

# The Greenland Analogue Project: Final Report

NWMO-TR-2016-12

September 2016

**Claesson Liljedahl L<sup>1</sup>, Kontula A<sup>2</sup>, Harper J<sup>3</sup>, Näslund J-O<sup>1</sup>, Selroos J-O<sup>1</sup>, Pitkänen P<sup>2</sup>, Puigdomenech I<sup>1</sup>, Hobbs M<sup>4</sup>, Follin S<sup>5</sup>, Hirschorn S<sup>4</sup>, Jansson P<sup>6</sup>, Kennell L<sup>4</sup>, Marcos N<sup>7</sup>, Ruskeeniemi T<sup>8</sup>, Tullborg E-L<sup>9</sup>, Vidstrand P<sup>1</sup>**

<sup>1</sup>Svensk Kärnbränslehantering AB, <sup>2</sup>Posiva Oy, <sup>3</sup>University of Montana, <sup>4</sup>Nuclear Waste Management Organization (NWMO), <sup>5</sup>Golder associates, <sup>6</sup>Department of Physical Geography, Stockholm University, <sup>7</sup>Saanio & Riekkola Oy, <sup>8</sup>Geological Survey of Finland, <sup>9</sup>Terralogica AB

**nwmo**

NUCLEAR WASTE  
MANAGEMENT  
ORGANIZATION

SOCIÉTÉ DE GESTION  
DES DÉCHETS  
NUCLÉAIRES



**Nuclear Waste Management Organization**  
22 St. Clair Avenue East, 6<sup>th</sup> Floor  
Toronto, Ontario  
M4T 2S3  
Canada

Tel: 416-934-9814  
Web: [www.nwmo.ca](http://www.nwmo.ca)

# **The Greenland Analogue Project: Final Report**

**NWMO-TR-2016-12**

September 2016

**Claesson Liljedahl L<sup>1</sup>, Kontula A<sup>2</sup>, Harper J<sup>3</sup>,  
Näslund J-O<sup>1</sup>, Selroos J-O<sup>1</sup>, Pitkänen P<sup>2</sup>,  
Puigdomenech I<sup>1</sup>, Hobbs M<sup>4</sup>, Follin S<sup>5</sup>, Hirschorn S<sup>4</sup>,  
Jansson P<sup>6</sup>, Kennell L<sup>4</sup>, Marcos N<sup>7</sup>, Ruskeenieni T<sup>8</sup>,  
Tullborg E-L<sup>9</sup>, Vidstrand P<sup>1</sup>**

<sup>1</sup>Svensk Kärnbränslehantering AB, <sup>2</sup>Posiva Oy, <sup>3</sup>University of Montana, <sup>4</sup>Nuclear Waste Management Organization (NWMO), <sup>5</sup>Golder associates, <sup>6</sup>Department of Physical Geography, Stockholm University, <sup>7</sup>Saanio & Riekkola Oy, <sup>8</sup>Geological Survey of Finland, <sup>9</sup>Terralogica AB

This report has been prepared under contract to NWMO, SKB and Posiva. The report has been reviewed by NWMO, but the views and conclusions are those of the authors and do not necessarily represent those of the NWMO.

### Document History

Title:	The Greenland Analogue Project: Final Report		
Report Number:	NWMO-TR-2016-12		
Revision:	R000	Date:	September 2016
Report Contributors			
Authored by:	<p>L. Claesson Liljedahl, J-O. Näslund, J-O Selroos, I. Puigdomenech, P. Vidstrand (Svensk Kärnbränslehantering AB)</p> <p>A. Kontula, P. Pitkänen (Posiva Oy)</p> <p>J. Harper (University of Montana)</p> <p>M. Hobbs, S. Hirschorn, L. Kennell (NWMO)</p> <p>S. Follin (Golder associates)</p> <p>P. Jansson (Department of Physical Geography, Stockholm University)</p> <p>N. Marcos (Saanio &amp; Riekkola Oy)</p> <p>T. Ruskeeniemi (Geological Survey of Finland)</p> <p>E-L. Tullborg (Terralogica AB)</p>		
Reviewed by:	L. Claesson Liljedahl (Svensk Kärnbränslehantering AB); A. Kontula (Posiva Oy);		
Independent review by:	Mike Thorne (Mike Thorne and Associates Ltd.); Joe Pearson (Ground-Water Geochemistry, United States); Shawn Marshall (University of Calgary)		
Approved by:	P. Wikberg (Svensk Kärnbränslehantering AB), T. Jalonen (Posiva Oy)		
Nuclear Waste Management Organization			
Reviewed by:	Monique Hobbs, Laura Kennell, Mark Jensen		
Accepted by:	Mark Jensen		

## EXECUTIVE SUMMARY

**Title:** The Greenland Analogue Project: Final Report  
**Report No.:** NWMO-TR-2016-12  
**Author(s):** Claesson Liljedahl L<sup>1</sup>, Kontula A<sup>2</sup>, Harper J<sup>3</sup>, Näslund J-O<sup>1</sup>, Selroos J-O<sup>1</sup>, Pitkänen P<sup>2</sup>, Puigdomenech I<sup>1</sup>, Hobbs M<sup>4</sup>, Follin S<sup>5</sup>, Hirschorn S<sup>4</sup>, Jansson P<sup>6</sup>, Kennell L<sup>4</sup>, Marcos N<sup>7</sup>, Ruskeeniemi T<sup>8</sup>, Tullborg E-L<sup>9</sup>, Vidstrand P<sup>1</sup>  
**Company:** <sup>1</sup>Svensk Kärnbränslehantering AB, <sup>2</sup>Posiva Oy, <sup>3</sup>University of Montana, <sup>4</sup>Nuclear Waste Management Organization (NWMO), <sup>5</sup>Golder associates, <sup>6</sup>Department of Physical Geography, Stockholm University, <sup>7</sup>Saanio & Riekkola Oy, <sup>8</sup>Geological Survey of Finland, <sup>9</sup>Terralogica AB  
**Date:** September 2016

### Executive Summary

This report summarises the key findings of the Greenland Analogue Project (GAP), a collaborative research project conducted between 2008 and 2013 by the national nuclear waste management organisations in Sweden (SKB), Finland (Posiva) and Canada (NWMO). The primary aims of the GAP were to enhance scientific understanding of glacial processes and their influence on both surface and subsurface environments relevant to the performance of deep geological repositories for spent nuclear fuel in crystalline shield rock settings. Based on its size, relative accessibility, and crystalline shield bedrock, the Greenland Ice Sheet (GrIS) was selected by the GAP as a natural analogue for glaciation processes expected to reoccur in Fennoscandia and Canada over *Deep Geological Repository* (DGR) safety-relevant timeframes.

The GAP study area is located east of Kangerlussuaq village on the west coast of Greenland and covers approximately 12,000 km<sup>2</sup>, of which approximately 70% is occupied by the GrIS. To advance understanding of glacial hydrogeological processes, GAP research activities included both extensive field work and modelling studies of the GrIS, focused into three main project areas: 1) surface-based ice sheet studies; 2) ice drilling and direct studies of basal conditions; and 3) geosphere studies. The main objectives and activities of these project areas are provided below:

1. Surface-based ice sheet studies aimed to improve the current understanding of ice sheet hydrology and its relationship to subglacial hydrology and groundwater dynamics. This work was based primarily on *indirect* observations from the ice sheet surface of the basal hydrological system, to obtain information on parts of the ice sheet which contribute water for groundwater infiltration. Project activities included quantification of ice sheet surface water production, as well as an evaluation of how water is routed from the ice surface to the interface between the ice and the underlying bedrock.
2. Ice drilling and direct studies of basal conditions also aimed to improve understanding of ice sheet hydrology and groundwater formation based on *direct* observations of the basal hydrological system, paired with numerical ice sheet modelling. Specific processes were investigated, including: 1) thermal conditions within and at the base of the ice sheet; 2) generation of meltwater at the ice/bedrock interface; and 3) hydrologic conditions at the base of the ice sheet. Activities included ice drilling of multiple holes at three locations on the ice sheet, at distances up to thirty kilometres from the ice sheet terminus, to assess drainage, water flow, basal conditions and water pressures at the interface between the ice and bedrock.
3. Geosphere investigations focused on groundwater flow dynamics and the chemical and isotopic composition of water at depths of 500 metres or greater below ground surface, including evidence on the depth of permafrost, redox conditions and the infiltration of glacial meltwater into the bedrock. Deep and inclined boreholes were drilled through the permafrost in the vicinity of the ice sheet

margin. The boreholes were hydraulically tested and instrumented to allow hydrogeologic and hydrogeochemical monitoring. The nature of ground conditions under a proglacial lake was also investigated, to assess if areas of unfrozen ground within the permafrost (taliks) may act as a potential pathway for exchange of deep groundwater and surface water.

The key findings from these three main project areas contribute towards improved scientific understanding of processes associated with the GrIS. Several highlights are summarised below, in terms of attributes relevant to assessing the long term safety of a DGR.

**Transient meltwater processes on the ice sheet surface:** Surface melt and runoff is a summer phenomenon limited to 3-4 months (May through September), during which time the ice surface lowers by up to 3-4 metres. The volume of meltwater generated at the surface each summer exceeds the amount of predicted basal melt by two order of magnitude (cm of basal melt vs. metres of surface melt). The summer melt period therefore completely dominates the annual cycle of available water volume.

Abrupt draining of supraglacial lakes (SGLs) into newly opened fractures is one of the key mechanisms for establishing surface-to-bed pathways. Nearly all surface melt eventually penetrates the ice and reaches the bed. Just above the *equilibrium line altitude* (ELA), where meltwater begins to pool, is approximately the interior limit where substantial surface melt has the potential to penetrate to the bed. Seasonal variations in water flow through the basal drainage system beneath the ablation zone occur mainly as the result of ice sheet surface melting.

**Basal thermal distribution and generation of water at the ice sheet bed:** Direct observations made in 23 boreholes drilled to the ice sheet bed at distances between 200 m and 30 km from the ice margin provide the first direct evidence that the entire outer flank of the study area has a melted bed, with liquid water present, rather than a universally or locally frozen bed. No evidence has been found to suggest that a complex pattern of patchy frozen/melted bed conditions exist in the ice marginal areas within the region studied.

Modelling results illustrate that the location of the boundary between melted and interior frozen conditions is highly sensitive to geothermal heat flux values, but relatively insensitive to longitudinal ‘pulling’ caused by fast sliding ice flow near the margin. For all choices of boundary conditions and modelling parameters believed to be reasonable, a central frozen area extends many tens of kilometres from Greenland’s central ice flow divide, but greater than 75% of the studied sector of the GrIS is subject to basal melting conditions.

**Hydraulic boundary conditions for groundwater simulations:** Hydrologic conditions at the ice sheet bed were found to vary across the width of the GAP study area. Between the ice divide and the margin, there is evidence for three different basal zones as defined by the amount and configuration of meltwater: the *frozen bed zone*, the *wet bed zone*, and the *surface-drainage bed zone*. The *surface-drainage bed zone* is further characterised by a zone with *distributed water drainage* and a zone with *transient conduit drainage*. These hydrological zones result from surface, bed, and internal ice flow processes, and may be representative of Northern Hemisphere ice sheets in a similar stage of development to the current GrIS.

This revised conceptual understanding of the drainage system developed through the GAP implies that much of the bed inward of the margin is covered by water, rather than mostly drained by discrete conduits with little water in between. Further, the drainage system would not be expected to undergo large pressure drops in response to water input forcing, as hypothesised for a conduit dominated system that rapidly drains high volumes of water from the bed. Taken together, hydraulic measurements and analyses from the ice boreholes imply that ice overburden hydraulic pressure (i.e. a hydraulic head

corresponding to 92% of ice thickness) provides an appropriate description of the basal hydraulic pressure as an average value for the entire ice sheet over the year.

**Role of permafrost and taliks:** The GAP study area is located in a region with continuous permafrost. Close to the ice sheet margin, the permafrost thickness reaches 350-400 m, as measured in the DH-GAP03 and DH-GAP04 boreholes. The main part of the base of the ice sheet in the study area, including marginal areas, has been shown to have basal melting conditions, with the exception of the central parts of the ice sheet. Taken together with the fact that most of the area presently glaciated was also glaciated throughout the past 10,000 years (and therefore, has not been subject to any sub-aerial permafrost development during this time), indicates that permafrost does not exist under the major part of the large, warm-based areas of the ice. An exception is at the ice margin, where a wedge of permafrost most likely stretches in under the ice. It is not known how far this subglacial permafrost wedge stretches (e.g. if it is a few hundreds of metres or several kilometres).

Where permafrost extends to depths of greater than 300 m, a lake diameter of approximately 400 m would be expected to maintain unfrozen areas throughout the entire permafrost thickness, e.g. through taliks, which provide a potential pathway for exchange of deep groundwater and surface water. Borehole DH-GAP01 was drilled underneath a lake ("Talík lake"), confirming for the first time, the existence of a through talík beneath a lake in an area of continuous permafrost. Furthermore, sampling of this borehole has provided the first information on groundwaters from within a talík located in close proximity to the ice sheet margin. Although it has been hypothesised that the Talík lake would act entirely as a discharge feature, evidence from hydraulic head measurements and the stable water isotopic composition of the sampled groundwaters are consistent with seasonal recharging conditions occurring at this location.

**Meltwater end-member water compositions:** The characteristics of a meltwater end-member are needed when evaluating water compositions in glaciated areas, as well as in any numerical modelling of groundwater flow and reactive solute transport. Based on analysis of meltwater compositions conducted as part of the GAP and reported in the scientific literature, a glacial meltwater end-member has depleted  $\delta^{18}\text{O}$  (-30 to -25‰) and  $\delta^2\text{H}$  signatures (-235 to -200‰) consistent with cold climate conditions and a very low total dissolved solids content, with solute concentrations ranging from practically zero to approximately 1 mM for the main solutes, such as  $\text{Ca}^{2+}$ .

**Depth of glacial recharge:** The stable water isotopic signatures ( $\delta^2\text{H}$  and  $\delta^{18}\text{O}$ ) indicate that the groundwater sampled in both boreholes (DH-GAP01, DH-GAP04) are of glacial meltwater origin. The millions of years of predominantly glacial conditions in this region, the local structural geology and fracture distribution, the presence of high hydraulic gradients and the presence of relatively low salinity fluids at depth in the rock mass have likely facilitated the penetration of glacial meltwaters at this site to depths of a least 500 m.

The relatively low concentrations of Na and Cl in the groundwaters likely originate from within the rock matrix through water-rock interactions and diffusion, whereas Ca and  $\text{SO}_4$  in these waters originate from dissolution of gypsum, which occurs as a fracture infill mineral at depths below approximately 300 m. A preliminary interpretation of dissolved He concentrations suggests that the deep groundwaters may have residence times exceeding hundreds of thousands of years. Together with the extensive persistence of gypsum (hydrothermal origin) below 300 m, which is a highly soluble mineral, this suggests stable conditions with limited groundwater flow at depths below 300 m at the DH-GAP04 location.

**Redox stability of the groundwater system:** Below the permafrost (and/or at depths greater than about 350 m), reducing conditions are interpreted to prevail in the study area. Past penetration into the bedrock of dissolved oxygen in meltwaters has been limited in depth, as indicated by the presence of pyrite in

fractures below approximately 50 m; iron oxyhydroxides are found in fractures only in the upper parts of the rock (down to 60 m), with only a few isolated occurrences of goethite down to 260 m depth.

The above examples illustrate ways in which research conducted within the GAP has advanced scientific understanding of hydrological processes related to the presence of an ice sheet, including the temporal and spatial nature of processes occurring on the ice sheet surface, conditions at the ice sheet bed (thermal and meltwater generation), and interactions between glacial meltwater and the underlying groundwater systems. In assessments of the potential risk to humans and the environment from DGRs for spent nuclear fuel, uncertainties related to process understanding are typically handled using assumptions which over- rather than underestimate the potential radiological consequences. The increased scientific understanding of glacial hydrological processes attained through the GAP, and the associated reduction of uncertainties, has provided new insights that will inform and strengthen future safety cases, including the safety assessments developed for DGRs in crystalline bedrock settings. Furthermore, the findings may allow a re-evaluation of the degree of pessimism in some of the assumptions made in previous safety assessments and modelling work.

# Contents

<b>1</b>	<b>Introduction</b>	11
1.1	Background	12
1.2	Objectives and scope of project	15
1.3	The present report and supporting documents	19
<b>2</b>	<b>Summary of GAP investigations and available data</b>	25
2.1	Overview of the GAP study area	25
2.1.1	Landscape	25
2.1.2	Topography and Quaternary Geology	27
2.1.3	Geological setting	29
2.1.4	Climate, permafrost and the 'Talík lake' study area	30
2.1.5	Characteristics of the GrIS in the GAP study area	34
2.1.6	Deglaciation history of southern West Greenland	36
2.2	Surface based ice sheet investigations	36
2.2.1	Remote sensing	37
2.2.2	Automatic weather station network	37
2.2.3	GPS measurements of ice motion	38
2.2.4	Ground-penetrating radar	39
2.2.5	Seismics – reflection and passive seismics	40
2.3	Ice drilling and direct studies of basal conditions	42
2.4	Geosphere investigations	46
2.4.1	Bedrock geology	49
2.4.2	Geophysics	49
2.4.3	Surface water characterisation	50
2.4.4	Bedrock borehole investigations	53
2.4.5	Measurements performed after drilling	57
2.4.6	Groundwater sampling and analysis	62
2.4.7	Sampling and analysis of rocks and fracture minerals	63
2.4.8	Monitoring of water pressure, temperature and electrical conductivity	64
<b>3</b>	<b>Summary of main areas where process understanding was increased through the GAP</b>	65
3.1	Ice sheet hydrology	65
3.1.1	Basal thermal conditions	65
3.1.2	Surface water generation	70
3.1.3	Water pressure level and variability	72
3.1.4	Generalised hydraulic potential field	79
3.2	Hydrogeology	80
3.2.1	Previous knowledge base	80
3.2.2	New knowledge obtained by GAP	81
3.2.3	Key findings	85
3.2.4	Remaining challenges	86
3.3	Hydrogeochemistry	86
3.3.1	Previous knowledge base	87
3.3.2	New knowledge obtained by GAP	94
3.3.3	Remaining challenges	100
<b>4</b>	<b>Contributions towards answering the six guiding project questions</b>	101
4.1	Where is meltwater generated under an ice sheet?	101
4.2	What is the hydraulic pressure situation under an ice sheet, driving groundwater flow?	102
4.3	To what depth does glacial meltwater penetrate into the bedrock?	104
4.4	What is the chemical composition of glacial water when and if it reaches repository depth?	105
4.5	How much oxygenated water will reach repository depth?	105

4.6	Does discharge of deep groundwater occur in the investigated proglacial talik in the study area?	106
<b>5</b>	<b>Conceptual understanding of conditions and processes at the GAP site</b>	107
5.1	Hydrological conditions of the ice sheet	107
5.1.1	Surface conditions	107
5.1.2	Bed conditions	109
5.2	Permafrost and taliks	110
5.3	Hydrogeological system at the ice sheet margin	111
5.4	Hydrogeochemical system at the ice sheet margin	112
<b>6</b>	<b>Conclusions</b>	117
6.1	Scientific results and understanding attained through the GAP	117
6.2	The GAP: Applicability to safety assessments for nuclear waste repositories	120
	<b>Acknowledgements</b>	121
	<b>References</b>	123
<b>Appendix A</b>	GAP bibliography – list of journal publications	135
<b>Appendix B</b>	Monthly mean air temperatures from the DMI weather station in Kangerlussuaq	139
<b>Appendix C</b>	List of abbreviations	141

# 1 Introduction

The *Greenland Analogue Project* (GAP) Final Report is the second of two final technical reports documenting the results from the GAP. The fieldwork was conducted during 2008 to 2013 near Kangerlussuaq in Western Greenland (Figure 1-1). The first final technical report ‘The Greenland Analogue Project: Data and Processes’ (Harper et al. 2016a, from here on referred to as the Data Report 2016) presents the collected datasets, and the conceptual understanding within each discipline developed during the GAP. The present report is a synthesis report that presents the key data/understanding gained during GAP and aims to summarise and integrate the conceptual models presented in the Data Report 2016. The overall focus of this Final Report is to demonstrate the advances in process understanding, as relevant to the long term safety of *deep geological repositories* (DGRs) for spent nuclear fuel, that have resulted from the GAP, i.e. how the understanding of glacial hydrology, and of hydrological, hydrogeological and geochemical processes under glacial conditions in a crystalline setting has improved as a result of the work performed as part of the GAP.

The main authors of this report are listed in Table 1-1.

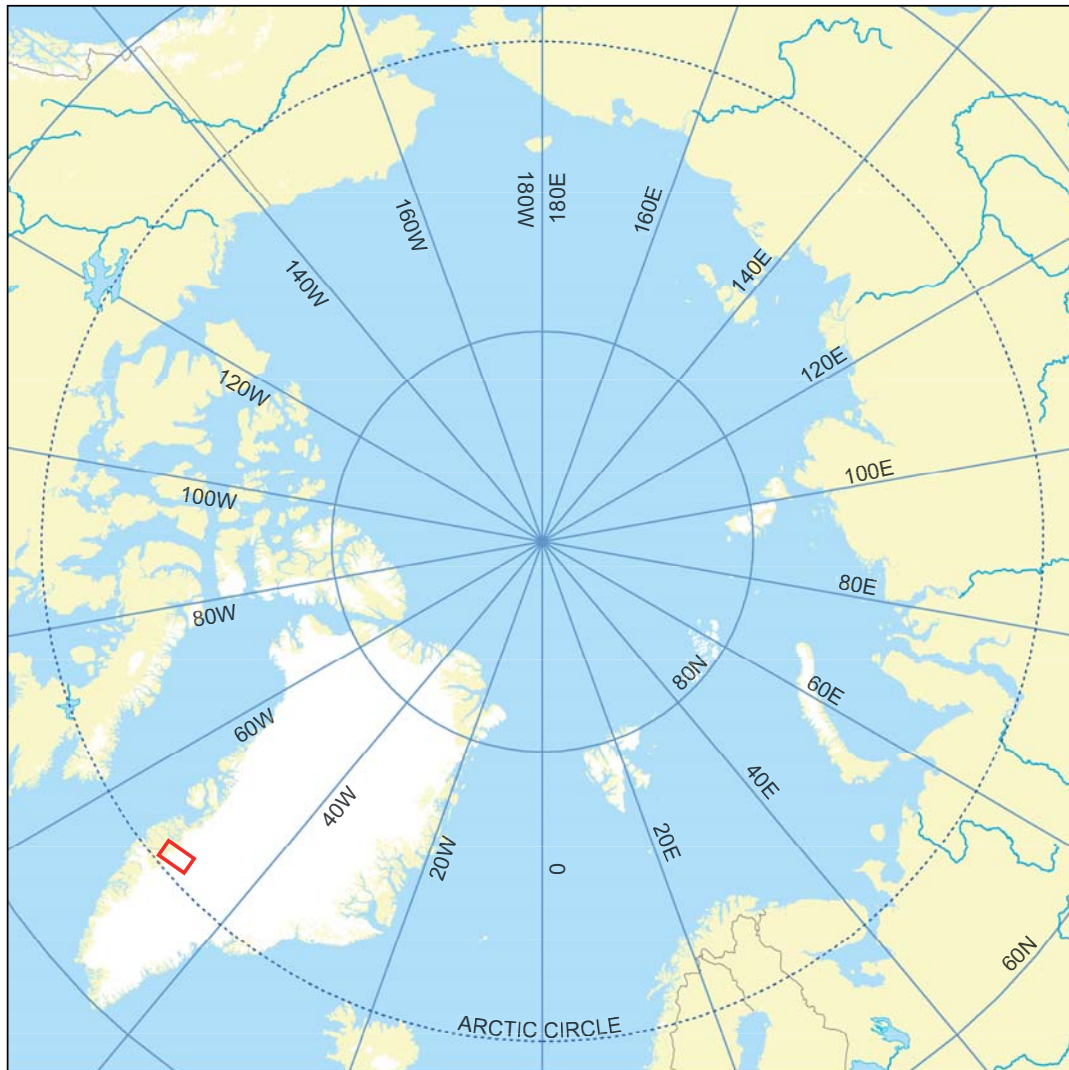


**Figure 1-1.** Circumpolar map of the northern hemisphere showing the location of the GAP study area (red rectangle).

**Table 1-1. Authors of the report and the sections for which they are responsible and to which they have contributed. The GAP was initiated and funded by Svensk Kärnbränslehantering AB (SKB) in Sweden, Posiva Oy (Posiva) in Finland and the Nuclear Waste Management Organization (NWMO) in Canada.**

Author	Organisation	Responsible for section(s)	Contributing to section(s)
Claesson Liljedahl, Lillemor	SKB	2, 5.2	1, 2, 3, 4, 5, 6
Follin, Sven	Golder associates		3.2, 4.2, 4.6, 5
Harper, Joel	University of Montana	3.1, 5.1	3.2, 4.1, 4.2, 5, 6
Hirschorn, Sarah	NWMO	Executive summary	4, 6
Hobbs, Monique	NWMO	5.4, 6	3.3
Jansson, Peter	University of Stockholm		3.1, 5.3
Kennell, Laura	NWMO		3.3
Kontula, Anne	Posiva	1	3
Marcos, Nuria	Saario & Riekkola Oy		1, 3.1, 3.3
Näslund, Jens-Ove	SKB	4.1	3.1, 5, 6
Pitkänen, Petteri	Posiva	4.3	3.3, 4.4, 4.5, 5
Puigdomenech, Ignasi	SKB	3.3, 4.4, 4.5	4.3, 5, 6
Ruskeenieni, Timo	Geological Survey of Finland		2, 3.3
Selroos, Jan-Olof	SKB	3.2, 4.2, 4.6, 5.3	5, 6
Tullborg, Eva-Lena	Terralogica AB		3.3, 5.4
Vidstrand, Patrik	SKB		3.2, 4.2, 5

## 1.1 Background

*Deep Geological Repositories* for spent nuclear fuel are being considered in a number of countries that are designing and/or implementing practical solutions for the long term safety and isolation of spent nuclear fuel. The DGR concept (Figure 1-2) is based on a multi-barrier principle. For example, in Sweden and Finland, the DGR concept (the KBS-3 vertical deposition concept shown in Figure 1-2) includes copper canisters, each with a cast iron insert and containing spent nuclear fuel that are emplaced in individual deposition holes bored in the floors of deposition tunnels. To seal the deposition holes, the canisters are to be surrounded by a swelling clay buffer material (bentonite). The deposition tunnels, the central tunnels and the other underground openings, including the main access shafts and/or ramps, are to be backfilled with materials of low permeability once the repository is filled.

Long term safety in nuclear waste management requires that the spent nuclear fuel, including its original radionuclide inventory and associated decay by-products, is kept isolated from the ground surface biosphere on a time scale of 100,000 years up to one million years. Over this time frame, glacial conditions are expected to occur repeatedly in regions that have been glaciated from the mid Pliocene onwards. Climate-induced changes, such as the advance and retreat of ice sheets and development of permafrost, will influence and alter the surface and subsurface environment, including its hydrology, hydrogeology, geochemistry and stress state, which may impact repository performance. In assessments of glacial impacts on long term repository safety, simplified models and cautious assumptions are used, e.g. in relation to the representation of ice sheet hydrology, generation of dilute meltwater and the penetration of that dilute meltwater into the underlying rock. Observations from existing ice sheets help to reduce uncertainties and provide a stronger scientific basis for the treatment of glacial impacts in safety assessments (e.g. SKB 2011, Posiva 2012, NWMO 2012).

In 2008, the international GAP was initiated collaboratively by Svensk Kärnbränslehantering AB (SKB) in Sweden, Posiva Oy (Posiva) in Finland and the Nuclear Waste Management Organization (NWMO) in Canada. The goal of the GAP is to advance the understanding of processes associated with glaciation and their impacts on the long term performance of a DGR in crystalline bedrock. An additional aim of the GAP is to contribute to an increased understanding of a glaciated environment by obtaining an integrated view of ice sheet hydrology and groundwater flow and chemistry. Using the *Greenland Ice Sheet* (GrIS) as a modern analogue for future continental-scale ice sheets

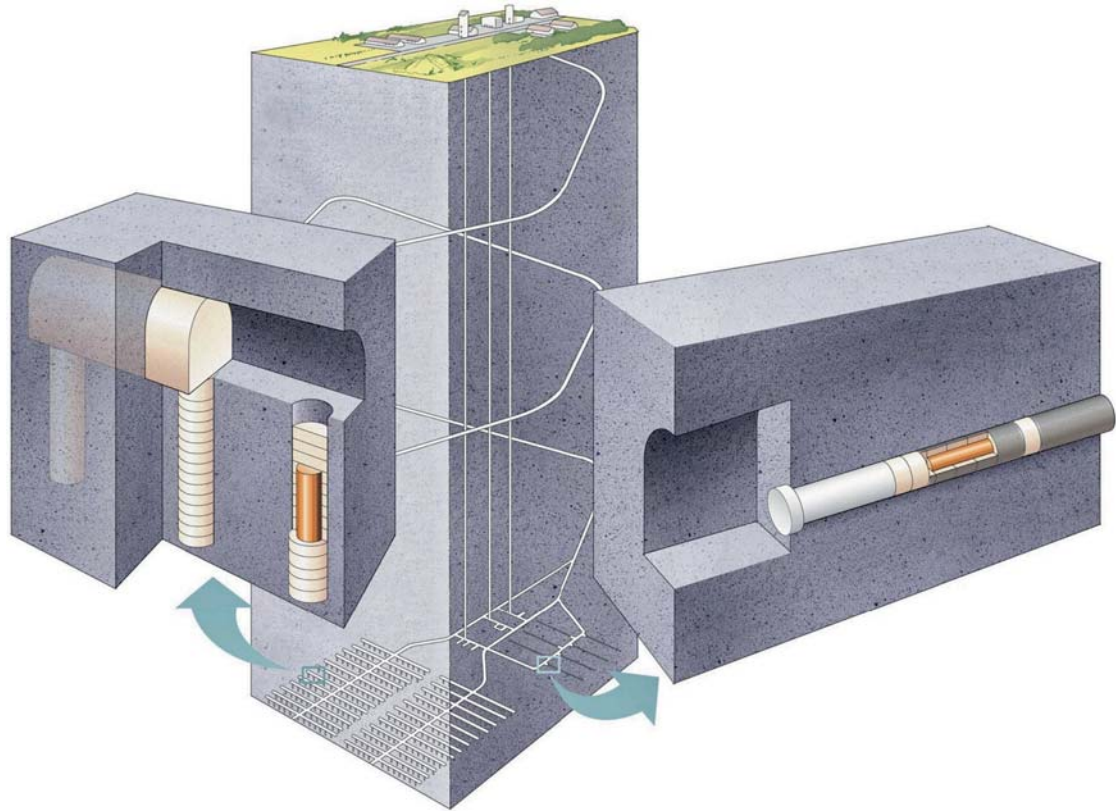


**Figure 1-2.** The multi-barrier deep geologic repository concept (here illustrated by the KBS-3 concept), showing the vertical deposition concept to the left and the horizontal deposition concept to the right. SKB ©.

in previously glaciated regions, field and modelling studies of the GrIS and subsurface conditions were undertaken. The GrIS was chosen because it is of about the same size as those ice sheets known to have formed, and expected to form in the future in Fennoscandia, which suggests that the scale of processes and response times could be similar during the glaciation and deglaciation phases. Moreover, the bedrock in the study area is crystalline, with similarities to the crystalline bedrock in Sweden, Finland and Canada in terms of composition, fracturing and age. These characteristics make the study site an appropriate analogue of the conditions that are expected to prevail in Fennoscandia and, to some degree, in Canada during future glacial cycles. However, the suggested repository sites in Finland and Sweden are located in regions of low topography, whereas the GAP study area is characterised by moderate relief (few hundreds of metres), which among other factors, needs to be considered when transferring knowledge obtained from GAP to other regions.

The study area chosen for GAP is located close to the Kangerlussuaq village (Søndre Strømfjord in Danish) on the west coast of Greenland, just north of the Polar Circle at 67°N and 51°W and approximately 160 km from the Atlantic Ocean (Figure 1-3). The GAP study area measures approximately 200 km from east to west, extending from the Kangerlussuaq fiord and up on the GrIS and measures 60 km from north to south (Figure 1-3). The study area was chosen to meet the following criteria: 1) the field area is logistically easy to reach compared with other areas in Greenland; 2) its long axis is parallel to the general ice flow direction; 3) it was assumed to include both frozen and wet conditions at the base of the ice sheet; and 4) the proglacial area is within continuous permafrost and includes larger lakes with potential taliks.

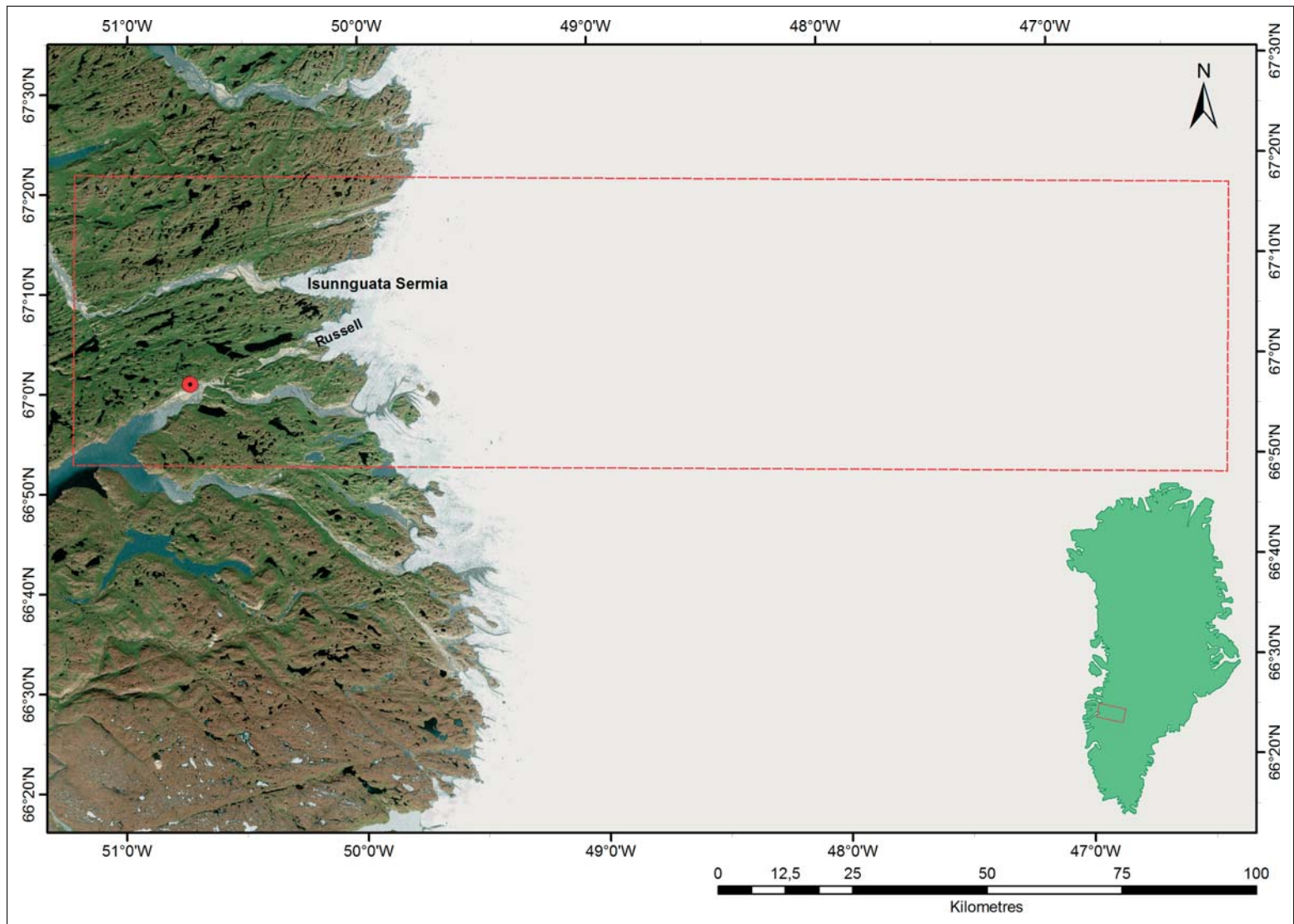


**Figure 1-3.** Overview map showing the GAP study area (red dashed rectangle). Inset map shows the location of the study area on the Greenland scale. The key outlet glaciers in the GAP study area, Isunnguata Sermia and Russell glacier are indicated. Red circle shows the location of Kangerlussuaq village and the Kangerlussuaq International Airport (SFJ). Background image is a World Imagery esri satellite image acquired 2 October, 2014.

## 1.2 Objectives and scope of project

Safety assessment of geological disposal of nuclear waste requires a multidisciplinary and iterative approach (IAEA 2012) used to develop an overall understanding of the long term performance of the repository and its surroundings. The repository system includes multiple engineered barriers which, together with the surrounding geosphere, are designed to contain and completely isolate the nuclear waste. Features, events and processes (natural and anthropogenic) that could potentially affect the safety of the repository system are identified and possible releases to the environment are assessed, as well as the consequences of such potential releases.

Given the long time span covered by safety assessments of DGRs for nuclear waste (100,000 years up to one million years), scientific information and knowledge on processes related to cold climate conditions are required. Previous safety assessments have shown that, for sites located in previously glaciated terrain, the impacts of glacial (ice sheet) and periglacial (permafrost) processes need to be included and addressed. These processes influence the environment around a repository and have the potential to directly or indirectly affect the engineered barrier system, the geosphere and, consequently, repository safety (e.g. SKB 2011, NWMO 2012, Posiva 2012). In this context, specific factors of importance for repository safety include changes in groundwater flow, hydrogeochemistry, hydrostatic pressure and bedrock stresses. In addition, these processes affect the surface biosphere and landscape development at a repository site, which in turn could influence the effects of a potential release from a repository.

Scientific research to better understand processes associated with continental-scale glaciation, in terms of both glacial and periglacial conditions, has increased in the past decade (e.g. Kleman et al. 2008, Pitkäranta 2009, Vizcaíno et al. 2010, Jansson 2010 and references therein, SKB 2010a and references therein). The area in which the lack of information is most significant for glacial regions concerns permafrost characteristics and development, groundwater flow and its chemical composition, and bedrock stress and rock mechanical characteristics. However, conducting such research remains challenging, due to the remote nature and extreme environmental conditions associated with ice sheets in both Greenland and Antarctica. Within fields where available scientific information has been limited, uncertainties have been handled using conservative assumptions in safety assessments. To reduce these uncertainties and in order to better evaluate and improve the assumptions made in previous, ongoing and future safety assessments, the GAP aims to advance scientific understanding of hydrological, hydrogeological and geochemical processes under glacial conditions.

The prime processes not directly addressed by the GAP relate to hydro-mechanical couplings induced by the ice load. The bedrock in the investigated region in Greenland was expected to be comparable to that found in typical Fennoscandian Shield conditions. In such hard (high strength), fractured (permeable) crystalline rock, all pressure changes during a glacial cycle are often assumed to be instantaneous (Vidstrand et al. 2013) and modelling has shown that with realistic hydraulic and mechanical properties and boundary conditions, this assumption is valid (Lund et al. 2009, Lönnqvist and Hökmark 2010, Hökmark et al. 2010). Furthermore, assuming the GrIS at the site to be wet-based, the load and the pressure rise occur instantaneously and no change in effective stress occurs. The two assumptions stated above comprise the prime reason for omitting the hydro-mechanical coupling in primary analyses and the reasoning behind the prioritisation of studying only the hydrological, hydrogeological and hydrogeochemical aspects of glacial conditions in the GAP.

To achieve the required increase of understanding, GAP research focused on obtaining information that contributes to answering the following six overall project questions:

- 1) Where is meltwater generated under an ice sheet?
- 2) What is the hydraulic pressure situation under an ice sheet, driving groundwater flow?
- 3) To what depth does glacial meltwater penetrate into the bedrock?
- 4) What is the chemical composition of glacial water if, and when, it reaches repository depth?
- 5) How much oxygenated water will reach repository depth?
- 6) Does discharge of deep groundwater occur in the investigated proglacial talik in the study area?

These questions cover areas where process understanding based on observations from an actual ice sheet setting or the extent of the process (in terms of duration, magnitude or scale) were very limited prior to the GAP. These questions also highlight areas where substantially conservative assumptions have been necessary in safety assessment analyses. Specifically, the first two questions relate to reducing uncertainties associated with the influence of the ice sheet on the groundwater system (including seasonal variations) and to better constraining the hydraulic boundary conditions to be used in groundwater modelling. Questions 3 through 5 are posed to better understand potential changes in groundwater chemical composition that could affect redox conditions at repository depth (e.g. oxygen in the infiltrating/penetrating meltwater), or that may influence bentonite stability through an adverse change in pH and/or ionic strength. The final question contributes to a better understanding of periglacial processes (especially hydrogeological) where permafrost occurs. In the final question the term “deep groundwater” is used and it concerns the groundwater system found at depths greater than 300 m. In the context of this study, groundwaters from the surface to approximately 300 m depth are denoted “shallow groundwaters”.

The six project questions were deliberately formulated in a condensed and simplified fashion and they have been used only as general guidelines for planning research conducted in the GAP. In reality, each question encompasses a range of specific research goals that were included in activities conducted in the GAP.

The GAP was originally divided into three subprojects 1) surface based ice sheet studies; 2) ice drilling and direct studies of basal conditions; and 3) geosphere studies, each with specific individual objectives collectively aimed at contributing understanding and inputs relevant to the answering of the six project questions listed above. The specific objectives of the three subprojects are described below. Figure 1-4a and Figure 1-4b shows the extent of the GAP study area and highlights the field areas in which the subprojects carried out fieldwork.

- 1) **Surface based ice sheet studies** aimed to improve the understanding of interactions between ice sheet hydrology and subglacial hydrology in order to gain insight into the prerequisites for groundwater formation. This was done by indirect observations from the ice sheet surface to increase the understanding of the basal hydrological system and specifically, to identify which parts of the ice sheet contain basal water available for bedrock infiltration. The latter aspect includes quantification of ice sheet surface water production, as well as how water is routed from the ice surface to its basal interface. This subproject included remote sensing, as well as direct measurements of vertical ice displacement and horizontal velocity fluctuations, and examined the variation of these parameters in space and time with variable surface meltwater production and routing.
- 2) **Ice drilling and direct studies of basal conditions** also aimed to improve understanding of ice sheet hydrology and the prerequisites for groundwater formation. However, these studies focused on direct observations and measurements to investigate the characteristics of the basal boundary conditions of the ice sheet. The main activity was drilling through the ice sheet at a number of locations where the ice sheet was observed to be wet-based to measure water pressures at the interface between the ice and the bedrock. This information provided important input for the conceptualisation of hydraulic pressure during glacial conditions for groundwater models applicable in Fennoscandia and Canada, including spatial and temporal variations in those pressure gradients.
- 3) **Geosphere investigations** focused on studying the infiltration of glacial meltwater into the bedrock, as well as groundwater flow dynamics and the chemical composition of water when, and if, it reaches typical repository depths (approximately 500 m depth or more). The main activities involved deep bedrock drilling near the ice sheet margin and subsequent downhole surveys and thermal, hydrogeological and hydrogeochemical instrumentation, sampling and monitoring. In order to investigate whether or not taliks may act as discharge points for deep groundwater formed under an ice sheet, a borehole was also drilled into a lake area where a talik was assumed to exist.

It should be noted that the intention of the GAP was never to perform a full site characterisation similar to those carried out by SKB and Posiva in Forsmark and Olkiluoto, for example. The data obtained during 2008–2013 are presented in detail in the Data Report 2016.

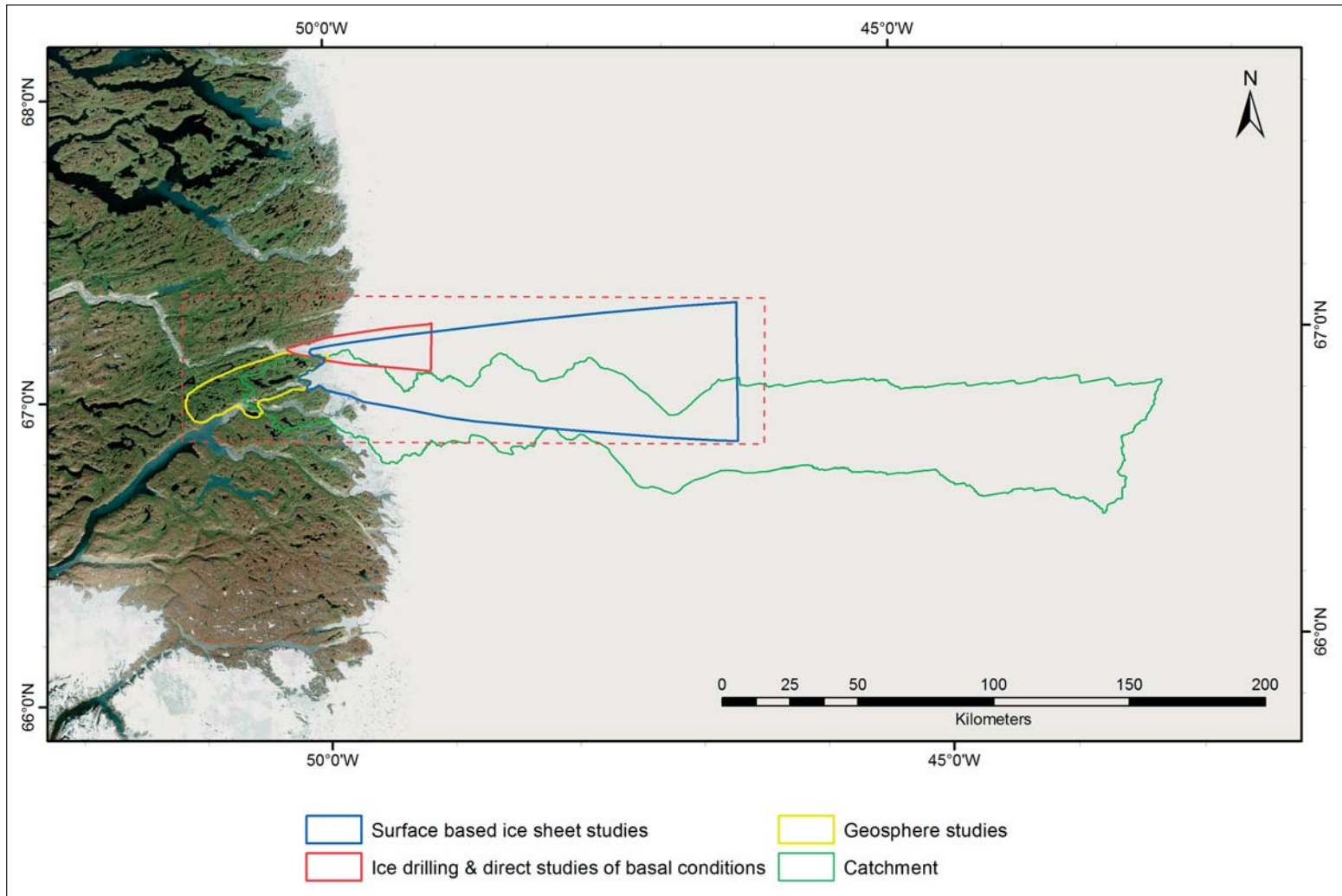


**Figure 1-4a.** Satellite image of the GAP study area (red dashed line) and the borders of the different field study areas within the GAP. Green line delineates the surface catchment area defined by Mikkelsen *et al.* (2013). The eastern border of the catchment coincides with the ice divide. The surface based ice sheet investigations were carried out in the blue bordered area (see Section 2.2), the ice drilling and direct studies of basal conditions were carried out in the red bordered area which overlaps with the surface based ice sheet investigation area (blue bordered area) (see Section 2.3). The yellow bordered area shows where the geosphere investigations were carried out (see Section 2.4).

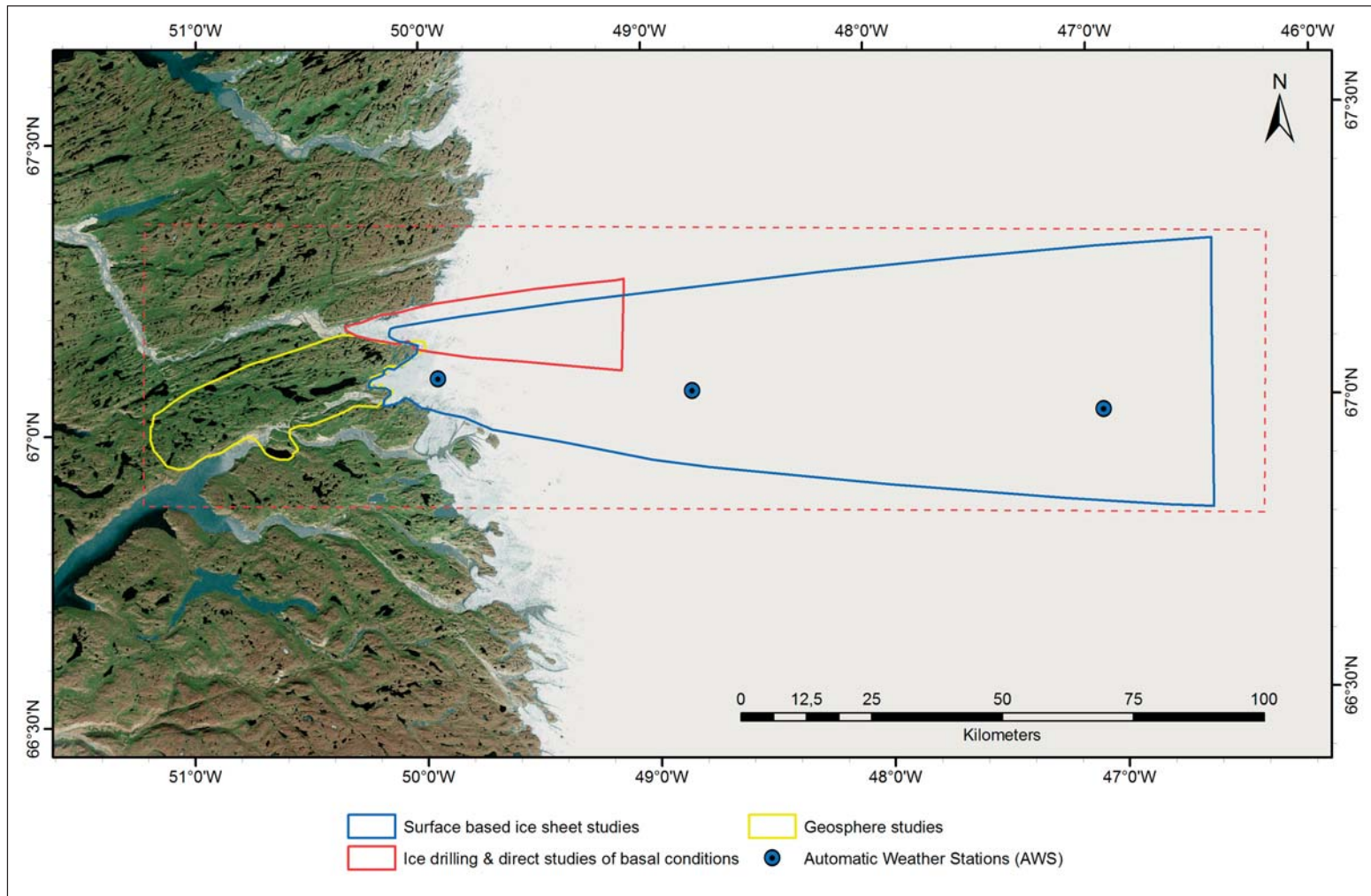


**Figure 1-4b.** Close up view of the GAP field study areas. Blue circles show the locations of the three GAP automatic weather stations, which form part of the surface based ice sheet investigations (for details see Section 2.2.2). Background image is a World Imagery esri satellite image acquired 2 October, 2014.

### 1.3 The present report and supporting documents

There are six main chapters included in this report.

Chapter 1 provides an introduction to the study and report.

Chapter 2 provides an overview of the GAP study area, the field investigations and available data.

Chapter 3 summarises the topics for which important process understanding was increased by the GAP.

Chapter 4 summarises contributions towards answering the six guiding project questions.

Chapter 5 proposes a conceptual understanding of the GAP site.

Chapter 6 presents the overall conclusions of the project.

Below is a summary of the background information reports, fieldwork and data reports and ground-water modelling work produced by the GAP to date. The results of GAP have been published in scientific journals and presented at scientific meetings. A full publication list is shown in Appendix A. Scientific publications from GAP will continue to be published over the coming years.

#### Background information reports

*Jansson P, 2010. Ice sheet hydrology from observations. SKB TR-10-68, Svensk Kärnbränslehantering AB.*

This report summarises the understanding of ice sheet hydrology as determined from observations made in Antarctica and Greenland before the GAP was initiated. Much of the general understanding of ice sheet hydrological processes was based on work performed on valley glaciers. There were few glacial hydrological investigations on ice sheets, but were increasing in number due to increased focus on both Greenland and Antarctica from the scientific community in the light of effects from climate change. Many of the new studies on ice sheet hydrology that were being performed fell into two categories. One related to verification of well-documented processes but on an ice sheet scale; the other related to ice sheet-specific features.

*Nielsen A B, 2010. Present conditions in Greenland and Kangerlussuaq. Posiva Working Report 2010-07, Posiva Oy, Finland.*

This report summarised the present climate, fauna, vegetation and bedrock conditions in Greenland and especially in Kangerlussuaq. Kangerlussuaq is located in the dry, continental area of central west Greenland and in the southernmost part of the continuous permafrost zone. This summary of present-day conditions in Kangerlussuaq was helpful in planning and carrying out the investigations in the study area.

*Wallroth T, Lokrantz H, Rimsa A, 2010. The Greenland Analogue Project (GAP), Literature review of hydrogeology/hydrogeochemistry. SKB R-10-34, Svensk Kärnbränslehantering AB.*

This report reviewed available information on the hydrogeology and hydrogeochemistry of central Western Greenland, with special emphasis on the area around Kangerlussuaq. The relevant information on this area was very limited and the review was extended to briefly consider studies made in other regions with similar conditions in terms of geology, climate and glaciology. It was obvious that both hydrogeological and hydrogeochemical conditions are highly localized and site-specific. Hence, data from other Arctic regions can only be seen as indicative and provide knowledge on processes that may or may not be relevant for the geographical area of primary interest in GAP.

Engels S, Helmens K, 2010. **Holocene environmental changes and climate development in Greenland**. SKB R-10-65, Svensk Kärnbränslehantering AB.

This report gave an overview of the Holocene environmental and climatic changes in Greenland and described the development of the periglacial environment during the Holocene. Special emphasis was given to the influence of the ice sheet on its surroundings, as a function of both time and in space.

The report focused on palaeoecological studies, as it was intended to assemble basic information for future studies on adaptation of the biosphere to changes in climate. There was a bias towards pollen- and macro-remains-based reconstructions of past changes, as these dominate palaeoecological studies that have been performed in Greenland; unfortunately, only a limited number of studies exist that include more modern proxies, such as diatoms or chironomids (of value as indicators of climate), but, where available in the literature, these were also included in the review.

### **Field and data reports**

Aaltonen I, Douglas B, Frapé S, Henkemans E, Hobbs M, Klint K E, Lehtinen A, Claesson Liljedahl L, Lintinen P, Ruskeeniemi T, 2010. **The Greenland Analogue Project, Sub-Project C, 2008, Field and data report**. Posiva Working Report 2010-62, Posiva Oy, Finland.

This report presented the field investigations and subsequent laboratory studies prior to the initiation of GAP. The main emphasis was on geological bedrock mapping and hydrogeochemical surface water characterisation of selected areas. Geological mapping provided information on the main rock types and fracture patterns. Hydrogeochemical sampling covered an area (2×6.5 km) between the Leverett and Russell glaciers, where the mapping survey investigated a large number of non-meltwater lakes and ponds. The sampling aimed to obtain a good cross-section of the variation in hydrological / hydrogeochemical conditions close to the ice margin and to observe the possible indirect influence of meltwaters through groundwater circulation.

SKB, 2010b. **The Greenland Analogue Project. Yearly report SKB 2009**. SKB R-10-59, Svensk Kärnbränslehantering AB; Posiva Working Report 2011-54, Posiva Oy, Finland.

This report presented the outcome of the activities carried out within the GAP during 2009. Major activities included preparatory work, testing of equipment, reconnaissance studies, establishment of monitoring networks in the field and preliminary data processing. Two bedrock boreholes were drilled in front of the ice sheet for subsequent downhole surveys and hydrogeological/hydrogeochemical instrumentation, sampling and monitoring. In addition to the fieldwork activities, regional groundwater flow modelling under ice sheet conditions was carried out.

Follin S, Stigsson M, Rhén I, Engström J, Klint K E, 2011. **Hydraulic properties of deformation zones and fracture zones at Forsmark, Laxemar and Olkiluoto for usage together with Geomodel version 1**. SKB P-11-26, Svensk Kärnbränslehantering AB.

This report presented trial datasets comprising structural-hydraulic properties suitable for flow modelling on different scales. The properties provided in this report were based on data and groundwater flow modelling studies conducted for Forsmark, Laxemar and Olkiluoto. The hydraulic properties provided are simplified to facilitate ready application with the GAP Geomodel version 1.

Engström J, Paananen M, Klint K E, 2012. **The Greenland Analogue Project. Geomodel version 1 of the Kangerlussuaq area on Western Greenland**. Posiva Working Report 2012-10, Posiva Oy, Finland. SKB P-11-38, Svensk Kärnbränslehantering AB.

This report describes a lineament model that was constructed as an interpretation from *Danish Geological Survey* (GEUS) ArcGIS data, with topographical, geological and geophysical data acquired from the updated GEUS map over Western Greenland (Gaarde and Marker 2010). The report included a suggested connection to the regional tectonic history and also a possible simple stress history; however, due to the limited amount of site information that had been collected, these should be referred to as tentative analyses.

Harper J, Hubbard A, Ruskeeniemi T, Claesson Liljedahl L, Lehtinen A, Booth A, Brinkerhoff D, Drake H, Dow C, Doyle S, Engström J, Fitzpatrick A, Frape S, Henkemans E, Humphrey N, Johnson J, Jones G, Joughin I, Klint KE, Kukkonen I, Kulesa B, Landowski C, Lindbäck K, Makahnouk M, Meierbachtol T, Pere T, Pedersen K, Pettersson R, Pimentel S, Quincey D, Tullborg E-L, van As D, 2012. **The Greenland Analogue Project. Yearly report 2010.** Posiva Working Report 2012-16, Posiva Oy Finland. SKB R-11-23, Svensk Kärnbränslehantering AB.

This report presented the outcome of all the activities within the GAP during 2010. The main field activities in 2010 included: ice radar investigations; operation and maintenance of the GPS and automatic weather station (AWS) network; active and passive seismic studies; ice drilling; tracer and slug tests; subglacial hydrological and hydrogeochemical investigations; groundwater and surface water sampling; borehole monitoring; and water-rock interaction studies. A number of activities were carried out in conjunction with the field investigations, which included: design and fabrication of equipment, such as the ice drilling rig and downhole sensors; remote sensing analysis; numerical ice sheet and hydrological modelling of the ice sheet; and logistical planning of the deep bedrock drilling for 2011.

Pöllänen J, Heikkinen P, Lehtinen A, 2012. **Difference flow measurements in Greenland, drillhole DH-GAP04 in July 2011.** Posiva Working Report 2012-13, Posiva Oy, Finland.

This report presented the principles of the difference flow measurements method and the results of measurements carried out in borehole DH-GAP04 in July 2011. The aim of the Posiva Flow Log (PFL) measurements was to find transmissive fractures (fractures with flow into the borehole) to aid in borehole instrumentation that would allow water sampling in borehole DH-GAP04. Suitable fractures for water sampling with positive hydraulic head (flow direction into the borehole when the borehole is at rest) were found in the borehole between 540 m to 640 m below the top of the casing.

Harper J, Hubbard A, Ruskeeniemi T, Claesson Liljedahl L, Kontula A, Booth A, Brinkerhoff D, Chandler D, Drake H, Dow C, Doyle S, Engström J, Fitzpatrick A, Frape S, Helanow C, Henkemans E, Humphrey N, Johnson E, Johnson J, Jones G, Klint KE, , Kulesa B, Landowski C, Lindbäck K, Luckman A, Maddoc L, Makahnouk M, Meierbachtol T, Pere T, Pettersson R, Pimentel S, Quincey D, Tullborg E-L, van As D, 2016b. **The Greenland Analogue Project. Yearly report 2011.** Posiva Working Report 2012-79, Posiva Oy, Finland.

This report presents an overview of the activities as well as research results obtained within the GAP during 2011. The main field activities in 2011 included: remote sensing, ice radar investigations; operation and maintenance of the GPS and AWS network; passive seismic studies; ice drilling; tracer and slug tests; subglacial hydrological and hydrogeochemical investigations; groundwater and surface water sampling; DH-GAP04 borehole drilling; borehole instrumenting and monitoring; and water-rock interaction studies.

Harper J, Hubbard A, Ruskeeniemi T, Claesson Liljedahl L, Kontula A, Brown J, Dirkson A, Dow C, Doyle S, Drake H, Engström J, Fitzpatrick A, Follin S, Frape S, Grały J, Hansson K, Harrington J, Henkemans E, S Hirschorn, M Hobbs, Humphrey N, Jansson P, Johnson J, Jones G, Kinnbom P, Kennell L, Klint K E, Liimatainen J, Lindbäck K, Meierbachtol T, Pere T, Pettersson R, Tullborg E-L, van As D, 2016a. **The Greenland Analogue Project: Data and Processes (in the present report referred to as the Data Report 2016).**

This report presents the objectives of the GAP research and investigations, and presents the different datasets collected as part of the GAP project during 2008-2013. The report further describes the conceptual models developed by the GAP and describes how the data collected support these conceptual models.

## Groundwater modelling reports

The different nuclear waste organisations are using different type of groundwater models, and hence a number of different parallel groundwater modelling studies have been performed for the GAP study area.

*Jaquet O, Namah R, Jansson P, 2010. Groundwater flow modelling under ice sheet conditions. Scoping calculations. SKB R-10-46, Svensk Kärnbränslehantering AB.*

Within the framework of the GAP project, a regional groundwater flow model under ice sheet conditions was developed for a specific location in Greenland. This model integrated the currently available data and information related to topography, ice thickness, talik location and ice margin position as well as analogue data for boundary conditions, hydraulic parameters, permafrost distribution and deformation zones derived from previous studies.

Conceptually, the groundwater flow system was considered to be governed by infiltration of glacial meltwater in heterogeneous faulted crystalline rocks in the presence of permafrost and taliks. The geological medium with conductive deformation zones was modelled as a 3D continuum with five hydrogeological units whose hydraulic properties were assigned using a stochastic simulation method. Based on glaciological concepts, a stochastic model was proposed for describing the subglacial permafrost distribution correlated to bed elevation. Numerical modelling of groundwater flow was performed at a regional scale under steady state conditions for various sensitivity cases that included variations in boundary conditions and permafrost distribution.

*Jaquet O, Namah R, Siegel P, Jansson P, 2012. Groundwater flow modelling under ice sheet conditions in Greenland (phase II). SKB R-12-14, Svensk Kärnbränslehantering AB.*

The second phase of groundwater flow modelling aimed at a more in-depth understanding of groundwater flow conditions likely to occur underneath ice sheets. This modelling phase enabled the development of an improved regional model that has led to a better representation of groundwater flow under ice sheet conditions. New data in relation to talik geometry and elevation, as well as to deformation zones, were integrated in the numerical model. In addition, more realistic hydraulic properties were considered for groundwater flow modelling. The major improvements were related to: 1) the assimilation of the subglacial boundary conditions using pressure and meltwater rates provided by a dynamic ice sheet model, which enabled simulation of a more plausible flow field in the Eastern part of the domain; 2) the integration of all potential taliks within the modelled domain provided better characterisation of the flow field under ice sheet conditions, and 3) the characterisation of the permafrost depth distribution was improved using a coupled description of flow and heat transfer. Finally, the distribution of glacial meltwater produced by the ice sheet was modelled for the determination of the potential depth and lateral extent that could be reached or influenced by such glacial water.

*Yin Y, Normani S, Sykes J, Barnard M, 2013. Preliminary hydrogeologic modelling of a crystalline rock setting in Western Greenland. NWMO TR-2013-20, Nuclear Waste Management Organization, Canada.*

This report describes preliminary, regional-scale groundwater modelling undertaken in support of the GAP. Through the use of parameter perturbation and case analyses, the effect of geosphere parameter and process uncertainty on groundwater system stability at depth is illustrated. Scenarios investigated in the report include: *Total dissolved solids* (TDS) vs. fluid density relationships; TDS vs depth relationships; permeability vs. depth relationships for the deformation zones; characterisation of permafrost, both in front of and beneath the ice sheet, and glacially-induced mechanical coupling.

*Vidstrand P, 2015. Concept testing and site-scale groundwater flow modelling of the ice sheet marginal area of the Kangerlussuaq region, Western Greenland. SKB R-15-01, Svensk Kärnbränslehantering AB.*

This study had two main objectives. First, the influence of recharge variations on groundwater flow and pressure in a subglacial environment is addressed. The relevance of top boundary conditions from large-scale groundwater flow models for use in detailed models is also investigated. Second, a number of sensitivity studies concerning the top boundary condition have been performed using the traditional specified-pressure top boundary condition. Also, sensitivity studies on subglacial permafrost have been performed. The results include a first set of supporting models of the ice sheet fore field including recharge and discharge characteristics in talik lakes, complemented with an analysis of the flow and pressure system within the area in the vicinity of the DH-GAP04 cored borehole.

*Jaquet O, Namar R, Jansson P, Siegel P, 2015. Groundwater flow modelling under ice sheet conditions in Greenland (phase III). SKB R-15-12, Svensk Kärnbränslehantering AB.*

This third groundwater flow modelling phase of the GAP has enabled the assimilation of data from dynamic ice sheet modelling into simulations conducted over time frames relevant to the safety assessment. Modelling of density-driven groundwater flow, heat transfer and permafrost using transient boundary conditions representing ice sheet displacement was performed for a full glacial cycle in Greenland. Details of subglacial topography, deformation zones, borehole data and talik locations are integrated in the model. The impact of various hydraulic parameterisations for the rock domain and deformation zones is investigated based on data from three sites located in the Fennoscandian shield (Laxemar, Forsmark and Olkiluoto). The changing distribution of meltwater from the ice sheet is modelled in order to determine the potential depths reached by glacial water for various glaciation scenarios. Major improvements in terms of representing subglacial boundary conditions have been achieved based on results from the GAP field investigations, leading to a reduction in uncertainties, and consequently, to an improved assessment of selected measures of repository performance.



## 2 Summary of GAP investigations and available data

This chapter presents the general characteristics of the GAP study area and gives an overview of the field investigations carried out from 2008–2013 by the GAP, with a focus on why they were done and what information they provided. Sections 2.2, 2.3 and 2.4 present the various field and laboratory studies carried out by the GAP. Selected results from these investigations are presented in these sections under the heading ‘**key output**’ as they are considered essential contextual information. However, the key results of the GAP are presented and discussed in Chapters 3 and 4 and conceptualised in Chapter 5. A detailed description of the available GAP datasets and investigations are provided in the Data Report 2016.

Throughout the present report, unless otherwise stated, all geographical data are presented in the *World Geodetic System 1984* (WGS-84) latitude and longitude. Elevations are presented relative to the WGS-84-datum reference ellipsoid. Time is presented as Coordinated Universal Time (UTC).

### 2.1 Overview of the GAP study area

Greenland is the world’s largest island and hosts the second largest ice sheet in the world after the Antarctic Ice Sheet. The GrIS covers approximately 1,700,000 km<sup>2</sup>, which is roughly 80% of the surface of Greenland (Figure 2-1). The ice-free area, found mainly along the coast, covers approximately 410,000 km<sup>2</sup> (Statistics Greenland 2008).

The Kangerlussuaq region is the part of southwestern Greenland where the distance from the coast to the ice sheet is the largest (Figure 2-2), approximately 200 km (Funder 1989). The position far from the sea and the proximity to the ice margin influences the local climate (see Section 2.1.4). The GAP study area (see Figure 1-3 and Figure 1-4) measures approximately 200 km from east to west and 60 km from north to south. Approximately 70% of the study area is covered by the GrIS. There are a large number of proglacial lakes in the ice-free part of the study area (Figure 2-3).

The Kangerlussuaq village has a population of approximately 500 people and is centred on the *Kangerlussuaq International Airport* (SFJ), which is the largest civilian airport in Greenland. In Greenlandic terms it is an easily accessible area, which in combination with the access to the *Kangerlussuaq International Science Support centre* (KISS) and the gravel road leading up to the ice sheet and Point 660, forming an easy access point to the ice sheet (Figure 2-3), makes the area an international research hub.

#### 2.1.1 Landscape

The landscape in the Kangerlussuaq area is typical of central west Greenland, which is a fiord landscape with numerous long (typically around 25 km), narrow and up to 600 m deep fiords that terminate in U-shaped valleys. Some of these valleys contain an outlet glacier and terraces, whereas others are partially filled with terraces of glaciofluvial and marine sediments (Ten Brink 1975). The latter is true for the valley where Kangerlussuaq is located. The Kangerlussuaq fiord is approximately 170 km long and 1 to 6 km wide, and receives the majority of the meltwater discharge from the large area south of the Russell Glacier, whereas the majority of the meltwater from the terminus of Isunnguata Sermia is transported via Kugssup Alangua (Figure 2-3) to the Sisimiut Isortuat fiord, north of Kangerlussuaq.

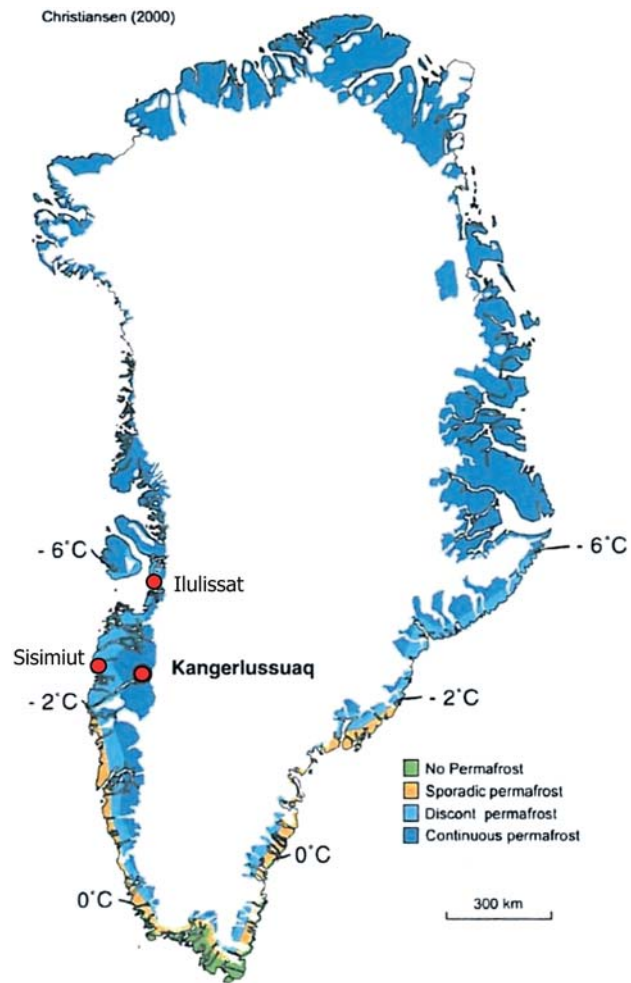


**Figure 2-1.** Location of the Kangerlussuaq, Ilulissat and Sisimiut villages, the extent of the ice sheet and the permafrost distribution (from Christiansen and Humlum 2000, in Jørgensen and Andreasen 2007). Permafrost does not apply to the ice sheet area (white area). Temperature indications show average mean annual ground temperature (MAGT). Figure reprinted with permission from Elsevier.

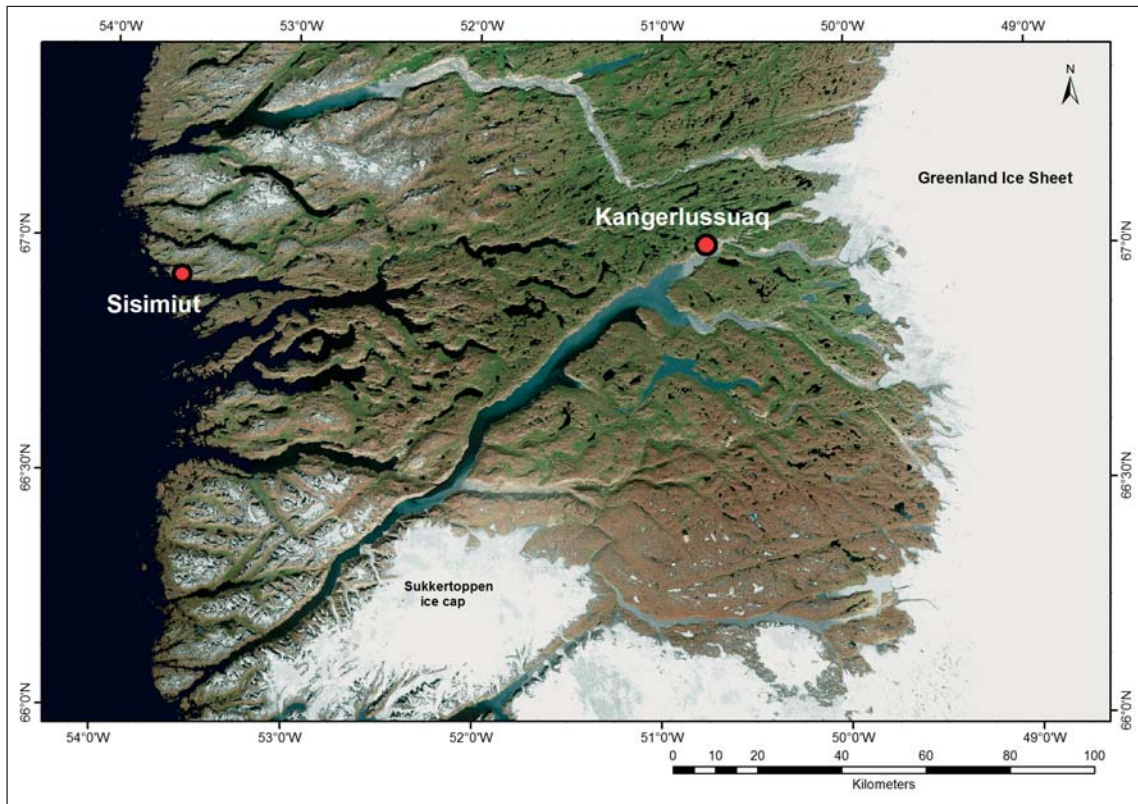


**Figure 2-2.** Map of the Kangerlussuaq region, including the approximately 170 km long Søndre Strømfjord/Kangerlussuaq fiord, extending from the Atlantic Ocean in the SW to Kangerlussuaq. Background image is a World Imagery esri satellite image acquired 2 October, 2014.

The proglacial area constitutes a gentle WSW-ENE trending hilly landscape, hosting numerous lakes of varying size, river valleys in the lower parts, abundant bare bedrock and sparse vegetation cover (Figure 2-3 and Figure 2-4). Two valleys running roughly east-west extend from the end of the Kangerlussuaq fiord to the ice sheet, i.e. Sandflugtdalen (which translates to Sand drift valley) and Ørkendalen (which translates to Desert Valley), and merge 3 km east of Kangerlussuaq (Figure 2-3).

The rivers are often frozen from October/November until April/May. Maximum discharge occurs from June to August. Abrupt drainage of ice dammed lakes occurs frequently in the area. The timing of these outburst floods, often at the end of the runoff season, is attributed to a sudden reduction of subglacial water pressure, caused by the annual reduction in meltwater production, which facilitates inflow of lake water to the glacier plumbing system (Russel 2009, Russell et al. 1990, 2011, Mikkelsen et al. 2013).

### 2.1.2 Topography and Quaternary Geology

The relief in the Kangerlussuaq region is typically a few tens of metres and some peaks reach 200–300 m above the lowest stream valley, but the total elevation range is from 0 m a. s. l. (at the Watson river in Kangerlussuaq) to 600 m a.s.l. (close to the ice margin). The same kind of highly variable relief observed in front of the ice sheet also exists under the ice sheet. In places, the bed beneath the ice sheet reaches hundreds of metres below sea level (Lindbäck et al. 2014, Lindbäck and Pettersson 2015).

Bedrock surfaces are often striated and erratics are common in the area. Fresh bedrock faces with striations are typical of surfaces that have been exposed for only a relatively short period of time (a few thousands of years). Periglacial features, such as patterned ground, hummocks and ice-wedges, as well as erratics with honeycomb weathering and loess characteristics, are observed in lowlands (Aaltonen et al. 2010). Valley floors and bedrock depressions are typically filled with till. Till cover on elevated areas is usually rather thin and heavily eroded by wind, or absent. Due to the arid conditions, and the supply of fine-grained sediments, various types of eolian deposits are widespread in the area (Willemsen et al. 2003).

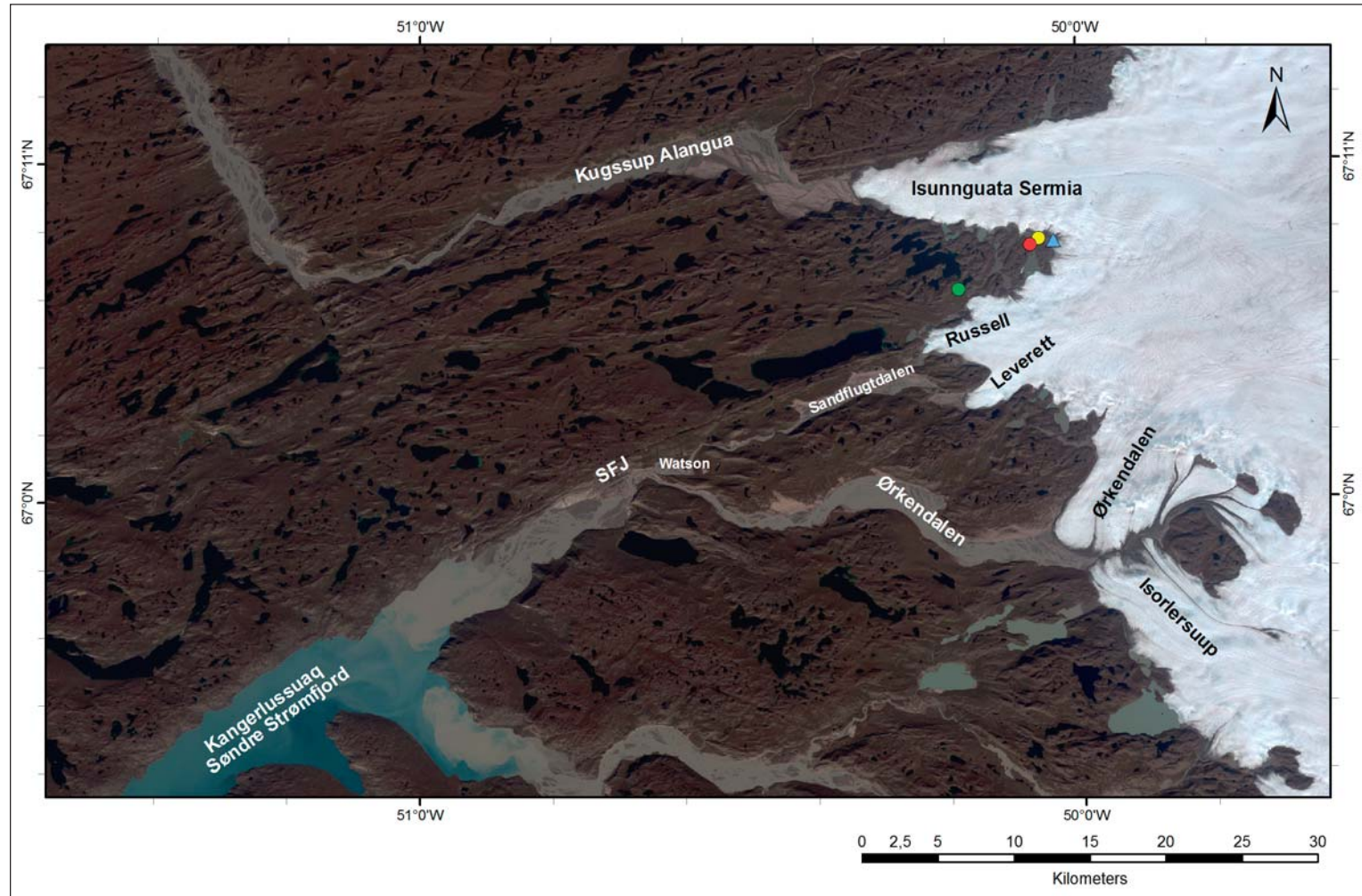


**Figure 2-3.** Map of the ice marginal and proglacial areas, including the many proglacial lakes. Light grey coloured lakes are glacial meltwater lakes, dark blue lakes are lakes without inflow of glacial meltwater. The northernmost tip of the approximately 170 km long Søndre Strømfjord is shown in the lower left corner. Isunnguata Sermia, Russell, Leverett, Ørkendalen and Isorlersuup form the major outlet glaciers in the area. Sandflugtdalen and Ørkendalen are the major valleys and meltwater rivers in the area. The Watson river extends from the head of the Søndre Strømfjord and up through the Sandflugtdalen to the Russell and Leverett outlet glaciers. Locations of the bedrock boreholes drilled by the GAP are indicated as coloured circles. Green circle = DH-GAP01, red circle = DH-GAP03, and yellow circle = DH-GAP04. Blue triangle shows the location of Point 660. SFJ = Kangerlussuaq International Airport. Background Landsat image was acquired 23 August, 2000.



*Figure 2-4. The rolling hills directly east of Kangerlussuaq. The river transports meltwater from the Russell and Leverett glaciers to the Kangerlussuaq fiord (Søndre Strømfjord). Photograph is from 2009 and was taken by Lillemor Claesson Liljedahl.*

Meltwaters from the Russell Glacier and the Leverett glacier drain through the two branches of the Watson River, which merge at the 2–3 km wide Sandflugtdalen floodplain, at the terminus of the Russell Glacier. The thickness of the glaciolacustrine and glaciofluvial deposits in this valley is up to 80 m (Storms et al. 2012). Southwest from the Sandflugtdalen, the valley narrows resulting in thinner deposits. Close to the Kangerlussuaq village, the sediments are typically 30 m thick. The head of the Søndre Strømfjord is filled with terraces of glaciofluvial and marine sediments of Holocene age (Storms et al. 2012).

The highest marine limit (based on the elevation of marine clays terraces) is located at an elevation of  $40 \pm 5$  m a.s.l. (Ten Brink 1974). However, since marine clays do not necessarily refer to a palaeo coastline elevation, this is considered a minimum value on the highest marine limit (Storms et al. 2012). The vertical displacement rate of the bedrock during Neoglacial time (i.e. the last 4,000 years of the Holocene) has varied between 20 mm/a (Weidick 1993, 1996) and  $-5.8$  mm/a (Wahr et al. 2001). The vertical subsidence displacement is attributed to the Neoglacial re-advance of the ice sheet during the past 3,000–4,000 years (Tarasov and Peltier 2002, Dietrich et al. 2005). Dietrich et al. (2005) report a current subsidence rate of  $-3.1$  mm/a for Kangerlussuaq.

### **2.1.3 Geological setting**

Greenland is dominated by crystalline rocks of the Precambrian shield, where the oldest areas constitute a basement shield composed of strongly folded gneissic rocks representing the root zone of Archean (3,800–2,550 Ma old) and Proterozoic (2,000–1,750 Ma) fold belts (orogenic belts). These belts are now welded together to form a stable coherent block surrounded by sedimentary basins formed in the Proterozoic, the Cambrian-Silurian period and the Devonian-Neogene period (Funder 1989, Henriksen et al. 2000). The Kangerlussuaq area is located in the Precambrian region of west Greenland (Henriksen et al. 2000), where bedrock is dominated by gneisses (Figure 2-5). The area is situated within the southern part of the Nagssugtoqidian Orogen, which consists of an approximately 1,900 to 1,800 Ma old fold belt that formed in a collision zone between two parts of a previously rifted large Archaean continent. The rocks in the Nagssugtoqidian Orogen are predominantly Archean

ortho-gneisses, with minor amounts of amphibolite and metasedimentary rocks that were reworked under high-grade metamorphic conditions in the Palaeo-proterozoic (van Gool et al. 2002, Garde and Hollis 2010). In addition, occasional intrusions of mafic dykes occur across the study area (Mayborn and Leshner 2006). The primary structures reflect the ductile to semi-ductile nature of the regional deformation, including macroscale folds, a penetrative gneissic fabric and evidence of shearing. The more brittle structures, such as open faults and fractures, are regarded as having been formed in a younger shallow, colder and, hence, more rigid environment.

According to regional lineament studies by Wilson et al. (2006), which focused on the on-shore expression of continental break-up and sea-floor spreading in central West Greenland, five main lineament systems were identified: N–S, NNE–SSW, ENE–WSW, ESE–WNW and NNW–SSE. Based on lineament interpretation and field observations in the GAP study area, over a hundred major deformation zones/large lineaments were identified (Engström et al. 2012). Apart from confirming the five systems identified by Wilson et al. (2006), a sixth sub-horizontal system was identified in the study area (Engström et al. 2012).

#### 2.1.4 Climate, permafrost and the 'Talík lake' study area

The present-day climate in the GAP study area is considered low Arctic continental, with continuous permafrost (Willemse et al. 2003). The region is characterised by a steep climate gradient from the coast to the inland, with mild winters and cool summers with varying weather in the coastal zone and warmer, stable summers but colder winters in the inland zone. The GrIS, reaching an elevation of 3,000 m a.s.l., has a dominant influence on precipitation and winds (Jørgensen and Andreasen 2007).

The *Danish Meteorological Institute* (DMI) operates a weather station in Kangerlussuaq. Figure 2-6 shows the mean monthly air temperatures from this station for the period 1961–2013 (Cappelen et al. 2001, Cappelen 2012). For detailed temperature information see Appendix B. The *mean annual air temperatures* (MAAT) at the Kangerlussuaq International Airport average  $-5.1^{\circ}\text{C}$ , ranging from  $-9.1$  to  $-0.3^{\circ}\text{C}$  (temperature record spanning 1977–2011, Cappelen 2012), whereas the *mean annual ground temperature* (MAGT) close to the airport is approximately  $-2^{\circ}\text{C}$  at 1.25 m below ground surface (van Tatenhove and Olesen 1994). Closer to the ice sheet margin, at the DH-GAP01 drill site (Figure 2-3) by the 'Talík lake' (see below), the MAGT for the years 2010–2013 was measured to be  $-3.0^{\circ}\text{C}$  at 1.25 m depth and  $-2.8^{\circ}\text{C}$  at 0.25 m depth (Johansson et al. 2015a). The MAAT for the same location and period was  $-4.2^{\circ}\text{C}$ . Sub-zero air temperatures typically prevail at Kangerlussuaq between October to May, with winter temperatures down to  $-40^{\circ}\text{C}$  and summer temperatures up to  $20^{\circ}\text{C}$ .

Although the weather naturally fluctuates from year to year, the GAP was carried out during a period with significantly warmer temperatures than during the 1961–1990 period (Figure 2-6). The 1961–1990 period is considered to represent a period during which the GrIS was in approximate mass balance (e.g. van Angelen et al. 2012). A clear negative precipitation gradient is present from the coast to the inland. At Sisimiut, situated by the coast (Figure 2-1), the annual mean precipitation is 383 mm (long term normal 1961–1990). The corresponding value at Kangerlussuaq, approximately 170 km from the coast, (DMI weather station) is 173 mm (measured 1977–2011), i.e. a desert-like annual precipitation (Cappelen 2012). At Kangerlussuaq, 40% of the annual precipitation falls as snow and 60% as rain. Mean surface wind speeds are low (less than 5 m/s) in the ice-free regions of the GAP study area. Winds are dominantly easterly at ground level, an effect of thermally-induced katabatic winds and airflow channelling in the valleys (van den Broeke and Gallée 1996). The vegetation near the ice sheet margin consists of dwarf-shrub tundra and steppe, with fell fields present throughout the region (Willemse et al. 2003).

Kangerlussuaq is located in the southern part of the continuous permafrost zone (Brown et al. 1997). Based on the MAAT and MAGT, permafrost at the Kangerlussuaq airport was previously modelled to be 100–160 m thick (van Tatenhove and Olesen 1994). Close to the ice margin and at higher elevations, such as at the GAP bedrock borehole sites, the permafrost thickness reaches approximately 350–400 m (see Section 2.4.5 and Data Report 2016). It is likely that permafrost exists some distance in under the ice sheet; however, no data are currently available to indicate how far it extends. The active layer in the area between Kangerlussuaq and the ice sheet margin has a thickness of 0.15 to 5 m (van Tatenhove and Olesen 1994). Areas with sandy inorganic soils and discontinuous vegetation, such as at the Talík lake (see text below), tend to have warmer soil temperatures and a deeper active layer than organic soils covered with dense vegetation (van Tatenhove and Olesen 1994). Periglacial features such as pingos and ice-wedges are found in the area (e.g. Scholz and Baumann 1997).

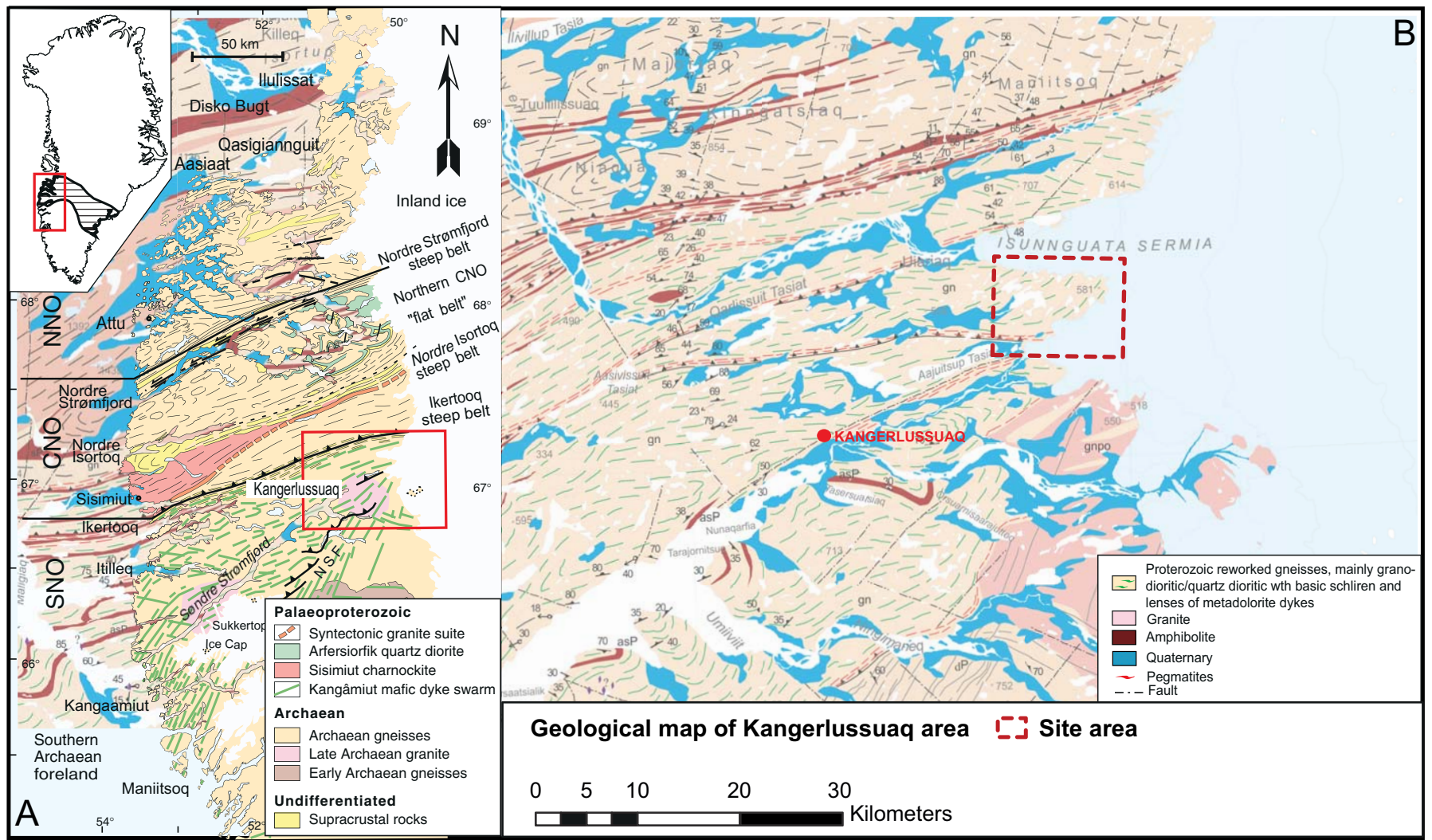
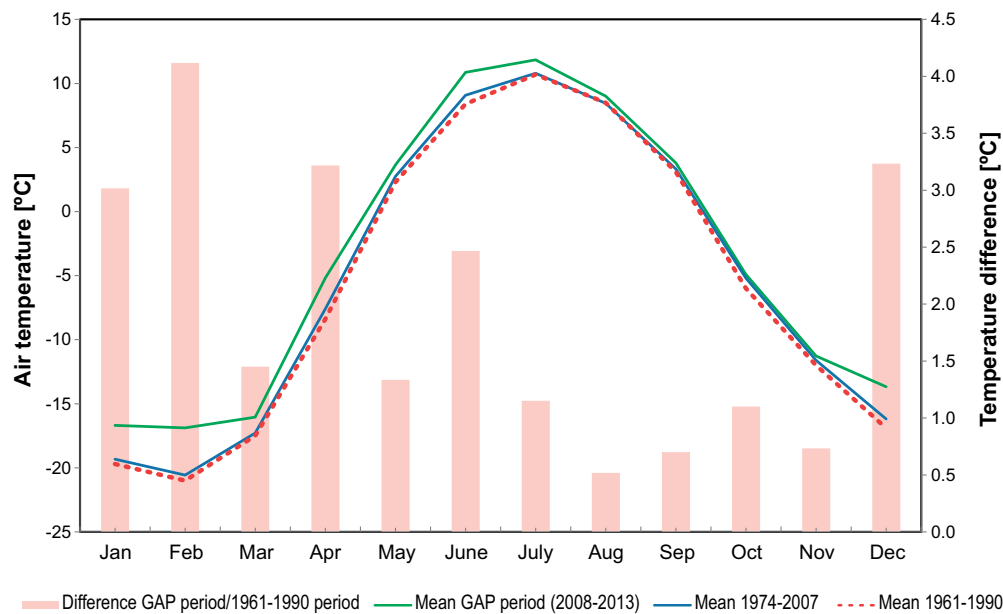


Figure 2-5. A) Geological map showing the area between the GrIS and the Atlantic Ocean, and B) the regional site domain. The red dashed rectangle denotes the area where the GAP carried out geologic mapping. (Map modified from Garde and Marker 2010, and Garde and Hollis 2010).



**Figure 2-6.** Monthly mean air temperatures from the DMI weather station in Kangerlussuaq for the periods 1961–1990, 1974–2007 and the GAP period 2008–2013. The 1961–1990 period is considered to represent a period during which the GrIS was in approximate mass balance (e.g. van Angelen et al. 2012). The temperature difference between the GAP period and the 1961–1990 period is shown as coloured bars.

Permafrost has a great impact on the hydrological cycle (White et al. 2007). Due to the fact that extensive permafrost acts as a largely impermeable layer, groundwater recharge and discharge are reduced, and, in areas with continuous permafrost, groundwater recharge and discharge are restricted to taliks, i.e. unfrozen zones in the permafrost (e.g. Kane et al. 2013, Bosson et al. 2012). Taliks are assumed to be abundant in the GAP study area and occur beneath large lakes, rivers and fiords. Through taliks, i.e. taliks extending through the entire thickness of the permafrost, are hypothesised to provide exchange of deep and shallow groundwater, a process that has been investigated and observed within the GAP and the *Greenland Analogue Surface Project GRASP*, which is an SKB-funded project focusing on hydrology and ecosystem issues (Johansson et al. 2015a, b).

Thermal modelling to evaluate the required size of a water body to retain a through talik was undertaken using circular lakes (SKB 2010a). The results from this simplified study showed that a lake radius of 0.6 times the thickness of the surrounding undisturbed permafrost is sufficient for a deep lake to maintain a through talik. Tentative thermal modelling of the so-called ‘Talik lake’ (see below) in the GAP study area has shown that through taliks can form through a 300 m deep layer of permafrost in less than 500 years, if the lake is wider than about 200 m. Open taliks (i.e. open to surface but confined by frozen ground at depth) can form in less than 100 years beneath lakes that are about 100 m wide (Harper et al. 2011, Data Report 2016). Considering an approximate permafrost depth of approximately 300 to 350 m (see Section 2.4.5) in the GAP study area, a lake diameter of approximately 360–420 m is required to maintain through taliks. The GAP study area encompasses several hundreds of proglacial lakes (Figure 2-3). About 20% of these lakes (6% of the land surface area) have a diameter larger than 400 m (Figure 2-7), which suggests that the permafrost in this area is perforated by through taliks, and flow pathways available for exchange of surface water and deep groundwater through the permafrost are abundant.

### The ‘Talik lake’ area

The ‘Talik lake’, which refers to a specific lake/talik system in the proglacial part of the GAP study area (Figure 2-3 and Figure 2-8) was investigated as part of the GAP (SKB 2010b, Harper et al. 2011, Data Report 2016). The lake, with a lake surface elevation of 369 m, is situated approximately 800 m from the ice sheet margin, has a surface area of 0.37 km<sup>2</sup> and a catchment area of 1.56 km<sup>2</sup>. The average and maximum lake water depths are 11.3 m and 29.9 m, respectively (Johansson et al. 2015a). The

lake is situated in an area characterised by continuous permafrost, but results from the GAP project have shown that the lake most likely supports a through talik (Data Report 2016, Harper et al. 2011). Borehole DH-GAP01 is located beside the lake at approximately 20 m distance from the lake shoreline. The borehole is angled and is dipping beneath the lake. Temperature profiling in borehole DH-GAP01, shows that the upper approximately 20 m of the borehole is within permafrost and that unfrozen soil/bedrock conditions exists under the lake, which allows for hydraulic contact between the lake and the deep groundwater system below the permafrost (Harper et al. 2011).

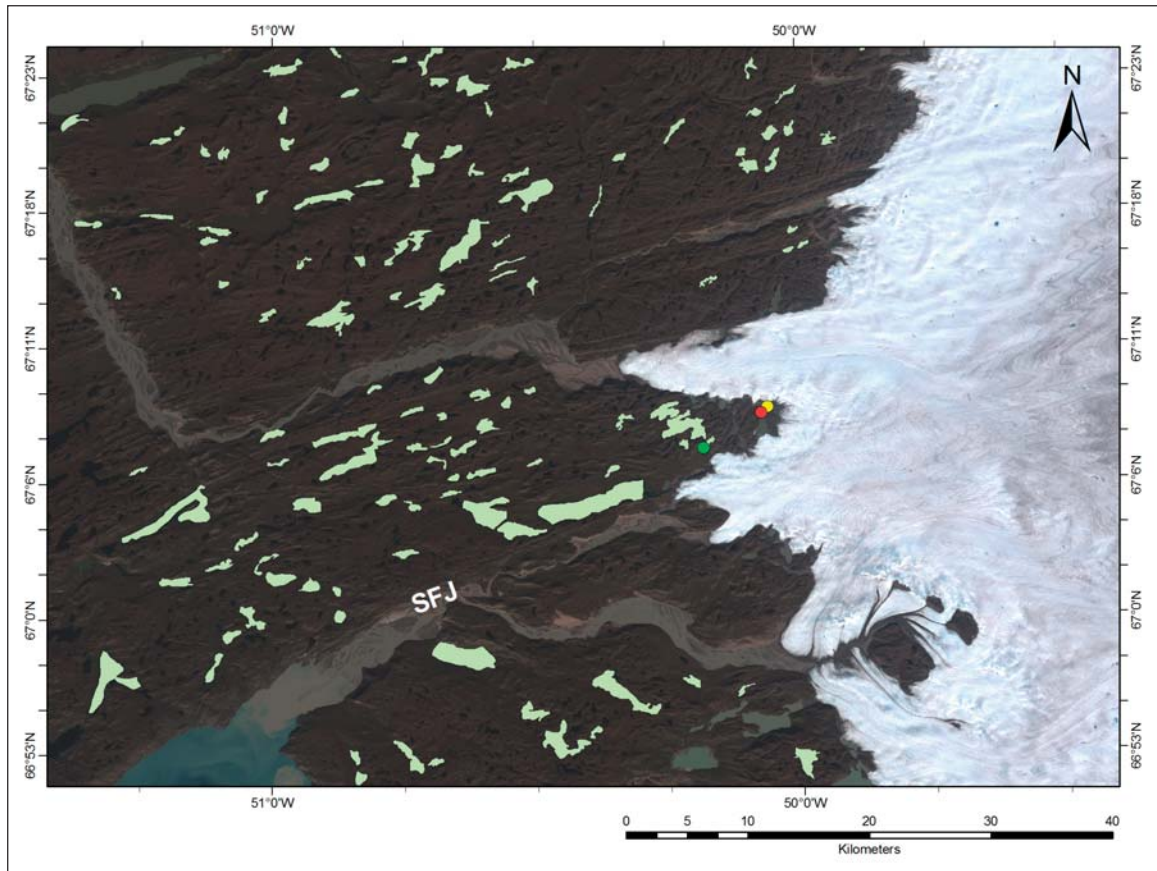


**Figure 2-7.** Map of the proglacial region of the GAP study area where lakes with a diameter  $\geq 400$  m, and thus may host through taliks, are shown in light green. Bedrock boreholes are shown as coloured circles. Green circle = DH-GAP01, red circle = DH-GAP03, yellow circle = DH-GAP04. SFJ = Kangerlussuaq International Airport. Background Landsat image was acquired 23 August, 2000.



**Figure 2-8.** The 'Talik lake' and the location of borehole DH-GAP01 (green dot). Location of the lake and the borehole is shown in Figure 2-3 and 2-7. Photograph is from 2012 and was taken by Tobias Lindborg.

Johansson et al. (2015a) summarise the Talik lake catchment characteristics as follows: The catchment area is dominated by glacial till and glaciofluvial deposits which to a large part are overlain by a layer of eolian silt to fine sand. The total depth of eolian sediments and glacial deposits ranges from 7–12 m in the valleys to zero along the hill sides. In the lake, a sediment thickness of up to 1.5 m has been observed (Petroni et al. in review). It is assumed that the observed depth of glacial deposits in the valleys of the catchment is also present in the lake, i.e. the lake sediments are underlain by approximately 10 m of glacial till. The glacial till was deposited under the ice sheet and glaciofluvial sediments were deposited mostly in front of the ice margin during deglaciation of the area. Eolian silt to fine sand has periodically been deposited after the area was deglaciated (Willemse et al. 2003). The catchment hydrology is a precipitation-driven system, with no meltwater inflow from the ice sheet occurring over the catchment boundary. Vegetation in the catchment is dominated by dwarf-shrub heath. There are no trees, and bushes rarely exceed a height of 0.5 m. The poor vegetation results in relatively low transpiration even though the total evapotranspiration in the catchment is relatively high. The only visible stream is at the lake outlet. Due to the low precipitation in the area, the stream at the outlet of the lake is dry during long periods and the summer of 2009 was the last time, as of September 2014, that surface water outflow was observed to occur from the lake. The surface water and the groundwater divide are assumed to coincide.

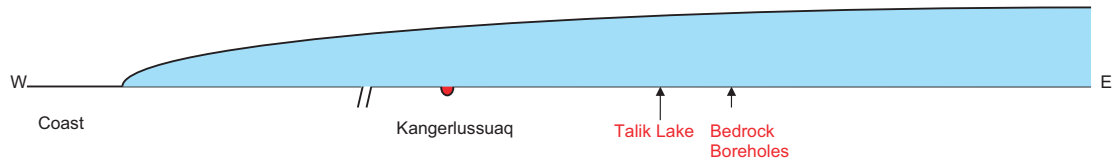
### 2.1.5 Characteristics of the GrIS in the GAP study area

The GrIS is the largest reservoir of ice in the Northern Hemisphere and marine records suggests that the GrIS has existed for millions of years. However, the timing of onset of glaciation on Greenland remains undetermined. It is believed that the Northern Hemisphere only experienced ephemeral glaciations during late Eocene to early Pliocene, and that the onset of extensive glaciations occurred around mid-Pliocene, approximately 3 Ma BP (Maslin et al. 1998, Flesche Kleiven et al. 2002, Bartoli et al. 2005). The present-day ice divide runs near the eastern ice sheet margin, so that most of the ice sheet flows towards the west. The GrIS contains approximately 11% of all fresh water on Earth, and has the potential of contributing up to 7.4 m of global mean sea level rise, if it were to entirely melt (Bamber et al. 2013, Vaughan et al. 2013). Because of the GrIS's high elevation and north-south orientation, the mean westerly atmospheric circulation is affected and as a result the GrIS impacts the climate in the entire Northern Hemisphere (Clark et al. 1999). The maximum ice thickness is 3,400 m, with an average thickness of 1,600 m (Thomas et al. 2001), and a total volume of 2.9 million km<sup>3</sup> (Bamber et al. 2001). The current ice in the ice sheet is 110,000 years old at a depth of 2,800 m (Meese et al. 1997) at the Summit location in central Greenland. The current mass balance of the GrIS is negative, and over the time period January 2011 to January 2014 the volume loss for the entire GrIS was  $-375 \pm 24$  km<sup>3</sup>/yr (Helm et al. 2014).

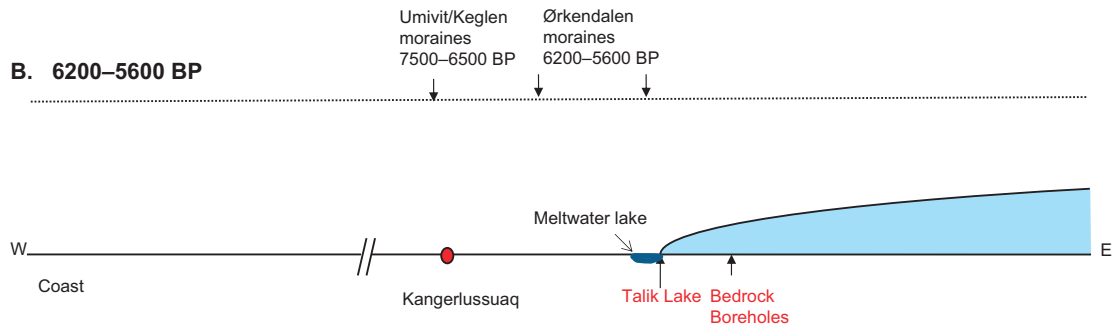
The ice sheet part of the GAP study area includes the Isunnguata Sermia, Russell, Leverett, Ørkendalen and Isorlersuup outlet glaciers and their catchment areas (see Figure 2-3). The ice thickness in the study area reaches approximately 1,500 m with a mean value of approximately 800 m, but is highly variable due to the steep and undulating subglacial topography (Lindbäck et al. 2014). The ice flow direction in the area is generally directed from east to west, with a mean surface velocity of approximately 150 m/yr (Joughin et al. 2010). The glaciated part of the GAP study area is one of the most studied regions of the GrIS including previous and parallel studies of mass balance (e.g. van de Wal et al. 2012) and ice dynamics (e.g. van de Wal et al. 2008, Bartholomew et al. 2011, Palmer et al. 2011, Sole et al. 2013). One reason for the research interest in this area is related to the fact that the land-terminating outlet glaciers here are isolated from marine influences and exhibit changes in ice dynamics that are remote from tidewater influences and are directly attributable to surface-melt forcing (Fitzpatrick et al. 2014).

The period 1961–1990 is often used as a reference to when the GrIS was considered to be in approximate steady state, whereas during the past 20 years the mass balance has turned negative (van Angelen et al. 2012). A recent strong warming over the western part of the GrIS is recorded by e.g. weather stations in the GAP study area (van As et al. 2012, van Angelen et al. 2014). The negative mass balance has resulted in a larger melt extent of the GrIS, increased surface runoff and discharge (Hanna et al. 2008, Ettema et al. 2009, Fettweis et al. 2011, van As et al. 2012).

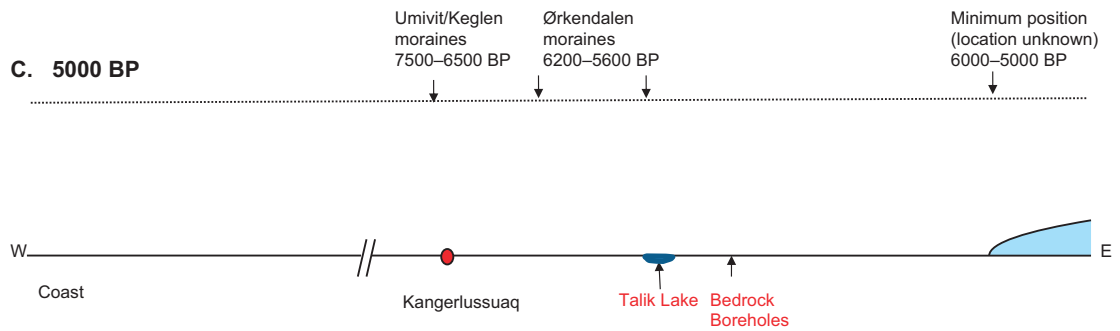
**A. 16,800–11,100 BP**



**B. 6200–5600 BP**



**C. 5000 BP**



**D. Re-advance**

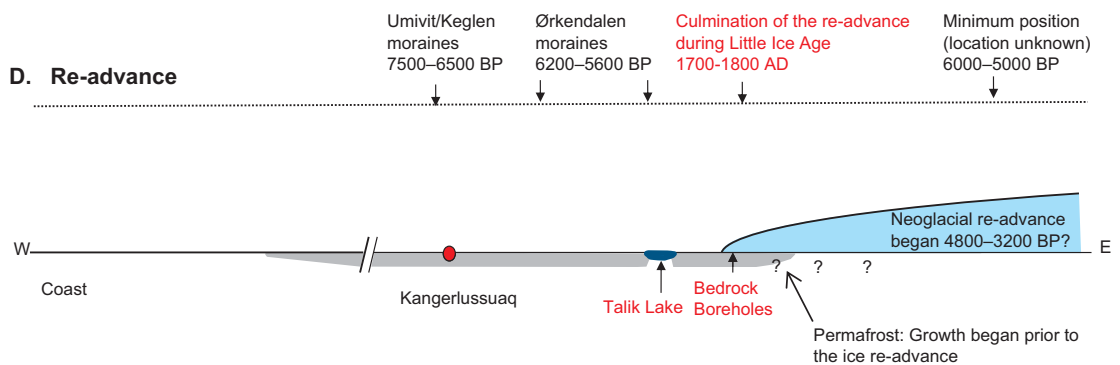


**Figure 2-9.** Cartoon showing the deglaciation history of the Kangerlussuaq area since the Last Glacial Maximum (LGM). Many of the present lakes were likely formed as soon as the area was exposed from the retreating ice sheet. These lakes were first filled with meltwaters and later turned into non-glacial lakes, implying that the growth of permafrost was prevented under these lakes when the climate started to cool during the neoglacial re-advance. Moraine ages are presented as <sup>14</sup>C BP and are from van Tatenhove et al. (1996).

### 2.1.6 Deglaciation history of southern West Greenland

The average long term climate conditions (glacial-, periglacial-, or temperate climate) that have prevailed at the GAP bedrock drill sites are of interest for e.g. geochemical-, geothermal- and permafrost analyses. A rough estimate of the average conditions at the GAP site was made by employing a glacial history perspective. The present configuration of the GrIS is to a major extent a result of the warm Holocene interglacial climate conditions (Figure 2-9). During glacial periods, the ice sheet is typically significantly larger. For the past millions of years, glacial conditions have dominated Earth's climate (e.g. Lisiecki and Raymo 2005). In Northern Hemisphere high- to mid-latitudes, this has resulted in larger ice sheets than at the present-day. In e.g. Fennoscandia, the typical ice sheet distribution for at least the past 1 Ma therefore contained significantly more ice than the present, very restricted, mountain glaciation (Porter 1989, Kleman et al. 2008). Also, it is likely that the average configuration of the GrIS has been larger than the present one for the past million years, since this was the case for both the Fennoscandian and Laurentide ice sheets at similar latitude (Porter 1989).

Given that the GAP boreholes are located at the very margin of the present-day ice sheet configuration, it is thus likely that the drill sites have been dominated by ice-covered conditions, on average, for the past 1 Ma. During the relatively shorter interstadial and interglacial periods, the drill sites could either have experienced periglacial climate conditions (i.e. with presence of permafrost) or temperate climate conditions (here defined as a warm climate without presence of permafrost or an ice sheet), but on average for the whole 1 Ma period, glacial conditions most probably have dominated.

During the *Last Glacial Maximum* (LGM), the GrIS was considerably more extensive than at present and the ice sheet margin extended offshore, at least onto the continental shelf (Funder 1989, Bennike and Björk 2002). By the beginning of the Holocene, the ice margin had retreated towards the east to a position close to the modern coast line (Funder and Hansen 1996). Subsequently due to increasing air temperatures, and low annual precipitation (Anderson and Leng 2004, Aebly and Fritz 2009), the ice margin started to retreat, which resulted in a series of regional moraine systems being formed during temporary halts in the retreat. These moraine systems have been mapped and dated by Ten Brink and Weidick (1974), van Tatenhove et al. (1996), Forman et al. (2007) and Levy et al. (2012). Deglaciation of the present-day coastal area in southern West Greenland started around 12,300 years BP, and most of the ice sheet margin reached its present position between 6,500 and 7,000 years BP (Ten Brink and Weidick 1974, van Tatenhove et al. 1996). The retreat was fast and, at approximately 6,000 years BP, the ice margin was behind the present position and remained there until the *Little Ice Age* (LIA) re-advance (van Tatenhove et al. 1996, Forman et al. 2007). It is assumed that the minimum position was reached by 5,000 years BP (Weidick 1993). Neoglacial re-advance may have started as early as 4,800 years BP and culminated about 2,000 years BP (van Tatenhove et al. 1996, Forman et al. 2007). The climate then started to warm and, around 1,000 years BP, it was warmer than at present. The ice sheet advanced again during the LIA, when the ice margin of western Greenland was approximately 1–2 km west from its current position (Csatho et al. 2005). The Isunnguata Sermian edge of the ice margin was only 50–200 m beyond its present margin (Forman et al. 2007). The maximum position was reached around 1850 AD. Forman et al. (2007) reported that the ice sheet has retreated to its present position over the past 100 years. Thinning of the ice sheet at elevations below 1,500 m a.s.l. has accompanied this retreat (Krabill et al. 2000, Johannessen et al. 2005). Based on current understanding, neither of the GAP bedrock borehole drilling sites (see Section 2.4) were ice-covered during the LIA (cf. Forman et al. 2007).

## 2.2 Surface based ice sheet investigations

This section presents a summary of the investigations carried out on the ice sheet by the GAP during 2008–2013 to address two of the GAP project questions: 1) *Where is the meltwater generated under an ice sheet?*, and 2) *What is the hydraulic pressure situation under an ice sheet, driving groundwater flow?* Figure 1-4 shows where the different ice sheet investigations were carried out. A summary of the remote sensing, the automatic weather station network, GPS monitoring, radar surveys and seismic studies, focussing on why these studies were carried out, is given in the subsections below. A detailed presentation of the results of these field investigations, remote sensing, numerical modelling and the available datasets, are provided in the Data Report (2016). The **'key outputs'** are presented in this section under each type of investigation, while the key results from the surface based ice sheet investigations relating to the GAP questions are discussed in Sections 3.1, 4.1, 4.2 and in the conceptualisation in Chapter 5.

### 2.2.1 Remote sensing

Remote sensing can be used to establish good spatial coverage of surface boundary conditions of the ice sheet that can further be used to direct/target detailed field-based research and to provide specific inputs such as supraglacial lake (SGL) water fluxes to the bed, surface flow distributions, and surface elevation changes for other analyses and modelling within the project. Remotely sensed data collected within the GAP have been used to determine the fluxes of surface meltwater to the bed of the ice sheet and the extent to which catchment-wide spatial and temporal variations in glacier velocity are linked to these changes, reflecting the basal boundary condition of the ice sheet. A considerable archive of remotely sensed data was assembled to meet the project aims, utilizing data from satellite and aerial platforms using optical and radar sensors. The remote sensing studies involved the following focus areas on the GrIS in the GAP study area; a) SGLs drainage events, b) structural mapping of the ice sheet surface to look at spatial patterns and their potential coupling to subglacial hydrological pathways, c) ice velocity mapping to investigate its spatial and temporal variability, and d) generation of high-resolution *Digital Elevation Models* (DEMs) to investigate thinning rates.

#### Key outputs

The storage and drainage of approximately 200 seasonally occurring SGLs across the GAP study area were quantified (Fitzpatrick et al. 2014). Although the SGLs in the study area occupy a relatively small portion of the catchment (2%), they store a disproportionate volume of bulk runoff (13%) of annual surface meltwater production and have important implications for the ice dynamics through the release of surface meltwater into the subglacial hydrological system via rapid *in situ* drainage or through overflow into moulins (Fitzpatrick et al. 2014).

Structural mapping reveals that patterns of foliation on the ice surface are longitudinally extended in areas of faster ice flow corresponding to the location of subglacial troughs, suggesting that the spatial patterns of faster ice flow can be attributed to surface and bed slope acting in unison to determine subglacial hydrological pathways.

Spatial and temporal variations in ice velocity are complex. Although they are influenced by the amount of water that is routed from the surface to the base of the ice sheet and the rate of flow of that water from the surface to the base, other factors, such as bedrock topography, are of importance and need to be taken into account (Fitzpatrick et al. 2013).

### 2.2.2 Automatic weather station network

Determining the availability of meltwater in the supra-, en- and subglacial systems was one of the goals of the GAP. Most meltwater originates at the surface of the ice sheet, where ice melt is caused by energy received from the sun and atmosphere. Net mass input by snow accumulation in higher regions occurs and compensates for the melting at low elevations. Cooling climates reduce the rate of surface melting, and warming climates, such as Greenland is presently experiencing, enhance the rate of surface meltwater production. Water is also generated at the bed from melting of ice due to heat energy supplied from geothermal sources, friction from the ice mass sliding over its bed, and internal deformation of the ice.

To determine the surface meltwater production in the study area, GAP chose a common observation-based method, which involves *automatic weather stations* (AWS) placed on the ice sheet and used to quantify the energy exchange at snow and ice surfaces. So-called *surface energy balance models* (SMB) use the AWS observations to calculate the separate heat sources and sinks, not only providing an accurate melt estimate, but also offering the possibility to investigate the relative contributions of heat sources and changes therein in a warming climate. Three AWS (KAN\_L, KAN\_M and KAN\_U) were installed in the Kangerlussuaq sector of the GrIS in September 2008 and April 2009 (Figure 2-10 and Table 2-1). The GAP AWS adds to the K-transect (stations S5, S6 and S9 in Figure 2-10) operated by the *Institute for Marine and Atmospheric Research in Utrecht* (IMAU), and makes this a well-instrumented part of the GrIS, allowing investigation of factors influencing SMB and meltwater runoff. The 21 year-mean *mass balance equilibrium line altitude* (ELA) is in this region at an altitude of approximately 1,600 m a.s.l. (van de Wal et al. 2012); thus KAN\_L is placed in the lower ablation zone<sup>1</sup>, KAN\_M is in the upper ablation zone and KAN\_U is placed well into the accumulation zone.

---

<sup>1</sup> Ablation zone is the area of the ice sheet where mass losses exceed mass gains. As a result, this area has bare ice (no snow) exposed during the summer months.

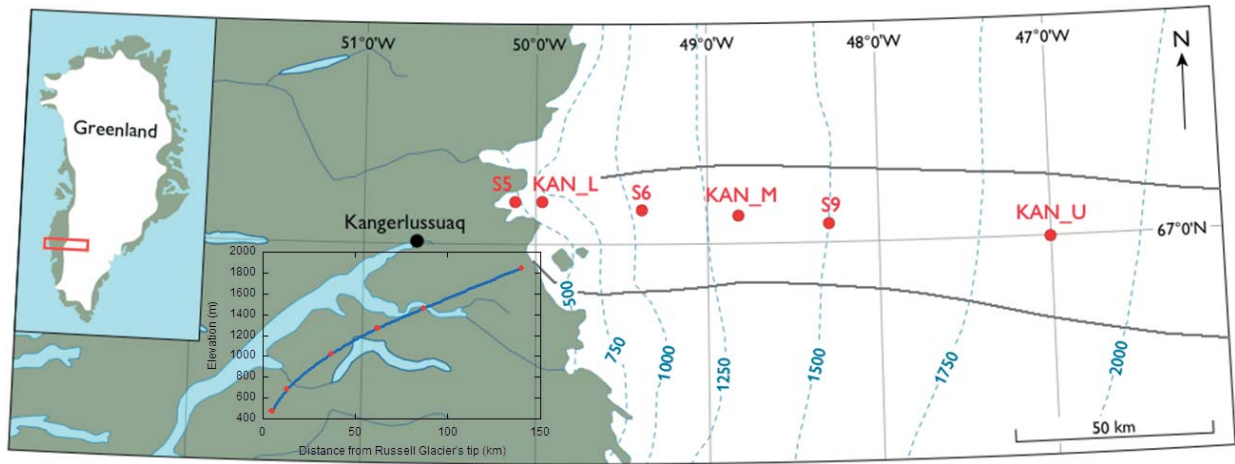


**Figure 2-10.** Map of southwest Greenland including the positions of the GAP (KAN\_L, KAN\_M and KAN\_U) and the Institute for Marine and Atmospheric research Utrecht/IMAU automatic weather stations (S5, S6 and S9 stations belonging to the K-transect, described in e.g. van de Wal et al. 2012) and catchment delineation (grey lines). Blue dashed lines represent elevation contours. The mass balance equilibrium line in this region is situated at an altitude of approximately 1,600 m a.s.l. (van de Wal et al. 2012).

**Table 2-1. Locations and deployment dates of the GAP AWS.**

Station name	Latitude (°N)	Longitude (°W)	(WGS-84) (m)	Deployment date
KAN_L	67.097	49.933	710	1 Sep 2008
KAN_M	67.066	48.818	1,310	2 Sep 2008
KAN_U	67.000	47.017	1,880	4 Apr 2009

### Key output

The SMB results (see Figure 3-5 in Section 3.1.2) show that nearly all melt in the GAP study area takes place during the three summer months. Interannual variability is large though, both in length of the melt season and the melt intensity. Most of the meltwater ran off the ice sheet during the four year monitoring period, implying that only a smaller portion refroze in snow and firn. Refreezing increases with increasing elevation.

### 2.2.3 GPS measurements of ice motion

Observations of surface ice motion provide an indirect method for investigating the role of water at the ice sheet's basal interface. Pressurised subglacial water causes hydraulic ice-bed separation and can enhance basal sliding by reducing bed friction. The resulting rapid, transient accelerations and vertical displacement events that occur during the summer period with surface melting are detectable using geodetic-quality *Global Positioning System* (GPS) receivers. Measurements of ice motion from a network of GPS receivers deployed across the GAP study area (Figure 2-11, Data Report 2016) may constrain when water accesses the bed and how basal water pressure and ice motion respond to it. The GAP GPS datasets have allowed detailed studies of the seasonal and diurnal velocity cycles, supraglacial lake drainage events, rainfall events and influence of moulins on drainage and on the basal hydrology of the ice sheet (e.g. Doyle et al. 2013, 2014). It should be noted that velocity changes may or may not indicate basal pressure changes (e.g. Fountain and Walder 1998, Jansson and Näslund 2009).

### Key outputs

The seasonal velocity cycle of ice motion in the GAP study area is characterised by an initial maximum at melt onset (the so called 'spring event') followed by a gradual decline to an all year minimum in the autumn.

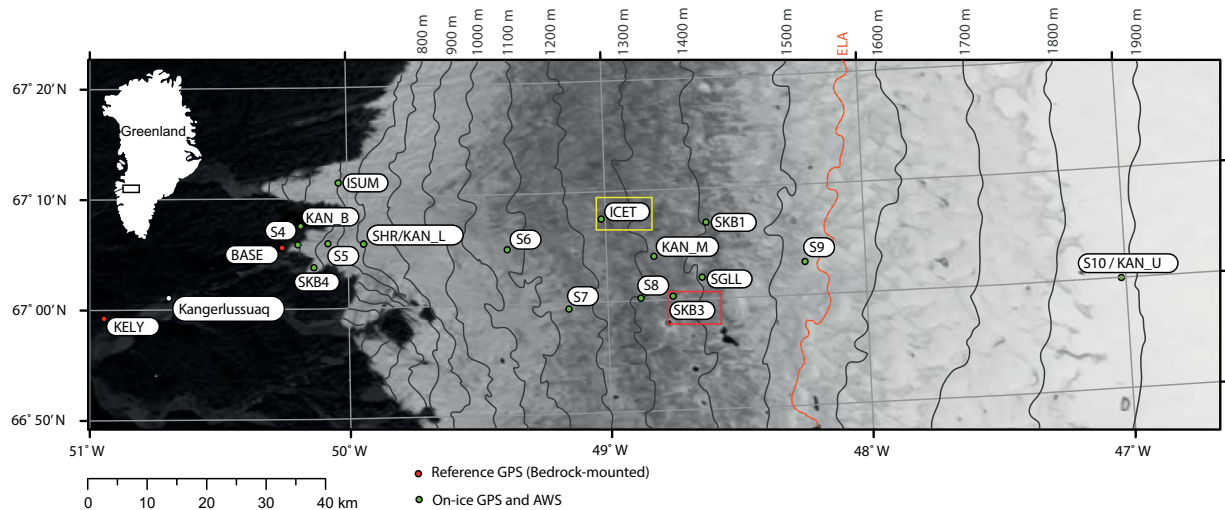


**Figure 2-11.** Map of the GAP GPS network showing the locations of a) GPS receivers, b) K-transect sites (S4, S5, SHR, S6, S7, S8, S9 and S10, van de Wal et al. 2012), c) the GAP AWS (KAN\_B, KAN\_L, KAN\_M and KAN\_U), d) Kangerlussuaq town and airport, e) the bedrock-mounted Kellyville reference GPS (KELY) maintained by UNAVCO and f) the locations of two passive seismic experiments around a SGL (SKB3, red box) and moulin (ICET, yellow box). The twenty-one (1990–2011) year mean mass balance equilibrium line altitude (ELA) estimated by van de Wal et al. (2012) at 1,553 m a.s.l. is indicated with an orange line. The elevation contours are based on the DEM of Howat et al. (2013). The MODIS background image was acquired on 17 August, 2011.

A drainage event of a SGL was successfully captured in 2010 where the GPS stations recorded the opening and closure of the fractures through which the lake was drained, showing that SGLs rapidly can deliver large volumes of water to the ice-bed interface (Doyle et al. 2013).

Surface velocity measurements from the s10/KAN\_U GPS station high up on the ice sheet (Figure 2-11) show a year-on-year (from 2009 to 2012) increase in annual velocity well above the ELA (Doyle et al. 2014). Doyle et al. (2014) suggest that this is due to increased penetration of water to the ice-bed interface, which drives faster ice motion at high elevations on the GrIS.

## 2.2.4 Ground-penetrating radar

The objective of the ground-penetrating radar work conducted within the GAP project was to establish good spatial coverage of subglacial topography and basal thermal and hydrological conditions of the ice sheet within the GAP study area. Radar surveys also contribute to address, in different ways, the first two GAP project questions (see Section 1.2). Radar data can be used to derive potential flow paths and hydraulic potential distributions under the ice, provided that the subglacial topography and ice surface are known with accuracy. The returned power from the bed reflections in the radar data can also give an indication of the distribution of meltwater and the basal thermal boundaries. During the GAP, approximately 1,500 km of radar profiles using two ground-based impulse radar systems were collected (Figure 2-12). From this dataset, and other available datasets including the ICEbridge and Danish Technical University (DTU) datasets, DEMs of ice thickness and bed topography were obtained (Figure 2-12 and Figure 2-13) (Lindbäck et al. 2014).

### Key outputs

Figure 2-13 summarises the key results from the GAP radar investigations. The ice thickness generally increases towards the ice divide and the maximum ice depth is 1,460 m. The mean ice thickness in the area is 830 m (Lindbäck et al. 2014). The bed shows a highly variable subglacial topography resembling the landscape in front of the ice sheet. Major valleys aligning NE-SW or SE-NW directions likely follow the dominant zones of geological weakness. The deepest troughs are found under Isunnguata Sermia with an elevation of  $-510$  m below the WGS-84 ellipsoid and a difference, at that

location, of approximately 1,000 m between the valley bottom and the hills on each side. The highest subglacial peak in the area is 1,060 m above the ellipsoid. The relief of the bed topography decreases towards the ice divide, but is generally variable throughout the area.

## 2.2.5 Seismics – reflection and passive seismics

### *Reflection seismics*

The objective of the seismic reflection survey was to establish detailed spatial coverage of subglacial topography and basal sediment characteristics under the ice. Reflection seismic data were collected in July and August 2010 at four sites (PLOP, F-Lake, SHBAM and SHR) (Figure 2-14) to image the elastic properties of the ice sheet subsurface and were applied in the GAP study area to determine the geometry and characteristics of the material at the ice-bed interface. Applying *amplitude versus angle* (AVA) analysis provided further information on the material characteristics, such as sediment porosity, sediment density and spatial changes in water content.

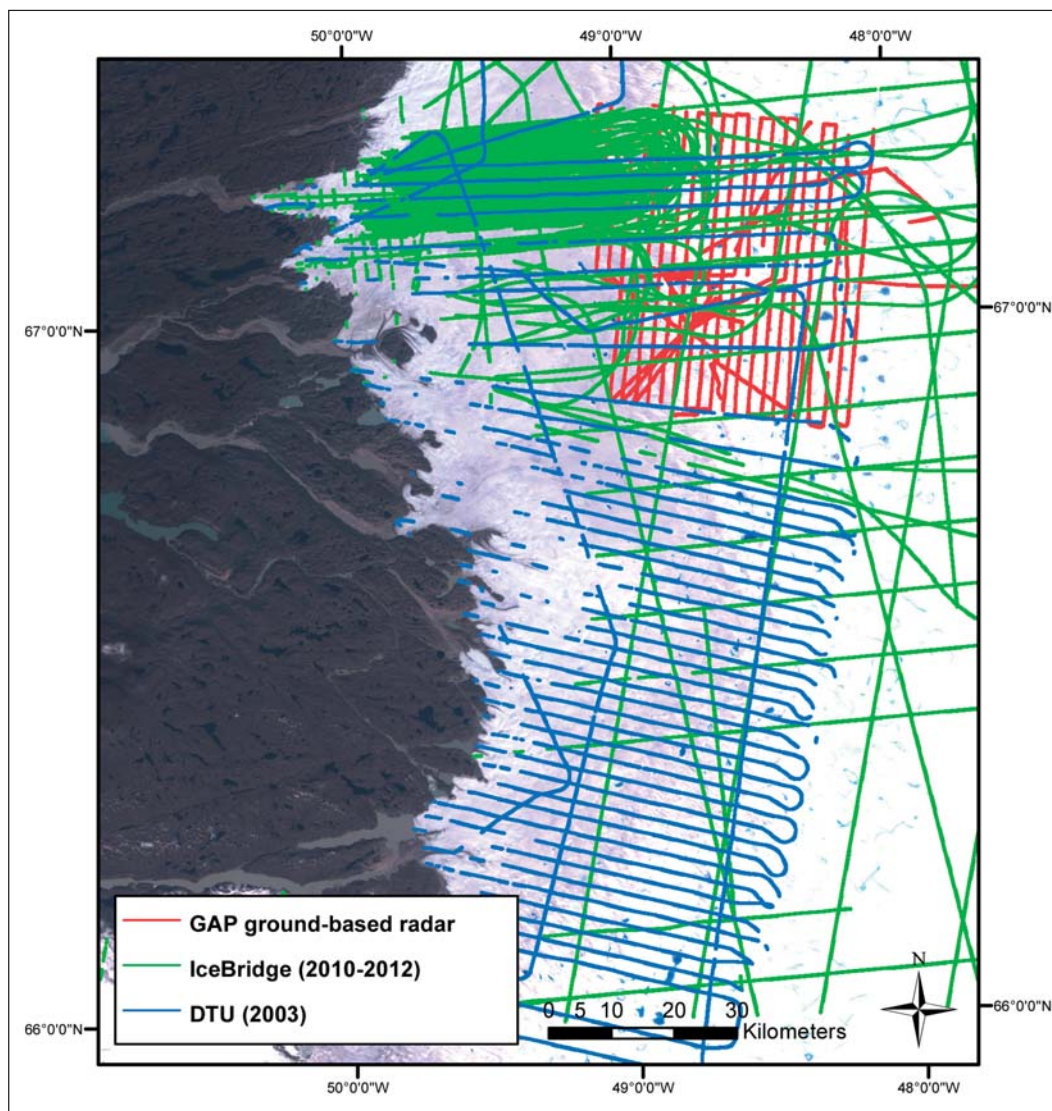


**Figure 2-12.** Available radar datasets for the GAP study area. DTU and ICEBridge data were generated by and provided to the GAP by other projects and initiatives.

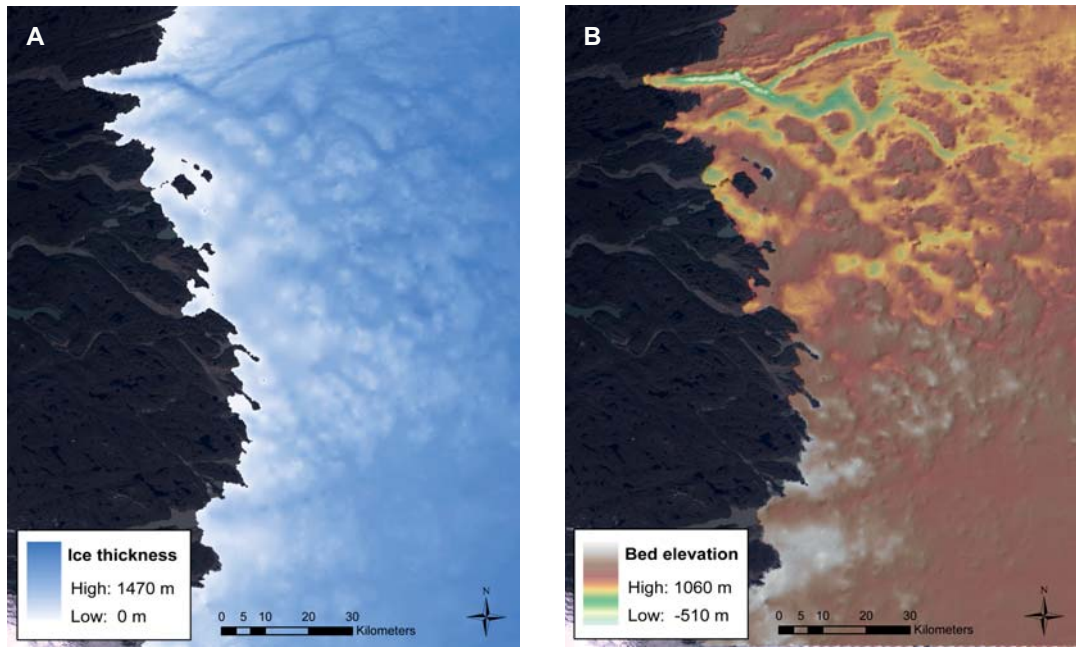


**Figure 2-13.** A) Ice thickness, and B) basal topography over part of the GAP area (in m above the WGS-84 ellipsoid). The ice thickness and basal topography maps extend further south than the GAP study area since the DTU airborne radar was available for this part of the ice sheet (Figure 2-12).

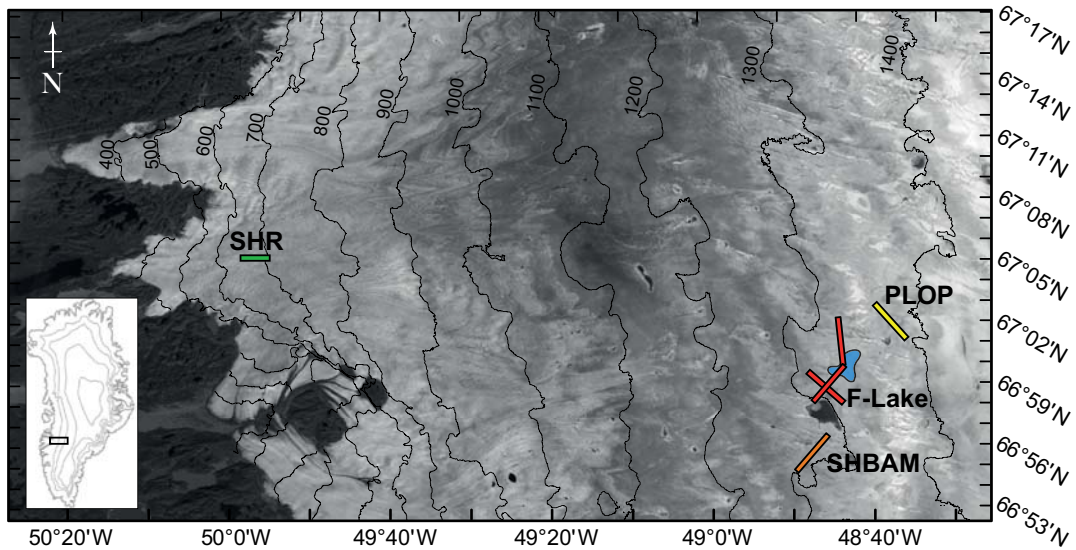


**Figure 2-14.** Landsat image from July 18, 2010 with the reflection (active) seismic lines and sites (PLOP, F-Lake, SHR and SHBAM) marked in colours.

### **Key outputs**

Reflection seismic data collected from four sites (Figure 2-14) indicate the widespread occurrence of till with varying material characteristics. Soft till is seen in basins to the south (SHBAM) and north (PLOP) of the F-lake field site with a third line near the lake (F-lake) indicating the presence of lodged till. Closer to the terminus, analysis of the SHR seismic data suggests that weak and wet (although not dilating) subglacial sediment is present in the region (Dow et al. 2013).

### **Passive seismics**

Passive seismic analysis provides a technique for ‘listening to’ and ‘triangulating on’ specific energy signatures associated with fracture material, movement and/or the flow of fluids within a medium. In this context, the objective of the passive seismic experiments conducted within the GAP project was primarily to confirm and establish linkages between surface meltwater production and its englacial transmission to the ice sheet basal interface, and secondly, to determine the subsequent destination of that water and how it impacts the ice sheet’s subglacial hydro-thermal environment. Two passive seismic experiments were conducted within the GAP (for location of experiments see Figure 2-11). In June, 2010, a SGL was instrumented with geophones prior to its drainage to determine the triggering mechanism and hydraulic pathways by which it would rapidly drain. In May, 2011, a moulin was instrumented to identify to what extent such surface to bed hydraulic connections persist and reactivate from year-to-year, i.e. remaining open over winter with no meltwater inputs, and to understand the impact of surface water on the subglacial hydraulic environment.

### **Key outputs**

Based on the acquired passive seismic data combined with lake pressure and GPS motion data (described above), a rapid lake drainage event involving ice tectonic deformation, hydrofracturing and consequent drainage of water was characterised (Doyle et al. 2013).

## **2.3 Ice drilling and direct studies of basal conditions**

This section presents a summary of the ice drilling carried out by the GAP to conduct comprehensive and direct observational research on the basal hydrological system of the GrIS. The ice drilling related studies directly contributed towards addressing the following GAP project questions: 1) *Where is the meltwater generated under an ice sheet?* and 2) *What is the hydraulic pressure situation under an ice sheet driving groundwater flow?* In addition, the results from the ice drilling studies provided direct observation of basal conditions, which is relevant to understanding ice surface conditions and groundwater/chemical conditions investigated by other parts of the GAP (see Sections 2.2 and 2.4). The ice drilling further provided input data to the numerical modelling of basal conditions. For a detailed presentation of the results of the ice drilling related studies, see Harper et al. (2011) and Data Report (2016). Due to the wealth of data generated from the ice drilling and related studies, the ‘**key outputs**’ of these investigations are not presented in this section, but they are instead presented and discussed in detail in Sections 3.1, 4.1 and 4.2 and conceptualised in Chapter 5.

### **Overview of the drilling and borehole sites (Margin, Interior, Trough)**

To study all relevant aspects of interest with respect to the basal conditions, direct observational, multi-faceted field observations were combined with numerical modelling. The core of the observational campaigns was direct measurement of basal water via borehole experiments and monitoring. Ancillary observations, such as ice velocity, surface meteorological conditions, and geochemical analyses of basal water and sediment, were also essential to advance understanding. For example, changes in ice velocity can act as an indicator of the distribution of water at the bed, which is relevant to the overall project goals. In addition, ice sheet models are too under-constrained to run in isolation without feedback from as many different types of field observations as possible, such as ice surface velocity, ice temperature, etc.

The basic measurements and their purpose with respect to overall goals of this project were as follows:

- **Basal water pressure** – a direct measure of the hydraulic pressure within the basal hydrological system. This is measured by placing a water pressure transducer at the base of the open boreholes. These data are relevant to characterising the basal hydraulic conditions, and are often transformed into a prescribed head boundary condition to model groundwater flow near and beneath ice sheets.
- **Borehole impulse tests** – experiments conducted by artificially perturbing the water level in open boreholes. Three types of impulse tests were performed in boreholes drilled to the bed: 1) *drilling breakthrough tests* to measure the borehole water level in response to initial intersection with the basal drainage system; 2) *slug tests*, i.e. repeatable, low magnitude, short duration impulse tests in which a set volume of water is rapidly injected into the borehole and the subsequent water level recovery is documented; and 3) *injection tests*, i.e. long duration impulse tests in which water is pumped into the test hole at a continuous rate for a set period of time. Results from the impulse tests provide information about the state of the ice sheet's basal hydrological system and its ability to respond to transient perturbations.
- **Basal water and sediment chemistry** – geochemical analyses of subglacial waters and subglacial sediments collected in boreholes drilled to the bed of the ice sheet, and by sampling of outlet streams. These data can reveal basic water flow processes at the bed, as well as chemical conditions at the groundwater/ice interface. Thus, the measurement of water chemistry in the GrIS allows analysis of the variability in sub-ice water-rock interactions and an assessment of the role of the GrIS in the overall geochemical cycle.
- **Surface velocity** – measured by installation of continuously logging GPS stations mounted on the ice and referenced to a station in front of the ice margin (these GPS stations are individual GPS stations installed in the ice drilling study area and are not part of the GPS network as described in Section 2.2.3). Although poorly constrained, time changes in sliding velocity often indicate changing basal hydrological conditions. However, constraining the changing hydrological conditions exactly is difficult.
- **Surface meteorology** – measured by installation of sensors on the glacier surface. These data are used for direct comparison with meltwater generation and the effects of meltwater forcing on basal processes.
- **Ice temperature** – measured by installation of temperature sensors at intervals along boreholes. Data are used for comparison with numerical model output; including models used to investigate the effects of frozen versus melted conditions at the ice sheet bed.

In addition to the field measurements, numerical simulations (ice sheet modelling) of e.g. basal temperature and basal water production were done for comparison to field observations and to provide boundary conditions for groundwater modelling.

For a detailed description of the different measurements, the ice sheet modelling, their purpose and methodology see Data Report 2016.

Field research was conducted each year from 2010 to 2013. Ice boreholes were drilled and instrumentation was installed during June and July of each of the study years. The sites were revisited each September to download data and to prepare some instruments for over-wintering. All boreholes were drilled using hot water methods (Taylor 1984, Engelhardt et al. 1990, Humphrey and Echelmeyer 1990). A new hot water drill was built for the GAP so that the deep and cold ice in the GAP study area could be penetrated (Figure 2-15). Water used for drilling was captured in surface streams and transferred to a storage reservoir where the drill water was spiked with a dye (Data Report 2016).

The field efforts were focused on data collection at three different case-study regions located within the GAP study area (Figure 2-16). Each of the case-study regions is wet-based and they were selected to represent specific glaciological settings based on ice thickness, basal and surface topographic gradients, and proximity to the ice margin. Data exist for a total of seven sites (Figure 2-16) spread among the three case-study regions (Data Report 2016). The case-study regions included sites located 1) close to the ice margin, 2) within the ice sheet interior, and 3) over a deep bedrock trough (Figure 2-17). Four margin region sites were installed 0.1–3 km from the ice edge, and two interior region sites were installed 15 and 30 km inland from the nearest exposed land. Multiple boreholes were installed at each study site, with a total of 26 boreholes installed. A total of 23 of these boreholes reached the bed. These case-study regions are described in more detail below.

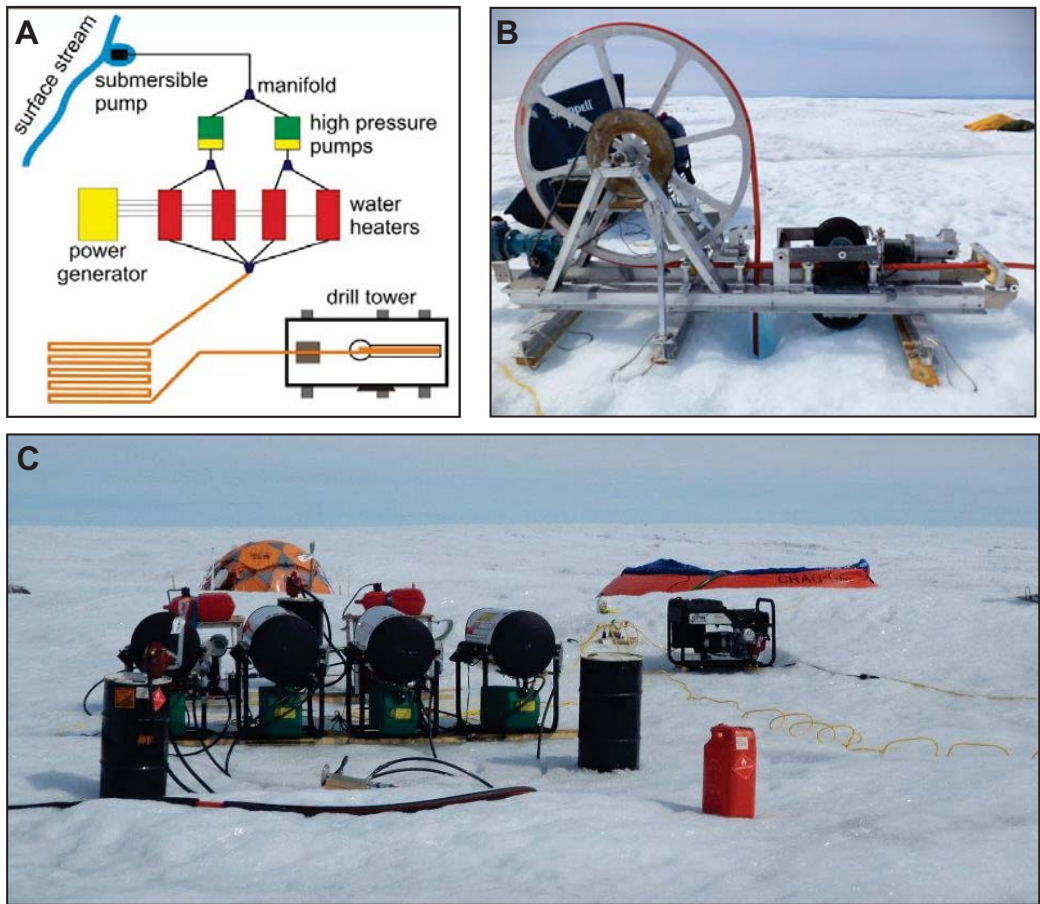


Figure 2-15. A) Schematic of power plant and drill, B) photograph of drill, and C) photograph of the power plant. Photographs were taken by Arlan Dirkson during the 2012 field season.

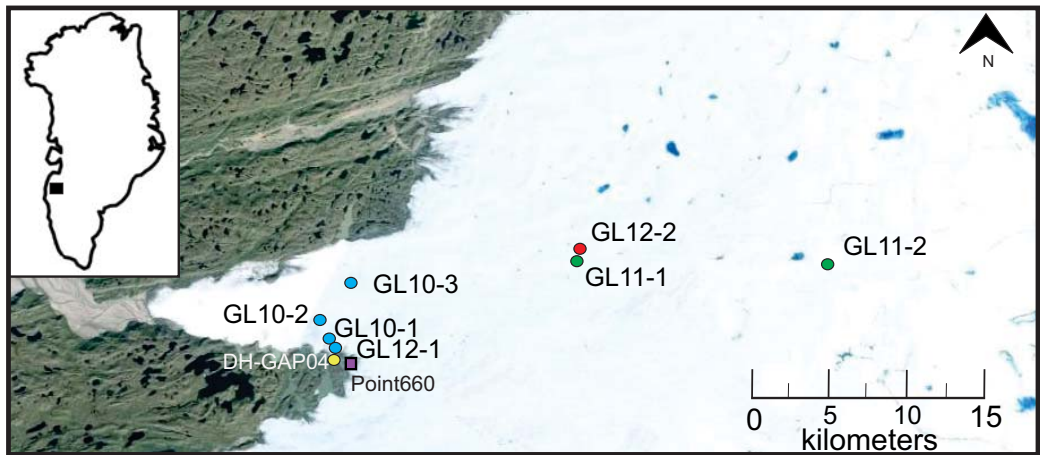
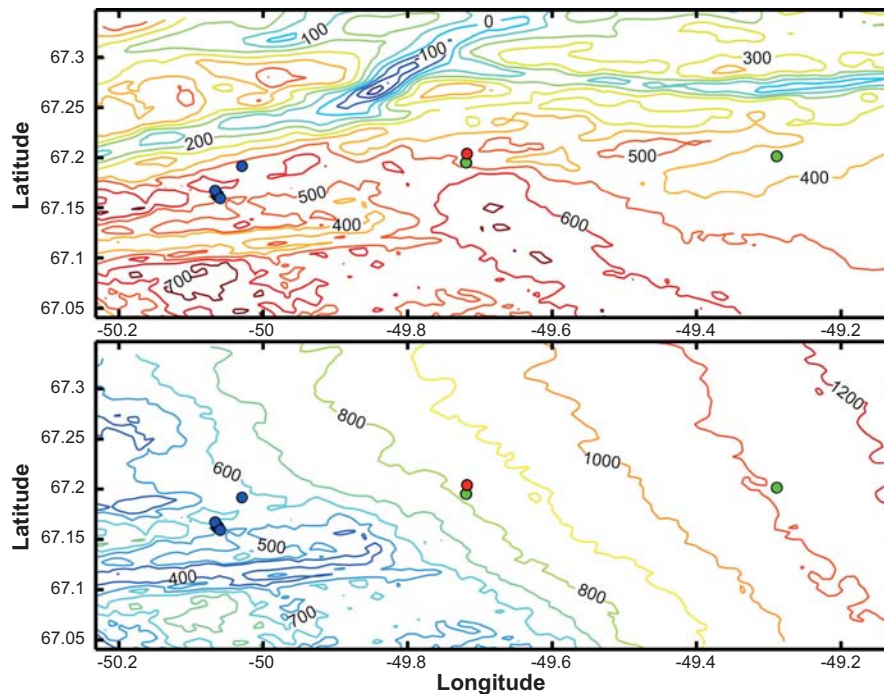


Figure 2-16. Map showing GAP study sites; colour of each circle on the ice indicates the site region: margin = blue, interior = green, trough = red. Yellow circle = location of bedrock borehole DH-GAP04. Purple square = location of Point 660. Dark blue areas show the location of supraglacial lakes (SGLs).



**Figure 2-17.** Bed (top) and surface (bottom) topography for the GAP study area, highlighting site locations using the same colour scheme as Figure 2-16. Contours are labelled by elevation and are spaced at 100 m, with mapping done on a 54×25 (x, y) km grid.

#### **Margin case-study region: sites GL 10-1, GL 10-2, GL 10-3, GL 12-1**

This region addressed ice sheet conditions adjacent to the land-terminating margin of the GrIS. The sites were chosen to investigate ice sheet basal conditions near the margin, where the ice is thinner and the climate is warmer relative to the interior of the ice sheet. Moreover, this site was chosen to provide constraining information for the deep bedrock borehole (DH-GAP04) drilled near the ice margin, and which extends in under the ice sheet (see Section 2.4.4). These sites represent the near-field boundary conditions in DH-GAP04.

Data were collected from this case study region in 2010 (sites GL 10-1, GL 10-2, GL 10-3) and 2012 (GL 12-1). These sites are located from 100 m to approximately 3 km from the ice margin. All sites are located on the ice sheet adjacent to a marginal area, and near bedrock borehole DH-GAP04. Multiple boreholes were drilled at each site. The ice thickness in this region ranges from zero at the margin to 100–200 m approximately 1 km inland from the margin, and then rapidly increases towards the main trough of Isunnguata Sermia where the ice thickness is many hundreds of metres just 3 km inland from the margin. The bed topography is also variable, with locally steep slopes (Figure 2-17). The ice surface topography in this area is steep and hummocky within 2 km of the ice sheet margin. The surface slope is highly variable. Surface ablation (surface melt) is very high, though spatially variable; ablation of more than 3 m/yr is common.

A total of 15 boreholes were drilled in this region, and 13 of these holes reached the bed. Borehole and other data collected included:

- Basal water pressure.
- Ice temperature.
- Results from borehole impulse experiments.
- Borehole water samples.
- Stream outlet water samples (these samples represent a natural averaging of subglacial conditions collected from the terminal outlet of the Isunnguata Sermia Glacier).
- GPS surface velocity values.
- Meteorological data.

### ***Interior case-study region: sites GL 11-1, GL 11-2***

This region was selected to represent ice sheet basal conditions beneath thicker ice and away from the margin. This is representative of a higher degree of glaciation in terms of ice thickness, with approximately 460 m to 825 m of ice overlying the geosphere. In addition, with straight-line distances of 15 and 30 km from DH-GAP04, these sites represent the far-field boundary conditions for the deep bedrock borehole.

Data were collected from this case-study region during 2011. Two sites were installed, one located 15 km inland from Point 660 (GL 11-1), and one located 30 km inland from Point 660 (GL 11-2).

The ice surface topography at GL 11-1 is characterised by a lower slope relative to that near the margin, but with a steeper gradient than farther inland (Figure 2-17). The surface melt is on the order of 2.5 m/yr and the ice thickness is approximately 460 m.

The ice surface topography at GL 11-2 is the flattest of the sites (Figure 2-17). The melt rate here is about 2.5 m/yr and the ice is 825 m thick with a relatively flat bed.

A total of 7 holes were drilled and instrumented at these sites, with 6 extending to the bed. Measurements collected include:

- Basal water pressure.
- Ice temperature.
- Results from borehole impulse experiments.
- Borehole water samples.
- GPS surface velocity values.
- Meteorological data.

### ***Interior trough case-study region: site GL 12-2***

This site was selected to represent deep basal conditions (Figure 2-17), where water is potentially routed along the bed to the subglacial trough beneath the ice sheet. This region is located 15 km inland from the ice edge, and just 1 km north of GL 11-1. The trough region is distinctly different than the nearby interior region because it overlies a deep bedrock trough, with the ice thickness increasing by more than 50% over the trough. Ice thickness at the trough site is approximately 700 m, whereas just 1 km south, at the interior site, the ice thickness is only 460 m. The trough has relatively steep walls, but the ice surface shows no apparent changes in elevation over the trough area. Data were collected in this region in 2012 and 2013. The surface melt is on the order of 2.5 m/yr.

A total of 4 boreholes were drilled to the bed at this site. Measurements collected include:

- Basal water pressure.
- Ice temperature.
- Results from borehole impulse tests.
- Borehole water samples.
- GPS surface velocity values.
- Meteorological data.

## **2.4 Geosphere investigations**

In addition to the investigations on the ice sheet, field investigations were performed in the proglacial part of the GAP study area (Figure 2-18). Laboratory tests and analyses were carried out in parallel to the field studies. The aim of the geosphere investigations was to increase the understanding of hydrogeochemical and hydrogeological conditions in the bedrock down to repository depths (500 to 1,000 m). These studies were planned and designed to directly or indirectly address the following GAP project questions: 3) *To what depth does glacial meltwater penetrate into the bedrock*, 4) *What is the chemical composition of glacial water when and if it reaches repository depth?*, 5) *How much oxygenated water will reach repository depth?*, and 6) *Does discharge of deep groundwater occur in the investigated proglacial talik in the study area?* In addition to the questions listed above, the geosphere investigations provided indirect information to address question 2) *What is the hydraulic*

*pressure situation under an ice sheet, driving groundwater flow?* The subsections below give an overview of the different investigations. For a detailed explanation of the investigations and the results see the Data Report (2016), Harper et al. (2011) and SKB (2010b). For contextual purposes the ‘**key outputs**’ of the geosphere investigations are indicated under each relevant section, whereas the key results from the geosphere investigations (e.g. surface and groundwater chemistry, fracture infillings, results of borehole monitoring) relating to the GAP questions are discussed in Sections 3.2, 3.3 and 4.3–4.6 and conceptualised in Chapter 5.

The main geosphere activity in the GAP was the drilling and instrumentation of three cored bedrock boreholes<sup>2</sup>, DH-GAP01, DH-GAP03 and DH-GAP04 (Figure 2-18 and Table 2-2). These boreholes were drilled in order to: 1) study a potential through talik beneath a lake (DH-GAP01); 2) define the depth of permafrost close to the ice margin (DH-GAP03); 3) collect drill core material for geological and structural studies (DH-GAP01, DH-GAP03 and DH-GAP04); and 4) provide groundwater sampling, hydraulic testing opportunities and to allow groundwater monitoring (DH-GAP01 and DH-GAP04). In addition to the bedrock drilling, a range of supporting field studies was carried out. Besides the bedrock borehole sites, the Talik lake (where DH-GAP01 is drilled), the Leverett spring (in front of the Leverett glacier) and the Ice dammed lake (at the ice sheet margin and close to DH-GAP03 and -04) formed key hydrogeochemical investigation sites (Figure 2-18).

The geosphere supporting studies are grouped into five main themes, each of which included several lines of research:

#### **Geology:**

- Geological surface mapping, including lithologies and structures, at different scales.
- Drill core logging of lithologies, fractures and fracture infillings, orientation of the planar structural features.
- Petrophysical measurements from drill cores.
- Aeromagnetic interpretation of lineaments and ground-truthing/characterisation of lineament sets.

#### **Permafrost:**

- Temperature profiling of boreholes and the ‘Talik lake’.
- Geophysical soundings.
- Geothermal modelling.

#### **Hydrogeochemistry:**

- Surface water studies, including lakes, springs, rivers and glacial meltwaters.
- Groundwater studies, including sampling of DH-GAP01 and DH-GAP04 and the Leverett spring.
- Monitoring of pressure, temperature and electrical conductivity in DH-GAP01 and DH-GAP04.
- Matrix porewater studies – crush and leach of core samples and porewater extraction from preserved core samples.
- Microbial investigations of borehole and lake water.

#### **Mineralogical and geochemical studies:**

- Fracture infillings and drill core observations.
- Stable isotopes and fluid inclusions in calcites.
- Mineralogical and isotope geochemical studies on sulphur and sulphate phases.
- Observation of redox conditions based on fracture infillings.

#### **Hydrogeology:**

- Hydraulic testing of DH-GAP04.
- Slug tests of DH-GAP01.
- Pressure and electrical conductivity monitoring in DH-GAP01 and DH-GAP04.

---

<sup>2</sup> A fourth borehole, DH-GAP02, was drilled at the same site as DH-GAP03, but this borehole had to be abandoned due to drilling difficulties as the drill string hit a fault zone.

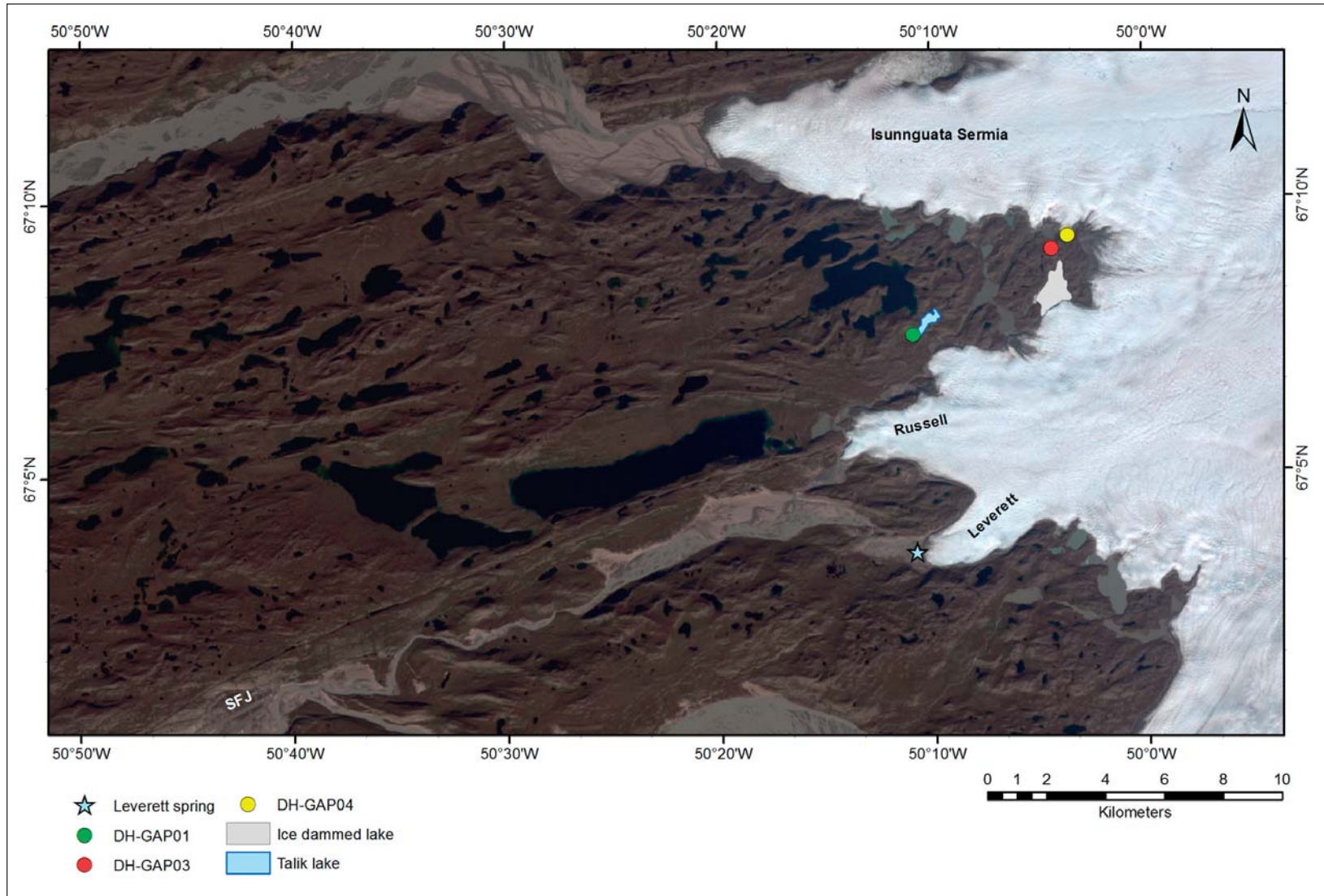


**Figure 2-18.** Map of the area where geosphere investigations were carried out. The key geosphere investigation and monitoring sites: bedrock boreholes, the Leverett spring, Talik lake and the Ice dammed lake, are highlighted. SFJ = Kangerlussuaq International Airport. Background Landsat image was acquired 23 August, 2000.

**Table 2-2. Technical details of boreholes DH-GAP01, DH-GAP03 and DH-GAP04. Elevations are in m relative to the WGS-84 ellipsoid. TOC = top of casing, EOH = end of hole.**

Borehole	Top of Casing (TOC) elevation (m)	Borehole length (m)	Vertical depth below TOC (m)	Elevation of end of borehole (EOH) (m)
DH-GAP01	374.7	221.5	190.7	184.0
DH-GAP03	484.9	341.2	321.7	163.2
DH-GAP04	526.2	687.0	649.1	-122.9

### 2.4.1 Bedrock geology

In order to enhance understanding of the geology and structure of the study area, geological mapping of the region was conducted during 2008–2013. Detailed geological investigations included scanline mapping of fractures and faults and characterisation of the foliation and main rock types at seven different key locations in 2008 (Aaltonen et al. 2010). Later mapping campaigns aimed at increasing the general understanding of the complex geology of the area and providing sufficient information to generate a geological map of the drilling sites (SKB 2010b, Harper et al. 2011, Data Report 2016). Detailed geological mapping focused on a transect extending from Kangerlussuaq to the ice margin and a smaller subarea surrounding the sites selected for the drilling of the three boreholes (Figure 2-18). Aeromagnetic lineament interpretation and ground-truthing of these lineaments was also done within the site area. Due to several generations of large-scale folding overprinting the bedrock, the site area (in close proximity to the three boreholes) shows a complex geology (e.g. Engström and Klint 2014). Figure 2-19 shows an overview of the geological framework of the study area including the interpreted structural form lines (foliation, fold hinge line, fault and shear zone traces) overlain on a high-resolution aerial image. Following the drilling of DH-GAP01, DH-GAP03 and DH-GAP04, detailed information was made available to help expand the 2D mapping information into a 3D-understanding, through the creation of a 3D geosphere model (Engström et al. 2012). The report by Engström et al. (2012) describes the geological structures and lineaments occurring in the Kangerlussuaq area, which form the basis for the GAP Geomodel version 1. Drill core investigations included detailed fracture characterisation, lithological mapping, and mapping of foliations and deformation zones (Pere 2014).

The three GAP bedrock boreholes were drilled in a complex geological environment with different geological settings in terms of dominating rock types.

#### Key outputs

The rock types in the boreholes can be divided into four main types: felsic gneiss, mafic gneiss, intermediate gneiss and granitic pegmatite. The relative amount of mafic/felsic minerals have been used as a guideline when defining the rock types. The felsic gneisses consist typically of K-feldspar, quartz and plagioclase with some biotite. The mafic gneisses typically are massive or slightly foliated and contain large amounts of garnet with amphibole and pyroxene. The intermediate gneisses resemble mafic gneisses but contain more plagioclase and biotite than amphibole and pyroxene. DH-GAP01 is situated in foliated felsic gneiss which has both mafic and intermediate layers. In DH-GAP03, alternating layers of felsic and mafic gneisses dominate. DH-GAP04 is dominated by mafic garnet gneiss in the upper 300 m, with more foliated intermediate to felsic gneiss below. For a comprehensive presentation of the core logging, see Pere (2014).

### 2.4.2 Geophysics

A wide-band frequency-domain electromagnetic sounding (SAMPO) system was used in the study area to test its applicability to detect permafrost both in the proglacial area and under the ice sheet. In 2012 and 2013, a total of 260 sounding points (see Figure 2-20) were measured on the ice and in front of the ice sheet.

## Key output

The SAMPO profiles from the GAP study area provided a consistent cryogenic structure for the soil and crystalline bedrock in front of the ice sheet, which included: 1) a low resistivity active layer, 2) highly resistive permafrost, and 3) lower resistivity bedrock beneath including a weak, deep (550–750 m deep) conductor. In the ice-covered area (i.e. the area directly east of borehole DH-GAP04), four layers were preliminarily distinguished: 1) glacier ice, 2) an unfrozen layer, 3) permafrost, and 4) a low-resistivity feature at depth, i.e. the same deep conductor as observed in the ice-free areas (Data Report 2016). The weak conductor at depth seen in almost all of the GAP profiles at 550–750 m depth could possibly indicate the base of permafrost. However, based on the temperature profiling in the GAP boreholes, it is known that the permafrost in the GAP study area extends to depths of 350–400 m. The most likely explanation of the weak, deep conductor is that it coincides with the depth where the salinity of groundwater exceeds a certain threshold level and becomes observable (Data Report 2016).

In the area where the SAMPO survey was carried out, no supporting information or data exist to help in elucidating the presence or non-existence of subglacial permafrost in the ice-covered area. It should also be noted that no other types of studies investigating subglacial permafrost near the ice margin were carried out by the GAP.

### 2.4.3 Surface water characterisation

Surface water characterisation began in 2008, during the initial evaluation of the Kangerlussuaq region for its suitability to host the GAP. Overall, 44 lakes were sampled for main chemical and isotopic analyses, including  $\delta^{18}\text{O}$ ,  $\delta^2\text{H}$ ,  $^3\text{H}$ ,  $\delta^{37}\text{Cl}$ ,  $^{87}\text{Sr}$ , and  $\delta^{34}\text{S}$  and  $\delta^{18}\text{O}$  of  $\text{SO}_4$ . In addition, meltwaters were sampled in several locations at Leverett glacier and Isunnguata Sermia for chemical and isotopic analyses. Ice samples were analysed for  $\delta^{18}\text{O}$ ,  $\delta^2\text{H}$  and tritium. Locations of sampled lakes, boreholes and ice samples are shown in Figure 2-21. Springs at the drained lake bed of the Ice dammed lake (Figure 2-18) were also considered to represent surface water (and possibly groundwater), and were therefore sampled by the GAP.

The aims of the surface water characterisation were to:

1. Define end-members for various geochemical parameters (compositional and isotopic) for lakes and meltwaters. Groundwater characteristics could then be interpreted within the framework of a dynamic system of groundwater transport and mixing, and water-rock interactions. This was particularly important for meltwaters – to help determine the depth to which meltwater penetrates into the subsurface.
2. Understand possible interactions between groundwaters and surface waters, and determine whether or not there were geochemical indicators for groundwater upwelling into lakes through taliks.
3. Examine the source of salinity in the lakes so that the cryogenic concentration model of salinity development (i.e. freeze-out or solute exclusion) in front of ice sheets (Herut et al. 1990, Starinsky and Katz 2003) could be evaluated.
4. Compare and distinguish the chemical and isotopic similarities and differences between suspected glacial recharge and surface meteoric recharge from lakes.
5. Provide understanding of the geochemical systems for key elements, such as sulphur and strontium, which can help to determine flow paths and interpret the geochemical evolution of groundwaters.

For a detailed description of the different water types, sampling methodology and results see Data Report 2016.

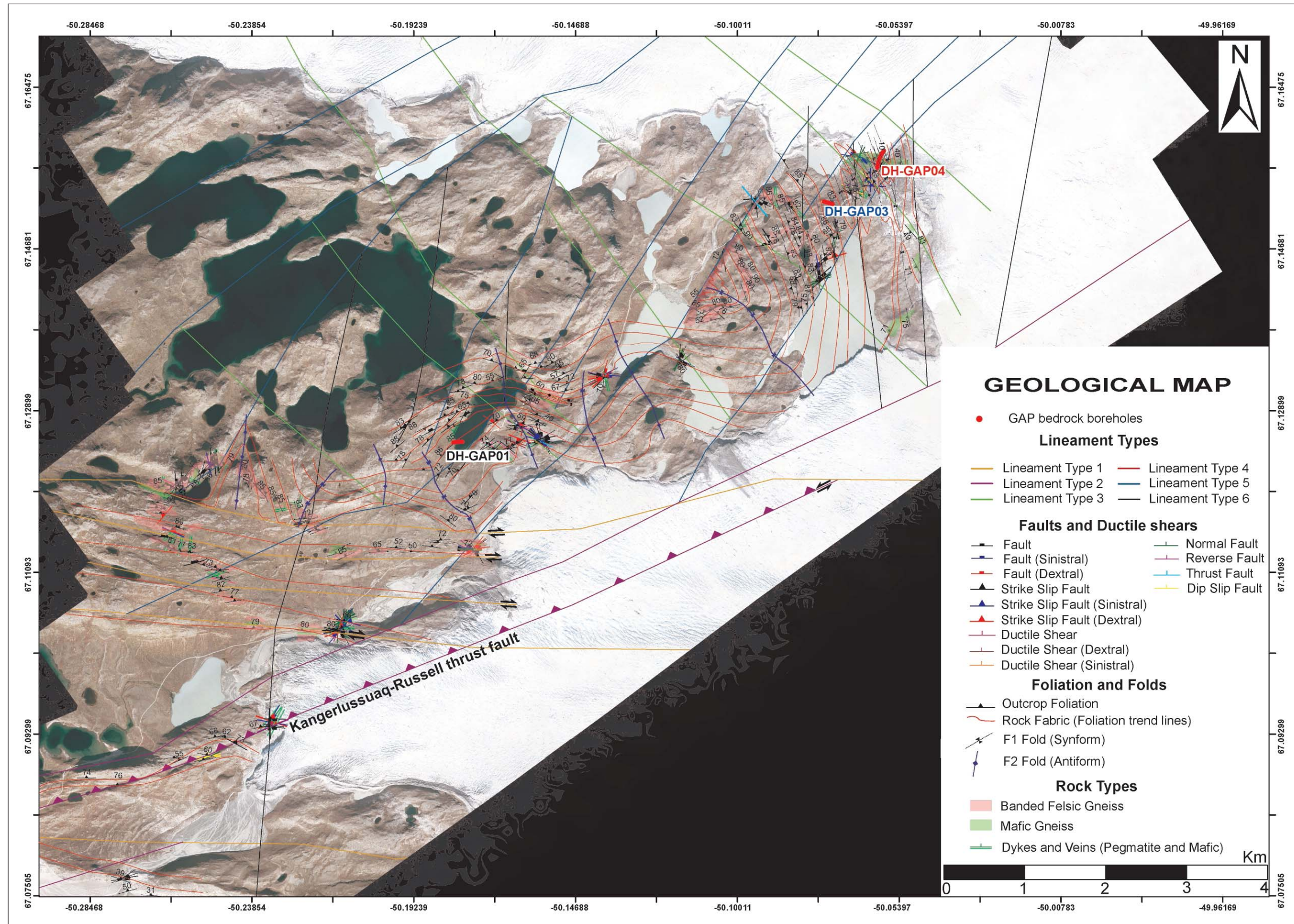
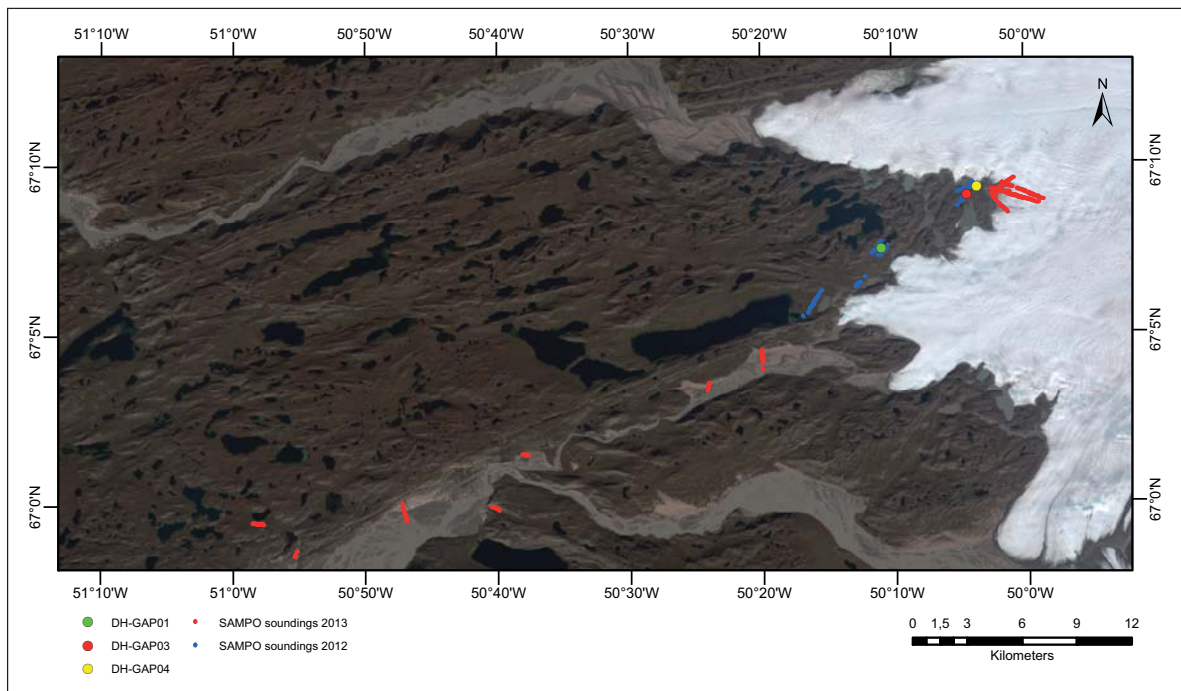


Figure 2-19. Aerial image from May 2006 overlain by the mapped and inferred rock fabric (foliation), rock types and structural elements. The macro-scale structure outlines large-scale folding overprinted by various shear zones and more brittle fault zones. The three bedrock boreholes are displayed as DH-GAP01, DH-GAP03, and DH-GAP04.





*Figure 2-20. Locations of the SAMPO soundings made in 2012–2013.*

## 2.4.4 Bedrock borehole investigations

### ***Drilling of bedrock boreholes***

Two 57 mm (DH-GAP01 and DH-GAP03) and one 76 mm bedrock (DH-GAP04) boreholes were drilled by the GAP using standard core drilling techniques (Figure 2-18, Table 2-2 and Table 2-3). DH-GAP01 is the shallowest and DH-GAP04 the deepest; hydrogeological data were successfully acquired from these two boreholes. Due to technical problems, only temperature information was obtained from DH-GAP03. DH-GAP04 is drilled approximately 200 m from the ice margin of the Isunnguata Sermia outlet glacier. DH-GAP03 is located approximately 800 m SW of DH-GAP04. Both boreholes are interpreted to penetrate a tight synformal syncline that dips gently under the Isunnguata Sermia margin. DH-GAP01 is located approximately 6 km SW of DH-GAP04 and approximately 1 km from the nearest ice margin (Figure 2-18).

Due to the presence of permafrost and the risk of freezing limiting the time available for borehole testing and instrumentation, the drilling was performed with heated (up to 60°C) drilling water. A local, geochemically well-characterised water source was used as drilling water (Data Report 2016) and the drilling water was further spiked with sodium fluorescein dye ( $C_2OH_{10}Na_2O_3$ ) to evaluate the drilling water contamination in subsequent geochemical sampling. Technical details of these boreholes are presented in Table 2.2. Table 2-3 gives an overview of when the boreholes were drilled, instrumented and tested. Detailed information about the drilling of these boreholes can be found in SKB (2010b), Harper et al. (2011) and the Data Report (2016).

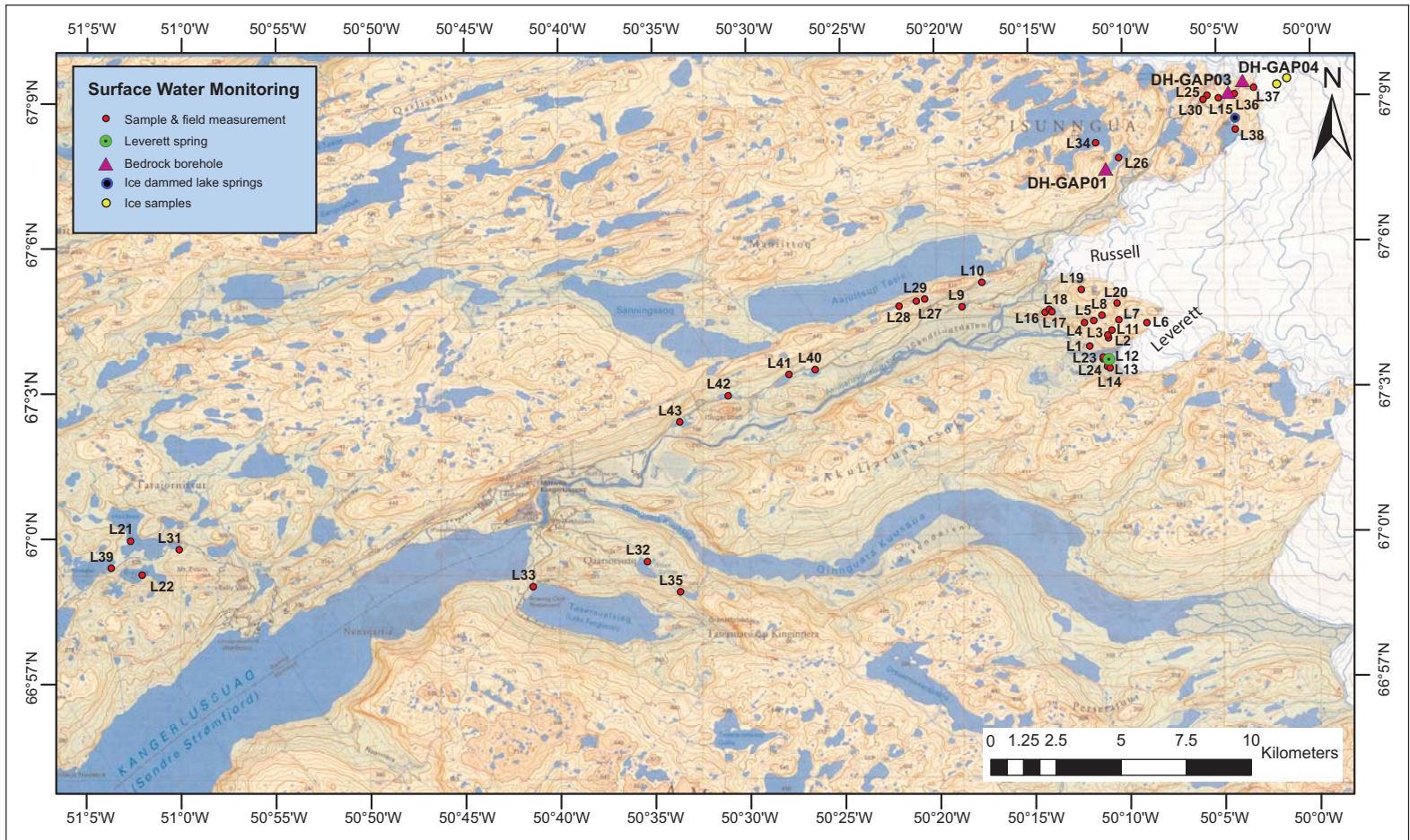
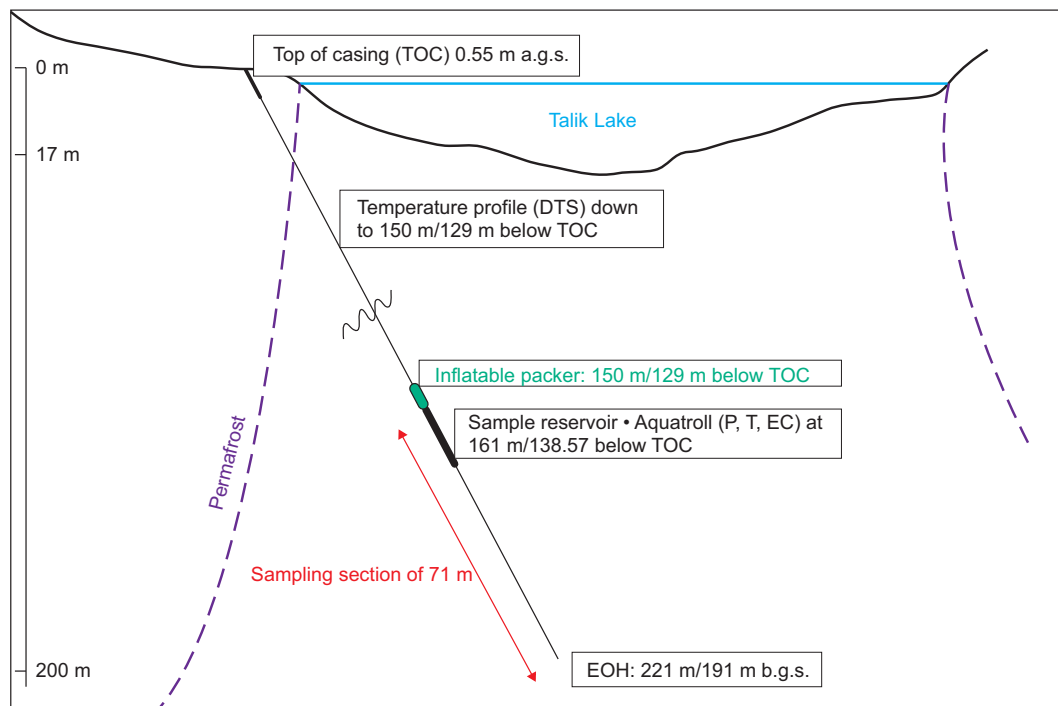


Figure 2-21. Locations for surface and groundwater hydrogeochemical sampling.

### DH-GAP01: drilling and instrumentation

DH-GAP01 was drilled to confirm the existence of, and to study, a possible through talik structure under a lake. Selection of the lake for talik investigations was based on general knowledge of the formation of taliks, experience gained from the Permafrost Project in the Canadian Arctic (e.g. Stotler et al. 2009) and the field investigations carried out in the study area. The main criteria were that the water body should be large and deep enough not to freeze to the bottom during winter and, since taliks are often assumed to be zones of discharge/recharge, that the lake should preferably be located in a lineament or fault to increase the probability of higher bedrock hydraulic conductivity (Figure 2-3 and Figure 2-19). The selected lake (Figure 2-8, Figure 2-18, Figure 2-19 and Figure 2-21), is referred to as the Talik lake (see Section 2.1.4) by the GAP (SKB 2010b, Johansson et al. 2015a). DH-GAP01 was drilled beneath the lake basin approximately 20 m from the lake shoreline (Figure 2-22). The borehole was oriented towards the NNW and is drilled with an inclination of 60° from horizontal. The borehole is 221 m long, which equals 191 m vertical depth. No hydraulic testing was carried out before instrumentation. Based on examination of the core, DH-GAP01 is unevenly fractured, having narrow, highly fractured borehole intervals and also fully intact sections. The average fracture frequency is 2.23/m (Pere 2014).

DH-GAP01 was equipped with a U-tube sampling device (Freifeld et al. 2005), which includes one inflatable packer, a water sampling unit and sensors to monitor in situ pressure, temperature and electrical conductivity of the water (for a detailed description of the installation, see SKB 2010b). The packer was placed at 150 m borehole length (129 m vertical depth) in an intact bedrock section. The sample intake and sensors are located at 161 m borehole length (138.57 m below TOC) (Figure 2-22). Groundwater sampling is achieved by applying nitrogen gas pressure in a tube running down to the sampler. In addition to the downhole sensors, a fibre optical *Distributed Temperature Sensing* (DTS) cable was installed to provide temperature profiling from the surface down to the packer. Although there is no knowledge as to how the mapped geological structures, including delineated fracture zones and fault zones, contribute to groundwater flow, their character and scarcity tend to support a model of sparsely fractured bedrock with a small number of flowing fractures (Data Report 2016).



**Figure 2-22.** Schematic plan of the borehole DH-GAP01, the instrumentation and the hydrogeological context. The location of the base of the permafrost (dashed purple line) is approximate, except for at the location of the borehole. The top of casing (TOC) is 0.55 m above the ground surface (m a.g.s.) and serves as the reference for depth measurements; m b.g.s. = metres below ground surface; EOH = end of the hole. The section length between the packer and the bottom of the hole is 71 m and its volume is 174 L.

### ***DH-GAP03: drilling and instrumentation***

This borehole was drilled close to the margin of Isunnguata Sermia, about 5 km NE of the Talik lake and DH-GAP01 (Figure 2-18 and Figure 2-19). The aim of this borehole was to determine the maximum depth of permafrost, based on the assumption that the MAAT would be lowest near the ice margin at a high elevation, where the snow cover, vegetation and other potentially insulating factors would be minimised. When investigating permafrost thickness, it is important to remember that this depends to a great extent on the historical ice cover at this site, i.e. whether the ice sheet extended over the site during the neoglacial or LIA. Additional considerations for siting of this borehole included the presence of sparsely fractured bedrock, which would best represent the preferred conditions for a deep geologic repository, balanced with a proximity to zones of increased fracturing if possible (SKB 2010b). Information about the permafrost thickness was of importance for the general understanding of the GAP study area but also provided critical information when planning for and designing the instrumentation of borehole DH-GAP04 (see below). The borehole was orientated towards NWW and was drilled with an inclination of 70° from horizontal. The borehole is 341 m long, which equals 320 m vertical depth. DH-GAP03 is unevenly fractured, having narrow, highly fractured borehole intervals and also fully intact sections. Fracturing generally increases with depth. The average fracture frequency is 3.36/m (Pere 2014). A small pond (L25) about 500 m from the drilling site was used for drilling water. Due to technical problems during installation of the instrument string it was not possible to instrument this hole with a similar U-tube device as was installed in DH-GAP01. However, a fibre optical DTS cable extending to 329 m borehole length (309 m vertical depth) providing temperature data was successfully installed. No hydraulic testing was carried out in this hole.

### ***DH-GAP04: drilling and instrumentation***

The aim of this borehole was to provide groundwater sampling and monitoring opportunities down to, or below, typical nuclear waste repository depths (approximately 500 m or more), and it was intended that the hole would extend beneath the ice sheet (Harper et al. 2011). The borehole was drilled towards the north with an inclination of 70° from horizontal at approximately 210 m from the ice margin (Figure 2-18, Figure 2-19 and Figure 2-23). DH-GAP04 measures 687 m in length, which equals 649 m vertical depth relative to the TOC at the drilling site. The bottom of the hole is under the ice sheet, approximately 20 m beyond the ice margin (Figure 2-23). However, it should be recalled that the GrIS is currently melting and thinning, and although the melt is not as substantial in the GAP study area as within other parts of the ice sheet, the ice margin has retreated a few metres at the borehole site during the course of the project. The upper 2.5 m of the borehole are cased. DH-GAP04 is fairly evenly fractured, but contains intact sections. Overall it is less fractured than DH-GAP01 and DH-GAP03. The average fracture frequency is 1.97/m (Pere 2014, Data Report 2016). The same pond (L25) that was used for drilling water for DH-GAP03 was also used when drilling this hole. Hydraulic testing was done after completion of drilling to identify flowing fractures to optimise the positioning of the downhole instrumentation (see Section 2.4.5).

The borehole was instrumented to provide information about the hydrogeochemical and hydrogeological conditions. The instrumentation contains a two-packer system (each packer is 1 m long) isolating a section between 561 to 571 m vertical depth (i.e. from top of upper packer to top of lower packer), dividing the hole into three sections (Figure 2-24). The upper 400 m of the borehole are frozen since this part is within permafrost. The sections are named: the upper section (Sect-up), the mid-section (Sect-mid) and the lower section (Sect-low) and are all equipped with both pressure and electrical conductivity sensors. The mid-section is also equipped with a temperature sensor. A fibre optical DTS cable extends from the surface down to the lowermost packer and allows temperature profiling. The design of the instrumentation and its components are described in detail in the Data Report (2016).

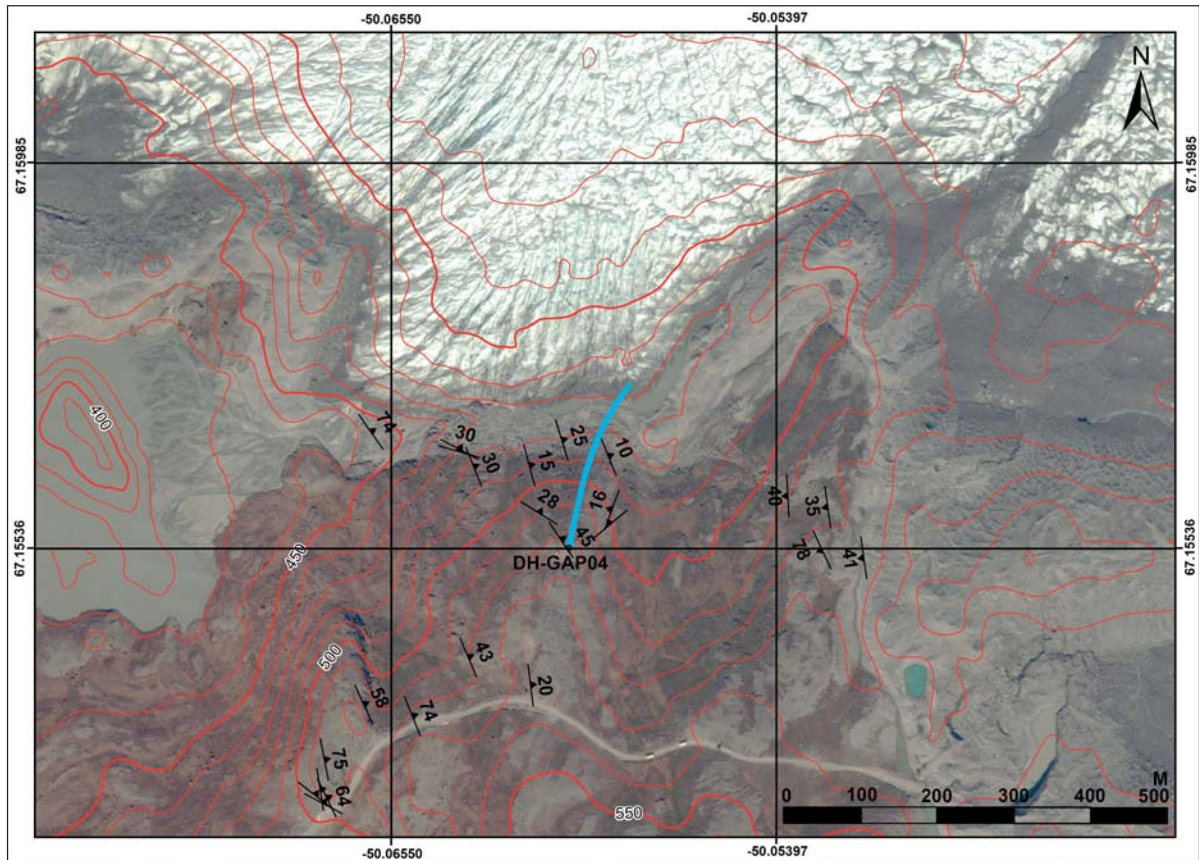


**Figure 2-23.** Location of the DH-GAP04 drilling site with the trace of the borehole (blue line). Foliation measurements are given, indicating the strike, dip direction and dip angle. Red lines are elevation contours with a 10 m interval. Background image is a Quickbird acquired 4 July, 2011, which is when DH-GAP04 was drilled.

## 2.4.5 Measurements performed after drilling

### **Pressure response test DH-GAP01**

In order to measure transmissivity and hydraulic conductivity, two pressure response tests associated with water withdrawal from borehole DH-GAP01 were performed in September 2010. In this test water was removed from the 71 m long borehole section below the packer and the downhole pressure responses were monitored with the downhole pressure sensor (Figure 2-22). The pressure recovery following water removal was evaluated, allowing calculation of transmissivity and hydraulic conductivity using evaluation methods for slug tests. The tests had short durations and involved small water volumes, implying that the evaluated parameters relate to the rock immediately surrounding the borehole.

### **Key output**

The results of the evaluation of the two pressure response tests suggest a total transmissivity for the tested section of the DH-GAP01 borehole of approximately  $10^{-6}$  m<sup>2</sup>/s.

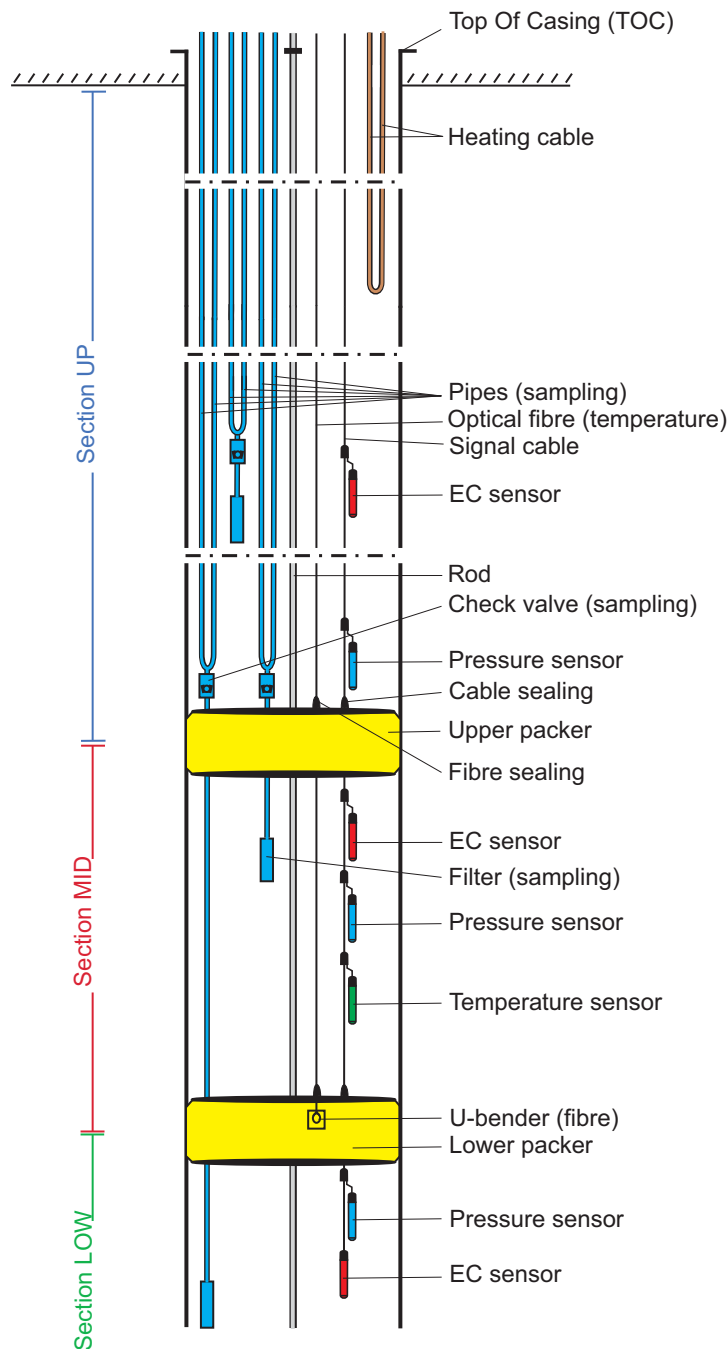


**Figure 2-24.** Equipment in borehole DH-GAP04. Each packer is 1 m long. The upper 400 m of the hole is within the permafrost and is naturally sealed with ice within this part of the hole. The top of the upper packer is located at a depth of 561 m below TOC. The top of the lower packer is located at a depth of 571 m below TOC. Sect-up is approximately 190 m and extends from the base of the permafrost to the uppermost packer, its volume is 840 L. Sect-mid is isolated by the two packers and is 10 m long and has a volume of 44 L. Sect-low is 80 m long and extends from the lowermost packer to the bottom of the hole with a volume of 350 L. A heating cable is installed to a depth of approximately 450 m allowing melting of the water within sample tubes for water sampling campaigns.

### Posiva Flow log DH-GAP04

Hydraulic testing in DH-GAP04 was conducted using the *Posiva Flow Log method* (PFL) (Pöllänen et al. 2012). PFL measures the flow rate into or out of a defined test section and simultaneously observes a number of parameters from which the transmissivity and hydraulic head (given as fresh water head) of a fracture can be calculated. The method is based on tracking of both the dilution (cooling) of an electronically generated thermal pulse and transfer of the pulse by the moving water (Pöllänen et al. 2012). During measurement, the test section is isolated with rubber disks, which improves the detection of weak features. Due to time constraints related to downhole freezing conditions, the testing program was designed to optimise both critical data needs and testing time. A 10 m test section was used with a two metre step, giving a total error, including the strain of the cable, of  $\pm 3.3$  m for this testing geometry. Due to the high risk that the borehole would freeze there was no time to await steady state flow conditions; therefore the testing was completed only two days following drilling completion. For this reason, it is important to remember that the measurements were carried out, partially, in transient flow conditions.

The primary motivation for carrying out PFL testing in DH-GAP04 was to find the best location for the downhole instrument system; however, the data from the PFL testing were useful also for hydrogeological characterisation of the tested bedrock volume, a requirement to understand the hydrogeology of the ice marginal area.

### Key output

The PFL testing identified nine flowing features (Figure 2-25). The measured specific capacities (flow rate in  $\text{m}^3/\text{s}$  per metre of head change) in these flowing features range from  $1.6 \cdot 10^{-9}$  to  $3.3 \cdot 10^{-6}$   $\text{m}^3/\text{s}$ . In addition to the PFL testing, further hydraulic evaluations of pressure data collected during water sampling campaigns in September, 2011 and September 2013 were carried out (Data Report 2016).

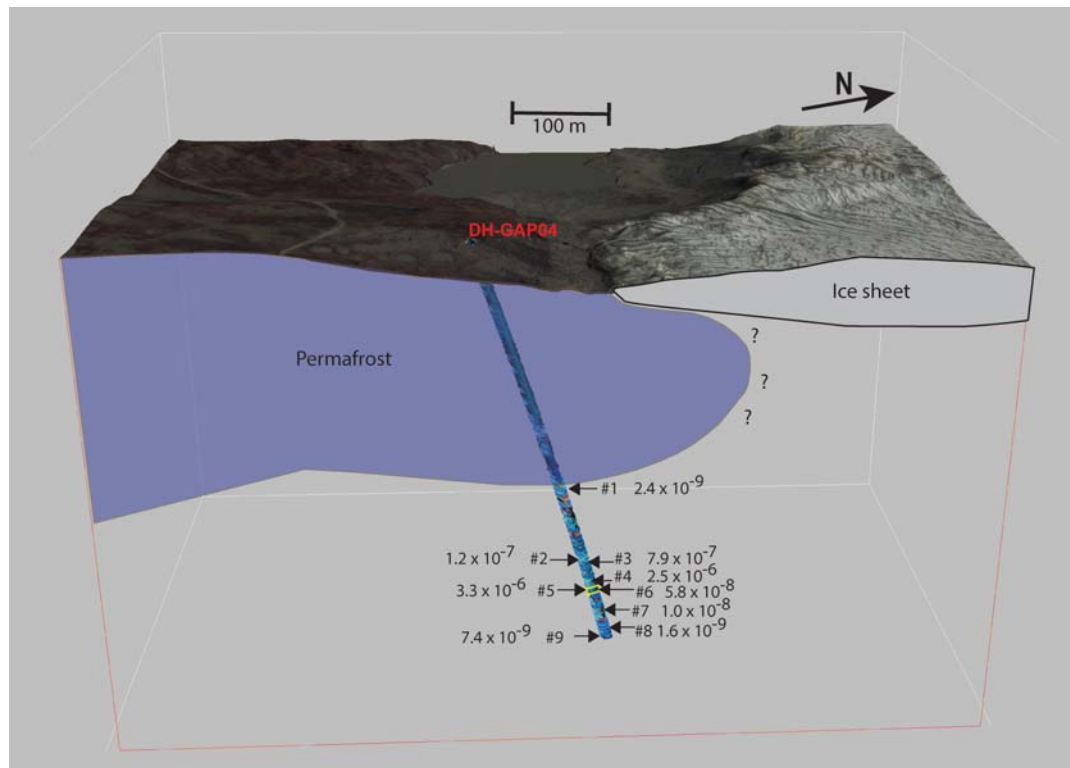


**Figure 2-25.** Schematic presentation of the topography and the nine water-conducting features (indicated by arrows) with measured specific capacities (flow rate in  $\text{m}^3/\text{s}$  per metre of head change) in DH-GAP04. The two yellow lines at approximately 600 m borehole length indicate the location of packers. Purple area denotes permafrost. The base of the permafrost is defined as the 0-degree isotherm.

### ***Distributed temperature sensing of DH-GAP01, DH-GAP03 and DH-GAP04***

Boreholes DH-GAP01, DH-GAP03 and DH-GAP04 are equipped with optical fibres that allow accurate, high-resolution temperature profiling utilizing the DTS technique (e.g. Selker et al. 2006, Tyler et al. 2009). Temperature profiling of DH-GAP01 and DH-GAP03 was completed immediately after the hot water drilling in 2009, and was repeated again in DH-GAP01 in May and September 2010 and in DH-GAP03 in May 2010 (SKB 2010b, Data Report 2016). The aim in 2010 was to observe if the 2009 measurements still showed evidence of the hot water drilling. Once steady state temperatures are reached, it is not expected that the bedrock temperatures would vary much below the upper 10–15 m of seasonally affected bedrock temperatures.

#### **Key output**

Temperature profiling of DH-GAP01 confirmed that as soon as the borehole advanced beneath the lake basin, the bedrock temperature increased to values above zero (see Figure 2-26a). The temperature is continuously above 0°C (Figure 2-26a) from approximately 20 m to 130 m vertical depth. The separate temperature sensor at a depth of 140 m (Figure 2-22 and Figure 2-26a) maintained a temperature of  $1.3 \pm 0.2^\circ\text{C}$  from mid-July, 2009. These observations show the absence of permafrost and support the hypothesis that a through talik exists under the lake (SKB 2010b).

Temperature profiling of DH-GAP03 was completed to estimate the maximum permafrost depth in the region close to the ice margin, prior to the drilling of the deep bedrock borehole that was to be instrumented. The results from the 2010 measurements indicate that, at the DH-GAP03 site, the base of the permafrost (i.e. the 0-degree isotherm) is located at  $335 \pm 14$  m vertical depth (Figure 2-26b). However, it is probable that these temperature measurements still remained affected by the drilling conducted in 2009 (SKB 2010b, Data Report 2016).

Bedrock temperatures in DH-GAP04 have been measured continuously since July 2011, with different measurement intervals depending on the purpose of the monitoring. Examples results are presented in Figure 2-26b. The borehole was initially cooling following the hot water drilling campaign. More stable temperature profiles were observed after December 2012 (Data Report 2016), when the effect of the drilling could be considered small. However, due to the heat added during drilling, and during the subsequent groundwater sampling campaigns, the borehole is still approximately 0.2°C from being completely thermally recovered. The base of the permafrost is located at  $405 \pm 10$  m vertical depth (Figure 2-26b).

To account for differences in the ground surface topography between the two drill sites, the elevation of a point at the ice margin directly north of DH-GAP04 was determined and used as a reference point to calculate permafrost thickness at each location. Using this approach, permafrost thickness is approximately 315 m at DH-GAP03 and approximately 350 m at DH-GAP04. The difference in permafrost thickness between the two borehole sites may be related to many different factors, such as different geology, different local surface conditions over time, slightly differing instrument calibration procedures (see Data Report 2016), etc.

Model calculations, DTS temperature profiling and petrophysical data from DH-GAP03 and DH-GAP04 were used to obtain the first estimates of *Heat Flux Density* (HFD, or geothermal heat flux) for the site. The HFD value for DH-GAP03 is  $34.8 \pm 1.9$  mW/m<sup>2</sup> (Harper et al. 2011), whereas the HFD from the deeper DH-GAP04 borehole is  $27.2 \pm 1.8$  mW/m<sup>2</sup>. The HFD difference between the boreholes could be related to the different climatic history of the borehole sites, since the ground surface at each site has been exposed for different periods of time since deglaciation i.e. DH-GAP03 has been ice-free for a longer time than DH-GAP04. The calculated HFD values are considerably lower than previous HFD estimates for this part of Greenland, e.g. the approximately 58 mW/m<sup>2</sup> estimate by Shapiro and Ritzwoller (2004) and the approximately 75 mW/m<sup>2</sup> value calculated by Fox Maule et al. (2009). The new HFD values are not corrected for climatic effects, i.e. the long term palaeoclimatic variations have not been considered. If a climate correction were to be made, the values would be somewhat higher, but still not as high as previous estimates. Furthermore, the difference between the new and old values is well within the large expected variability of HFD values in this type of geologic setting (cf. Näslund et al. 2005, Fox Maule et al. 2009). Sensitivity analysis suggests that the difference between the new and old HFD values is of importance in ice sheet modelling for this portion of the GrIS (see Section 3.1.1, Brinkerhoff et al. 2011 and Meierbachtol et al. 2015).

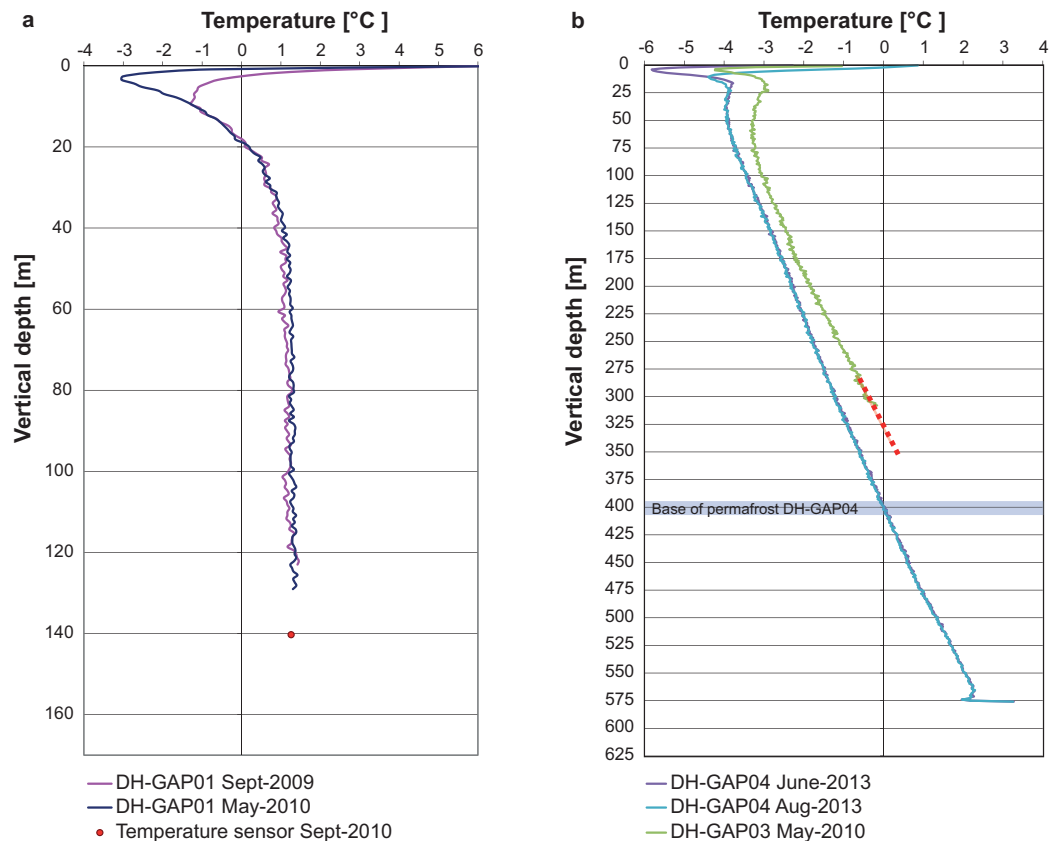


**Figure 2-26.** a) Temperature profiles from DH-GAP01. A temperature sensor at 140 m vertical depth provides an independent temperature reference. b) Temperature profiles from DH-GAP03 (green) and DH-GAP04 (blue and purple). The base of permafrost (i.e. the 0-degree isotherm) is reached at a vertical depth of 395 to 415 m in DH-GAP04. By extrapolating the temperature curve (red dashed line) in DH-GAP03 the base of permafrost is reached at a vertical depth of approximately 335 m. The temperatures in DH-GAP04 and DH-GAP03 differ by almost 1 degree. This is likely due to a combination of 1) that the borehole sites have been subject to different local surface conditions over time 2) the temperature in DH-GAP03 was probably still affected by the added heat from the drilling, and 3) the measurement protocol and data calibration procedure for DH-GAP03 differed slightly from the data calibration and measurement protocol for DH-GAP04. The boreholes have the following inclinations: DH-GAP01 60°, DH-GAP03 70° and DH-GAP04 70°.

### Microbial investigations in DH-GAP01

In order to obtain information on the anaerobic or aerobic nature of the groundwater in DH-GAP01 and to be able to provide input to GAP questions 4 and 5 (see Section 1.2), microbial investigations with the aim of characterising and classifying microbial DNA signatures in groundwaters from DH-GAP01 and from the Talik lake were carried out in July, 2009, and in September, 2010. Due to drilling fluid contamination, no uncontaminated water samples were available from DH-GAP04 for microbial sampling and analyses.

### Key output

Analysis of the total numbers of microorganisms did not show a significant difference between DH-GAP01 groundwater and the Talik lake water (Data Report 2016). However, according to DNA signatures, the microorganisms in DH-GAP01 groundwater were mostly anaerobic or facultative anaerobic microorganisms. On the contrary, the Talik lake water contained aerobic microorganisms, including species of Cyanobacteria that typically require light for growth. The number of different

DNA signatures found in the Talik lake water was higher than was observed for DH-GAP01 groundwater. None of the DNA signatures found in the Talik lake were found in the DH-GAP01 groundwater. These observations imply that the microbial communities differ between the borehole groundwater and the lake water. That is, some DNA signatures were similar, but none of the sequences were identical between the DH-GAP01 groundwater and the lake water. Most DNA signatures indicated anaerobic conditions in the DH-GAP01 borehole and aerobic conditions in the lake.

## 2.4.6 Groundwater sampling and analysis

One of the main focuses of the GAP was to increase knowledge about the interaction between ice sheets and groundwater. The bedrock boreholes were drilled to directly address this issue, and there was a requirement to be able to: 1) measure *water pressure* (P), *temperature* (T) and *electrical conductivity* (EC), and 2) collect water samples allowing chemical and isotopic characterisation of the groundwater both beneath and in front of the ice sheet. The data from these boreholes could then be used to calibrate and compare to groundwater models of other glaciated systems. The Leverett spring (referred to as a pingo by Scholz and Baumann 1997) in front of the Leverett glacier (Figure 2-18 and Figure 2-21) is also considered to represent groundwater, and has therefore been monitored during 2009 to 2012.

**Table 2-3. Drilling, installation and testing information for boreholes DH-GAP01, DH-GAP03 and DH-GAP04. Figures 2-22 and 2-24 show the equipment installed in DH-GAP01 and DH-GAP04, respectively. Note that not all activities lasted for full days, some only required a few hours. DH-GAP01 water sampling campaigns were carried out in September 2009 and May 2010. DH-GAP04 water sampling campaigns were carried out in September 2011 and 2013.**

Borehole DH-GAP01	Date	Comment
Drilling: borehole length 221.5 m and vertical depth 190.7 m	June 26–28, 2009	56.8 mm diamond drilling using double tube WL-56/39 equipment, providing a 39 mm core. Drilling water was heated and spiked with sodium fluorescein (C <sub>2</sub> OH <sub>10</sub> Na <sub>2</sub> O <sub>5</sub> ).
Deviation survey	June 28, 2009	DeviFlex method.
Installation of the U-tube sampling device and a fibre optical DTS cable.	June 28, 2009	Allows water sampling and monitoring of pressure, temperature and electrical conductivity of the water. The DTS cable allows temperature monitoring along the hole.
Pressure response tests	September 4–5, 2010	Pressure response tests were based on water removal (from the test section below the packer) and pressure recovery monitoring.
Borehole DH-GAP03	Date	Comment
Drilling: borehole length 341.2 m and vertical depth 321.7 m	June 30–July 3, 2009	56.8 mm diamond drilling using double tube WL-56/39 equipment, providing a 39 mm core. Drilling water was heated and spiked with sodium fluorescein (C <sub>2</sub> OH <sub>10</sub> Na <sub>2</sub> O <sub>5</sub> ).
Deviation survey	July 3, 2009	DeviFlex method.
Unsuccessful attempt to install a U-tube sampling device.	July 3, 2009	Due to technical problems the installation failed. Downhole sensors were later installed but these eventually failed. A fibre optical DTS cable was successfully installed allowing temperature monitoring along the hole.
Borehole DH-GAP04	Date	Comment
Drilling: borehole length 687.0 m and vertical depth 649.1 m	June 18–28, 2011	75.8 mm diamond drilling using double tube NQ2 equipment, providing a 50.7 mm core. Drilling water was heated and spiked with sodium fluorescein (C <sub>2</sub> OH <sub>10</sub> Na <sub>2</sub> O <sub>5</sub> ).
Deviation survey	June 29, 2011	GyroSmart method.
Circulation of hot water in the borehole	June 29–July 1, 2011	To prevent the borehole from freezing.
Posiva Flow Log testing	July 1–2, 2011	Measures the specific capacity and hydraulic head in fractures/fractured zones in cored boreholes.
Circulation of hot water in the borehole	July 2–7, 2011	To prevent freezing of the hole and to allow preparation of the downhole multipacker system.
Installation of multipacker system, fibre optical DTS cables and inflation of packers	July 7, 2011	Two inflatable packers and related instrumentation allowing groundwater sampling and monitoring from three sections.

The aims of the groundwater sampling and analysis campaigns were to:

1. Provide groundwater samples from a talik to increase understanding of the role of taliks in hydrogeological systems in continuous permafrost.
2. Enhance understanding of the geochemical evolution of groundwaters in a glacial environment, especially the influence of meltwater intrusion and permafrost formation. The achievement of these goals is aided by porewater and fracture mineral studies.
3. Examine water composition at depths of approximately 500 m below ground surface or deeper.
4. Provide chemistry data for modelling of the hydrogeological system.
5. Improve the understanding of the role of springs in the hydrogeological system, since springs, similar to taliks, could be potential locations of discharge.

Water samples from DH-GAP01 representing the water in the through talik beneath the Talik lake (L26) were collected in September, 2009, September, 2010 and September, 2011.

Water sampling of DH-GAP04 was carried out shortly after the drilling in September, 2011. A second sampling campaign was carried out in September, 2013.

Water types considered representative of groundwaters include the talik-related water in DH-GAP01, the deep waters in DH-GAP04, and the Leverett spring water (Figure 2-21).

Waters from DH-GAP01 and DH-GAP04 were analysed for a full suite of chemical parameters, as well as  $\delta^{18}\text{O}$ ,  $\delta^2\text{H}$ ,  $^3\text{H}$ ,  $\delta^{37}\text{Cl}$ ,  $^{87}\text{Sr}$ , and  $\delta^{34}\text{S}$  and  $\delta^{18}\text{O}$  of  $\text{SO}_4$ , and sodium fluorescein ( $\text{C}_2\text{OH}_{10}\text{Na}_2\text{O}_5$ ). In addition  $^{36}\text{Cl}$  was analysed in waters from DH-GAP04.

For a detailed description of the groundwaters, sampling methodology and results see Data Report 2016.

#### **2.4.7 Sampling and analysis of rocks and fracture minerals**

##### ***Fracture infilling studies***

Physical and chemical characteristics of secondary minerals within the fracture network in the study area were examined to provide insights into palaeohydrological processes in bedrock (e.g. hydrothermal, metamorphic or glacial events). Fracture infillings from the drill cores (DH-GAP01, DH-GAP03 and DH-GAP04) were mapped to investigate the mineral distribution, providing a general insight into the fluid history, and analysed in three different ways:

1. Analysis of carbonate minerals and sulphates (gypsum) to study their mineralogy in the drill cores.
2. Analysis of stable isotopes and fluid inclusions of calcite infillings to characterise past fluid environments in terms of trapping temperature.
3. Examination of redox-sensitive minerals (Fe-oxyhydroxides, pyrite, Mn-oxyhydroxide) and redox-sensitive elements (Ce U, Mn and Fe) to 1) gain information on redox transitions in the bedrock fractures (i.e. the change from oxidizing conditions near the ground surface to reducing conditions prevailing at greater depth); and 2) gain information about the depth of intrusion of oxygenated waters in the bedrock fractures. *Uranium Series Disequilibrium* analyses (USD) were conducted to provide constraints on the timing of changes in redox conditions.

##### ***Porewater studies (crush and leach, DH-GAP04 porewater analysis)***

Two methodologies were used to investigate the matrix porewater end-member and to observe possible long term changes in the groundwater system. The crush and leach technique was applied by the University of Waterloo (Data Report 2016). Two additional porewater extraction techniques (diffusive exchange and out-diffusion) were employed by the University of Bern (Eichinger and Waber 2013).

##### ***Petrophysical studies DH-GAP01, DH-GAP03 and DH-GAP04***

To provide an overview of the variations in rock type and in rock physical properties, which have impacts on many of the features investigated by the GAP, petrophysical analyses were performed using material from DH-GAP01, DH-GAP03 and DH-GAP04 drill cores. Parameters such as porosity,

density and thermal conductivity are essential when studying the growth of permafrost and the interactions between matrix waters and fracture waters, as well as for interpreting geophysical investigations (e.g. SAMPO) and carrying out thermal modelling. The Data Report (2016) presents the results of the petrophysical analyses.

### **Key outputs**

The felsic and mafic rock types from the GAP cores have different densities as expected. In general, the felsic and mafic rocks have similar matrix porosities. In DH-GAP01 and DH-GAP03 matrix porosities range from 0.2 to 0.6%, averaging around 0.45%, whereas the range for the matrix porosities in DH-GAP04 is 0.2 to 1.32%. This broader range is related to a group of felsic rocks, with matrix porosities of 0.9 to 1.32%, occurring between 500–650 m borehole lengths in DH-GAP04. The reasons for these higher porosities are currently unknown. The range of porosities for intact rock is relatively wide (0.2–1.32%). Although only little information on the mineralogy or the geochemistry of the rocks in the research area exists, it can be assumed that the mineralogical compositions of the main rock types differ, which potentially contributes to differences in their thermal properties. The average radiogenic heat production for felsic rocks in DH-GAP04 is  $0.36 \mu\text{W}/\text{m}^3$ , whereas the average for the mafic rocks is  $0.22 \mu\text{W}/\text{m}^3$ . The thermal conductivity does not correlate with rock type: the calculated average  $2.50 \text{ W}/\text{mK}$  for all three drill cores is considered to be representative of bedrock in the research area. The results suggest that geology in the research area has only a minor impact on permafrost thickness due to its relatively uniform thermal properties.

### **2.4.8 Monitoring of water pressure, temperature and electrical conductivity**

Boreholes DH-GAP01 and DH-GAP04 are instrumented with downhole sensors allowing monitoring of P, T and EC. These quantities have been monitored in DH-GAP01 since June 2009, and in DH-GAP04 since July 2011. Lake level variations in the Talik lake (L26, Figure 2-21) have been monitored by the GRASP since September 2010.

The aims of the instrumentation were to obtain continuous long term monitoring records of the hydraulic and hydrogeochemical behaviour of: 1) the presumed through talik (data from borehole DH-GAP01), and 2) groundwater below the permafrost (data from borehole DH-GAP04). It was particularly important to cover the onset of melting during spring and freezing during the fall, when changes in hydraulic gradients are expected.

The purpose of the monitoring of the GAP boreholes was to obtain high quality chemical, physical and hydrogeological information about the sub-permafrost environment, and to enhance knowledge about underlying, often complex processes that govern time-dependent variations in the monitored parameters. For detailed information on the monitoring see the Data Report (2016). The results are also discussed in this report in Sections 3.3 and 4.3–4.6 and conceptualised in Chapter 5.

### 3 Summary of main areas where process understanding was increased through the GAP

This chapter presents the different scientific disciplines where process understanding was increased through the GAP. These disciplines are **ice sheet hydrology** (Section 3.1), **hydrogeology** (Section 3.2) and **hydrogeochemistry** (Section 3.3). Each section starts by presenting the knowledge base prior to the GAP, after which the key findings and advances are presented and discussed, followed by remarks concerning remaining challenges. Given that there were differences in the level of process understanding between these three disciplines at the initiation of the GAP, the level and maturity of technical details in the knowledge obtained vary between the disciplines. More specifically, the reasons for the differences between the disciplines and results presented are the following:

- The understanding of the GAP site, including the processes acting within the site, prior to the start of the GAP was quite different for each of the three disciplines. The ice sheet hydrology group started the project with a conceptual understanding of the site that relied on numerous field investigations and numerical modelling studies of glaciated settings, whereas both the hydrogeology and hydrogeochemistry disciplines started the project with a solid knowledge of numerical modelling work on glaciated sites and understanding of previously glaciated areas, but these disciplines had essentially no field data from the GAP or similar sites at the start of the project.
- The ice sheet data and interpretations presented by the GAP are not as site dependent as the hydrogeology and hydrogeochemistry data. Also, the latter two disciplines have data from a few boreholes only, whereas the investigation program on the ice sheet had a much greater spatial range.

#### 3.1 Ice sheet hydrology

Early understanding of ice sheet hydrology was largely based on generalised knowledge transfer from small glacier hydrology (in this case, specifically, valley glacier hydrology), which had been developed over many decades e.g. summarised in Jansson et al. (2007). Questions have been raised as to what extent the understanding of smaller glaciers, typically a few or a few tens of km in length, could be applied to processes at the ice sheet scale. The lack of field investigations prior to the GAP provided little opportunity to gain sufficient insight on ice sheet processes, other than speculations and estimates based on indirect information and modelling using the best possible, yet still poorly constrained, boundary conditions. The status of knowledge on ice sheet hydrology was summarised by Jansson (2010).

A ground-breaking study by Zwally et al. (2002) showed that water inputs from surface to bed could be responsible for ice sheet velocity variations despite a kilometre thick sub-freezing ice sheet. Such a coupling had previously been inferred from palaeoglaciological observations, but evidence for the mechanisms involved had not previously been published. The Zwally et al. (2002) study prompted initiation of many studies in Greenland simultaneous with the initiation of the GAP project.

##### 3.1.1 Basal thermal conditions

The basal thermal boundary condition is one of the key aspects of the interaction between ice sheet hydrology and groundwater hydrology because liquid water can only exist at the bed when the ice temperature is at the pressure melting point. The thermal conditions at the base of an ice sheet are determined by the balance of many different heat sources and sinks which are generally governed by climate, geothermal and thermo-mechanical ice flow processes. Important factors include the vertical (both up and down) and horizontal advection of ice, geothermal heat flow at the basal boundary, conductive heat exchange with the atmosphere, mass accumulation and loss, strain heating as the ice deforms, frictional heating where the ice slides over its base, and latent heating where water refreezes. The relative contribution of each factor varies tremendously in time, and with position within the ice sheet.

## **Previous knowledge base**

In the GrIS, the modelled conditions within the ice are poorly constrained without information on the geothermal fluxes at the base of the ice sheet. Näslund et al. (2005) showed how modern-day geothermal fluxes vary substantially across the Fennoscandian shield based on extensive field measurements. Similar conditions could be expected beneath the GrIS as well, but due to the presence of the ice sheet only a few point measurements exist across the entire ice sheet.

The GAP starting point for understanding the ice sheet's basal conditions was a conceptual picture common in the glaciological literature over prior decades. In this conceptual model, the bed was considered to have a frozen central area surrounded by an area of melted conditions, which in turn gives way to frozen conditions in a zone of thin ice near the edge of the ice sheet. The only way to constrain thermal zonation is by numerical models, because direct measurement over wide areas of the ice sheet is not possible. Unfortunately, reported model outputs varied from almost entirely frozen conditions to almost entirely melting conditions, depending on model structure, input parameters, and the chosen boundary conditions. Hence, previous modelling results provided few conclusive constraints on conditions at the GAP area.

In addition to the general zonation of basal conditions, there was an agreement that the bed might also exhibit patchiness with melting conditions in lower elevation areas, and frozen conditions in areas where the bed is more elevated. Since the topography in front of the ice sheet was assumed to continue beneath the ice sheet, the relief seen in the proglacial area would also be reflected in the basal topography. It was, of course not known to what extent these conditions would prevail as one moves further in under the ice sheet except that the relief was thought to decrease inland. The latter was a postulate based on existing coarse resolution bed topography datasets (Bamber et al. 2001).

## **New results**

The GrIS investigation undertaken by the GAP project has resulted in new and detailed information about the basal thermal field under ice sheets. This knowledge has been gained from both direct field measurements, and new advances in numerical modelling guided by the field observations collected by GAP, and by assimilation of other newly available observational datasets (e.g. Joughin et al. 2010) as discussed below.

### ***Direct measurements of basal temperatures***

**Bed observations** – The GAP project yielded direct observations of thermal conditions at the basal boundary via the network of boreholes drilled to the bed (Section 2.3). All boreholes intersecting the ice sheet bed (23 in total) revealed melted bed conditions and abundant water. These boreholes are concentrated near the outer margin of the ice sheet, from 30 km inland to less than 200 m from the ice margin. These observations provide the first direct evidence that near the ice sheet margin the ice is not frozen to the bed. In addition, since the boreholes were widely distributed, it is highly unlikely that the boreholes only intersected discrete water pathways (i.e. subglacial channels) leaving wide expanses of frozen bed between the holes. The GAP borehole data therefore strongly suggest that the entire bed, extending from the margin to several tens of km inland, is melted rather than primarily frozen. Furthermore, the analysis of radar data collected within GAP suggests that the bed has abundant water from the margin to at least 120 km inland where the surface altitude reaches 1,200 to 1,400 m a.s.l.

**Ice temperatures** – The GAP project also documented the internal temperature of the ice mass through borehole temperature measurements (Section 2.3). These investigations have revealed a complex thermal profile exemplified in Figure 3-1. The surface is influenced by seasonal swings, and then temperatures cool with depth to about half way through the ice thickness. In the lower half of the ice thickness, temperatures increase with depth toward the bed until reaching the pressure melting point. The ice is at the pressure melting point in a layer above the bed, and this layer increases in thickness along the ice flow direction from tens of m thick at 45 km from the ice margin, to more than 150 m by 30 km from the ice margin. This implies that local heat sources warm the ice near the bed, from frictional heating and/or latent heat supplied by freezing basal water and perhaps strain heating from enhanced deformation in the warm layer. Within a few km of the ice margin, the entire thickness of ice is at the pressure melting point. Ice near the margin may also experience warming from above by refreezing meltwater, and from within by strain heating.

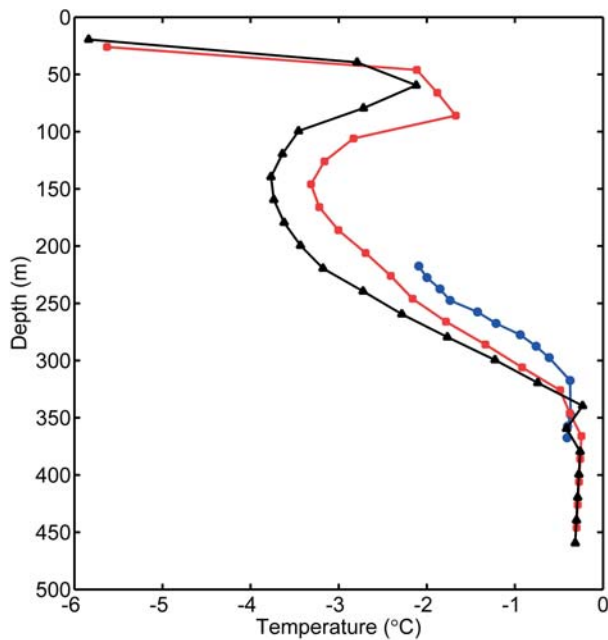


**Figure 3-1.** Ice temperatures for boreholes GL 11-1A (blue), GL 11-1B (red) and GL 11-1C (black). The three boreholes are about 20 m apart, and are located approximately 30 km from the Isunnguata Sermia terminus (see Figure 2-16). Data capture from GL 11-1A did not yield a full profile. Depth units are relative to the initial ice surface at the top of the borehole. The ice-bed boundary is located approximately 5 m below the lowermost temperature measurement.

The presence of a layer of temperate ice again suggests that melted bed conditions are widespread across the ablation zone, since it is unknown how such a thick warm basal layer could develop only locally. The internal ice temperatures also provide valuable constraints for increasing confidence in numerical investigations of the ice-bed boundary. Those studies have been primarily focused on the ice sheet's movement; but they do offer useful overlap with and are complementary to the GAP's goals of understanding the subglacial hydrological conditions.

### **Modelling of basal temperatures**

**Frozen/Melted Transition** – Initial modelling efforts as part of the GAP employed a full stress (i.e. including all components of the stress tensor), thermo-mechanically coupled numerical model to explore the interaction between motion and basal thermal conditions in the GAP study area (Brinkerhoff et al. 2010). This work investigated the boundary between the frozen interior of the ice sheet and the melted outer regions. The boundary was termed *the frozen/melted boundary* (FMB).

The precise location of the FMB cannot be accurately predicted from modelling, since numerous poorly constrained parameters must be input to any ice sheet model. For example, HFD (or geothermal heat flux) beneath the ice is a key input parameter, which originates from interpolated datasets derived from geologic models which carry substantial uncertainty. Consequently, this study explored the sensitivity of the FMB to changes in sliding speed and to prescribed geothermal heat fluxes spanning a wide range, including the values measured in the proglacial GAP bedrock boreholes, by applying perturbations to each of these parameters. This resulted in model outputs depicting the thermal field of the entire ice mass, including the basal temperature field (e.g. Figure 3-2).

The position of the FMB was shown to be highly sensitive to the prescribed geothermal heat flux below an upper threshold. With higher heat flux values, the entire bed except for the area immediately below the ice divide is melted, and the small frozen area remains relatively robust to choices of geothermal heat flux. The position of the FMB is relatively insensitive to perturbations applied to the basal traction field. This insensitivity is due to the short distances over which longitudinal stresses act in an ice sheet. Hence, a rapid increase in the sliding speed of the ablation zone does not have the effect of “pulling” the interior frozen portion of the bed toward the margin, or vice versa.

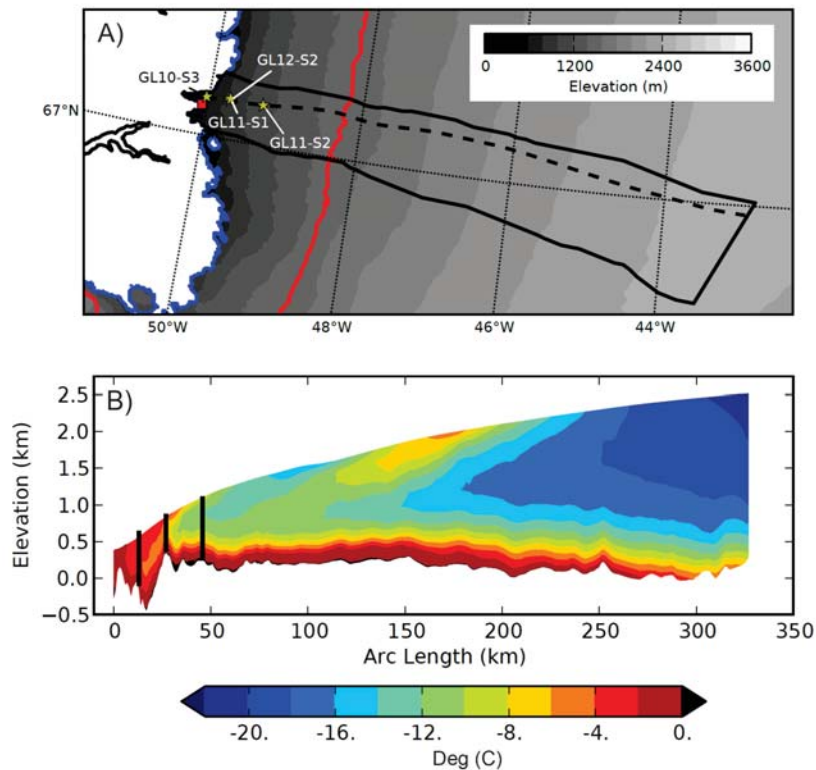


**Figure 3-2.** Modelled ice temperature field along a transect through the GAP study domain. A) 3D model domain shown by solid black line and 2D transect shown below is indicated by dashed line. Red line indicates approximate position of the equilibrium line. Grey shading indicates surface elevation bands. S in the borehole ID:s (e.g. GL 11-S1) stands for site, such as Site 1 or Site 2 etc. B) Modelled temperature field. Vertical black bars denote locations of boreholes with temperature measurements, some of which are slightly out-of-plane with the model domain.

The position of the FMB was also found to be highly sensitive to not just the basal boundary condition, but also the surface boundary condition. This prompted a focused and detailed study of the impact of improved surface and bed boundary conditions on the modelled basal thermal field (Meierbachtol et al. 2015). The boundary conditions were improved by incorporating new and detailed field data from the region. The surface boundary was shown by measurements to be far warmer than predicted by the atmospheric models for the 2 m ice temperature (i.e. RACMO2, MAR) that are typically used to constrain ice sheet models (Figure 3-3). The measured near-surface temperatures are warmer than common surface temperature datasets by up to 14°C in the percolation zone, and 10°C in the ablation zone. This substantial difference is reflected in the new data-driven surface boundary which is, on average, more than 5°C warmer than the RACMO surface temperature. The GAP's geothermal gradient measurements were combined with other observational data in southern and central Greenland to generate a new observationally-based interpolation of geothermal heat flux. Due to low heat flux values in both the GAP borehole and other observations, the new basal boundary had a substantially lower heat flux than the values derived from geologic models. For example, much of the domain had heat flux values on the order of 30–40 mW/m<sup>2</sup>, which is nearly half the heat flux represented in prior models.

The refined boundary conditions were implemented into the numerical ice flow model for the study domain. Taken alone, the lower geothermal heat flux caused substantially colder bed conditions with frozen basal conditions across the ablation zone. When the warmer surface (from refreezing of surface meltwater) was taken into account, however, melted basal conditions resulted, with the model output more closely matching the observations (Figure 3-4). Warmer surface ice and firn introduced several times more energy to the ice mass than the decrease at the bed due to reduced basal heat flux. Hence, meteorological and latent heat processes at the surface and within the ice, play a key role in dictating the spatial distribution of melted conditions and the quantity of basal meltwater that can be generated

(Meierbachtol et al. 2015). Although a precise description of the transition from frozen to melted conditions is neither possible from observations nor model output, all the results imply that the vast majority of the bed is not frozen. For all choices of boundary conditions and modelling parameters believed to be reasonable, the frozen area extends many tens of kilometres away from the ice divide but greater than 75% of the study transect is in a basal melted state.

### Key advances

GAP research has provided both direct evidence and modelling results that advance the understanding of basal thermal conditions of this region of the GrIS. Direct borehole evidence suggests the entire outer flank of the ice sheet (i.e. the ablation zone) has a melted bed rather than a universally or locally frozen bed. The boundary between melted and interior frozen conditions is highly sensitive to geothermal heat flux values, but relatively insensitive to the sliding speed of the ice which generates frictional heat (Brinkerhoff et al. 2010). However, the surface boundary condition can also have a strong influence on the spatial distribution of frozen/melted bed conditions.

Several aspects of the new knowledge are directly relevant to safety assessments of deep geological repositories. The GAP found no evidence to suggest that a complex pattern of patchy frozen/melted bed conditions must be considered in the marginal regions of an ice sheet in a state of retreat (i.e. an ice sheet in a similar state to the present GrIS). Evaluation of the heat budget at the bed must take into account both the sliding speed of the ice, and the role of the surface boundary condition in influencing internal ice temperature all the way to the bed. Wet-based conditions are extensive across a wide reach of this region of the ice sheet, and this consistency during deglaciation phases makes its representation in models relatively straightforward. Further, geothermal heat flux has been shown to be a highly influential uncertainty for understanding this setting in Greenland, where the presence of ice prevents direct measurement of heat flux in bedrock. In contrast to Greenland, geothermal heat flux can be measured at proposed repository sites and their surrounding regions, which in turn results in better constrained model predictions.

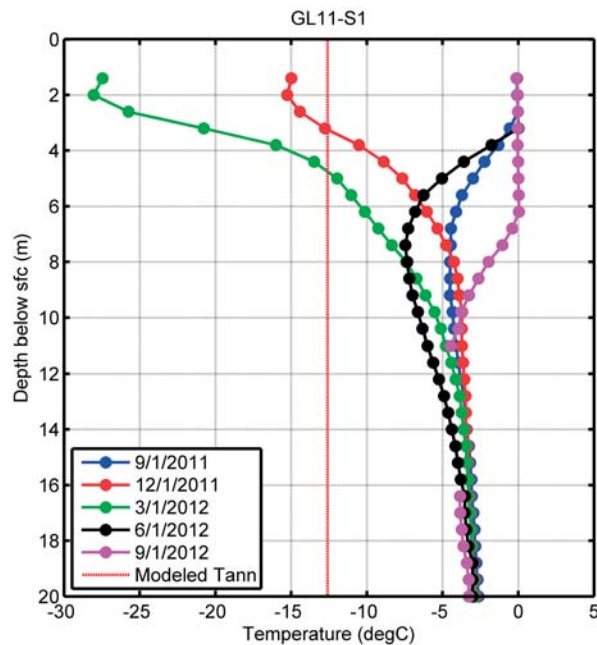


**Figure 3-3.** Measured temperature profiles at a site located 30 km inland from the terminus of Isunnguata Sermia. The different time slices shown bracket the seasonal temperature swings of surface ice, and define the mean annual temperature to which values converge near 20 m depth. The vertical red line shows mean annual temperature of the ice as modelled with the RACMO2 atmospheric based model. S in GL 11-S1 stands for Site 1. Sfc = surface.

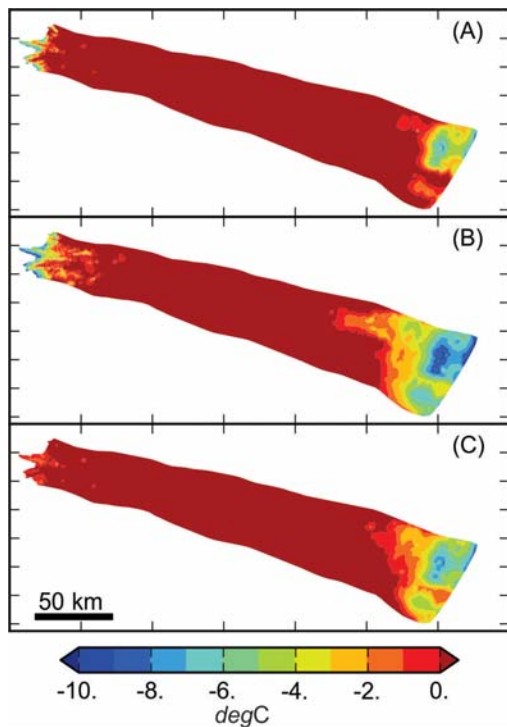


**Figure 3-4.** Basal temperature showing frozen and melted regions from three different modelling scenarios: (A) Previous (pre-GAP project) datasets for geothermal heat flux; (B) recently determined geothermal heat flux values which are lower than past values; and, (C) both lower geothermal heat flux and warmer surface conditions, which is considered the most plausible situation (Meierbachtol et al. 2015). Colour bar is consistent across all three panels. Scenario B produces the greatest region of frozen bed, with areas both near the margin and the interior frozen. Scenario C has a slightly subfreezing margin area, which measurements show to be incorrect, likely because the model does not sufficiently account for latent heat from meltwater. Figure 3-2 shows the model domain with respect to ice sheet margin which is located at the left side of the figure.

### Remaining challenges

The new findings demonstrate discrepancies between the measured upper boundary condition and the ice surface boundary condition simulated by current atmospheric models, and that this difference impacts modelling of the ice sheet's internal and basal temperature fields. The first order representation of basal thermal conditions is insensitive to the two different surface boundary conditions, but further refinement of the surface boundary condition is needed to improve important details of the basal thermal field. Further, although this project has yielded the most comprehensive direct measurement of an ice sheet's internal temperature distribution to date, the data still represent a small number of observations within a very large ice sheet. Additional measurements, some of which are currently underway, will further refine modelling efforts and reduce uncertainties.

### 3.1.2 Surface water generation

On an ice sheet's surface, water is generated from rain and from melting of snow, firn and ice. Due to the large elevation variation of the ice sheet surface, there is usually a zonation from completely sub-freezing conditions and no runoff at higher elevations, to increasingly warmer conditions at lower elevations and eventually, substantial amounts of runoff. This zonation has been shown to vary substantially from year-to-year on Greenland (Abdalati and Steffen 2001). The ELA marks the elevation where long term average annual gains and losses match, but melt does occur above the ELA and a relatively minor fraction is assumed to run off. Where liquid water at the surface is abundant enough to induce runoff flow, features such as slush swamps, streams, and lakes commonly form, and the pooled water can, in principle, also reach the bed.

## Previous state of knowledge

From earlier studies, connections between the ice surface and the bed were known to be common in the ice sheet margin areas. For example, Thomsen et al. (1989) mapped the surface hydrology of an approximately 20×40 km section of the ablation area of the GrIS and showed that hundreds of catchments existed, each terminating with a moulin draining water below the ice surface, and eventually to the bed of the ice sheet. Evidence was also emerging that surface-to-bed connections were possible through the cold and km-thick ice higher on the ice sheet near the ELA. Several theoretical (e.g. Alley et al. 2005, van der Veen 2007) and observational (e.g. Das et al. 2008) studies undertaken after Zwally et al. (2002) provided a basis for our understanding that surface-to-bed connections do exist through substantial ice sheet thicknesses of cold, sub-freezing temperature ice.

## Key improvements

By adding the GAP automatic weather stations (i.e. energy balance stations, Section 2.2.2) to the K-transect along the southern extent of the GAP study area (van de Wal et al. 2005), a denser dataset has been gathered for the purpose of facilitating modelling of ice surface melt on diurnal, seasonal and annual time scales. These data have been used to drive a highly detailed melt model for the GAP region (van As et al. 2012), which provides high-resolution coverage in both time and space of melt variations over the GAP study area. The ice surface across the study region melts by up to 3–4 m/yr. Rainfall adds a less substantial volume to the water available at the surface. The volume of surface melt produced in the Russell catchment is highly variable from year-to-year, for example approximately 0.3 km<sup>3</sup> in 2009 and 0.8 km<sup>3</sup> in 2010 (Figure 3-5). Similarly, while the peak melt typically occurs in July, the length of the melt runoff season varies between years with significant runoff starting sometime in May and ending sometime in September. Importantly, surface melt and runoff are a summer phenomenon limited to 3–4 months in duration. The meltwater generated at the surface each summer exceeds the amount of modelled basal melt by two orders of magnitude (cm of basal melt at the bed vs. m of surface melt). The summer melt period therefore completely dominates the annual cycle of water availability beneath the ice.

Surface lakes on the ice sheet have attracted much attention in recent scientific literature. An understanding of the importance of and role of these lakes in the hydrological system has developed over the course of the GAP. Observations indicate that lakes are often associated with the establishment of surface-to-bed drainage (Das et al. 2008). The propagation of a crack requires pressures higher than ice pressure at the crack propagation point; an open fracture completely filled with water fulfils this requirement. Lakes constitute storage of water that can aid the crack propagation process by providing an ample water supply during formation. A reasonably sized lake may correspond to several days of discharge in a river flowing on the ice sheet surface. For example, a 1 km<sup>2</sup> lake with an average depth of 5 m contains the same volume of water as provided by a surface river discharging 10 m<sup>3</sup>/s for 5.8 days. Thus, if crack propagation towards the bed requires a volume that is not easily met by river discharge alone, a lake is the only possibility to provide the extra water required.

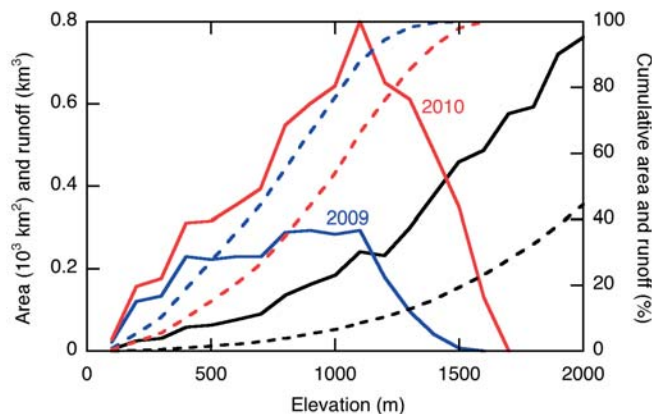


**Figure 3-5.** Russell Glacier catchment surface area (black) and surface meltwater runoff for 2009 (blue) and 2010 (red) per elevation bin. Dashed lines illustrate cumulative values (from van As et al. (2012)). For catchment delineation see Figure 1-4 and Figure 2-10.

While lake drainage events are one of the mechanisms for establishing moulin drainage features, their role in the overall hydrological system is not dominant. A detailed study of the Russell catchment found that lakes cover about 2% of the ice surface (Fitzpatrick et al. 2014). By storing water, the lakes delay the runoff of 7–13% of the bulk meltwater eventually discharged from the region (Figure 3-6). Less than one third of the lakes drain rapidly (i.e. in drainage events shorter than 4 days). Further, many lakes only drain to other streams and downstream lakes, and do not drain directly to the bed. However, when lakes do drain catastrophically to the bed, the pattern of ice surface uplift in the immediate vicinity (an area of 100s of m to 1 km in diameter) implies that the basal hydrological system is subject to volume increases and perhaps increased pressure (Das et al. 2008, Doyle et al. 2013). Such perturbations resolve after a period of a few days at most.

### Remaining challenges

Melt and melt proxies continue to be measured for a variety of projects and the Russell Glacier/Isunnguata Sermia sector remains one of the most intensely studied areas on Greenland, ensuring continuous environmental data for future use in evaluating the GAP data. Much remains to be learned about routing of meltwater once it is generated, for example the routing from the surface to the bed. However, it has clearly been established that substantial surface meltwater does penetrate the ice and eventually reaches the bed.

### 3.1.3 Water pressure level and variability

#### Previous status of knowledge

Information about the hydraulic pressure regime at the base of the ice sheet was severely lacking at the start of the GAP. There were recent observations that parts of the GrIS experiences daily and seasonal changes in velocity, which implied that the basal drainage system is equally dynamic. The first study to demonstrate this (Zwally et al. 2002) was published less than a decade prior to the start of the GAP and was considered a major paradigm shift in the understanding of ice sheets. Numerous similar studies have since followed and have clearly documented the time-space variability of surface velocity and inferred a link to changes in sliding speed caused by changes in the water drainage system.

With the growing body of literature focused on interpretations of the basal drainage conditions inferred from measurements of surface velocity, many details regarding the state of Greenland's basal water system remained unknown or unverified. In particular, much speculation existed regarding the seasonal development of a subglacial conduit network. In mountain glaciers, conduit systems are known to develop during the summer months and serve to increase the efficiency of the drainage system in response to the large input of surface meltwater during the peak melt season (Cuffey and Paterson 2010). The high capacity of the conduits effectively dewater the bed, increasing the coupling between ice and bedrock. Secondly, since melt varies on a daily cycle, the conduit networks experience very low pressures during times of low input (i.e. morning hours) and high pressures when water input peaks (i.e. during late afternoon or during rain storms).

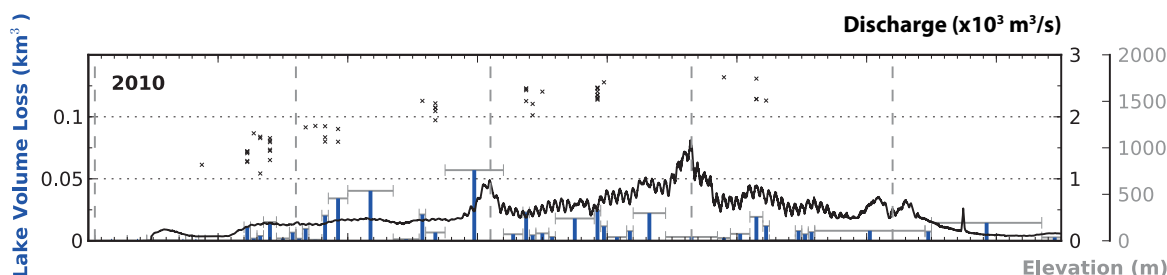


**Figure 3-6.** Lake volume loss within the Kangerlussuaq sector of the GrIS and Watson River discharge in 2010. Blue bars show estimated volume loss scaled to the left axis. Error bars represent uncertainty in timing. Black curve shows measured discharge of Watson River, scaled to the first right axis. The drainage date and elevation of rapidly draining supraglacial lakes are also shown (black dots), with their elevations referenced to the second right axis. From Fitzpatrick et al. (2014).

The sediment cover on the bed also influences the development of the basal drainage system and the distribution of water across the bed. The bed condition is therefore an important consideration for determining groundwater recharge. Observations at the terminus do not uniquely constrain the bed conditions further upstream: debris-charged ice is not necessarily a sign of a basal sediment layer but may represent the existence of loose material that can be entrained by the basal ice; also, turbid water may indicate active crushing by ice moving over its substrate and is, as such, not necessarily an indicator of a sediment layer. Direct observations of the bed were only point observations at ice divides; places where basal motion is low and the bed is frozen, and thus sediment is more easily preserved.

### **Key improvements**

Water pressure at the bed of the ice sheet can be characterised by several different metrics. Any analysis that includes the water pressure of the basal boundary should consider the form of basal water pressure that is most relevant to the problem. Factors that govern the metrics relevant to a given problem include: 1) the significance of points in time relative to time-averaged pressure; 2) the significance of local conditions relative to space-averaged conditions; and, 3) the relative significance of the absolute magnitude of pressure versus the gradients in pressure over time and/or space.

The GAP project investigated these issues by drilling 23 ice boreholes to the bed for directly measuring basal water pressure and for conducting related experiments. The discussion below is limited to the ablation region of the ice sheet within approximately 30 km of the ice margin, as targeted by the ice borehole study. Discussions of conditions above the ELA are conceptual in nature, and are therefore presented in Section 5.1.

### **Bed Conditions**

Observations made in the network of ice boreholes used multiple methods for investigating bed cover, including direct sampling of bed materials (Figure 3-7), ice borehole photography, bed-penrometer tests, and interpretations of pressure gradients during both passive monitoring and active impulse tests. Results from all 23 ice boreholes are consistent in implying that the bed consists of bedrock covered by a relatively thin veneer of sand and gravel-sized sediment (Figure 3-8, Data Report 2016). The sediment cover appears to be patchy, with some areas having minimal sediment coverage and others with a sediment cover reaching several decimetres in thickness. Fine sediment was noticeably lacking, implying that such grain sizes are washed away with flowing water. The ice itself often carries debris in a layer extending to, at most, approximately 10 m above the bed. The size of the debris may extend up to very large boulders plucked from the bed, based on observations of glacial erratics (large boulders deposited by ice) at the margin.

Whereas the ice borehole results imply a veneer of coarse sediment, they also suggest that no continuous layer of thick and soft till, i.e. fine grains with altered mechanical and hydrological properties, extended beneath any of the ice borehole sites. No clays or even silts were sampled in ice boreholes and the nature of the pressure changes in particular, is inconsistent with a till layer. For example, high pressure gradients (e.g. 50 m of head difference) were observed over distances of just 20 m (Figure 3-9). Such large gradients and sudden gradient changes would not be expected from Darcy-type flow through a homogenous sediment layer, but are consistent with a basal drainage system developed on a 'hard' bed with irregular and perhaps transient pathways for water flow.

Importantly, interpretations of seismic data collected on Russell Glacier implied sediment cover beneath the study sites (Booth et al. 2012, Dow et al. 2013). Because the crevassed ice surface yields highly noisy data, new methods for seismic analysis were required to interpret the data. Those methods implied that the 500 m long study region was underlain by sediment. This finding does not necessarily conflict with the above ice borehole observations for several reasons. First, the characteristics of the sediment cover remained unclear from the seismic analysis, leaving open the possibility for agreement with the coarse sediment observed in ice boreholes. Second, the ice borehole measurements are point measurements and the seismic data were collected along two short transects located many 10s of km away from the ice boreholes. The bed conditions likely vary in space across the study reach.



**Figure 3-7.** Photograph showing sample of bed material collected in a 700 m ice borehole GL 12-2B located about 30 km from the terminus. Sand size grains dominate the sample and fine grains and clays are notably lacking.

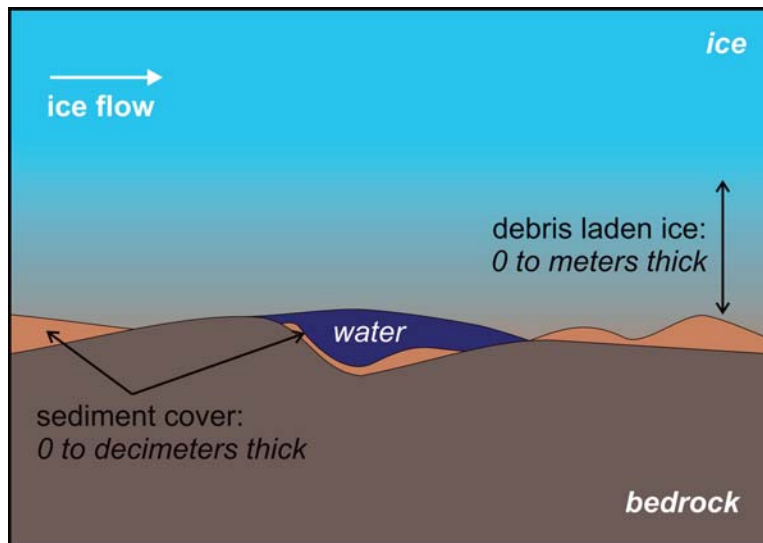


**Figure 3-8.** Conceptual view of bed conditions based on several types of observations in ice boreholes (see text). Note that cartoon is not to scale. Sediment cover on the bed is mostly gravel and sand sized grains, and occupies a patchy network with occasional areas of bare bedrock. Entrained sediment in ice is 0% to perhaps as much as 20% by volume. High water transmissivity can occur in basal drainage system where water cavities are highly linked. Basal drainage system transmissivity is time variable, and related to 1) the water flux that can open/close connectivity through melting of the ice walls and/or uplift of the ice mass, and 2) the sliding speed of ice over the bed which can open/close cavities in the lee side of bedrock bumps.

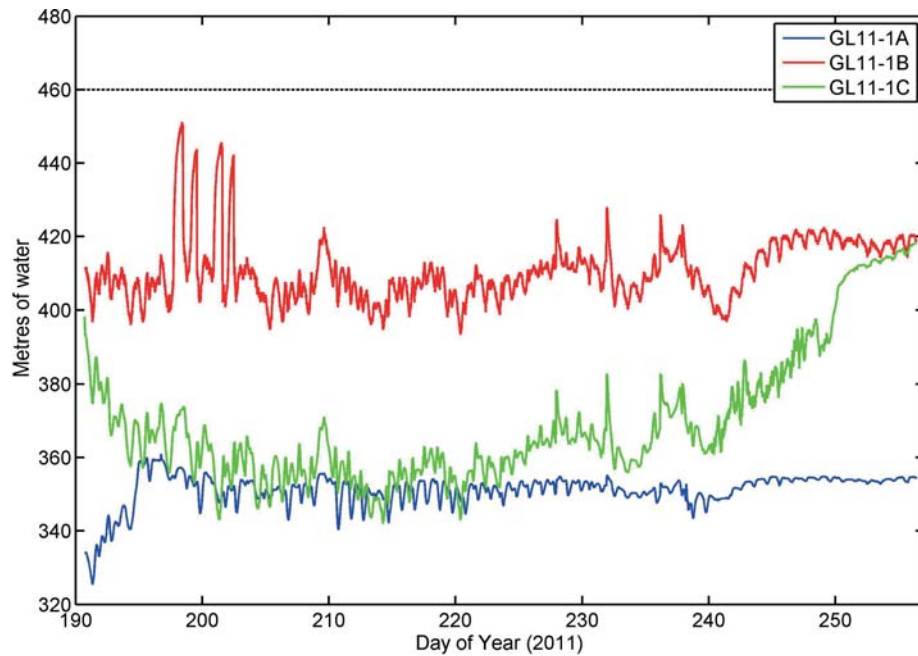


**Figure 3-9.** Basal water pressure over a 60 day period of 2011 at site GL 11-1, located about 30 km from the terminus of Isunnguata Sermia. Y-axis shows basal pressure expressed as a column of 0 degree Celsius water. The three ice boreholes are arranged in a triangular pattern with 20 m on a side. Day 190 is 9 July; day 250 is 7 September. Black horizontal line at 460 m denotes ice thickness at borehole sites. Note the large pressure gradients between hole GL 11-1B and the two other ice boreholes.

### Basal Water Pressure

The GAP *in situ* measurements of water pressure, collected in 23 ice boreholes and spanning time intervals of minutes-to-years, have elucidated the envelope of basal pressure conditions within 30 km of the ice margin. The relative consistency of the multiple measurements at each of the sites, and between the different sites, implies that conditions would not be expected to differ substantially in other comparable ice sheet settings. The basal water pressure was not found to be a constant value, but was shown to vary depending on the time and spatial scales. Hence, the pressure must be described by both its magnitude and by its spatial and temporal gradients. The spectrum of pressure limits is summarised in Table 3-1.

#### Long Time/Length Averages

The ice borehole water pressure measurements suggest that the basal water pressure is most appropriately described as the ice overburden pressure when distances of km and time periods of years are considered. All ice borehole sites demonstrated pressures near overburden pressure for the majority of the year (Figure 3-10). Overburden pressure is typically a slight over-estimate of actual pressure, as the measurements suggest water pressure is most commonly slightly below this value. Note that the calculated overburden pressure is dependent on chosen ice density, which has not been measured and can vary by several percent due to bubble content. A standard assumed density of  $900 \text{ kg/m}^3$  was used here.

Diurnal and seasonal changes in pressure occur at all locations, causing the pressure to drop below overburden pressure for some time periods. However, reduced pressures occur only during a limited time-fraction of the day and year, and the magnitude of the reduction diminishes with distance inward from the margin. In locations where the pressure does drop substantially below ice overburden pressure, this occurs for limited portions of the day. Further, such locations are not likely to be uniformly distributed over the bed. Theory suggests that the low pressure regions are limited to portions of the bed that are well-connected to high transmissivity drainage features, and our measurements show that points only tens of metres away from a location with fluctuating pressure may remain steady at overburden pressure. Hence, the high pressure areas located between lower pressure zones increases the average pressure for the region as a whole relative to just the lower pressure high transmissivity zones.

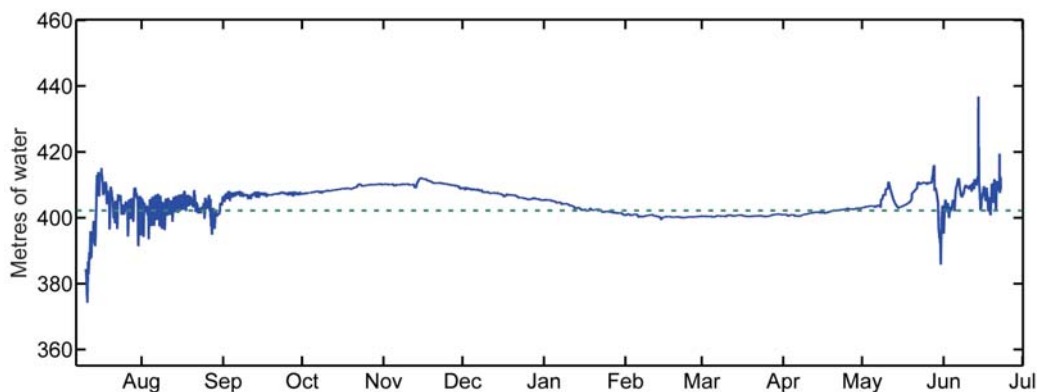


**Figure 3-10.** Pressure record from borehole GL 11-1C for period July 2011 to late June 2012. Data plotted as m of water equivalent above the bed; full ice thickness is 460 m. Dashed green line shows time-average water pressure for the period of record, and corresponds to 98% of overburden pressure.

### *Time/Space Gradients*

Since the magnitude of the basal water pressure is a direct function of the thickness of the ice, pressure gradients closely follow changes in the ice thickness. The ice overburden pressure increases from the margin inward due to the general increase in ice thickness from 0 at the margin to approximately 1,500 m near the equilibrium line. Superimposed on this regional gradient are gradients caused by local changes in ice thickness associated with bedrock troughs and ridges (e.g. see Figure 3-12). Most deep troughs have length scales of several km in width. Note that gradients in the basal water pressure magnitude are not the same as the overall head gradient driving groundwater flow. Since the hydraulic head in the groundwater system is related to both the bedrock elevation and ice thickness, the head gradients are far smoother and mimic the parabolic profile of the ice sheet surface elevation.

Local and regional pressure gradients are further altered by changes in the basal drainage system, where temporary reductions of water pressure below overburden result from increased efficiency of the basal drainage system and melt-back of the ice enclosing the water system. Hence, the spatial gradients in basal water pressure related to drainage system dynamics develop during summer months in response to surface meltwater input, with pressure during the remainder of the year returning to near overburden pressure (Figure 3-10). The further towards the interior, the smaller the fractional pressure reductions during summer, and so the smaller the local gradients caused by basal drainage system evolution.

Basal water pressure was found to be highly coupled to surface melt conditions on a daily time scale. Diurnal swings in basal water pressure occurred at all ice borehole sites during the summer months of July and August (Figure 3-11). Pressures reached or exceeded overburden by 5–7% during the late afternoon or early evening hours, and then fell below overburden during the early morning hours. The magnitude of the diurnal pressure swings diminished with distance inward from the margin. Within a few km of the margin pressures fell during morning hours by as much as 70%, whereas 30 km inward pressures only fell by 10% or less. Importantly, the low-pressure morning periods are approximately balanced each day by high pressure afternoon periods.

Large drops in basal water pressure on diurnal cycles are interpreted to result from the development of a conduit network with high water moving efficiency. The spatial pattern of water pressure variations (large pressure drops near the margin, but not in the interior) observed in the GAP ice boreholes was investigated using numerical simulations (Meierbachtol et al. 2013). Results indicate that as a conduit network grows from the margin toward the interior of the ice sheet, it quickly encounters less favourable conditions for continued expansion. Water flux decreases following the surface melt gradient, and the surface slope diminishes rapidly away from the steep margins. The result is a lower-and-lower hydraulic gradient which reduces viscous heating of flowing water, thereby diminishing ice melt and the growth of the conduits. At some location inward from the margin, the seasonal conduit network terminates its head ward propagation. A key finding of the GAP is that this location is not only set by the heat energy generated in the water system below, but also by the water input from above. In the GAP study area, that location is on the order of 20 km inward from the steep margin.

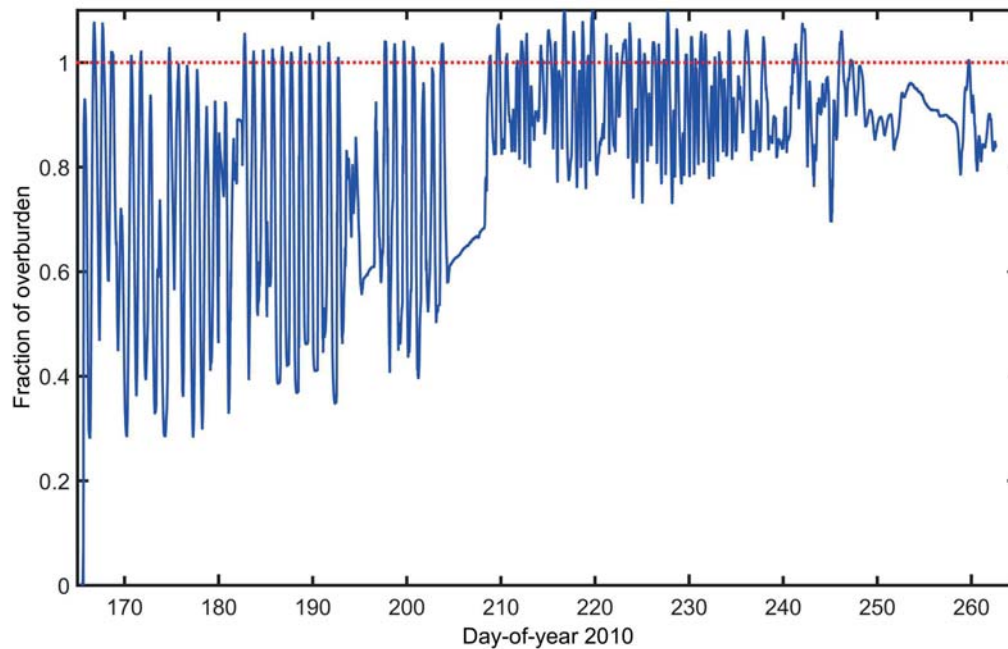


**Figure 3-11.** Water pressure record from ice borehole 1D at GL 10–Site 1. During mid-summer the water levels show large diurnal swings, sometimes reaching 70 m of water level change, and fluctuating between 30% of overburden and 105% of overburden. In late summer, the typical diurnal pattern breaks down and daily pressure variations become irregular during a transition to relatively steady pressure in winter. In fall, repeated high frequency pressure variations cease and the pressure varies at differing time scales about a relatively high water pressure.

#### *Transient Changes*

Basal water pressures approaching atmospheric or far-exceeding overburden could only be transient events, if they occur at all. This is because the ice surrounding basal waters is compliant, and will close-in if the pressure is low or will deform in response to a high pressure. Brief but large pressure deviations at the bed are theoretically possible where the basal drainage system experiences a sudden change in discharge. Local pressure increases are likely, for example, in the case of lake drainage events. Flash flow during a rainstorm could also lead to a sudden pressure spike. The pressure increases associated with these events are locally limited by the ice thickness which sets the maximum height above the bed of a potential column of water. This upper limit is equivalent to 110% of the ice overburden pressure (Table 3-1), owing to the density difference between water and ice. Alternatively, sudden and large pressure drops could also occur for very brief periods (i.e. seconds to perhaps minutes) if water input to a high capacity drainage system were to be quickly shut off. This might happen when a supraglacial stream draining into a moulin is suddenly diverted. Rapid sliding events that open cavity space could also cause short term pressure drops. Such events as described above were never measured and, while theoretically possible, are expected to be rare if they occur at all. Nevertheless, the impact of transient pressure spikes and drops may be important to some processes.

**Table 3-1. Spectrum of pressure limits in the hydraulic system.**

<b>High pressure in the basal drainage system</b>	
Greater than 110% of overburden* pressure (i.e. greater than the pressure at the base of a column of water extending through the full thickness of the ice).	Not measured; likely to be highly transient if occurring at all.
Equal to 110% of overburden pressure ('ice thickness pressure').	Not directly measured, but expected in cases of supraglacial lake drainage. However, lake drainage events are isolated in time and space, and therefore do not relate to mean conditions across the bed.
<b>Low pressure in the basal drainage system</b>	
Atmospheric	Not measured, but expected in exit channels very close to the ice sheet margin (i.e. within 100s of m). In other locations, very low pressures are theoretically possible in circumstances where water input undergoes a sudden and large discharge drop, but not expected for sustained periods of time.
<b>Time and space average pressure of the basal drainage system</b>	
Near overburden	All measurements indicated pressures near overburden occurred for the majority of the year. Pressures fell below overburden by no more than approximately 10% at locations 30 km or more from the terminus. Pressures fell below overburden by up to 70% at locations close to the margin, but only during summer months and for a portion of each day. Overburden pressure represents a relatively small over-estimate of the time/space average of pressure.

\* Overburden is defined as the water pressure resulting from the weight of the ice resting on subglacial waters. Because the density of ice is less than water, overburden pressure expressed in metres of water equivalent is equal to about 92% of the ice thickness.

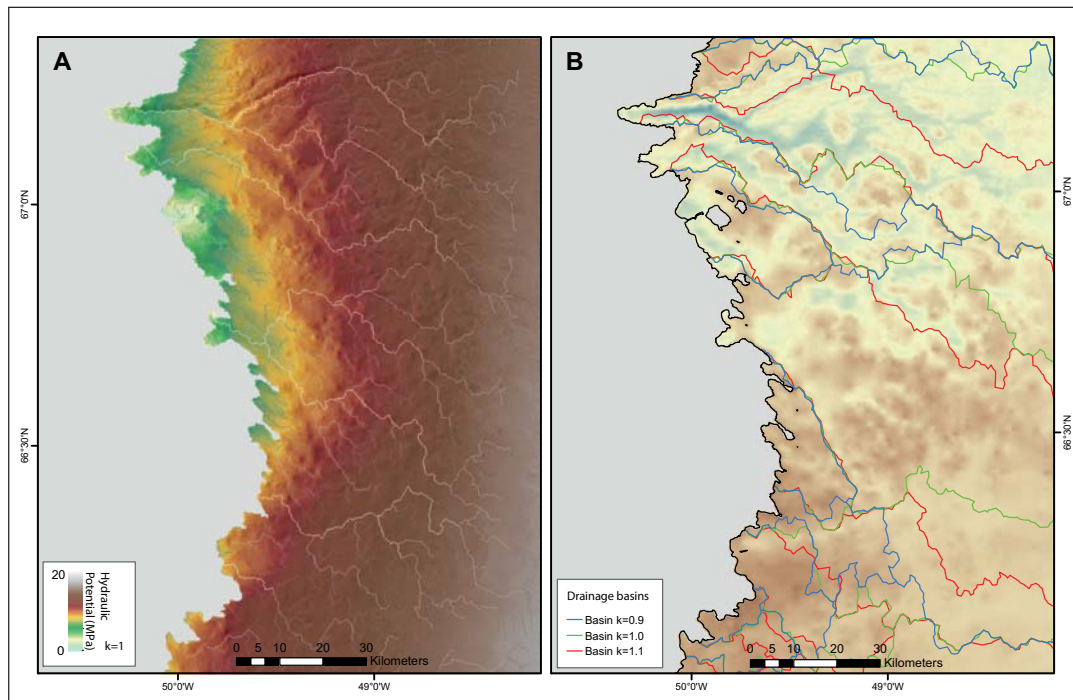


**Figure 3-12.** A). Calculated hydraulic potential with pathways of accumulated water flow. The shadowed map in the background depicts bed topography. B) Map showing the topography of the study area and subglacial drainage basins for major proglacial river derived using various assumptions about basal water pressure ( $k$  values represent basal water pressure as a fraction of overburden, see inset); colouring depicts elevation with brown colours higher than blue colours. Note the large changes (up to 100% area change) of subglacial drainage basins that occur for different scenarios of basal water pressure.

## **Remaining challenges**

An unresolved issue is that there are no estimates of the fraction of the bed submerged by water in the basal drainage system and experiencing pressure fluctuations. This fraction is expected to change in time and space. Direct measurement is not possible, and even bounds are difficult to establish. Ongoing work related to impulse tests in adjacent boreholes may yield additional information on this issue. A related problem is that the thickness, spatial continuity, and physical characteristics (i.e. permeability and porosity) of sediment at the bed are not fully resolved. This too, is expected to change in time and space, influencing the fraction of the bed having access to large volumes of water with variable pressure. Future seismic studies may extend the coverage of observations, but current limitations of the seismic analysis imply that the required information may not be well constrained by this approach. Despite these unresolved issues, the assumption that the entire bed is in contact with water represents a justified upper bound for purposes of defining the ice sheet boundary of the groundwater system.

As pressure was not measured at high time resolution (i.e. seconds), it is not clear whether occasional high frequency changes occur (as are known to occur in some mountain glaciers). However, current research underway should soon resolve this question. The influence of the deep troughs in the study area on the overall hydrological conditions is not well constrained. This potentially influences the transferability of the observations from Greenland to potential disposal sites, where the topographic relief is much more subdued than in the GAP study area.

### **3.1.4 Generalised hydraulic potential field**

The routing of water beneath the ice sheet is governed by the hydraulic gradient at the bed, which drives water from higher to lower potential. The hydraulic potential of water within the basal drainage system is the sum of the elevation potential, set by bedrock elevation, and the pressure potential of the connected waters flowing at the bed. The pressure potential therefore varies in time and space as a result of changes in the basal drainage system (see Section above on water pressures). Here, the hydraulic potential is estimated from detailed bed elevation data, and using various fixed water pressure fields (particularly, ice overburden pressure) since measured water pressures are not available for all times and locations. The generalised calculations of hydraulic potential provide insight into the direction of water flow at the bed due to the interaction between topography and water pressure.

### **Previous state of knowledge**

The general understanding of hydraulic potential beneath glaciers goes back to Shreve (1972) who developed a generalised theory for hydraulic gradients driving water flow in glaciers. In Greenland, water was known to enter the ice sheet at multiple input points clearly identifiable on the surface of the ice, and exit through a few major rivers emanating from beneath the ice sheet. However, without more detailed information about basal topography and the hydraulic gradients at different water pressures, little could be determined about the hydraulic potential defining the extent of subglacial basin catchments in the GAP study area.

### **Key improvements**

A key part of the GAP has been to establish a more detailed bed topography, since the bed and ice surface topography along with water pressure, dictate the basal routing of water. The bed topography was poorly known prior to GAP, with a comprehensive network of measurements available in a narrow marginal zone only. GAP set up an extensive programme to provide additional data inland where much of the water input occurs. The new bed topography (Lindbäck et al. 2014, Lindbäck and Pettersson 2015) is useful for interpretation of numerous aspects of the GAP investigations (Figure 2-13 and Figure 3-12A).

As expected, the hydraulic potential within the study region shows the strongest gradients near the ice margin. About 25 km inward from the ice sheet margin, gradients in hydraulic potential are relatively small, but the values of potential are high reaching up to 15 MPa. An important finding is that the area of subglacial drainage basins changes substantially, by up to 100%, depending on the assumed basal water pressure. Further, the subglacial drainage basins do not directly coincide with the supraglacial basins and for some values of water pressure, the surface and bed basin drainage areas are substantially different (Figure 3-12B). Finally, a characteristic of hydraulic potential in

a subglacial water layer is that the bed slope must be 10 times greater than the surface slope in order for the bed elevation to be the driving component of the water flow direction (Cuffey and Paterson 2010). Such conditions are rare in most glacier settings; however, in the GAP study area there are some portions of the deep bedrock troughs where this condition is met.

### **Remaining challenges**

Detailed analysis has been completed of the hydraulic potential within the study area under various assumptions of basal water pressure. No critical barriers remain to this work. Higher resolution information on the bed topography will improve existing scenarios for water routing, but existing data are sufficient for most modelling purposes. Additional bed water pressure measurements will better constrain the time and space distributions of bed water pressure for purposes of case-specific analyses of hydraulic potential and gradients.

## **3.2 Hydrogeology**

Groundwater flow is strongly affected by the prevailing climatic conditions. Specifically, relative to the present temperate conditions at the suggested repository sites in Finland and Sweden, warm-based glacial conditions may imply large meltwater production with potential infiltration (recharge) into the subsurface and consequent increased groundwater flow. However, the existence of permafrost will impede both recharge to the groundwater and groundwater flow due to the formation of ice in the fractures and pore space of the rock in the subsurface. There are thus two key questions for hydrogeological modelling; first, how should the water generation under the ice sheet be formulated in terms of boundary conditions for groundwater flow models, and second, how should the formation of permafrost be manifested as changes in hydrogeological properties.

GAP had the objective to provide insight and answers to the questions above through the six guiding questions (see Section 1.2). In Sections 4.1 and 4.6, answers related to hydrogeology are provided. In the present section, the knowledge base, prior to and after completion of GAP, is summarised.

### **3.2.1 Previous knowledge base**

This section summarises the main assumptions and simplifications generally invoked in hydrogeological modelling of warm-based glacial conditions as performed by nuclear waste management organizations within safety assessment applications. Thus, the general knowledge base of hydrogeology in glacial and permafrost settings is not reviewed or summarised.

Vidstrand et al. (2013) provide a literature review of data on hydraulic properties and boundary conditions during periglacial and glacial climate conditions. Questions of importance for both conceptual and numerical groundwater flow and solute transport modelling include: 1) thickness and continuity of potential permafrost in the proglacial area as well as below the ice sheet, 2) hydraulic and hydrological conditions in the proglacial area, in particular the role of through taliks, 3) hydraulic and hydrological conditions in the basal drainage system, i.e. the interface between the base of the ice sheet and the bedrock surface, and 4) hydro-mechanical coupling (loading efficiency, i.e. how the ice overburden pressure is propagated at depth thus modifying bedrock and water properties, respectively). These questions are fundamental to modelling, in that they all affect the permeability distribution within the modelled system, and also specify the source term of water at the top boundary of the domain. When hydro-mechanical couplings are considered, volume changes in the pore space of the rock also need to be taken into account.

Vidstrand et al. (2013) concluded that various assumptions and simplifications are common in the literature for reasons including differences in modelling objectives, scale, geological conditions, and computational constraints; a common problem in numerical modelling is uncertainty due to a lack of detailed process-level understanding and lack of field data. Two assumptions of particular interest to the GAP are: 1) taliks considered to be through taliks are often assumed to be discharge zones, and 2) a hydraulic head in the basal drainage system equal to 92% of the ice thickness is generally assumed. This value is often used as it reflects the density difference between ice and water, and it is typically considered a conservative estimate since the full ice column is included in the calculation of the hydraulic head. The hydraulic and hydrological data acquired from the GAP through the studied

through talik, the basal drainage system beneath Isunnguata Sermia, and at large depth in the bedrock in front of and below the ice sheet margin of Isunnguata Sermia constitute unique contributions to the scientific understanding of these two questions.

### 3.2.2 New knowledge obtained by GAP

Results and new knowledge related to the DH-GAP01 site are described below under the heading *Talik lake site*, whereas results and new knowledge related to DH-GAP04 (and DH-GAP03) are presented under the heading *Ice sheet site*.

#### **Talik lake site**

DH-GAP01 was drilled to confirm the existence of and increase the understanding of a talik under a lake. The hydrogeological information acquired from DH-GAP01 is limited, as no hydraulic testing with the PFL method was carried out in this borehole before instrumentation. Pressure recovery data following water removal for chemical sampling purposes in a 71 m long sampling section (Figure 2-22) were used to estimate the transmissivity of the fractured bedrock adjacent to the sampling section. A total transmissivity (sum of all fracture transmissivities in the sampling section) of approximately  $10^{-6}$  m<sup>2</sup>/s is estimated using evaluation methods for slug tests (Section 2.4.5, Harper et al. 2011).

Figure 3-13 shows the hydraulic head in DH-GAP01 (here denoted borehole head) co-plotted with the hydraulic head in the Talik lake (here denoted lake head). Over the course of the monitoring period, the lake head varied from a minimum of -5.6 m (during winter 2011–2012) to a maximum of -5.3 m (in June, 2013) relative to the TOC of DH-GAP01. During the same time period, the borehole head varied from a minimum of -8.5 m (in July, 2011) to a maximum of -6.6 m (in June, 2010) relative to TOC of DH-GAP01. Thus, the borehole head in the monitoring section is lower than the lake head at all times. This indicates recharge from the Talik lake to the bedrock where the sampling section in DH-GAP01 is positioned (Johansson et al. 2015a). Further, the lake head and borehole head show some similarity in terms of timing of increase and decrease of head values, although the magnitude of variation are different with larger variations in the borehole head. The similar timing is likely due to the fact that both lake and borehole head vary according to seasonal changes.

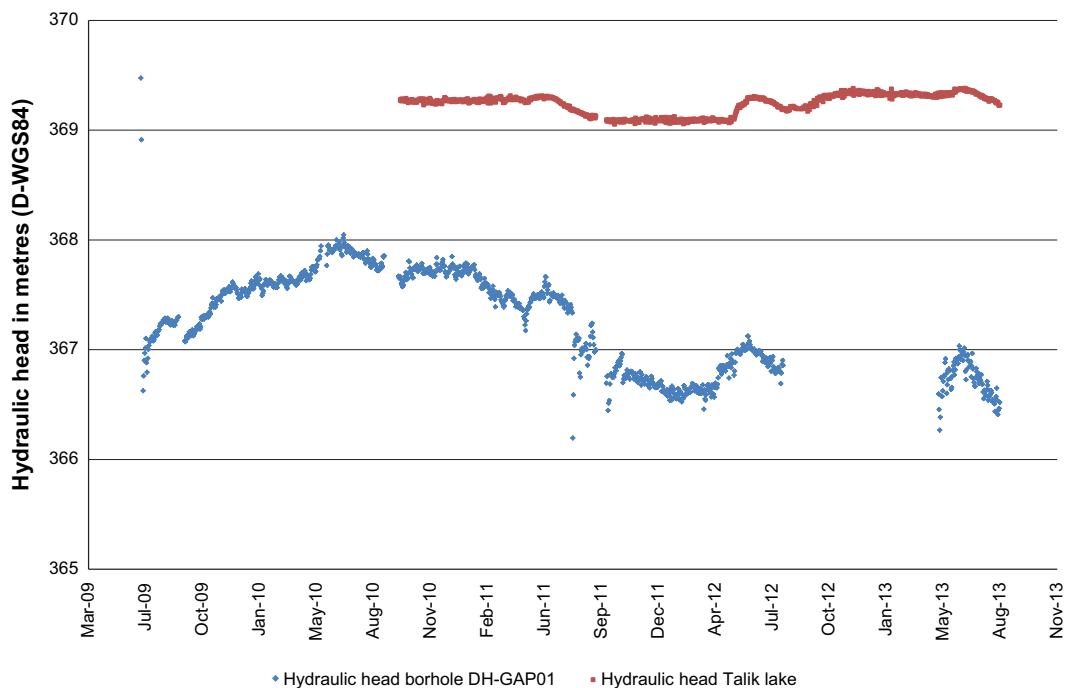


**Figure 3-13.** Daily average calculated hydraulic head (relative to TOC) for DH-GAP01 (red) from June, 2009, to August, 2013. Due to power problems, data from borehole DH-GAP01 are missing from July, 2012 to April, 2013. The lake head (blue) from the Talik lake, from Johansson et al. (2015a), is included for the period September, 2010 to August, 2013.

Johansson et al. (2015b) used the head information described above to set up an annual water balance for the lake. The calculated balance indicates that the recharge from the lake to the through talik below constitutes a very small part of the total water balance of the lake; the main components of the lake's water balance are precipitation, evapotranspiration and inflow to the lake from the surrounding catchment. Besides influences from local hydrological processes associated with the lake catchment, the hydraulic head in the through talik below the lake is probably also influenced by regional hydrological processes, e.g. seasonal variations in regional surface runoff, including hydrological processes at other lake catchments lying above neighbouring through taliks. That is, the hydraulic head envelope recorded in DH-GAP01 could be seen as a measure of "all" ongoing hydrological processes.

### Ice sheet site

Figure 3-14 shows a visualisation of all fractures mapped in the unfrozen part of DH-GAP04. The inset on the left shows the fracture characteristics below the permafrost. The fracture frequency increases significantly between 500 m and 600 m borehole length, showing a dominance of sub-horizontal fracturing (mainly parallel to foliation); steeply dipping fractures striking NE–SW with a moderate dip towards NW are also present. The fracture frequency decreases below 600 m borehole length showing a clear dominance of sub-horizontal fractures that dip gently in under Isunnguata Sermia. The inset on the right gives a detailed view of the fracturing around the packed-off section (Sect-mid). Immediately below the lower packer is an approximately 30 m thick bedrock unit where both the fracture frequency and specific capacity (Figure 3-14) drop considerably and the orientation of the few fractures available becomes almost uniformly sub-horizontal. According to acquired head data, this unit of bedrock apparently isolates Sect-low from the upper monitoring sections.

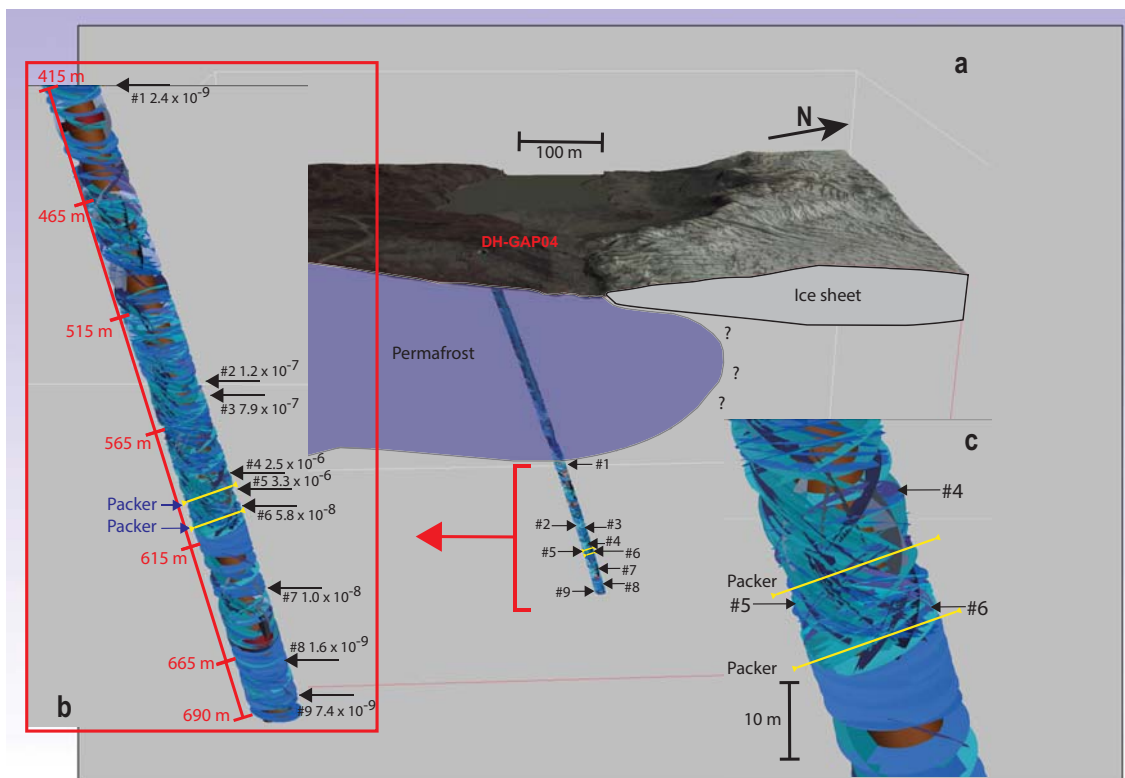


**Figure 3-14.** Visualisation of all fractures mapped in the unfrozen part of DH-GAP04 and water-conducting features (indicated by arrows). Purple area denotes permafrost. Inset on the left (b) shows the fracture characteristics below the permafrost. Measured specific capacities (flow rates in  $\text{m}^3/\text{s}$  per metre of drawdown) are shown for the nine water conducting features in figure (a). Inset on the right (c) gives a detailed view of the fracturing around the packed-off section (Sect-mid). An approximately 30 m thick unit of significantly less fractured bedrock (between 604–638 m borehole length) exists just below the packed-off section. The few fractures in this unit have almost uniformly sub-horizontal orientations.

The specific capacity (flow rate in m<sup>3</sup>/s per metre of drawdown) of DH-GAP04 was estimated based on measurements with the PFL (Pöllänen et al. 2012). The difference flow logging was run immediately after the drilling operations were completed and revealed measureable flow in the unfrozen part of DH-GAP04 (below approximately 400 m) for nine 2-m long borehole intervals. The recorded specific capacities (commonly referred to as “PFL transmissivities” in the supporting publications; i.e. the specific capacities are taken as proxy values of transmissivity) are shown in Figure 3-14.

Significant artesian conditions prevail with respect to the current elevation of the ice sheet margin at the location where DH-GAP04 extends in under Isunnguata Sermia; see Figure 3-15 for a schematic illustration.

The following is noted:

- The hydraulic heads measured in Sect-up and Sect-mid in Figure 3-16 are between 39–47 m above the elevation of the ground surface where DH-GAP04 extends in under the ice sheet margin.
- The hydraulic heads measured in Sect-low in Figure 3-16 are of the order of 25–35 m lower than the hydraulic heads in Sect-up and Sect-mid, depending on season, but still 10–12 m above the elevation of the ground surface where DH-GAP04 extends in under the ice sheet margin.

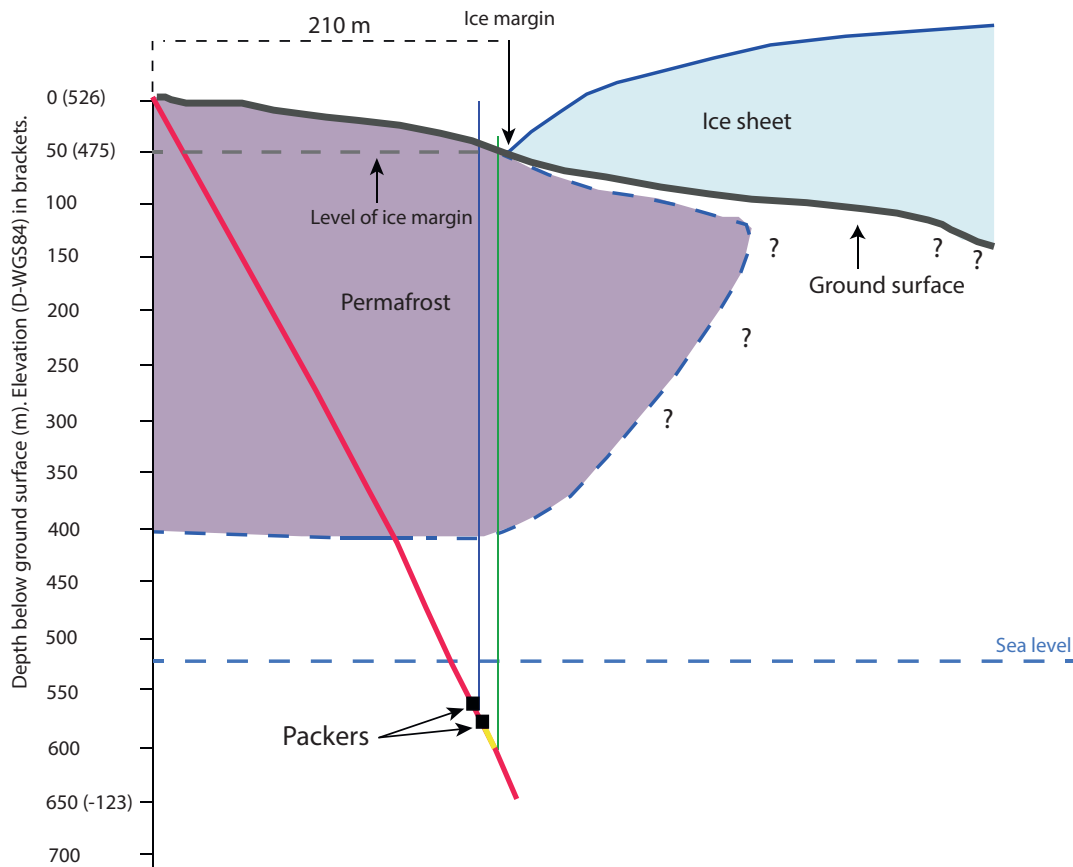


**Figure 3-15.** Schematic illustration of the ice sheet (light blue), permafrost (purple) extent and borehole DH-GAP04. The water levels in all three borehole sections are artesian with respect to the ground surface where the borehole extends in under the ice sheet (+475 m above the WGS-84 reference ellipsoid). The vertical green and blue lines represent the head values in Sect-low (+485 m) and Sect-mid (+520 m), respectively. The head in Sect-up is identical to the head in Sect-mid. The yellow colour shading along the borehole below the lower packer illustrates the approximately 30 m intact rock unit found at this depth in the borehole.

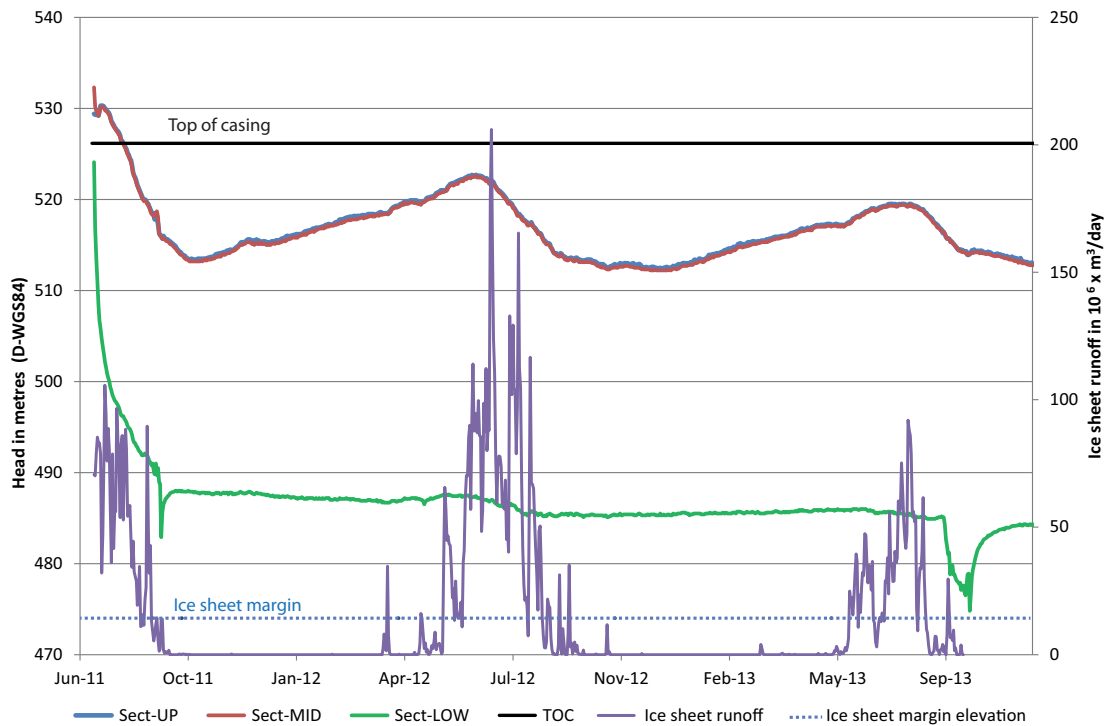


**Figure 3-16.** Daily average hydraulic heads in Sect-up, Sect-mid and Sect-low in borehole DH-GAP04 and surface meltwater runoff from the Kangerlussuaq sector of the GrIS. Runoff in the figure is represented as total modelled runoff within the delineated surface catchment (for catchment delineation see Figure 1-4a and for details see Data Report 2016). Note that the head curves for Sect-up (blue curve) and Sect-mid (red curve) overlie each other: TOC stands for top of casing. The dashed line shows the elevation of the ice sheet margin, indicating that pressure levels in the borehole are artesian. Successful water sampling campaigns were carried out in all sections in September 2011 and 2013.

Figure 3-16 reveals that the changes in the heads of both Sect-up and Sect-mid coincide with the changes in the calculated regional ice sheet runoff. The synchronised responses of Sect-up and Sect-mid imply that the flowing fractures intersecting these two monitoring sections (see Figure 3-14 for specific capacity values in Sect-up and Sect-mid) are interconnected. The fact that the responses also roughly coincide with changes in the calculated regional ice sheet runoff indicate that these borehole sections connect to the fracturing along geological structures that outcrop at locations below the wet-based Isunnguata Sermia Glacier. The cross-cutting fracturing within Sect-mid and in the lower part of the Sect-up probably explains why these sections appear to be hydraulically well connected (cf. Figure 3-14). To summarise, the rapid, synchronous and cyclic annual response of the hydraulic head values in the upper and mid intervals strongly indicate that this part of the bedrock is connected to, and hydraulically governed by, the basal drainage system under the ice sheet rather than by the flow conditions in front of the ice sheet (as manifested in borehole DH-GAP01). Also, the magnitudes of the annual changes in these two borehole sections strongly suggest a connection to the basal drainage system.

In comparison, the time series showing a consistently lower head in Sect-low in Figure 3-16 reveals a significantly weaker correlation to seasonal changes in the regional runoff envelope. This difference is attributed to the almost complete lack of steeply dipping fractures intersecting Sect-low (see figure 3-14 and Pere 2014), and by the generally lower specific capacity values at depth in DH-GAP04. Together, these conditions probably explain why the head values in Sect-low are considerably lower and less sensitive to pressure changes associated with seasonal changes in regional ice sheet runoff. To conclude, the significantly higher artesian heads in Sect-up and Sect-mid (relative to the ground elevation of the ice margin of Isunnguata Sermia directly north of DH-GAP04) are likely due to a better connection of the bedrock structures at these elevations to the basal drainage system, in combination with their ‘confined location’ between the upper ‘sealing’ permafrost boundary and the lower sealing intact 30 m thick bedrock unit. Figure 3-14 schematically illustrates how the upper two packed-off sections are connected to the basal drainage system, despite being

geometrically in between the permafrost and sealing bedrock units. The hydraulic pressure imposed in the basal drainage system under the ice sheet thus propagates to the packed-off sections through fractures in the bedrock circumventing the permafrost layer.

The head difference between the upper two sections and the lower section implies a quite strong vertical hydraulic gradient, on the order of 1 m/m, over the 30 m thick bedrock unit below the lower packer. Since the gradient acts over very low permeable rock, the resulting groundwater flux will be low. The horizontal gradient, which is linked to the slope of the ice sheet terminus, primarily implies large groundwater fluxes in the basal drainage system rather than in the rock itself. Overall, it is thus judged that the groundwater flow and associated advective velocities in the bedrock adjacent to DH-GAP04 at the depth of the monitoring sections are relatively low. The consistency between such groundwater flow estimates and groundwater age, as estimated by geochemical methods (mainly based on He contents, see Section 3.3.2), is further discussed in Section 5.4. The discharge of groundwater within the bedrock likely takes place in some of the taliks in front of the ice sheet, or in deep, unfrozen valley sediments below the ice sheet tongues. The GAP has not been able to locate or quantify this discharge.

### 3.2.3 Key findings

Through the drilling, instrumentation and sampling of borehole DH-GAP01, a first-of-its-kind inclined cored borehole beneath a through talik, the GAP has obtained unique information on hydrological processes in the proglacial area of a continental ice sheet down to approximately 190 m vertical depth.

A key finding from the Talik lake investigations is that the existence of a through talik in a proglacial area characterised by continuous permafrost in close proximity to a continental-scale ice sheet has been confirmed. The GAP has thus confirmed the initial hypothesis of a proglacial through talik being present (see also Section 3.3.2). This hypothesis was based on geometrical considerations only; i.e. based on lake surface area relative lake depth. Another key finding is the currently available time series of lake head and hydraulic head in DH-GAP01 suggesting a downward gradient in the area where DH-GAP01 is drilled; i.e. lake water recharges to the groundwater at this location (Data Report 2016, Johansson et al. 2015b).

It has also been demonstrated that the hydrology of the Talik lake catchment is a precipitation-driven system (Johansson et al. 2015b). Furthermore, there is no observed meltwater inflow from the glacier over the catchment boundary, thus supporting the catchment boundary which was calculated primarily based on digital elevation data. The through talik allows for hydraulic contact between the Talik lake and the deep groundwater system below the permafrost. Temperature measurements in borehole DH-GAP03 and DH-GAP04 indicate permafrost depths of the order of approximately 350 m (Harper et al. 2011, Data Report 2016).

Through the drilling, instrumentation and sampling of borehole DH-GAP04, a first-of-its-kind inclined cored borehole beneath the margin of a continental ice sheet, the GAP has obtained information on bedrock hydrogeology at vertical depths down to approximately 650 m.

The most striking result obtained from the hydrologic monitoring in DH-GAP04 is the prompt responses of the confined (artesian) hydraulic heads in the two upper sections in DH-GAP04, and how the recorded pressure changes in these two sections harmonise with the timing of the calculated seasonal ice sheet meltwater runoff. The repeated observation and reporting of the multi-year consistency in timing between the recorded hydraulic head transients in DH-GAP04 at approximately 520 m vertical depth below the ice sheet margin and the seasonal changes in the superficial meltwater runoff is another unique contribution of the GAP. It is hypothesised that the pressure changes at depth are linked to the seasonal development of the basal drainage system. Specifically, the hydraulic head falls in Sect-up and Sect-mid when an efficient drainage system develops under the ice sheet during the melting season, whereas the hydraulic head builds up during winter conditions when no surface water enters the basal drainage system which then closes, see also Section 3.1.3.

The observation of pressure responses at great depth due to hydrological perturbations at the surface has been recorded for temperate climate conditions at the Forsmark site during rain events (Follin et al. 2007); however, the unique contribution within GAP is the finding that ice sheet surface melting may result in fast pressure changes at depth in the bedrock. It is noted that these pressure changes are observed in the two upper-most sections while the lower section reacts less; this further indicates that these deeper parts of the bedrock may be more isolated from the surface.

It is concluded that the assumption of a hydraulic head in the basal drainage system equal to 92% of the ice thickness is not necessarily conservative in the sense of being overly pessimistic. Rather it appears to be the typical state based on data, from the ice holes drilled through the Isunnguata Sermia Glacier (for details see Section 3.1.3), except for the most near-frontal parts of the ice sheet. Therefore, using the ice sheet overburden pressure as a pressure boundary condition in groundwater modelling appears to be a reasonable and realistic assumption.

### 3.2.4 Remaining challenges

The duration of the GAP has been fairly short; thus, the time series data presented above are fairly short in duration. To gain a better understanding of how subsurface pressures change in time and may be related to ice sheet runoff, a combination of longer time series and additional modelling studies is required. Additionally, it was only possible to obtain pressure measurements beneath one location in the Talik lake area during the sampling period. It cannot be excluded that other parts of the Talik lake area may behave differently from the studied location, as preliminarily indicated by groundwater simulations<sup>3</sup>. More analyses and modelling studies of the Talik lake hydrology and hydrogeology will take place outside of the GAP.

It is noted that there are additional key hydrogeological questions related to glacial and permafrost conditions that are not covered by the data collection within the GAP. The prime question not directly addressed is hydro-mechanical couplings induced by the ice load. In modelling by Yin et al. (2013), bounding hydro-mechanical couplings were considered. Specifically, one-dimensional loading was assumed, which during melting of the ice sheet, induces a vertical upward groundwater flow in the bedrock at depths approximately below 1,000 m due to the hydro-mechanical coupling through glacial unloading. The results of Yin et al. (2013) thus support the neglect of hydro-mechanical couplings when studying the GAP site down to relevant repository depths (see Section 1.2).

## 3.3 Hydrogeochemistry

Most of the hydrogeochemical processes that involve groundwaters in fractured rock under temperate climate conditions also take place under periglacial or glacial climates. Some factors are, however, quite different under glacial and permafrost conditions. These include:

- a) the different groundwater flow conditions (increased hydraulic pressures close to the ice margin or reduced hydraulic conductivity in rock volumes where permafrost is present),
- b) the different composition of the infiltrating waters (glacial meltwater instead of soil porewaters), and
- c) the reduced biological activity/productivity in the basal drainage system of the ice sheet and in the permafrost active layer, compared with soils or sediments under temperate climate conditions.

These differences between temperate and glacial or periglacial climate conditions affect the processes controlling the composition and the redox conditions of the groundwaters. In particular, because the glacial meltwaters have a relatively low content of dissolved solids, it may be expected that infiltrating meltwaters in glaciated areas will be dilute, as suggested by recent model results (see for example Figure 11 in Vidstrand et al. 2014). However, for some sites, such as Olkiluoto in Finland, glacial meltwater infiltration at depth may be prevented by the structural geology and the hydrogeological conditions (Posiva 2013). Concerning the redox conditions, it might be expected that given that glacial ice has a large quantity of air incorporated, glacial meltwaters could also have higher concentrations of dissolved O<sub>2</sub> than the soil waters that infiltrate during temperate conditions, where biological and microbiological activities effectively consume dissolved oxygen.

From the arguments presented above, it may be concluded that when considering the long term safety of DGRs for nuclear waste, it is necessary to assess if the low salinity and potential dissolved O<sub>2</sub> contents of the groundwaters resulting from infiltrating glacial meltwaters can have negative impacts on the repository. Understanding the processes that can control the salinity and consume dissolved O<sub>2</sub> during glacial periods is therefore important, and development of such understanding is one of the aims of the GAP.

---

<sup>3</sup> Vidstrand P, in prep. Concept testing and site-scale groundwater flow modelling of the ice sheet marginal-area of the Kangerlussuaq region, Western Greenland. SKB R-15-01, Svensk Kärnbränslehantering AB.

### 3.3.1 Previous knowledge base

Geochemical data and process understanding of the basal drainage system of an ice sheet give clues to the chemical characteristics of the glacial meltwaters that may infiltrate into the subglacial rock. Several literature studies have discussed possible geochemical processes in the basal drainage system as sources for the solutes observed in glacial meltwaters from Greenland, Antarctica, Svalbard, Spitsbergen, and Alpine glaciers (Raiswell 1984, Irvine-Fynn and Hodson 2010, Skidmore et al. 2010, Wadham et al. 2010a, b, Graly et al. 2014) and references cited therein. The main processes listed in the literature are the same as those affecting temperate shallow groundwaters, namely:

- Hydrolysis of carbonates and silicates.
- Dissolution of fluid inclusions.
- Oxidation of organic matter and sulphides by O<sub>2</sub>.
- Ion exchange.
- Oxidation of organic matter and sulphides by other oxidants than dissolved oxygen, such as sulphate and Fe(III).

These geochemical processes, when combined with different subglacial hydrological conditions, result in meltwaters that range from anoxic to oxic (Brown et al. 1994, Bottrell and Tranter 2002, Wadham et al. 2007, 2010b, Irvine-Fynn and Hodson 2010), and with solute concentrations that are quite low, ranging from practically zero to approximately 1 mM for the main solutes, such as Ca<sup>2+</sup> (Brown 2002, Stumpf et al. 2012, Graly et al. 2014). When these meltwaters infiltrate, they will mix with groundwaters previously present in the rock, and this, together with weathering processes in the rock and with matrix diffusion, might affect the salinity of the resulting (mixed) groundwaters.

Perhaps the most recognisable characteristic for glacial meltwaters is, however, the stable isotope signatures, in particular for <sup>18</sup>O and <sup>2</sup>H (see for example Sveinbjörnsdóttir et al. 2001, Yde and Knudsen 2004). Large negative δ<sup>18</sup>O values in groundwaters are assumed to reflect either a glacial or a cold climatic origin.

The only data available on subglacial groundwaters before the start of the GAP were from a spring associated with an open pingo (Scholz and Baumann 1997, Wallroth et al. 2010), which is located in front of the Leverett glacier, in the GAP area (see Figure 2-18 and Figure 2-21), and from some springs in Ellesmere Island (Grasby et al. 2003). The interpretation of these groundwater data is uncertain, as it is not known from what depth these waters originate. Groundwater data from a few permafrost areas in the Canadian Shield were available as well (Stotler et al. 2009, 2010, 2012). Because of the general lack of hydrogeochemical groundwater data in glaciated areas, assessments of the long term safety of nuclear repositories relied mainly on the results of hydrogeological modelling. Overall, before the GAP, it was clear that acquiring groundwater hydrogeochemical data from glaciated and/or permafrost areas would increase confidence in assessments of the performance of nuclear waste repositories.

#### ***Previous evidence for groundwaters originating from glacial meltwaters***

In contrast to hydrogeological information, hydrogeochemical data can provide evidence of past infiltration of glacial meltwaters. Such evidence is of importance, as it provides support to hydrogeological conceptual and numerical models, and it also emphasises the importance of a proper consideration of glacial meltwater infiltration when evaluating the long term safety of nuclear waste repositories. The literature on effects of Pleistocene glaciations on groundwaters has been reviewed, with a focus on sedimentary basins, by McIntosh et al. (2012). The following subsections provide a short overview of data evidencing the penetration of glacial meltwaters in crystalline rocks of Fennoscandia and of Canada, mainly based on δ<sup>18</sup>O data.

#### **Paleoclimate conditions in Fennoscandia**

Several glacial periods have occurred during the Quaternary in Fennoscandia. Finland and Sweden were repeatedly covered by ice during the Elsterian period (approximately 500–414 ka ago), the Saalian period (approximately 380–130 ka ago) and finally the Weichselian period (approximately 115–11.5 ka ago). The Weichselian is divided into three different sub stages: Early (115–74 ka),

Middle (74–24 ka) and Late Weichselian (24–12 ka). During the Early Weichselian, the ice sheets only covered northern Finland (Andersen and Mangerud 1989, Johansson et al. 2011) and a large part of northern and central Sweden (Wohlfarth 2013). Geological observations suggest that large parts of Fennoscandia were ice-free during the early parts of the Middle Weichselian (e.g. Helmens 2013, Wohlfarth 2009). During the later part of the Middle Weichselian, a substantial ice sheet covered most of Fennoscandia. Late Weichselian glaciation started about 24 ka ago in Fennoscandia and the ice sheet reached its maximum (LGM) about 22–18 ka ago. At that time, Fennoscandia was under an 2–3 km thick ice cover. After the LGM, the ice sheet started to melt due to climate warming; however, a new, brief cold period, the Younger Dryas, started about 13 ka ago and the ice sheet remained stationary or started to advance slightly until about 11.5 ka ago (Figure 3-17). The Weichselian deglaciation was completed about 10 ka ago, but large parts of Fennoscandia remained below sea level.

## Finland

Glacial chemical and isotopic signals are observed in many Finnish groundwaters and these signals are interpreted as the consequences of glacial melt infiltration and mixing in groundwater (Posiva 2013, Stotler et al. 2012). For example, Olkiluoto, Hästholmen and Kivetty studied by Posiva as potential repository sites and Palmottu (a natural analogue site), see Figure 3-17, all show cold climate signatures, although they have different hydrogeological relationships to glacial and post-glacial evolution, as well as different groundwater salinities. Olkiluoto and Hästholmen are situated on the coastal line. They were submerged below the saline Littorina Sea between 8 ka and 3 ka ago, resulting in isotopically heavy sea water infiltration and mixing. This complicates direct interpretation of stable isotopic compositions because the heavy isotopic signal of sea water partly masks the cold climate signature (Pitkänen et al. 2001, 2004). However, a glacial stable isotopic signal is evident down to 200 to 300 m depth (Figure 3-18). Kivetty and Palmottu have been above sea level since the ice retreat. Groundwaters at Kivetty are fresh, meteoric with a minor glacial signal from 200 to 800 m depth. The hydrogeology is dominated by steep sub-vertical features contrary to the other sites discussed here (Pitkänen et al. 1998). Palmottu is situated at a former ice sheet margin, where the ice edge remained stationary for a few hundred years during the retreat of the Weichselian ice sheet. Therefore, the cold climate signature should be most prominent at Palmottu among these Fennoscandian sites. It seems limited to depths of 200 to 400 m, although the full profile of meltwater influence cannot be observed because of the lack of deeper boreholes at Palmottu (Smellie et al. 2002).

Regardless of evident glacial melt input in all sites, the groundwaters only contain a fraction of meltwater, up to several tens of per cent (Pitkänen et al. 2001, 2002, Posiva 2013). Undoubtedly, the shallow parts of bedrock were more diluted after glacial melt infiltration, but more recently infiltrating post-glacial waters have replaced the glacial water and its isotopic signal. Estimates of the fraction of glacial meltwater may also be disturbed by cold climate meteoric infiltration, which has occurred occasionally during the Quaternary period. For example,  $^{18}\text{O}$  and Cl data from Olkiluoto (Figure 3-18) suggest that dilution of deep highly saline groundwater to brackish Cl-type groundwater is due to ancient meteoric water from a slightly cooler climate than exists now at the site. For this infiltration to have taken place, the site must have been above sea level for a long period. The influence of Weichselian glacial melt is evident only in the most dilute brackish Cl type and brackish  $\text{SO}_4$  type groundwaters from the upper bedrock (see left diagram in Figure 3-18). Mass balance mixing calculations made using PHREEQC indicated a maximum meltwater fraction of 40 to 60% from samples taken from depths of less than 150 m. The fraction decreased below 30% at greater depth, and below 300 m, it was minor (Posiva 2013).

No evidence of deep penetration of oxygenated groundwaters has been observed at Olkiluoto either in groundwater or fracture infillings. The scarcity of iron oxyhydroxides from fracture surfaces below the uppermost ten metres also indicates anoxic conditions below these shallow depths. Pyrite and other iron sulphides are instead common in fractures with no indications of oxidative corrosion below ten metres depth (Sahlstedt et al. 2009, 2014a, b), indicating the presence of a strong lithological buffer against oxic waters over geological time scales.

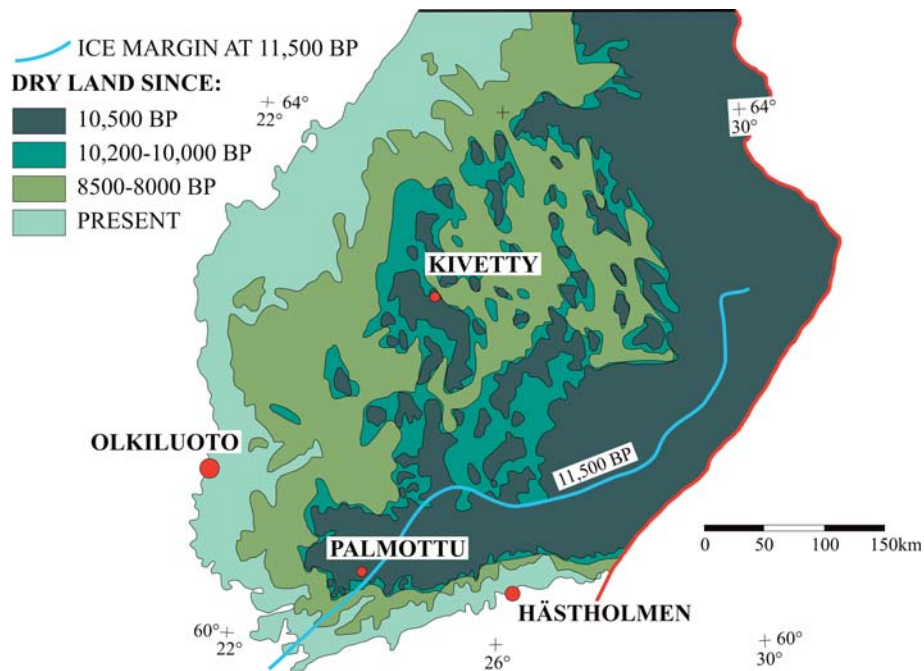


**Figure 3-17.** Palaeohydrology: Postglacial shoreline in southern Finland from about 11,500 years ago, when the ice margin remained stationary for several hundred years, until the present (after Eronen et al. 1995, Pitkänen et al. 2004). The illustrated ice margin at 11,500 BP is based on the deposition of the Salpauselkä end-moraine as the ice retreated towards the northwest from the margin. The illustrated marine regression and uplift was mainly due to crustal rebound after the Weichselian glaciation.

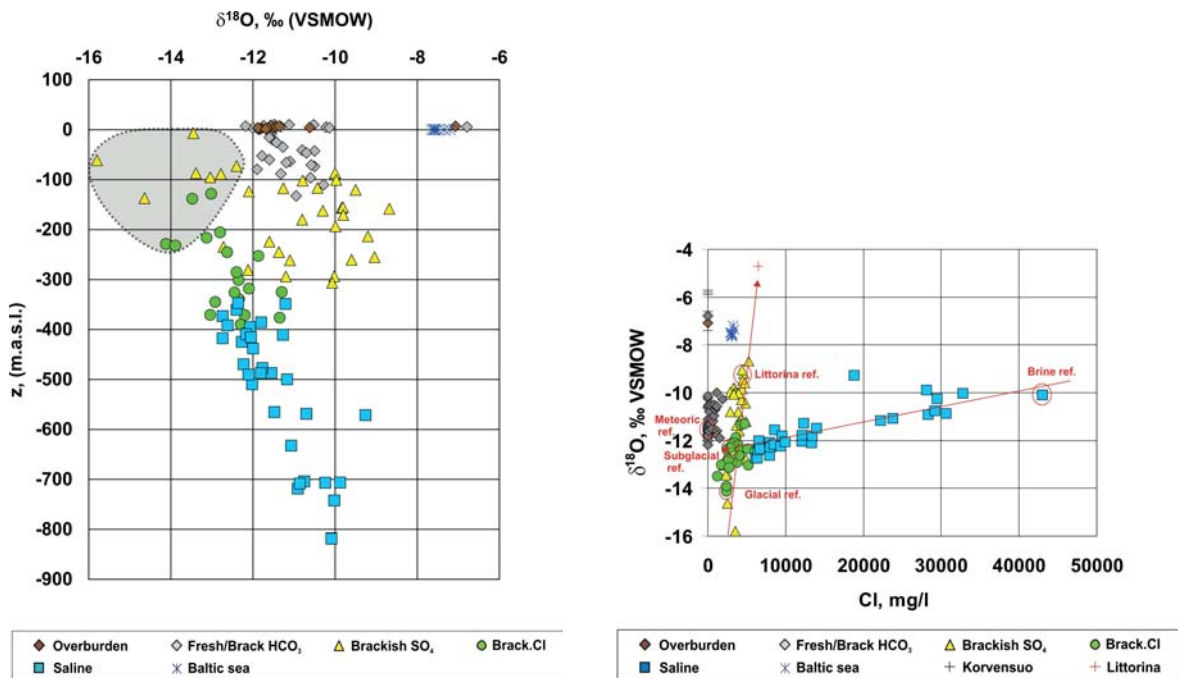


**Figure 3-18.** Olkiluoto groundwaters. Left:  $\delta^{18}\text{O}$  versus depth. The shaded area of low  $\delta^{18}\text{O}$  values in the upper part of the bedrock indicates an increased glacial water fraction near the surface, prior to the start of Littorina sea water infiltration. Subsequent sea water and meteoric water input has removed this signal from most of the other data. Right:  $\delta^{18}\text{O}$  versus chloride. Arrows indicate ancient dilution of brine to brackish Cl-type, and postglacial mixing between glacial meltwater and Littorina Sea water; the reference waters (circles) represent mixing end-member groundwaters. From Posiva (2013).

## Sweden

Glacial components in Swedish groundwaters have been recognised by their isotopic signatures, which are low  $\delta^{18}\text{O}$  in combination with no tritium and low  $^{14}\text{C}$  (the latter mostly analysed in inorganic carbon). These signatures rule out the possibility of low  $\delta^{18}\text{O}$  as a result of annual variations in recent precipitation. There is also a general indication of lower  $\delta^{18}\text{O}$  in waters with lower TDS, which is in strong support of a pre-Holocene recharge of fresh water with a cold climate signature. The glacial meltwaters, when found in the bedrock, are mixed with older waters (usually brackish to saline) that were already present in the bedrock at the time of recharge. After the glaciation/deglaciation stage when the upper part of the bedrock was filled with glacial meltwater, the Littorina stage of the Baltic Sea allowed more dense marine waters to penetrate by density effects. This description applies for several sites situated on the Swedish east coast, e.g. Forsmark (Laaksoharju et al. 2008b), Finnsjön (Andersson et al. 1991), Äspö (Laaksoharju et al. 1999a, Mathurin et al. 2012) and partly for Laxemar (Laaksoharju et al. 2009b).

Important parameters such as chloride, magnesium (to trace marine waters), and  $\delta^{18}\text{O}$  (to trace cold climate recharge) are plotted versus depth (Figure 3-19) for the Forsmark candidate site and for the low- and intermediate level radioactive waste underground repository located within the vicinity of the Forsmark nuclear power plant (SFR). The most evident glacial signatures are found in some less connected sections in the SFR at about 100 to 250 m depth (under the present Baltic Sea). An evaluation made using the multivariate analysis tool M3 (Gómez et al. 2006, 2008, 2009, Laaksoharju et al. 1999b, 2008a, 2009a) indicated a glacial component of 40 to 60% in the some of the Laxemar groundwaters at depths between 350 to 500 m (see Figure 4-22 in Laaksoharju et al. 2009b).

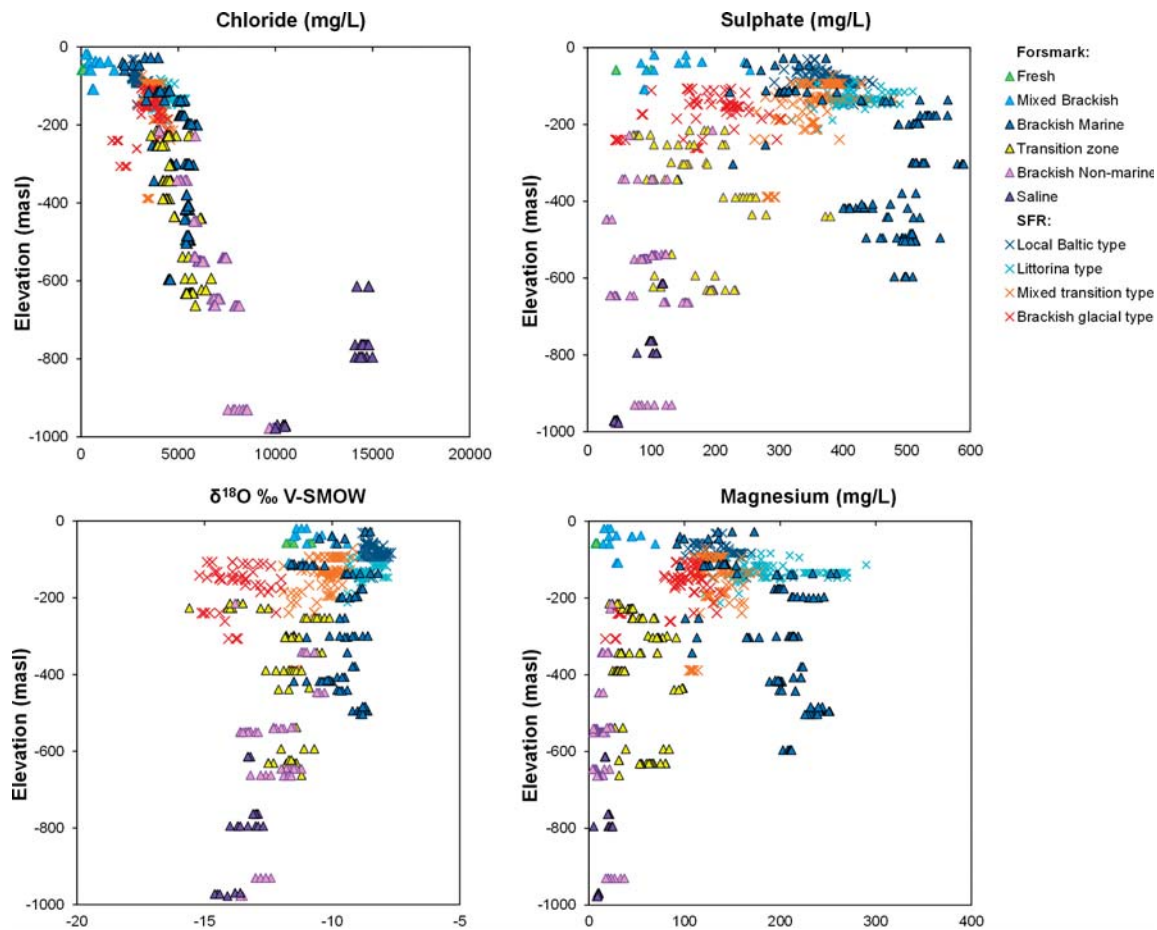


**Figure 3-19.** Distribution of chloride, sulphate,  $\delta^{18}\text{O}$  and magnesium with depth related to the different groundwater types defined for the Forsmark and SFR sites (Laaksoharju et al. 2008b, Nilsson et al. 2011).

During the Littorina Sea stage, brackish water with relatively high  $\delta^{18}\text{O}$  values (approximately  $-4$  to  $-5$  ‰) infiltrated and mixed with groundwaters of glacial origin, and the typical low  $\delta^{18}\text{O}$  signatures thus disappeared, making it more difficult to determine the glacial component in the present-day groundwaters, as seen from Figure 3-20 (Forsmark) and Figure 3-18 (Olkiluoto). However, after the deglaciation, most of the open fractures in the upper 300 m were filled with dilute glacial meltwater (and in some cases even deeper); this was the prerequisite for the denser Littorina Sea water to intrude. As pointed out above for Finland, one can assume that the low  $\delta^{18}\text{O}$  found in some deep saline waters in Sweden (e.g. at approximately 1,000 m depth in Forsmark) is the result of older glaciations. This is difficult to prove, and in many areas (as indicated from  $^{14}\text{C}$  analyses), the glacial meltwaters from the last glaciation reached greater depth at the Swedish sites than observed at Olkiluoto.

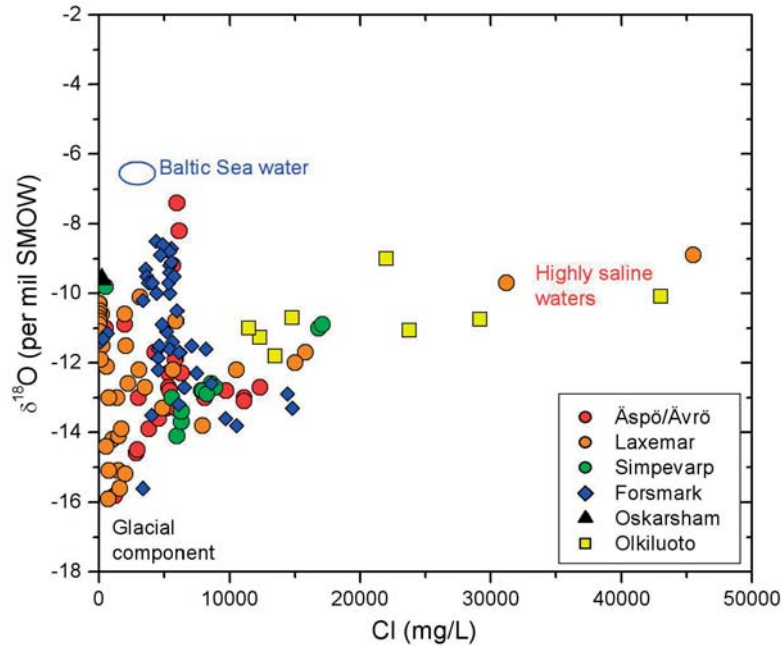


**Figure 3-20.**  $\delta^{18}\text{O}$  versus chloride (categories 1–4) for the most well documented sites around the Baltic (Smellie et al. 2008).

### Canada

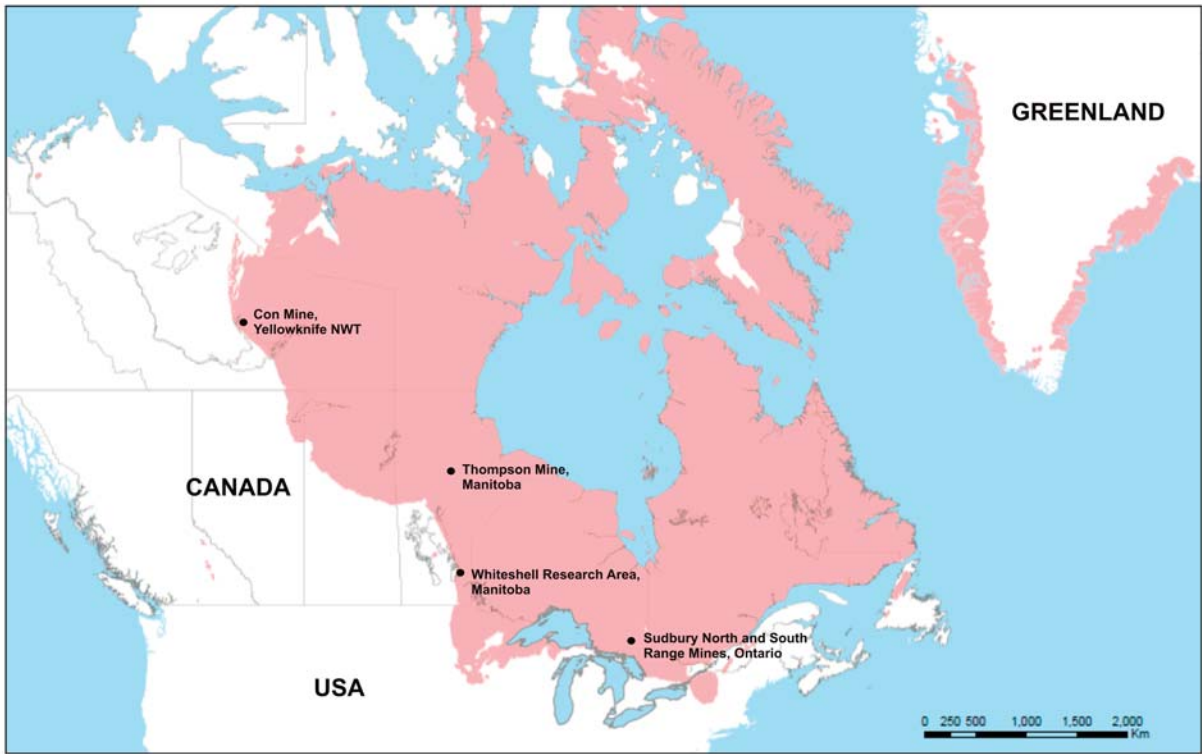
The Canadian Shield comprises igneous and metamorphic rock types, including volcanic, plutonic, metasedimentary and gneissic (e.g. Card 1990). The crystalline rocks of the Canadian Shield vary in composition and are divided into a number of geological provinces based on composition and geologic history. These rocks include gabbros and diorites, greenstones/schists, and granites and granodiorites.

Over the past one million years, the Canadian Shield has been subjected to approximately nine glaciation events, each lasting approximately 100,000–120,000 yr (e.g. Peltier 2003). Paleoclimate reconstructions, using the *University of Toronto Glacial Systems Model* (UofT GSM), indicate that during the last glacial cycle, involving multiple cycles of advance and retreat of the Laurentide Ice Sheet, up to 4 km of ice overrode parts of the Canadian Shield (Peltier et al. 2013).

Frape and Fritz (1987) have noted that brines across the Canadian Shield generally have a similar chemical composition, which suggests a common geochemical history. A general trend has been observed in the Canadian Shield with respect to groundwater chemistry and depth. Vertical zoning with respect to chemical composition is noted, progressing from dilute, oxygenated waters near the surface, to brackish and/or saline waters at depth (e.g. more than 500 m below ground surface; Singhal and Gupta 2010). Two general groundwater systems have been proposed by Singer and Cheng (2002) for the Canadian Shield: a shallow, generally fresh water system, and a deep, typically saline, system. The deep groundwater system in the Canadian Shield tends to be characterised by high TDS, Na-Ca-Cl or Ca-Na-Cl brackish or saline fluids, where transport is dominated by diffusion and the environment is reducing (McMurry 2004, Gascoyne and Kamineni 1994). The depth of the transition between the shallow and deep zones across the Canadian Shield is, in part, a function of the occurrence, frequency and interconnectivity of discrete fractures and fracture zones within the rock mass (NWMO 2012).

Figure 3-21 depicts the extent of the Canadian Shield and shows the location of a number of sites where data have been collected that contribute to the understanding of the geochemical history of Canadian Shield groundwaters. Figure 3-22 shows  $\delta^2\text{H}$  and  $\delta^{18}\text{O}$  signatures from fracture groundwaters at these sites (Con Mine, Yellowknife – Northwest Territories; Thompson Mine, Manitoba; Sudbury Mines, Ontario; Whiteshell Research Area, Manitoba), at depths in excess of 500 m, that have been characterised as brackish, saline or brine. One seepage porewater sample, collected from the unfractured rock matrix at approximately 420 m depth at the *Atomic Energy of Canada Limited Underground Research Lab* (AECL URL) in the *Whiteshell Research Area* (WRA), is shown as well. As shown in Figure 3-22, a common feature of deep Canadian Shield groundwaters is that their  $\delta^2\text{H}$ – $\delta^{18}\text{O}$  compositions typically plot to the left of the *Global Meteoric Water Line* (GMWL). The WRA groundwaters and porewater are discussed in greater detail below.

The Lac du Bonnet batholith, located in southern Manitoba within the WRA, has been characterised extensively in order to gain insight into groundwater chemistry and evolution in the Canadian Shield. Research carried out at the AECL URL found that groundwaters at depths of approximately 300 to 1,000 m had TDS concentrations typically ranging between 3 and 51 g/L (Gascoyne 2000, 2004). Based on an extensive dataset from the WRA, Gascoyne (2004) determined that shallow groundwaters in the fractured bedrock are generally dilute Ca-Na- $\text{HCO}_3$  fluids with modern-day meteoric water isotopic ( $\delta^2\text{H}$ ,  $\delta^{18}\text{O}$ ) signatures, indicative of an active groundwater system. Gascoyne (2004) suggests that groundwater residence time in the upper 100–200 m of bedrock is on the order of tens to hundreds of years. Intermediate fracture groundwaters (200–400 m depth) range in composition from Na-Ca- $\text{HCO}_3$  to Na-Ca- $\text{HCO}_3$ -Cl- $\text{SO}_4$  and the  $\delta^2\text{H}$ – $\delta^{18}\text{O}$  data indicate a glacial meltwater component, yielding estimates of residence time on the order of 1,000 to 100,000 years. The deep groundwater system (more than 500 m), where fracturing is minimal and transport is diffusion-dominated, contains Na-Ca-Cl- $\text{SO}_4$  waters of elevated salinity with  $\delta^2\text{H}$ – $\delta^{18}\text{O}$  signatures indicative of warm climate conditions (Gascoyne 2004). The interpretation of this deep chemistry is that the saline waters were recharged under conditions similar to present-day (Gascoyne 2004). Because these groundwaters underlie the zone containing glacial meltwaters, they are presumed to have resided in the system longer. As noted in Gascoyne (2004), this interpretation is consistent with isotopic and noble gas data that indicate long accumulation periods (more than 1 Ma) within the rock. Seepage porewater from the unfractured rock mass at the WRA was analysed and determined to be a high salinity (approximately 90 g/L) Ca-Cl fluid with  $\delta^2\text{H}$ – $\delta^{18}\text{O}$  composition plotting to the extreme left of the GMWL, beyond the typical range of Canadian Shield waters (Gascoyne 2004, Figure 3-22). It has been suggested that the porewaters may represent ancient basin brines that have evolved to their current chemical composition over long time periods (upward of one million years, possibly as long as 1,000 Ma). In addition to the groundwater and porewater analyses, uranium series age determinations on calcites from boreholes drilled near the AECL URL were performed (Gascoyne and Shewchuk 1998) and the results suggest that the infiltration of glacial meltwaters to depth in the rock mass surrounding the URL is limited in extent (less than 400 m depth).



■ Extent of the Canadian Shield (showing observed/interpreted extent in Canada and observed extent only in Greenland)

**Figure 3-21.** Depiction of the observed and/or interpreted extent of the Canadian Shield in Canada, as well as the observed extent of the Canadian Shield in Greenland (note: it is interpreted that the majority of Greenland is underlain by the Canadian Shield, however, the figure only depicts those areas where Canadian Shield basement rock has been observed – i.e. areas that have been mapped and are not currently glaciated).

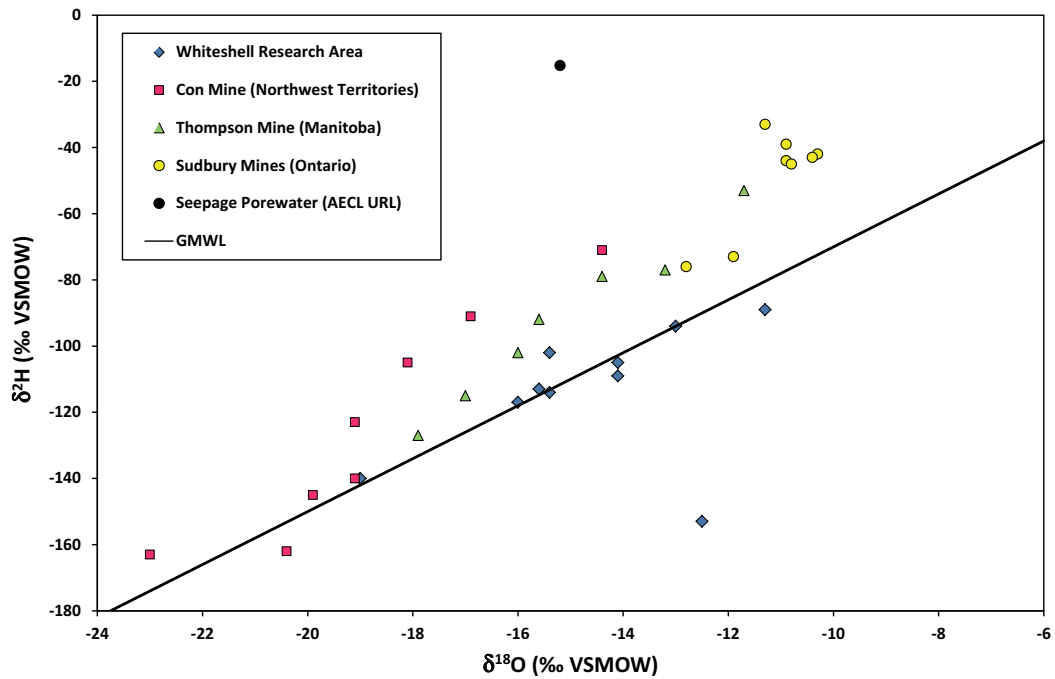


**Figure 3-22.**  $\delta^{18}\text{O}$  versus  $\delta^2\text{H}$  for groundwater samples collected on the Canadian Shield from Frapet and Fritz (1987) and Gascoyne (2004). For groundwaters from the Con Mine, Thompson Mine and Sudbury Mines, standard analytical error from mass spectrometry and distillation is  $\pm 0.15\text{‰}$  for  $\delta^{18}\text{O}$  and  $\pm 2\text{‰}$  for  $\delta^2\text{H}$  (Frapet and Fritz 1987); groundwaters from the WRA were analysed by mass spectrometry (Gascoyne 2004).

### **Evidence for glacial components in groundwaters of Fennoscandia and Canada: Implications**

As the subsections above have shown, there is ample hydrogeochemical evidence, mainly based on  $\delta^{18}\text{O}$  data, of penetration of glacial meltwaters in crystalline rocks in Fennoscandia and Canada. These data agree with the results from several model simulations (Lemieux et al. 2008, Normani and Sykes 2012, Vidstrand et al. 2014) which show the influence of ice sheets on groundwaters at potential repository depths. The experimental evidence summarised above, and the modelling studies, indicate the importance of the GAP investigations.

#### **3.3.2 New knowledge obtained by GAP**

To improve understanding and to obtain hydrogeochemical groundwater data for glacial climatic conditions, boreholes were drilled within the GAP in front of the GrIS, as described in Section 2.4.4. One of the conclusions from GAP is that it is possible to drill and take good quality groundwater samples, i.e. with a low content of drilling fluids, from boreholes in permafrost areas.<sup>4</sup> Three bedrock boreholes were drilled through permafrost, and for the first time a borehole was drilled in under an ice sheet. Even though working in such an environment has its unique challenges, datasets have been successfully collected in GAP, and because so few data were available before the GAP, these new acquired data will improve the understanding of fluid movement and geochemical evolution under cold climate conditions. Time series of groundwater samples were collected from four sections in two of the boreholes (three sections from DH-GAP04 and one section from DH-GAP01). More specifically:

- DH-GAP01: the sampled section, about 71 m long, was at the bottom of the borehole, cf. Figure 2-22.
- DH-GAP04: three sections were sampled. The upper section (Sect-up) is approximately 190 m long and extends from the base of the permafrost to the packer system. The mid-section (Sect-mid), between the two packers, is 10 m long; and the lower section (Sect-low) extends from the lower packer to the bottom of the borehole, being about 80 m long, see Figure 2-24 and Figure 3-15.

Groundwater sampling and analysis are described in the Data Report (2016); see also Section 2.4.5 and 2.4.6 for sampling dates. Porewater studies, and fracture-filling mineral investigations were also performed, as described in Section 2.4.7.

In addition to borehole investigations, hydrogeochemical groundwater data and understanding of processes taking place under glacial climatic conditions can also be obtained by investigating springs located at ice sheet margins. Observations of such groundwater discharges are uncommon, because permafrost likely impedes the flow of groundwater and some discharge points may remain undiscovered if they occur in areas covered by meltwater runoff or by lakes. Nevertheless, some reports exist of springs at glacier margins (Grasby et al. 2003, Pollard 2005, Scholz and Baumann 1997). In particular, the spring associated with a pingo in front of the Leverett glacier (Scholz and Baumann 1997), has been further investigated within the GAP. In addition, while searching for springs, samples were collected from groundwaters emerging at the bottom of the drained Ice dammed lake. For locations of these sample points see Figure 2-18 and Figure 2-21.

#### ***Main advances in geochemical understanding of glaciated sites***

##### **Groundwater origin**

Figure 3-23 shows  $\delta^2\text{H}$  and  $\delta^{18}\text{O}$  data obtained within GAP, including meltwaters, the Leverett pingo spring, the Talik lake, and the samples from the deep boreholes. The data show that the groundwaters sampled in DH-GAP04 originate from glacial meltwaters, whereas for groundwaters from DH-GAP01, the isotope signatures indicate that they are a mixture of glacial meltwaters and Talik lake waters. The  $\delta^2\text{H}$  and  $\delta^{18}\text{O}$  values from the DH-GAP01 waters also show a slight evaporation signature, which is consistent with some recharge from the Talik lake. The isotopic data from the GAP borehole groundwaters are unique, and the evidence obtained on the meltwater origin of the groundwaters at the GAP site confirms for the first time that some of the meltwater generated under a warm-based ice sheet is able to penetrate fractured rocks down to repository depths. This predominant meltwater origin at the GAP site is certainly the consequence of long periods of glacial and periglacial climatic conditions at the site (see Section 2.1.6), and therefore, groundwaters of other origins (e.g. meteoric recharge) would be expected at similar sites that have had only short glaciation periods.

<sup>4</sup> Although the samples obtained so far from the middle and upper sections of DH-GAP04 still contain approximately 35% of drilling fluid, it is expected that in the future representative samples can be collected.

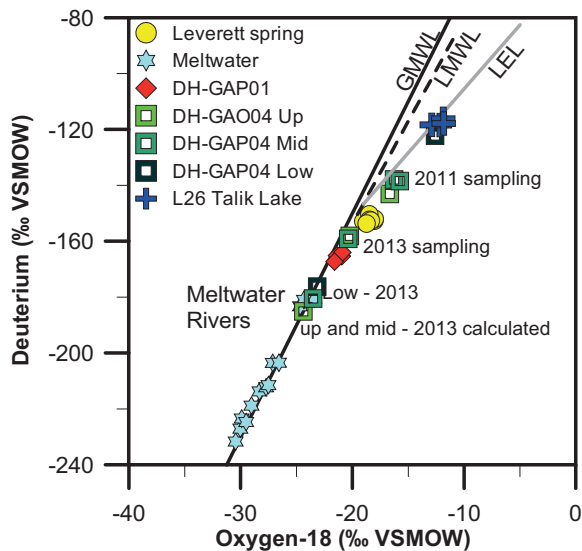


**Figure 3-23.**  $\delta^{18}\text{O}$  versus  $\delta^2\text{H}$  for groundwaters, meltwaters and the Talik lake (L26, the lake overlying DH-GAP01). The calculated isotopic composition of DH-GAP04 waters is based on a simple linear mixing model. LEL is the local evaporation line, and LMWL is the local meteoric water line.

### Salinity

The salinity of the DH-GAP04 groundwaters is relatively high (Figure 3-24), considering that, based on their isotopic signatures, they originate from glacial meltwaters. When examining the core from DH-GAP04, it was seen that gypsum ( $\text{CaSO}_4 \cdot 2\text{H}_2\text{O}$ ) is the major fracture infilling mineral. Gypsum is also found, although only from a few observations in fractures, in the core from DH-GAP01. There is evidence to suggest that this mineral has a hydrothermal origin (Data Report 2016). Gypsum is a readily soluble mineral, and the  $\text{Ca}^{2+}$  and  $\text{SO}_4^{2-}$  concentrations in the DH-GAP04 groundwaters show saturation with respect to this mineral. Graly et al. (2014) have shown that the subglacial meltwaters in the area have low sulphate contents, and it could be argued that all sulphate in the groundwaters originates from the dissolution of gypsum as these groundwaters flow in the rock fractures. Removing all cations equivalent to the sulphate in the groundwater sampled from the low section of DH-GAP04 (collected 2013-09-24) results in a groundwater containing 6.4 mM  $\text{Na}^+$  balanced by 4.9 mM  $\text{Cl}^-$ , and some bicarbonate, that is, if gypsum dissolution is excluded, only a limited amount of solutes have been acquired by the meltwaters since they infiltrated into the rock fractures. The low solute contents of the groundwaters, after removing the contribution from gypsum, provides no evidence for extensive freeze-out of salts, which could result in increased concentrations of salts (e.g. Skidmore et al. 2010). The estimated concentrations of solutes after removing the contribution from gypsum, are much higher than the reported data for subglacial meltwaters, which have less than 0.03 mM (Data Report 2016, Graly et al. 2014), although they are qualitatively comparable to the amounts of solutes in groundwaters from proglacial till in Antarctica and Svalbard (Cooper et al. 2002, Skidmore et al. 2010).

Long residence times and extensive water-rock interactions will, in general, not contribute significantly to increased concentrations of chloride in infiltrated meltwaters unless the rock itself contains chloride, for example in fluid inclusions. The results from the crush and leach and out-diffusion tests (Data Report 2016) suggest that the dissolved chloride found in the groundwaters sampled from the GAP boreholes originates from matrix diffusion and from weathering reactions involving the dissolved carbonic acid originally present in the glacial meltwaters. The groundwater emerging at the Leverett spring, i.e. the spring associated with the pingo at the margin of the Leverett glacier, judging from the temperature, has travelled to larger depths than those reached by the GAP boreholes, which may have resulted in some degree of mixing with deep-seated saline waters. However, the chloride content (approximately 1 mM) of these waters is lower than in groundwaters from the lower section of DH-GAP04.

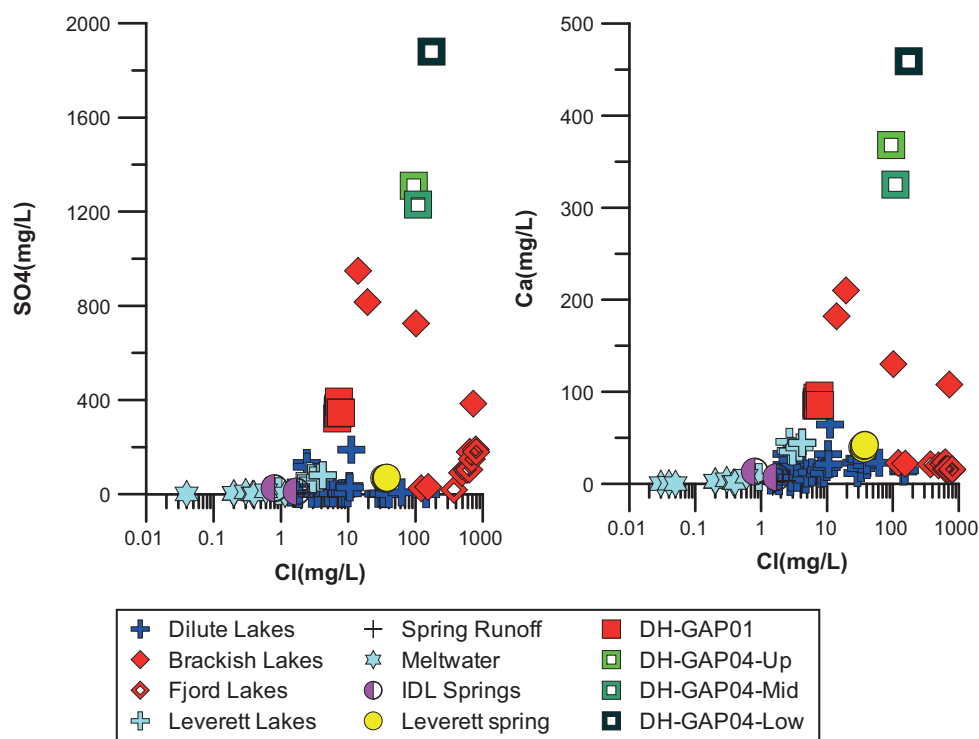


**Figure 3-24.** Sulphate and calcium plotted against chloride. Note that DH-GAP04 concentrations for the upper (Sect-up) and mid (Sect-mid) sections are based on samples that are still moderately contaminated with drilling fluid (38 and 33% respectively). Meltwater samples are shown, but often have large charge imbalances. IDL springs refer to Ice dammed lake springs. Figure from the Data Report (2016).

The hydrogeochemical data obtained within the GAP are unique; the low chloride contents of the groundwaters at the margin of an ice sheet, together with the meltwater origin of these waters, clearly confirms that fresh groundwaters can potentially reach repository depths during glacial conditions, and such waters could affect the stability of engineered barriers in a nuclear waste repository, for example by promoting bentonite buffer erosion. A key result of the GAP is therefore that it has provided support to the model calculations (e.g. Vidstrand et al. 2014) used in the long term assessment of the safety of nuclear waste repositories. However, whether low salinity groundwaters will be present or not at depth at a given site during a glacial period will depend on a number of site-specific factors, such as a hydrogeological setting favourable for meltwater infiltration, a rock devoid of soluble salts, and absence of saline groundwaters before the onset of the glaciation.

### Redox conditions

The laboratory gas analyses from the two samples from DH-GAP04 and those from the Leverett spring indicate anoxic conditions based on analysis of the methane and H<sub>2</sub> contents (Data Report 2016). Field measurements performed simultaneously with the sampling of DH-GAP04 using a dissolved oxygen sensor (accuracy ± 0.1 ppm) fitted into a plastic jar, indicated absence of dissolved O<sub>2</sub> in the groundwaters being pumped from all three borehole sections. These results are however somewhat uncertain because both degassing and dilution with the N<sub>2</sub> gas initially present in the electrode chamber cannot be excluded. The laboratory analyses showed the presence of some dissolved O<sub>2</sub>, probably from contamination during analysis. The Leverett spring samples, which were also analysed in a laboratory, also showed the presence of some dissolved O<sub>2</sub> (Data Report 2016), which could have originated from air bubbles in the ground ice buried in the till.

Evidence of anoxic conditions is also provided by the low, but measurable, Fe(II) and Mn contents. In DH-GAP04, the analysis of the latest sampling from the lower section shows Fe(II) approximately 0.1 mg/L, Mn approximately 0.5 mg/L, and a low concentration of U approximately 0.05 µg/L (the U concentration in general increases with increasing redox potential). The DH-GAP01 samples are taken from shallower depths, and the evidence of anoxic conditions is not so conclusive, as Fe(II)

is at or below the detection limit (0.03 mg/L), the concentration of Mn is also lower (approximately 0.02 mg/L) than in DH-GAP04, and the concentration of uranium is higher (approximately 0.4 µg/L). However, an additional indication of anoxic conditions is provided by the non-facultative anaerobic microbes (i.e. microbes that can only grow without oxygen) found in DH-GAP01. The Leverett spring waters have consistently high levels of Fe(II) (more than 5 mg/L), a clear indication of their anoxic condition.

The redox properties of fracture-filling minerals were investigated in a study financed by SKB and Posiva, using *scanning electron microscopy* (SEM), X-ray diffraction and USD (*Uranium Series Disequilibrium*) analyses to locate the transition between oxic and reducing conditions along each borehole. The results of this study are summarised in the Data Report (2016), see also Figure 3-25. In this study, evidence of reducing conditions is found through the presence of pyrite below approximately 50 m depth; oxidation of Fe (II)-containing minerals is found only in shallow fractures (down to 60 m below ground surface, with a couple of occurrences of goethite also found down to 260 m, see Figure 3-25) all from within the permafrost. In DH-GAP04, the deeper occurrences of goethite are, to a large degree, tiny crystals associated with sheared and slickensided chlorite-coatings, which shows that they were formed prior to a shearing event and are unlikely to have been formed recently. In all cases, the goethite occurrences are found within the present permafrost depths (Data Report 2016), and they are unlikely to be the result of a recent penetration of oxygenated groundwaters. It is to be noted that the oxidation observed in the upper few metres is within the active layer. USD provides indications of uranium mobilisation below the permafrost (from 431 m and 550 m depth, see Data Report 2016), suggesting that the redox conditions have changed in the past.

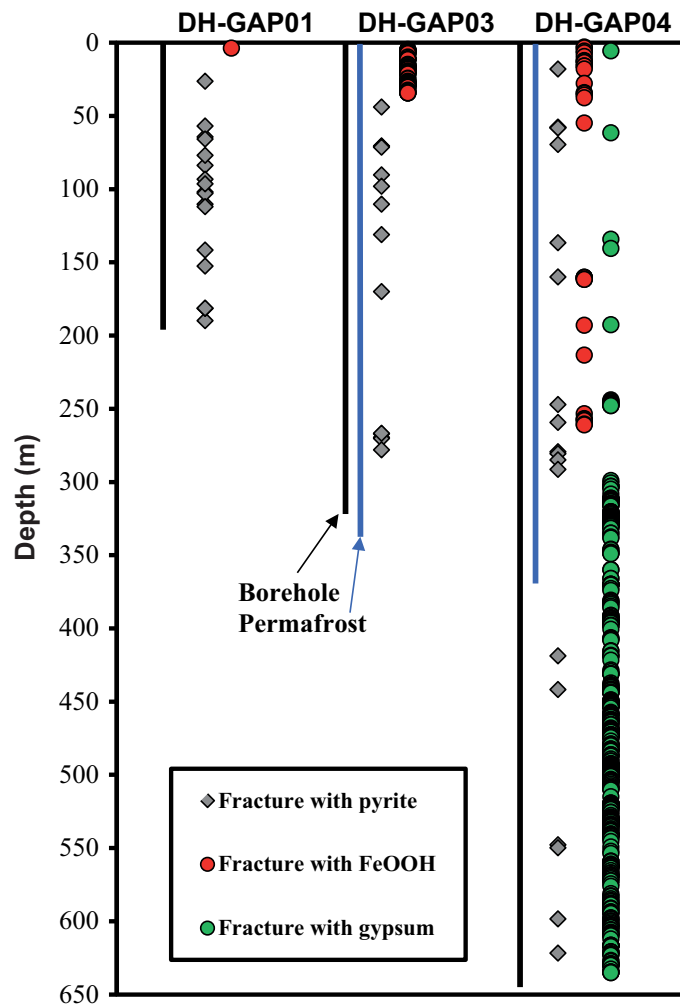


Figure 3-25. Mapping of fracture minerals, goethite (FeOOH), pyrite and gypsum vs. depth. On the x-axis, there is one column for each mineral in each of the boreholes. Y-axis shows vertical depth from top of casing (TOC).

A key finding of the GAP is, therefore, that oxygenated waters do not penetrate to depth close to the ice sheet margin, even though dilute glacial waters do penetrate, i.e. the redox potential is effectively buffered by the rock, thus providing evidence that confirms the results from modelling (Sidborn and Neretnieks 2008, Sidborn et al. 2010, Spiessl et al. 2008). GAP has therefore provided direct results that will increase confidence in future evaluations of the long term safety of nuclear waste repositories. However, there are limitations in the conclusions that may be drawn. These limitations are common for any analogue study: 1) the evidence of anoxic groundwaters at one site does not rule out the possibility of oxic meltwater infiltration to repository depths at other locations; and 2) there is uncertainty about the O<sub>2</sub> contents of the original meltwaters before they infiltrated into the rock, as the dissolved gas content of the basal meltwaters was not investigated (Data Report 2016). The evidence from fracture-filling minerals containing oxidised iron in the upper part of the bedrock does not contribute any information on this matter, as the oxidation may have taken place either during meltwater infiltration, or during periglacial climatic conditions, or both.

### Other considerations

#### *Groundwater dynamics:*

The Talik lake waters (isotope composition, dissolved solutes) do not show any indication of groundwater discharge (as compared with the DH-GAP01 data), and this is to be expected because the small volumes of groundwater that might perhaps enter the lake are insignificant compared to the volume of lake water. Possible recharge (from the lake into the rock) is indicated by the  $\delta^2\text{H}$  and  $\delta^{18}\text{O}$  signatures in the DH-GAP01 borehole water and by its  $^{87}\text{Sr}/^{86}\text{Sr}$  ratio, intermediate between radiogenic lake waters and the low (less than 0.71) ratios found from crush and leach derived waters and in the DH-GAP04 groundwaters. This is also consistent with measurements of hydraulic head, which suggest that water is recharging from the lake into the shallow groundwater system (Section 3.2.2). The Leverett spring in front of the Leverett glacier and the springs observed at the bottom of the (partially drained) Ice dammed lake (see locations in Figure 2-18) clearly show that some groundwater discharge exists close to the ice margin, but the evidence from GAP is that such discharges are negligible when compared to the amounts of melting ice.

Gypsum is widespread as fracture-filling mineral in the drill core of DH-GAP04 below approximately 300 m depth and was also identified dispersed in the rock matrix in core samples (Eichinger and Waber 2013). However, because gypsum is a readily soluble mineral, the fact that the sampled DH-GAP04 groundwaters are saturated with this mineral gives no indication about the residence time of these waters. Nevertheless, the widespread presence of gypsum in the fractures at this location indicates that volumes and/or durations of infiltrating meltwater have not been sufficient to dissolve these fracture infills. This interpretation is further supported by the absence of any chemical, isotopic or physico-chemical (EC or T) indications of changed flow conditions at depth, and by the slow decline in concentration of drilling fluid (Data Report, 2016). Even though groundwater flow occurs only in discrete fractures, widespread volumes of gypsum-free rock have not been observed in DH-GAP04 below approximately 300 m. It may therefore be concluded that either rather small volumes of meltwater infiltration have occurred to these depths or that large groundwater flows have occurred only during short time periods.

The source of dissolved gases could give an indication of groundwater dynamics. In the case of methane, the isotope signature of the Leverett spring gas sample ( $\delta^{13}\text{C}$  approximately  $-70\text{‰}$ ) suggests that its origin is microbial, either from the fermentation of organic matter or perhaps from methanogenesis sustained by deep crustal H<sub>2</sub>.

Chlorine-36 is a radioactive isotope (half-life 301,000 years) produced by cosmic radiation in the upper atmosphere and in the subsurface by *in situ* neutron flux. With time, <sup>36</sup>Cl will accumulate and decay until the rate of production equals the rate of decay (i.e. secular equilibrium). This occurs in a closed system after a period of approximately 1.5 million years. The <sup>36</sup>Cl/Cl<sub>Total</sub> ratio in the groundwater sample from the lowest section of DH-GAP04 is low ( $2.1 \times 10^{-14}$ ) and it is similar to the value calculated for <sup>36</sup>Cl at secular equilibrium with the surrounding rock in Finnish and Swedish sites (Gascoyne 2001, Posiva 2013, Smellie et al. 2008). The rate of generation of <sup>36</sup>Cl by *in situ* neutron flux in the groundwater, which mainly depends on U and Th contents in rock, is not established for

the GAP site, and therefore the  $^{36}\text{Cl}$  isotope ratio in secular equilibrium may deviate from those calculated for the Fennoscandian sites. However, the U and Th contents probably do not deviate significantly (i.e. by orders of magnitude) from the contents in granitic rocks at Olkiluoto, Forsmark and Äspö-Laxemar (Trincherio et al. 2014). A low  $^{36}\text{Cl}/\text{Cl}_{\text{Total}}$  ratio in the lower section of DH-GAP04 indicates that the chloride found in the groundwater has been isolated from the atmosphere for a period of approximately one million years or more. It should be noted that this residence time estimate concerns chloride ions, which may mostly originate from the rock matrix (e.g. in fluid inclusions) and may have been present much longer in the bedrock than the groundwater in fractures. Thus, the  $^{36}\text{Cl}/\text{Cl}_{\text{Total}}$  ratio of dissolved chloride does not provide evidence of the groundwater residence time. The  $^{36}\text{Cl}/\text{Cl}_{\text{Total}}$  ratios for the middle and upper sections of DH-GAP04 are much higher, but they can be approximately explained by simple mixtures of a surface water (i.e. drilling fluid) and a groundwater having “old” chloride.

Dissolved  $^4\text{He}$  can be used to estimate the time needed for that He to accumulate in groundwater in site-specific conditions, therefore indicating the residence time of groundwater (IAEA 2013, Trincherio et al. 2014). Gas data from DH-GAP04 do not include any isotopic analysis. However, He contents in the atmosphere is low, so the relatively high He concentrations observed in two samples from the upper section of DH-GAP04 (1.0 and 3.3 mL/L, Table 5–13 in Data Report 2016) are probably crustal in origin (from radioactive decay of U and Th and their  $\alpha$ -emitting daughters in rock minerals) and therefore, mostly  $^4\text{He}$ . The amount of He measured in DH-GAP04 suggests an *in situ* production time scale of one million years when compared with the calculated results for Olkiluoto, Forsmark and Äspö-Laxemar (Trincherio et al. 2014). Any residence time estimate from the He data available from DH-GAP04 is, however, uncertain for several reasons; 1) the time scale depends on the U and Th contents in the bedrock at the GAP site, which have not been determined; 2) the residence time may be overestimated, because additional  $^4\text{He}$  could be supplied from other sources, for example by a deep crustal He flux; and 3) the He contents of the two samples differs substantially.

A preliminary conclusion is that the He data from DH-GAP04 suggest that these deep meltwater-derived groundwaters have been isolated for long periods from the atmosphere and that they therefore have long residence times, possibly exceeding hundreds of thousands of years, which is much longer than what could be expected when considering the groundwater flow modelling results for Forsmark (see Figure G-23 in Vidstrand et al. 2010). This preliminary conclusion also suggests slow groundwater flows at DH-GAP04, which would be a consequence of the presence of permafrost, the geological structure and the hydrogeological setting at this borehole location, and it agrees with the observations and conclusions in Section 3.2.2. This is also consistent with the persistence of gypsum, as observed in DH-GAP04. As mentioned above there are several uncertainties and limitations to the He data. It should also be recalled that the He data are from the upper section of DH-GAP04, which still had a large amount of drilling fluid contamination. Isotope data on the carbon system ( $^{13}\text{C}$  and  $^{14}\text{C}$ ), if it becomes available in the future, might require a revision of this preliminary conclusion on the groundwater residence time.

#### *The maximum depth of glacial meltwater penetration*

The isotopic signature of the groundwaters from the low section in DH-GAP04 shows meltwater origin, so glacial meltwaters have penetrated at least to depths of 500 m, see Figure 3-15. The maximum penetration depth can therefore not be established from the GAP data as the GAP boreholes are not deep enough. Similarly, the groundwaters sampled in DH-GAP01 at depths below 140 m, have a glacial signature, and taking into account that the talik, where the borehole is located, is surrounded by several hundred metres thick permafrost, this indicates as well that the groundwaters have travelled down to repository depth.

The groundwater emerging at the spring in front of the Leverett glacier, which has a slight evaporation isotopic signature, is probably a mixture of a deep groundwater (of unknown age) and glacial meltwater in the gravel surrounding the spring. The groundwater component has travelled deep enough and for sufficient time to heat up so that it can keep the spring flowing year after year. The isotope signatures of the sampled spring waters suggests that the groundwater component is of glacial origin (or cold climate recharge), unless the proportion of moraine porewater in the samples is large (e.g. 50% or more).

Together, the isotope signatures of the groundwaters sampled at the three locations indicate that glacial meltwaters, or cold climate waters, are able to penetrate to depths of at least 500 m, at least locally, although this is certainly very dependent on the geometry of faults and fracture zones. This is in agreement with what could be expected from the information available before the GAP and presented above in Section 3.3.1.

### 3.3.3 Remaining challenges

Several aspects of the geochemistry of the groundwater samples are still not fully resolved. These include:

- The origin of the salinity that is not associated with gypsum dissolution, i.e. the chloride and bicarbonate. Data on the gypsum infills may be used to obtain better estimates of the amount of solutes originating from gypsum dissolution, and as a consequence, will lead to a better analysis of processes leading to the evolution of meltwaters into the observed groundwaters. As discussed above, the processes that lead to chloride contents are mixing with deeper saline groundwaters, perhaps of hydrothermal origin, or interactions with the rock, such as matrix diffusion and weathering reactions. The extent of mixing of deeper groundwater and recent superficial meltwaters at the outlet of the Leverett spring is difficult to establish and it may vary with time.
- Dissolved methane is, according to isotope evidence, of microbial origin, but the exact microbial processes involved are unknown.
- The content of drilling fluids remaining in the upper and middle sections of DH-GAP04 is still high. Further flushing and sampling will reveal more detail on the composition of the groundwaters in these sections. Isotope analyses, e.g. for  $^{13}\text{C}$  and  $^{14}\text{C}$ , are also needed to establish if the groundwaters in the three sections have different origins or if they have water components with different residence times.
- Drilling waters used during drilling were most probably air-saturated. Waters from lakes L26 (the Talik lake) and L25 were used for drilling of DH-GAP01 and DH-GAP04, respectively. The samples collected in 2013 from the upper and mid sections of DH-GAP04 still contain relatively large amounts of drilling water (approximately 30%). These samples show increased Mn concentrations compared with the drilling water, and the U content is low, but the Fe content is too low to indicate clearly anoxic conditions. Future samplings are needed to confirm that these borehole sections have recovered from the oxidizing perturbation caused by the drilling, and if so, to determine what microbial or inorganic processes have affected the consumption of oxygen.

## 4 Contributions towards answering the six guiding project questions

The motivation for the GAP project was derived primarily from experiences in past safety case applications where significant uncertainties and/or conservatisms regarding the role of glaciation on groundwater system stability and repository safety existed or were assumed. To this end, in the early stages of the GAP programme six key safety assessment related questions were posed to provide context for proposed work activities. The activities and research undertaken by GAP focused on obtaining information that contributes to answering these six questions.

### 4.1 Where is meltwater generated under an ice sheet?

The production of meltwater from an ice sheet can be divided into meltwater produced at the ice sheet surface and meltwater produced at the ice sheet bed. The latter component, referred to as basal water production, is, on an annual basis, two orders of magnitude smaller in terms of water volumes produced than the surface water production. The heat for the melting of basal ice comes from geothermal heat flow and, to a lesser extent, from frictional heat produced by basal sliding of ice and ice deformation. The production of water under an ice sheet is directly coupled to the ice sheet's basal thermal regime. In areas where the basal ice temperature is below the pressure melting point, the ice sheet is frozen to the bed and no free basal water is present. In contrast, in areas where the basal ice temperature is at the pressure melting point, the basal ice is melting and free water can be present at the ice sheet bed.

Studies performed within GAP, including direct and indirect observations as well as ice sheet modelling, have resulted in a conceptual view of ice sheet hydrology for the investigated section of the GrIS. This conceptual view includes three different basal hydrological zones, illustrated along a longitudinal ice sheet profile, see Section 5.1 and Figure 5-2. Under the ice divide, and extending many tens of km away from it, the basal ice temperature is below the pressure melting point and the bed is frozen, as indicated by radar data and ice sheet modelling. In this *frozen bed zone* no basal melting occurs, there is no basal hydrological system present and hence no groundwater recharge takes place.

Downstream of the *frozen bed zone*, there is a zone where the temperature of the basal ice is at the pressure melting point and basal meltwater is produced. In this *wet bed zone* free water is present at the bed and a basal hydrological drainage system transports the meltwater laterally. Even though there is surface melting taking place in this part of the ice sheet, the surface water does not reach the ice sheet bed. The amount of water produced by basal melting in the *wet bed zone*, available for groundwater recharge, amounts to close to zero at the upstream boundary towards the *frozen bed zone* and up to around 10 mm/yr (Brinkerhoff et al. 2011) at the downstream part of the zone, some 120 km from the ice margin. The water production from basal melting is relatively constant over the year, since the processes that result in basal melting do not vary over the seasons, with the potential exception of frictional meltwater generation associated with summer speedup. Although not observed within GAP, it is likely, from theoretical considerations and from ice sheet modelling, that the transition from the *frozen bed zone* to the *wet bed zone* is gradual, with a variable distribution of melted and frozen bed conditions. In such a transition zone, elevated parts of the bed are preferentially frozen whereas topographic lows typically have melted bed conditions.

Downstream of the *wet bed zone*, surface meltwater reaches the ice sheet bed. The GAP studies have shown that the surface water production is two orders of magnitude larger than the basal water production (Section 3.1.2). Therefore, surface water reaching the bed, in combination with the small amount of basal water production, results in considerably larger volumes of basal water than in the *wet bed zone*. This *surface-drainage bed zone* extends to the ice sheet margin, with an increasing amount of water produced at the ice sheet surface (upper panel Figure 5-2) approaching the ice margin. The sector of the GrIS that was investigated by GAP does not have the cold-based conditions along the ice sheet margin commonly observed on smaller polythermal glaciers in e.g. Scandinavia and Svalbard. Instead, the investigated section of the ice sheet seems to be entirely wet-based downstream of the central *frozen bed zone*.

The GAP has shown that, under the investigated sector of the GrIS, basal water is present under more than 75% of the ice sheet (Section 3.1.1), except in a central area where basal frozen conditions prevail. The areas where basal water is present have a hydrological system that varies considerably in characteristics over space and time (Section 3.1). In the extensive areas where basal water is present, groundwater recharge and discharge may take place.

It should be noted that the present distribution of meltwater and subglacial drainage under the GrIS, is a result of past and present-day climatological and glaciological settings. The associated hydrological systems in the bedrock, in particular the location of areas where groundwater recharge and discharge can take place, are affected by the local variations in elevation and hydraulic properties. It may be that similar conditions prevailed, and will prevail, during e.g. the deglaciation phases of past and future ice sheets over Fennoscandia and Canada. Nevertheless, during other phases of ice sheet cycles, such as during ice sheet growth, one has to consider that the distribution of e.g. hydrological zones may be different than in the observed example provided by the GrIS. For example, during peak glacial conditions the position of the ELA will be lower than at present, and the intensity of surface melt will be reduced from that at present. While the ice sheet would still have an ablation zone with wet summer conditions, this zone would be narrower and with less available water than observed on the present-day GrIS by GAP. Further, the margin of an advancing ice sheet may experience basal frozen conditions due to a colder climate, something not observed at the present-day GrIS.

## 4.2 What is the hydraulic pressure situation under an ice sheet, driving groundwater flow?

Data from the ice boreholes drilled from the surface of the Isunnguata Sermia Glacier to the bed of the ice sheet (the basal drainage system) provide information about hydraulic pressures under the ice sheet in the GAP study area. In addition, ice velocity data and radar measurements are utilized, as these provide indications of spatial variability in pressure and hydraulic potential in the basal drainage system under the ice sheet.

The hydraulic pressure characteristics under an ice sheet depend on factors such as the distance to the ice sheet margin, seasonal variations in meltwater runoff, the permeability of the basal drainage system including possible sediments therein, and the topography and permeability of the bedrock. The permeability of crystalline bedrock is of lesser importance for the hydraulic pressure under an ice sheet than the other factors due to the large hydraulic conductivity contrast between bedrock and basal drainage system, but important for the magnitude of local recharge of meltwater to groundwater.

The seasonal variations in water flow in the basal drainage system observed in the GAP study area mainly result from ice sheet surface melting, i.e. meltwater reaching the ice sheet bed through the en-glacial network. In addition, some water is generated within the basal drainage system due to basal melting (i.e. melting caused by geothermal and frictional heat and deformation of ice in the basal temperate layer). It is noted that the amount of water produced by basal melting is orders of magnitude smaller than the water generated by surface melting (see Section 3.1.2). However, whereas strong surface melting only occurs for 2–3 months each year, basal melting is a continuous process.

The ice thickness varies significantly within the GAP study area due to, among other things, the spatial variability of the bedrock topography (see Section 2.2.4 and 3.1.3). Specifically, the Isunnguata Sermia Glacier is situated above a deep bedrock trough that reaches several hundreds of metres below sea level. However, the surface of the ice is smooth and only in a subtle way reflects the bedrock topography beneath (Lindbäck et al. 2014, Lindbäck and Pettersson 2015). Significant depressions in the terrain typically have high hydraulic pressures and probably coincide with deformation zones in the bedrock, thus constituting potential recharge areas of meltwater to groundwater (Data Report 2016, Lindbäck and Pettersson 2015). The presence of permafrost below the ice sheet margin needs to be accounted for since frozen ground is significantly less permeable and reduces the potential for groundwater flow.

The ice boreholes drilled during GAP provide direct information on hydraulic pressure conditions at the base of the Isunnguata Sermia Glacier. Based on the acquired data in the ice boreholes and the results from ice sheet modelling, it is hypothesised that the bed of the ice sheet can be divided into three basal zones with contrasting thermal-hydrologic conditions. These are the *frozen bed zone*,

*the wet bed zone*, and *the surface-drainage bed zone*. The *surface-drainage bed zone* has two sub regimes, *the transient conduit region*, from the margin to 15–20 km inward, and *the high pressure region*, from 20 km to the ELA, see Sections 4.1 and 5.1 for details.

Meltwater flow in the basal drainage system in the frontal part of the *surface-drainage bed zone* is hypothesised to change character when the hydraulic pressure increases due to the abundance of meltwater during the summer months (Meierbachtol et al. 2013). During the ‘winter season’, the flow pattern in the basal drainage system is dominated by so-called linked-cavity flow (also called non-conduit flow), whereas during the ‘summer season’, the flow pattern in the basal drainage system is governed by flow in discrete conduits. As stated above, the conduits are believed to reach only some 15–20 km inland from the ice margin. It is envisaged that the pressure outside the conduits is lowered when conduits are formed, but remains higher than in the conduits, such that the flow of water is directed toward the conduits. Linked-cavity flow implies a poorly connected network of patches (cavities) of water, generated as a result of basal melting mainly and slowly draining under relatively high basal pressures. Also, the linked-cavity flow drainage system would not be expected to undergo such large drops in hydraulic pressure in response to water input forcing as hypothesised for a conduit-dominated system that rapidly drains high volumes of water from the bed. Rather, a relatively high hydraulic pressure is maintained at all times in the linked-cavity drainage system for moderate changes in meltwater runoff.

The hydraulic measurements and analyses from the ice holes imply that the ice overburden hydraulic pressure (i.e. a hydraulic head corresponding to 92% of the ice thickness, see Data Report 2016 for details) provides an appropriate description of the basal hydraulic pressure, as averaged over large distances and long time periods when considering the high pressure region of the *surface-drainage bed zone* and the *wet bed zone* (in the frozen bed zone, no recharge will take place). In the transient conduit region of the *surface-drainage bed zone*, the pressure drops substantially on a diurnal cycle during the summer months. Concerning water pressure, it is noted that because ice overburden pressure scales with ice thickness, the basal hydraulic pressure increases toward the centre of the ice sheet, from atmospheric pressure at the ice margin to more than 10 MPa where the ice becomes frozen to the bed, see Figure 4-1. Figure 4-1 indicates the measured (within the *surface-drainage bed zone*) and hypothesised (within the *wet bed zone*) water pressures along the same transect as shown in Figure 5-2; the horizontal gradient increases towards the ice margin where the ice surface slope is the steepest. It is noted in Figure 4-1 that it is the hydraulic head, not the shown water pressure, which drives groundwater flow. The hydraulic head equals the bedrock elevation plus 92% of the ice sheet thickness; thus, the hydraulic gradient is given by the slope of the ice sheet irrespective of the ice sheet thickness.

Local (i.e. a scale of 1–10 km) horizontal gradients in basal hydraulic pressure are superimposed on the ice overburden pressure gradient, as dictated by local changes in ice thickness and the length scale under consideration. Local hydraulic pressure gradients are substantial near the margin since the bed has large topographic relief and the ice sheet surface is steep. At locations where the local gradients in topographic relief are more than ten times the gradient of the ice sheet surface, the bed slope is the driving component of the water flow direction (Cuffey and Paterson, 2010). Such conditions are rare in most glacier settings; however, in the GAP study area there are some portions of the deep bedrock troughs where this condition is met.

Local pressure gradients are also altered by the basal drainage system, where flowing water can temporarily lead to water pressure being lower than overburden pressure, especially during summer months. These temporal gradients in hydraulic pressure were observed in the GAP study area.

As discussed above, data and analyses from the ice drilling provide direct, quantitative input on basal hydraulic pressures within the *surface-drainage bed zone*. In contrast, data measured on the ice sheet surface provide quantitative but indirect information on larger scales. Specifically, results from the GPS ice motion work (Data Report 2016) can be interpreted to support the ice borehole measurements suggesting the hydraulic pressure situation under the ice sheet as being variable in both space and time. High pressure events (inferred from surface accelerations) occur at the seasonal onset of melt (the so called ‘spring event’), during lake drainage, and during rainfall events. During summer, an efficient but high pressure, non-conduit, basal drainage at least within 40 km from the margin is interpreted to develop. Supraglacial lake drainage events may rapidly deliver large volumes of water to the ice-bed interface yielding temporary decimetre-scale uplift due to the massive input of water to the ice-bed. Lake drainage events also open up hydraulic pathways through km-thick ice, which continue to deliver supraglacial meltwater to the subglacial environment for the remainder of the melt season.

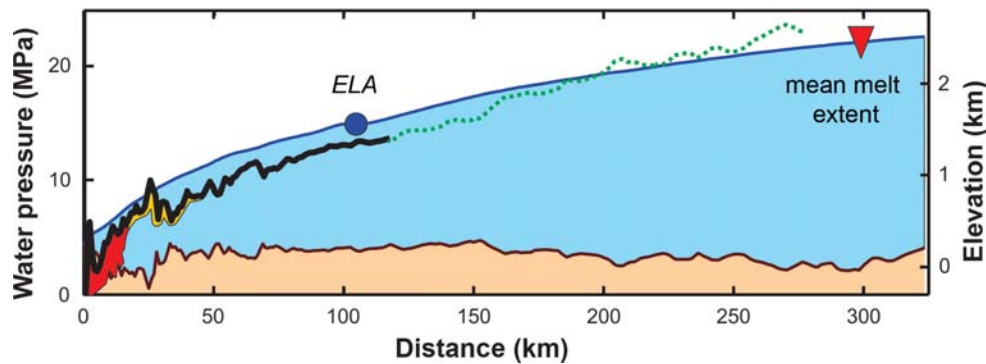


**Figure 4-1.** Cross section view of bedrock (brown) and ice sheet (blue) along the Greenland study transect extending from the ice divide to the ice margin. Conceptual understanding of water pressure in the basal drainage system shown as black curve. The red marking of the water pressure curve indicates the region that clearly develops a subglacial conduit network which can lower the water pressure far below that of the overburden (e.g. up to 70% below); the yellow marking indicates the region interpreted as not having a well-developed conduit network, but where pressure can still undergo a seasonal pressure drop (of 10 or at most 20% below overburden). The green dotted extension of the black pressure curve indicates that no measurements were made here; the curve is thus hypothesised. Red triangle is the 20 year average extent of any surface melt. The ice is shown in elevation and the pressure is shown in MPa; therefore, the green dotted line extends above the ice because it is plotted using the scale on the left. It is emphasised that groundwater flow is not driven by the water pressure alone, but by the hydraulic head which equals the bedrock elevation plus 92% of the ice sheet thickness.

GPR studies provide maps of the hydraulic potential that can indicate the regional hydraulic pressure distribution and water routing in the basal drainage system (Section 3.1.4, Data Report 2016). Although the hydraulic potential calculation is simplistic and has limitations, it provides an overview of regional trends. The hydraulic potential calculation shows a general decreasing trend towards the terminus, indicating flow in the area is generally towards the ice margin, but is modified with lower hydraulic potential in major subglacial valleys. Thus flow is expected to be focused into the valleys.

To summarise, the ice boreholes drilled in the transient region of the *surface-drainage bed zone* indicate that a low pressure conduit network develops up to ca 15–20 km from the ice margin during the melting season. There is no evidence of seasonal growth of a low pressure conduit network beyond this region. However, a broad spectrum may exist between efficient, low pressure conduits and inefficient, high pressure linked-cavities. The indication, from GPS data, of an efficient, high pressure linked-cavity system represents such a state.

It is concluded that the GAP has provided sufficient answers concerning the pressure situation under the ice sheet in order to formulate boundary conditions for groundwater flow modelling.

### 4.3 To what depth does glacial meltwater penetrate into the bedrock?

The isotopic results of DH-GAP04 groundwater samples show that glacial meltwater can reach depths of more than 500 m depth in the study area. Glacial melt infiltration at the GAP site may have been taking place continuously for hundreds of thousands of years, even millions of years (see Section 2.1.6), whereas the periods with glacial conditions over the suggested repository sites in Fennoscandia have been temporary and substantially shorter.

The groundwater data obtained in GAP and other sites (see Section 3.3) show the significance of palaeo-hydrogeological conditions on glacial meltwater infiltration in bedrock. Deep infiltration and meltwater features in deep groundwaters are influenced by several hydrogeological and hydrogeochemical factors:

- Long-lasting glacial conditions at or near ice margins favours meltwater infiltration (GAP, Palmottu).
- Favourable hydrogeological structure of bedrock contributes to meltwater infiltration (GAP, Kivetty).
- Existing highly saline and dense groundwaters may inhibit fresh and light meltwater infiltration to greater depths (Fennoscandian sites).

The GAP data cannot precisely answer how deep meltwater has penetrated in the bedrock of the GAP site; the data show only that meltwater has penetrated at least to typical repository depths (approximately 500 m). However, insufficient knowledge of site hydrogeology (gradients, spatial structure), and particularly on how long the glacial meltwater infiltration lasted, represent a substantial difficulty in interpretation in comparison with the sites in Fennoscandia, because this time span was probably considerably shorter in the other sites, even in Palmottu, which represents prolonged meltwater infiltration conditions at the ice margin. Detailed investigations at some other sites similar to Palmottu, with relatively low hydraulic gradients and known duration(s) of meltwater infiltration, and with stabilised hydrogeological conditions since ice retreat, could give more precise information to address this question. One such suitable site has been identified in south-eastern Finland, where the large lake Saimaa has stabilised the hydraulic conditions around the Salpausselkä end-moraine since the stationary ice margin stage approximately 11,500 years ago (Johansson et al. 2011).

#### **4.4 What is the chemical composition of glacial water when and if it reaches repository depth?**

Infiltrating glacial meltwaters are mixed with the groundwaters previously present in the rock, and the mixture will then be affected by matrix diffusion as well as by water-rock interactions. The composition of the resulting waters reaching repository depth will therefore depend on a number of factors:

- The composition of the groundwaters initially present in the fractures at the site, and in the pores of the rock matrix.
- Geological factors such as the spatial geometry of the dominant fracture zones, the porosity of the rock matrix, and the nature of the overburden (thickness, composition, etc.). These features will affect groundwater flow, and therefore affect the residence time of the waters in the fractures, and they will also influence the possibility of mixing with deep saline groundwaters.
- The geochemistry of the host rock (including fluid inclusions) and the fracture-filling minerals.
- The climatic history of the site: palaeohydrogeology, timing and duration of periods with glacial coverage, temperatures during past marine periods, etc.

The GAP has strengthened confidence in our understanding of the processes affecting the composition of the waters reaching repository depth. The groundwaters at depths at the GAP site down to approximately 500 m are essentially glacial meltwaters (Section 3.3.2). However, the data suggests that these groundwaters have had long residence times. An important process in DH-GAP04 is the dissolution of gypsum (calcium sulphate, present in relatively large amounts as a fracture-filling mineral) as groundwater travels along the fractures. The chemical composition of the groundwaters reaching DH-GAP04 is strongly affected by the dissolution of this mineral. At other sites, the factors listed above affect the groundwaters to varying degrees, such that the proportion of glacial meltwater as a function of depth will vary largely between sites, and the composition of the groundwaters will be correspondingly affected.

#### **4.5 How much oxygenated water will reach repository depth?**

The processes described in the previous section concerning the evolution of the chemical composition of infiltrating meltwaters will naturally affect the concentration of dissolved O<sub>2</sub> as well, although some factors are more important for oxygen than for other solutes, such as Ca. In particular, dissolved O<sub>2</sub> is consumed by reaction with dissolved Fe(II) originating from the dissolution of rock minerals. When Fe(II) is exhausted in the fracture minerals and groundwater, matrix diffusion plays an important role in making available larger amounts of Fe(II) for oxygen consumption (Sidborn et al. 2010, Spiessl et al. 2008). The Fe(II)-mineral contents of the host rock, its porosity and other factors affecting matrix diffusion are important for oxygen consumption. The GAP project has strengthened confidence in the processes that consume dissolved oxygen. Even though the groundwaters sampled in the boreholes are essentially glacial meltwaters in origin and although the reducing capacity of these groundwaters is low (e.g. in terms of the concentrations of dissolved Fe(II), manganese, methane, etc.), there are clear indications that the groundwaters are anoxic (Section 3.3.2).

The analyses of the gas samples from the Leverett spring and from DH-GAP04 are less conclusive, as they show traces of oxygen, possibly due to air contamination.

The presence of pyrite at depths greater than approximately 60 m provides evidence of anoxic, sulphidic conditions. In addition, all observed indications of oxidation of fracture-filling minerals are shallow and from within the permafrost and, therefore, these oxidations cannot have occurred under the current groundwater flow conditions (see Section 3.3.2). The deepest goethite samples (approximately 260 m depth) have experienced shearing and may be of relatively old age, so they are not strong evidence of oxidation at depth.

The body of data provided by GAP has shown that the processes that consume dissolved oxygen are effective at the site, and although the groundwaters are essentially of meltwater origin, no observation of oxic groundwaters has been made. The rate and the detailed characteristics of the oxygen depletion process cannot yet be determined because of several unknown factors: 1) the oxygen concentration of the infiltrating meltwaters; 2) the time of recharge, although estimated to be at least some hundreds of thousands of years; and 3) the detailed mineralogical and geochemical characteristics of the rock.

#### **4.6 Does discharge of deep groundwater occur in the investigated proglacial talik in the study area?**

In a proglacial landscape characterised by permafrost, recent numerical studies suggest that through taliks can act as either recharge or discharge pathways for deep groundwater flow (e.g. Vidstrand et al. 2013, Bosson et al. 2013), or that different through taliks may contain very different concentrations of glacial meltwater, i.e. water originating from the basal drainage system (Jaquet et al. 2012). Furthermore, high-resolution numerical studies of groundwater flow in permafrost landscapes indicate that individual taliks can contain both recharge and discharge within the same talik (Bosson et al. 2013)<sup>5</sup>. Thus, there is no *a priori* reason to assume that the investigated through talik in the GAP study area, and elsewhere in a similar setting, should be a discharge talik.

In order to increase the understanding of the proglacial hydrology, GAP (and the related GRASP) looked to understand how a through talik interacts with its surroundings by investigating the water balance of the catchment containing the lake under which the through talik is located. The borehole DH-GAP01 was drilled to confirm the existence of, and to study, a talik structure under the Talik lake in the GAP study area. DH-GAP01 was drilled to a vertical depth of approximately 190 m; for details of the borehole, see Section 2.4.4

As described in Section 3.2.2, Johansson et al. (2015b) used the hydraulic pressure (head) information measured in both lake and talik to set up an annual water balance for the lake. The calculated balance indicates that there is recharge from the lake to the talik, but that this recharge constitutes only a very small part of the total water balance of the lake.

There are also hydrochemical data indicating that lake water is recharging the groundwater. These indicators include the mixing of the  $\delta^{18}\text{O}/\delta^2\text{H}$  signature of the groundwater with the evaporative signature of the lake water, and a  $^{87}\text{Sr}/^{86}\text{Sr}$  ratio showing mixing between radiogenic lake waters and deep groundwater characteristic of the deep borehole DH-GAP04, see also Section 3.3. Groundwater in the monitored section of DH-GAP01 may, therefore, include mixing with recharging lake waters. However, based on the lack of a secondary tracer and limited geochemical information, the hydrochemical evidence provides only limited support to indicate recharge to groundwater from the lake. For the estimated geochemical mixing scenario outlined above, the DH-GAP01 groundwater would contain up to 25% lake water recharge. It is to be recalled that this borehole fully recovered from drilling contamination by May of 2010 (Data Report 2016) and therefore the mixing calculations were not influenced by drilling fluids.

To summarise, data collected within GAP, and within supporting independent field efforts (GRASP), conclusively indicate that a through talik exists beneath the Talik lake. In addition, water balance analysis and chemical data analysis indicate that water recharges from the lake to the talik. With longer time series of measured variables and with additional supporting modelling, more confidence can be placed in the description of the talik characteristics. It is noted that there are many potential through taliks in the proglacial region of the GAP study area, see Figure 2-7.

---

<sup>5</sup> Vidstrand P, in prep. Concept testing and site-scale groundwater flow modelling of the ice sheet marginal-area of the Kangerlussuaq region, Western Greenland. SKB R-15-01, Svensk Kärnbränslehantering AB.

## 5 Conceptual understanding of conditions and processes at the GAP site

The GAP included investigations of conditions at the surface and at the bed of the GrIS, as well as hydrogeological and hydrogeochemical conditions in the proglacial area directly in front of the ice sheet and extending just underneath the margin of the ice sheet. Significant bedrock structures (deformation zones) and strong topographical undulations are present in the proglacial area (see Sections 2.2.4 and 2.4.1), and measurements with ground-penetrating radar and airborne geophysics revealed that these conditions are also present below the ice sheet. The bedrock is predominantly crystalline and is heterogeneously fractured; its hydraulic conductivity is therefore expected to vary in space both laterally and with depth. Accordingly, the hydrological dataset acquired for the bedrock in the GAP area is expected to be site-specific at a local scale, whereas the hydrological datasets acquired on the surface of the ice sheet and at the base of the ice sheet (the ice-bedrock interface) are likely to be more broadly representative of a large region of western Greenland and perhaps other ice sheets with similar settings and boundary conditions.

Figure 5-1 illustrates the main hydrological and hydrogeochemical results and the conceptual understanding of the GAP study area. Figure 5-1a illustrates the larger GAP study area in which the GAP carried out field investigations and ice sheet modelling (cf. Figure 1-4). Locations of the ice boreholes, AWS and bedrock boreholes in Figure 5-1b are highlighted here. Figure 5-1b is a schematic cross-section of the dashed blue profile indicated as X-X' in Figure 5-1a, highlighting the key GAP data and conceptual hydrological and hydrogeochemical understanding. The goal of the surface based ice sheet investigations was to improve scientific understanding of 1) the seasonal interactions between ice sheet hydrology and subglacial hydrology; 2) the thermal regime at the base of the ice sheet; and 3) to examine supra-, en- and subglacial processes to understand where water is formed and/or present under the ice sheet and its routing through the ice. Ice drilling activities employed direct measurements to examine pressures at the base of the ice sheet and seasonal development of the basal drainage system close to the ice sheet margin. The geosphere investigations focused on improving understanding of hydraulic and hydrogeochemical conditions of deep groundwaters and of a talik, based on investigations of lakes, springs and bedrock boreholes.

The understanding of the hydrological observations acquired for the ice sheet and for the geosphere in the area studied by the GAP is summarised in Sections 5.1 and 5.3, respectively. The proglacial area is subject to permafrost with patches of unfrozen ground conditions (taliks). The presence of permafrost and taliks in the area studied by the GAP and the understanding of how these potentially affect recharge and discharge are summarised in Section 5.2. Considering together the geological, hydrogeological and hydrogeochemical information, the overall hydrogeochemical understanding of this area is presented in Section 5.4.

### 5.1 Hydrological conditions of the ice sheet

The understanding of the present-day hydrological conditions both at the surface and at bed of the ice sheet is presented in the following sections.

#### 5.1.1 Surface conditions

At the centre of the GrIS, approximately 300 km inland from the ice sheet margin in the GAP study area, low temperatures persist all year such that the snow-covered surface remains relatively dry, undergoing inconsequential melt or no melt. As the elevation decreases away from the ice divide following a parabolic surface profile, more of the winter snowfall melts each summer. Annual snowfall exceeds annual melt across a wide region between the dry snow area and the ELA (the elevation at which annual melt balances annual snowfall); surface melt in this region is generally retained as either refrozen ice and/or liquid water.

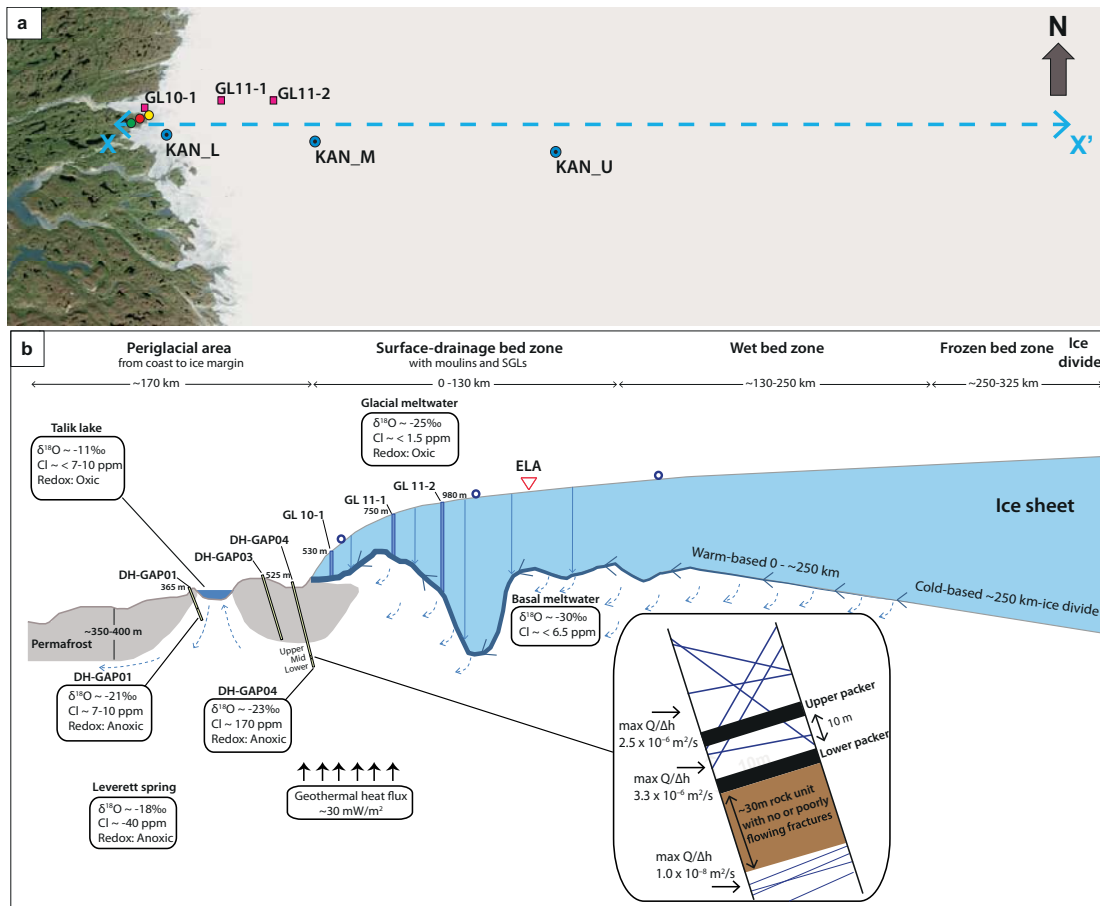


**Figure 5-1.** Synthesis of main results and conceptual understanding of the hydrology within the GAP study area. a) View showing extent of the area where GAP field investigations and ice sheet modelling were carried out. Automatic weather stations (AWS) shown as blue circles. Locations of ice boreholes GL 10-1, GL 11-1 and GL 11-2 shown as pink squares. Bedrock boreholes shown as coloured circles, where green = DH-GAP01, red = DH-GAP03 and yellow = DH-GAP04, respectively. The dashed blue line (X to X') denotes the approximate extent of the cross-section seen in the lower panel. b) Schematic cross-section highlighting key GAP data and conceptual hydrological and hydrogeochemical understanding. Ice boreholes shown as blue lines are projected from a few km out of plane of the transect. The different glaciohydrological basal zones in the upper part are from Figure 5.2 in Section 5.1. Note that the position of the frozen-melted boundary (FMB) zone is based on modelling results (for details see Section 3.1.1). Blue line at the ice sheet bed indicates basal flow. Numerical figures beside bedrock and ice boreholes represent measured hydraulic heads. Main hydrogeochemical results from GAP key locations are shown in boxes. No redox data could be collected from the basal meltwaters. Note the presence of permafrost near the ice sheet margin, including the existence of a through talik under the Talik lake. Recharge into the through talik was documented by the GAP data. Although not observed in this study, groundwater discharge could potentially also occur in the same talik, as indicated in the figure. Also note the considerable subglacial bedrock relief. Red triangle shows the approximate location of the ELA. Inset in b shows a schematic view of the fracturing and the measured transmissivity values around the monitoring sections in DH-GAP04 (see inset c in Figure 3-14).

The ablation area lies, per definition, below the ELA and extends all the way to the ice sheet margin. Here, all annual snowfall is melted and, with decreasing elevation, an increasing amount of ice is also melted. Liquid water is, therefore, most abundant in the ablation area. The volume of surface melt is highly variable from year-to-year, and is a summer phenomenon limited to 3–4 months in duration. The summer melt period completely dominates the annual cycle of water availability in terms of water volume.

The SGLs that form on the ice surface cover a small fraction of the ice in this region (i.e. 2%). Lakes delay the runoff of 7–13% of the melt; the remainder enters the supraglacial, englacial and basal drainage

systems. Catastrophic draining of SGLs into newly opened fractures, however, is one of the key mechanisms for establishing surface-to-bed pathways. These events occur during summer, and within an elevation band covering about the upper half of the ablation zone. Nearly all surface melt eventually penetrates the ice and reaches the bed; this is supported by the observation that there are no major rivers pouring off the ice sheet (Section 3.1). Just above the ELA, where melt begins to pool, is approximately the interior limit where substantial surface melt has the potential to penetrate to the bed.

### 5.1.2 Bed conditions

The hydrological conditions at the bed of the ice sheet are controlled by the ice sheet surface conditions discussed above and by thermo-mechanical processes within the ice and at the basal boundary, e.g. traction and geothermal flux. Between the ice divide and the margin, the bed is characterised by three distinctly different basal zones based on the amount and configuration of water present; a *frozen bed zone*, a *wet bed zone* and a *surface-drainage bed zone* (Figure 5-2). In the *frozen bed zone* near the ice divide, the bed will remain frozen under the present climate-, ice dynamic- and geothermal heat flux conditions (Brinkerhoff et al. 2011, Section 3.1). The bed condition across this zone is in a frozen state and, therefore, no recharge to the groundwater system occurs.

As the ice near the base of the ice sheet flows toward the warmer margins and away from the cold ice divide, it slowly warms from the heat supplied by geothermal heat flux. Deformation of the ice causes strain heating, and frictional heat is added where the ice slides across the bed. Eventually, the ice temperature reaches the pressure melting point and the bed becomes wet and remains wet across the entire melted zone (*wet bed zone*). Conduit water flow within the ice bed is very unlikely in this zone, because the low surface slope of this region and low water flux severely restrict the ability of conduits to develop by the melting of ice walls. The isolated nature of the water features coupled with very thick ice likely render basal pressure at or near overburden pressure (i.e. 90 to 100% of overburden) at all times. Although water is present in this zone at the bed, modelling suggests the basal melt produces only mm to 1 cm of water per year across this zone. If bedrock fractures and/or permeable bed conditions exist, groundwater may route water away from the bed of the ice sheet. If the transmissivity of bedrock fractures is very high, the recharge rate may be limited by water availability.

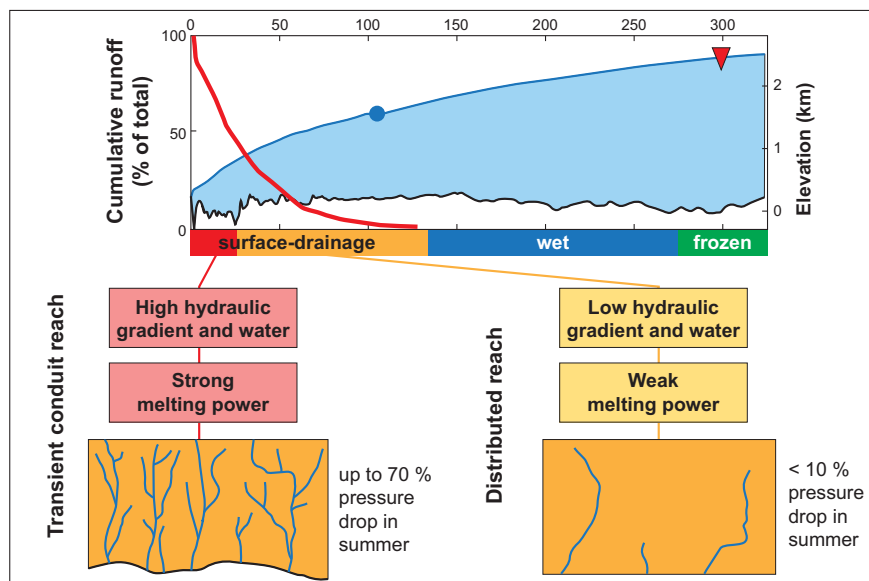


**Figure 5-2.** Schematic cross section through GAP study domain from the ice divide to the terminus of Isunnguata Sermia. Top panel shows ice surface and bed; blue dot on surface is the equilibrium line (ELA), and red triangle is the 20 year average extent of any surface melt. Red line shows 1958–2013 average meltwater runoff, accumulated from high-to-low along the ice surface, from the MAR model (Tedesco et al. CCNY Digital Archive). The top panel also shows the location and size of the three identified basal hydrological zones (here colored red/yellow, blue and green below the ice sheet), see the text. Bottom of panel shows a conceptual view of subglacial conditions.

The *surface-drainage bed zone* extends from the melted or *wet bed zone* outward to the ice sheet margin, and underlies the entire surface ablation area. This zone is distinct because it receives a substantial water input from the surface, and because basal sliding rates are high leading to drainage system/sliding speed interactions. An active and high flux basal drainage system develops in this zone. Boreholes in this region show that the drainage system evolves seasonally in response to changing surface conditions, and exhibits substantial spatial and temporal gradients. Water flows through linked-cavities and conduits melted into the ice roof in some places. The amount of water supplied to the bed far exceeds the amount of water that groundwater can accommodate and so the vast majority of the water exits to the terminus through a basal drainage system (Section 3.1.2). Water flux at the bed is so high from surface melt that losses or gains from the groundwater system can be expected to have an inconsequential impact on the basal drainage system.

The *surface-drainage bed zone* can be subdivided into two regions, based on distinct differences in the basal drainage system. Within about 15–20 km of the ice sheet margin, in the *Transient Conduit Reach* (Figure 5-2), the high basal water flux and steep surface slope along the outer flanks of the ice sheet cause a strong hydraulic gradient for driving water along the bed towards the margin. The gradient generates viscous heating in the water system, which enables the added heat to melt the overlying ice. The result is a transient conduit network that develops each summer in response to high water input from the surface. The network is established first at the outer margins sometime in early summer, and then propagates head ward under the ice as the summer progresses. Water pressures in the conduit network, and any highly connected adjacent regions, typically undergo large daily swings from 105% of overburden pressure to as low as 30% in response to meltwater input variability.

Along the conduit network head ward from the margin, water flux in the system decreases as the ice sheet surface melt rate declines. In addition, the ice sheet surface slope driving the generalised hydraulic gradient decreases rapidly away from the steep margins. These factors reduce the energy produced by viscous heating of flowing water, thereby diminishing ice melt and the growth of the conduits. A transient conduit network likely does not advance each summer from the margin and into this *Distributed Reach* (Figure 5-2), although there may be sparse conduits in select locations where sufficient water flux/pressure is maintained year-round. A key finding of the GAP project is that the growth of a summer conduit network into the interior of the ice sheet is strongly limited by diminishing melting power of the basal water system (Meierbachtol et al. 2013). Without the presence of a widespread conduit network, the *Distributed Reach* does not undergo the large daily swings in pressure (i.e. 30% to 105% of overburden pressure) observed lower on the ice sheet. Nevertheless, the water flux across this region has been observed to be relatively large – it must be in order to accommodate the surface input.

This conceptual view of the basal drainage system implies that much of the bed inward of the margin is covered by water, rather than mostly drained by discrete conduits with little water in between. Further, the drainage system would not be expected to undergo large pressure drops in response to water input forcing, as hypothesised for a conduit dominated system that rapidly drains high volumes of water from the bed. Rather, a relatively high pressure (approximately 90% of the ice thickness) can be maintained at all times despite variable water input.

## 5.2 Permafrost and taliks

The GAP study area is located in a region with continuous permafrost. At the Kangerlussuaq airport, permafrost has been estimated to be around 100–160 m thick (van Tatenhove and Olesen 1994), whereas at the nearby ice sheet margin, at a higher elevation, the permafrost thickness reaches 350–400 m, as measured in the DH-GAP03 and DH-GAP04 boreholes. As described in Section 3.1.1, the main part of the base of the ice sheet in the study area, including the marginal areas, is at the pressure melting point (with the exception of the central parts of the ice sheet where frozen bed conditions prevail). This, together with the fact that most of the area glaciated at present were also glaciated throughout the Holocene (and hence not been subject to any subaerial permafrost development), indicates that permafrost does not exist under the major part of the large warm-based areas of the ice. An exception to this is the ice margin where a wedge of permafrost most likely stretches in under the ice. It is not known how far this subglacial permafrost wedge stretches, e.g. if it is a few hundreds of m or several km. Considering that borehole DH-GAP04 is close to being a vertical borehole (drilled with a 70°

inclination from the horizontal), which penetrated the base of the permafrost and does not extend far beneath the ice margin, it is not possible to draw any further conclusions about the lateral extent of the subglacial permafrost from borehole data.

The existence of deep permafrost in the ice-free part of the GAP study area has a major impact on the proglacial hydrogeological system as it reduces groundwater recharge and discharge in the proglacial area, restricting it to taliks. Based on observations in the DH-GAP01 borehole (approximately 190 m deep; Table 2-1), and studies of the Talik lake where the borehole is located (Figure 2-8, Figure 5-1b, Figure 5-3a), the existence of unfrozen areas through the entire permafrost thickness, so-called through taliks, has been confirmed in the GAP study area. These through taliks are interpreted to be important features in the hydrological system, providing a potential pathway for exchange of deep groundwater and surface water.

Although the time series of collected data are short, the data from the Talik lake and DH-GAP01 borehole studies (see Section 3.2.4) show a gradient in a downward direction, suggesting recharge, i.e. flow from the lake to the talik. In addition, groundwater modelling<sup>6</sup> suggests that parts of the same talik (i.e. the through talik underlying the Talik lake) might experience groundwater discharge. A longer time series, involving possibly significant changes in weather conditions, and additional pressure measurement locations could yield more insight into the Talik lake dynamics.

As shown in Figure 2-7, the GAP study area encompasses several hundred proglacial lakes. Many lakes in the study area are larger and deeper than the investigated Talik lake, indicating that through taliks are likely to be common features in the hydrological system in this study area. Simplified permafrost/talik modelling has provided information on lake sizes required to support through taliks (SKB 2010a). The results suggest that about 20% of the proglacial lakes in the study area may support through taliks. This, in turn, suggests that, on a GAP study area scale, there is a significant potential for exchange of deep groundwater and surface water in the proglacial area, by recharge and discharge in taliks, despite the fact that the landscape is dominated by thick permafrost.

Regardless of whether the investigated Talik lake constitutes a recharge or discharge talik, or a combination of the two, the main and unique finding of the GAP in this respect is the confirmed existence of a through talik in close proximity to a continental-scale ice sheet, where deep groundwater has the potential to reach the ground surface, and surface water may enter the hydrogeological system.

### 5.3 Hydrogeological system at the ice sheet margin

Figure 5-3a shows a close up of the ice-free area between Isunnguata Sermia and Russell Glaciers, together with the location of nearby boreholes, i.e. six ice sheet boreholes and three bedrock boreholes (DH-GAP01, DH-GAP03, and DH-GAP04). The observations made based on DH-GAP01 were discussed in the previous sections (Section 3.3, 4.6 and 5.2). Boreholes DH-GAP03 and DH-GAP04 are deeper and drilled much closer to the ice sheet margin than DH-GAP01 (Table 2-2). Both DH-GAP03 and DH-GAP04 are interpreted to intersect a tight synformal syncline, which in turn is interpreted to be intersected by several steeply dipping fracture zones (see Figure 2-19, Figure 3-14 and Figure 5-1). The hinge area of the syncline is interpreted to dip gently towards the Isunnguata Sermia Glacier. The conceptual block shown in Figure 5-3b does not show the syncline but does highlight other features considered important for the interpretation of the hydraulic and hydrological observations in borehole DH-GAP04, e.g. fracture zones, elevation and thickness of Isunnguata Sermia and Russell Glaciers, undulations in bedrock topography, and the extent of the permafrost. Neither hydraulic nor hydrological measurements were possible in DH-GAP03 (Section 2.4.4).

The data representing hydraulic heads in the upper and middle sections of DH-GAP04 are between 39–47 m above the elevation of the ground surface where DH-GAP04 is under the ice sheet margin of Isunnguata Sermia at 475 m (Figure 3-14, Figure 3-15, Figure 3-16 and Figure 5-1). This indicates that the hydraulic conditions in the uppermost monitoring sections are strongly artesian with respect to the elevation of the ground surface. Observed seasonal hydraulic head transients are on the order

<sup>6</sup> Vidstrand P, in prep. Concept testing and site-scale groundwater flow modelling of the ice sheet marginal-area of the Kangerlussuaq region, Western Greenland. SKB R-15-01, Svensk Kärnbränslehantering AB.

of 8–10 m. Taken together with the rapid, synchronous and cyclic annual responses in these hydraulic heads to changes in regional ice sheet runoff, these observations suggest that the upper and middle borehole sections connect to geological structures that outcrop in locations below the Isunnguata Sermia Glacier where melting conditions prevail. In comparison, the data representing hydraulic head in the lowest section of DH-GAP04 are 25–35 m lower than the hydraulic heads in the upper and middle sections depending on the season, but are still artesian (approximately 10–12 m above the elevation of the ground surface under the ice sheet margin). The head difference between the upper two sections and the lower section is indicative of a strong vertical gradient over the 30 m thick section unfractured bedrock present between the middle and lower sections.

A potential conceptual hydrogeological model for the observed artesian heads in DH-GAP04 is that the thick permafrost (approximately 400 m) observed in this borehole acts as a confining layer for groundwater flow at depth. The hydraulic pressure imposed in the basal drainage system under the ice thus propagates to the packed-off sections through fractures in the bedrock circumventing the permafrost layer. The difference in head between the upper and middle sections and the lower section are interpreted to be due to observed differences in structural-hydraulic properties with depth, e.g. differences in fracture intensity, orientations and transmissivities. As shown in Figure 3-14 and Figure 5-1, the most transmissive fractures that intersect the upper and middle sections are 100 times more transmissive than those intersecting the lower section and the orientations of the fractures are also different (Data Report 2016).

The observations of hydraulic head with time made in DH-GAP04 are unique; these are the first measurements ever made under the margin of the ice sheet and are a significant contribution of the GAP. Based on available data, it cannot be determined whether or not the transmissive fractures intersecting the upper and middle sections of the borehole are connected to the fracturing along geological structures that outcrop at locations where melting basal conditions prevail (Figure 5-1b). As stated previously, the entire ice sheet up to around 250 km from the margin has melting bed conditions in the study area. The time series of lower heads in the lowest section of the borehole is consistent with the lack of steeply dipping fractures intersecting this section and the lower fracture transmissivities discussed above.

The formation of crevasses near the ice margin prohibited long time series of basal pressure to be recorded in the ice sheet boreholes because sensor cables were severed when new crevasses opened. However, records collected during the summer and fall months indicate that the pressure transients observed at the bed of the ice sheet during melt changed by the hour (Figure 3-11) and can exhibit pressure gradients between boreholes (e.g. Figure 3-9). The dynamic variations in basal pressure during melt may reflect diurnal changes in the flow system properties (see Section 3.1.3).

## 5.4 Hydrogeochemical system at the ice sheet margin

Prior to the GAP, the information available on groundwater compositions in close proximity to an ice sheet was limited. In the Kangerlussuaq region, southwest Greenland, information was available only for a spring related to an open pingo (Scholz and Baumann 1997), referred to as the Leverett spring by the GAP. The GAP has provided the first information on groundwaters from within a through talik located in close proximity to the ice sheet margin (DH-GAP01) and on deeper groundwaters located directly under the ice sheet at its margin (DH-GAP04). Borehole DH-GAP01 was drilled in an area approximately 1 km NW of the northern flank of Russell Glacier, approximately 4 km south of Isunnguata Sermia and approximately 6 km SW of borehole DH-GAP04 (Data Report 2016, Pöllänen et al. 2012). Detailed information on the chemical and isotopic compositions of these groundwaters was integrated with complementary information from porewater and mineralogical studies and used, together with the geological and hydrogeological understanding of the site, to examine the origin and evolution of the groundwaters (Sections 3.3, 4.3, 4.4 and 4.5). In the following discussion, groundwaters are considered based on depth of occurrence within the bedrock: shallow refers to groundwaters sampled within the upper 300 m of bedrock, whereas deep refers to groundwaters sampled from below 300 m.

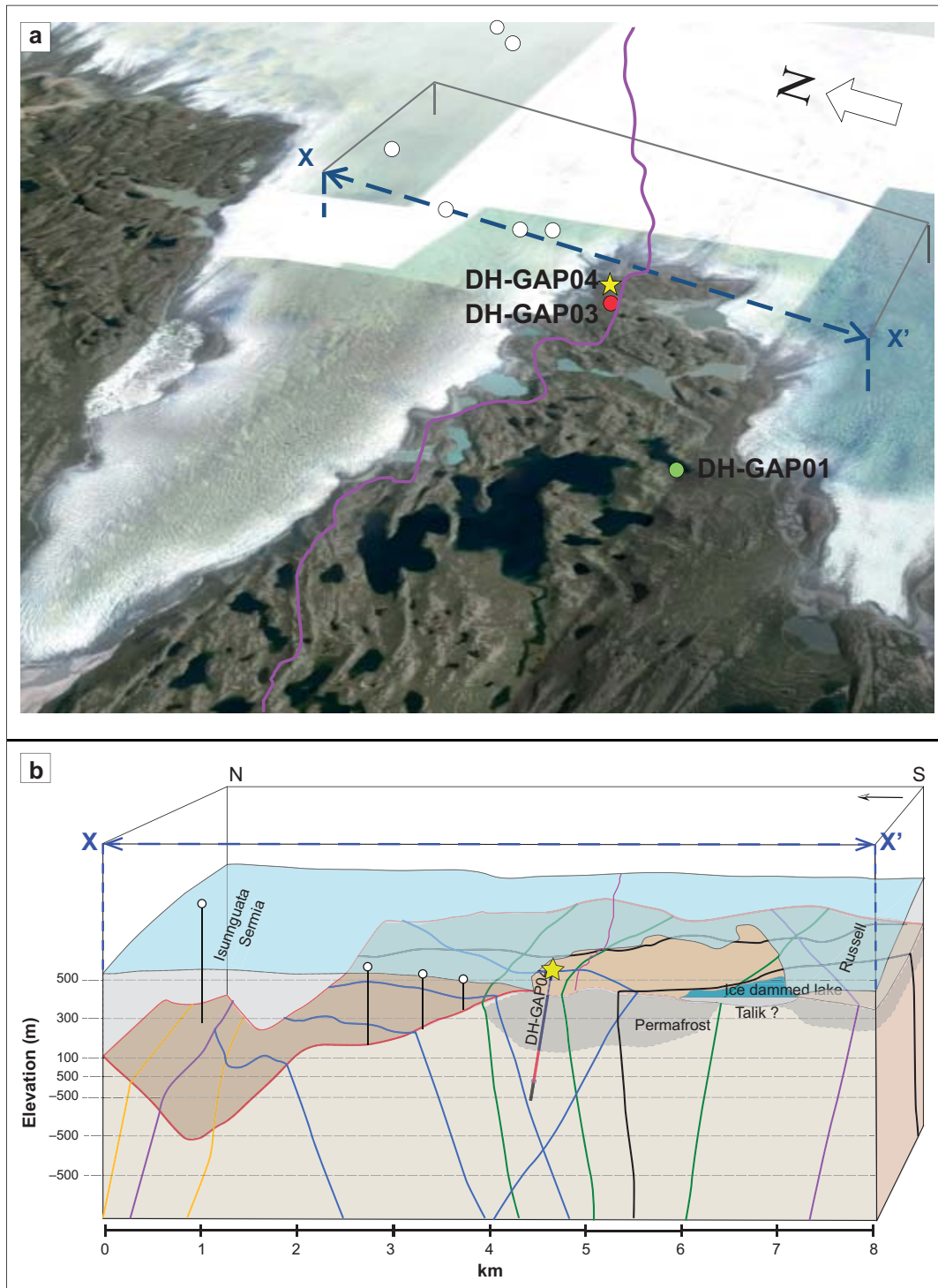


**Figure 5-3.** a) View showing the area between Isunnguata Sermia and Russell Glaciers. White spots indicate positions of six ice sheet boreholes. Green spot, red spot and yellow star indicate positions of bedrock boreholes, DH-GAP01, DH-GAP03 and DH-GAP04, respectively. Purple line indicates the position of the border of the surface catchment (see Figure 1-4 b) Conceptual block model with the frontal plane parallel to blue dashed line (X to X') in a. Note the considerable bedrock undulations (100s of m) and the thick permafrost in the proglacial area and in DH-GAP04. Coloured solid lines indicate modelled fracture zones. Fracture zones of lower order are conceived to intersect DH-GAP04 at approximately 500 m depth.

### Shallow bedrock (0 to 300 m depth)

Where permafrost occurs, depending on its depth, groundwaters within the shallow bedrock may be completely frozen. At the ice sheet margin, permafrost was observed to extend from the surface to approximately 350 m vertical depth. Hydraulic testing was not conducted in the upper 350 m of bedrock due to the presence of permafrost. In DH-GAP01, water-conducting features were detected as discrete peaks in the borehole temperature profile, as the hot water (up to 60°C) used in drilling the borehole cooled (Data Report 2016). In the temperature profiles for DH-GAP04, no evidence for water-conducting features was observed between the ground surface and the bottom of the permafrost, despite the presence of open fractures as observed in the drill core. This demonstrates effective sealing of any potentially transmissive fractures by permafrost.

Groundwaters sampled within shallow bedrock are from within a through talik located under a lake near the ice margin; approximately 1 km from Russell Glacier and 4 km south of Isunnguata Sermia (DH-GAP01). The first 20 m of this borehole were drilled through permafrost (Data Report 2016). Fresh, Ca-Na-SO<sub>4</sub> type water with a Cl<sup>-</sup> concentration of approximately 8 mg/L was sampled in an interval between 139 and 191 m below the ground surface. Although the concentrations of dissolved Fe(II) and Mn in these waters are low, their presence suggests conditions may be anoxic, consistent with the identification of anaerobic microbes (Harper et al. 2011, Data Report 2016). Stable water isotopes indicate that recharge of this water occurred under cold climate conditions ( $\delta^{18}\text{O} - 21.5 \pm 0.3\text{‰}$ ,  $\delta^2\text{H} - 167.5 \pm 2\text{‰}$ ), but the water is more enriched in both isotopes than the range of meltwater compositions currently observed in the area, suggesting that it may be influenced by mixing with evaporatively enriched water from the Talik lake. Fracture infillings in the drill core were observed to be predominantly calcite; gypsum occurs only as a trace mineral associated with calcite.

### Deeper bedrock (below 300 m depth)

Groundwaters of Ca-Na-SO<sub>4</sub>-Cl type were collected from deeper within the bedrock (more than 300 m) at the GAP site, from three monitoring sections located between 400 and 650 m (vertical depth) in DH-GAP04. The salinity of the groundwater in the lowest monitoring section was approximately 170 mg/L Cl. The salinity of groundwaters in the upper and middle sections are likely similar, once corrected for the approximately 35% drill fluid remaining in the samples. Corrected stable water isotopic signatures (corrected for remaining drill fluid contamination) for waters from the upper and middle monitoring sections are similar:  $\delta^{18}\text{O} - 25 \pm 0.5\text{‰}$ ,  $\delta^2\text{H} - 190 \pm 3.6\text{‰}$  and  $\delta^{18}\text{O} - 24 \pm 0.4\text{‰}$ ,  $\delta^2\text{H} - 180 \pm 3.3\text{‰}$ , respectively. Groundwater from the lower section (Sect-low) also has a similar isotopic composition ( $\delta^{18}\text{O} - 23.9 \pm 0.3\text{‰}$ ,  $\delta^2\text{H} - 178 \pm 2\text{‰}$ ). All three groundwaters are at the enriched end of the range of stable water isotopic signatures measured for meltwaters ( $\delta^{18}\text{O} - 23$  to  $-35\text{‰}$ ), indicating recharge during cold climate conditions. The presence of dissolved Fe(II) and Mn in the groundwaters suggests conditions are anoxic and gases sampled in the upper interval contain CH<sub>4</sub> and H<sub>2</sub>, which is also consistent with reducing conditions in the groundwater. In the lowest section of the borehole, <sup>3</sup>H is below detection (less than 0.8 TU) in the groundwater. A preliminary interpretation of dissolved He concentrations from the upper section of DH-GAP04 suggests that the deep groundwaters may have residence times exceeding hundreds of thousands of years (Section 3.3.2).

A distinctive aspect of the geology in DH-GAP04 is the presence of abundant gypsum in fractures below 300 m vertical depth (Figure 3-25). Gypsum present as fracture infillings has a cross-fibrous mineralogical texture suggesting a high temperature (hydrothermal/metamorphic) origin (Section 3.3.2, Data Report 2016). Gypsum was also identified as very fine to fine-grained, rounded crystals dispersed in the rock matrix in core samples from depths between 501 and 652 m borehole length (Eichinger and Waber 2013), or approximately 470 to 612 m vertical depth. Above 300 m in DH-GAP04, only a few, single gypsum-filled fractures occur (Figure 3-25). Below 300 m, the increased abundance of gypsum-filled fractures coincides with a change in rock type from mafic to felsic/intermediate gneisses (Data Report 2016), suggesting that the distribution of gypsum currently observed in the fractures may be related to the rock type available for interaction with hydrothermal fluids when precipitation of the fracture minerals occurred.

There is currently no groundwater flow in bedrock above 400 m depth in the vicinity of DH-GAP04 as a result of freezing conditions within the permafrost. However, under warmer climate conditions in the past, recharge through the fractures in this upper section could have dissolved gypsum, if originally present. This interpretation is consistent with evidence for past recharge of oxygenated waters to a maximum depth of 260 m, as indicated by the presence of iron oxyhydroxides in fractures (Figure 3-25). Although pyrite is observed in fractures below 300 m, iron hydroxide minerals were not observed. Taken together with the extensive persistence of gypsum below 300 m, which is a highly soluble mineral, there is strong evidence of stable conditions with limited groundwater flow since precipitation of gypsum (Data Report 2016) at depths below 300 m. Low groundwater flow in the bedrock surrounding the monitored sections in DH-GAP04 is supported both by hydrogeological observations (Section 3.2.2) and hydrogeochemical observations (in particular, dissolved He concentrations, as discussed above and in Section 3.3.2).

These observed differences in past groundwater flow between the shallow and deeper systems likely reflect, in part, the existence of vertical fractures in the upper 300 m of bedrock as observed in DH-GAP04, whereas below 300 m, vertical fractures become rare and sub-horizontal fractures dominate (Data Report 2016).

### **Groundwater evolution**

Groundwaters from within the shallow and deep bedrock evolved from meltwater recharge (Na-K-HCO<sub>3</sub> type, Graly et al. 2014) followed by water-rock interactions. Interaction of these meltwaters with higher salinity porewaters within the matrix, as identified in out-diffusion and crush and leach studies (Section 3.3.2, and Data Report 2016) resulted in increased concentrations of sodium and chloride in the groundwaters. Dissolution of gypsum is an important process as groundwater travels along fractures, strongly influencing the chemical composition of groundwaters; in particular, those sampled from DH-GAP04. This interpretation is supported by the similarity between the sulphur and strontium isotopic signatures ( $\delta^{34}\text{S}$ ,  $^{87}\text{Sr}/^{86}\text{Sr}$ ) of the groundwaters and those of the fracture minerals, gypsum and celestite (Data Report 2016).



## 6 Conclusions

In this chapter, the scientific results and understanding of the *Greenland Ice Sheet* (GrIS) attained through the GAP are presented in terms of attributes relevant to assessing the long term safety of a *Deep Geological Repository* (DGR) (Section 6.1). The applicability of these findings to safety assessments is summarised at the end of the section (Section 6.2).

### 6.1 Scientific results and understanding attained through the GAP

#### ***Transient meltwater processes on the ice sheet surface***

Surface melt and runoff is a summer phenomenon limited to 3–4 months (May through September). Within the ablation region, the ice surface melts and lowers by up to 3–4 m each summer. The volume of meltwater generated at the surface each summer exceeds the amount of modelled basal melt by two orders of magnitude (cm of basal melt vs. m of surface melt). The summer melt period therefore completely dominates the annual cycle of available water volume.

Abrupt draining of supraglacial lakes into newly opened fractures is one of the key mechanisms for establishing surface-to-bed pathways. Nearly all surface melt eventually penetrates the ice and reaches the bed; this is supported by the observation that there are no major rivers draining the ice sheet surface. Just above the *equilibrium line altitude* (ELA), where meltwater begins to pool, is approximately the interior limit where substantial surface melt has the potential to penetrate to the bed. Seasonal variations in water flow through the basal drainage system in the ablation zone mainly result from ice sheet surface melting.

#### ***Basal thermal distribution and generation of water at the ice sheet bed***

GAP research has provided both direct evidence and modelling results which advance the understanding of the thermal (and melt) conditions at the bed of the GrIS. Direct observations made in 23 boreholes drilled to the ice sheet bed at distances between 200 m and 30 km from the ice margin provide the first direct evidence that the entire outer flank of the study area has a melted bed, with liquid water present, rather than a universally or locally frozen bed. No evidence has been found to suggest that a complex pattern of patchy frozen/melted bed conditions exists in the ice marginal areas within the region of GrIS studied.

The modelling results illustrate that the location of the boundary between melted and interior frozen conditions is highly sensitive to geothermal heat flux values, but relatively insensitive to longitudinal ‘pulling’ caused by fast sliding speeds near the margin. However, additional processes influencing the surface boundary thermal condition – for example, the heat released by refreezing meltwater – can also have a very strong impact on the spatial distribution of frozen/melted bed conditions. For all choices of boundary conditions and modelling parameters believed to be reasonable, the frozen area extends many tens of kilometres away from the ice divide, but greater than 75% of the studied sector of the GrIS is subject to basal melting conditions.

Although the geothermal heat flux was calculated for the GAP bedrock boreholes (DH-GAP03:  $34.8 \pm 1.9$  mW/m<sup>2</sup>, DH-GAP04:  $27.2 \pm 1.8$  mW/m<sup>2</sup>), the uncertainty in the precise location of the frozen/melted transition is related to the inability to directly measure geothermal heat flux beneath the existing ice sheet. In contrast to Greenland, geothermal heat fluxes can, and have been, measured at proposed repository sites and their surrounding regions, which in turn result in better constrained model predictions. The existence of extensive melted bed conditions across a wide reach of the ice sheet, as suggested from GAP observations, could simplify the representation of wet-based conditions in models.

#### ***Hydraulic boundary conditions for groundwater simulations***

Hydrologic conditions at the ice sheet bed were found to vary across the width of the GAP study area. Between the ice divide and the margin, there is evidence for three different basal zones as defined by the amount and configuration of meltwater: the *frozen bed zone*, the *wet bed zone*, and the *surface-*

*drainage bed zone*. The *surface-drainage bed zone* is further characterised by a zone with distributed water drainage and a zone with transient conduit drainage. These zones result from surface, bed, and internal ice flow processes, and are likely representative of Northern Hemisphere ice sheets in a similar stage of development to the current GrIS.

Data and analyses from the ice drilling provide direct, quantitative input on basal hydraulic pressures within the surface-drainage base zone. In contrast, data measured on the ice sheet surface provide quantitative but indirect information on larger scales. Considered together, the results support the interpretation that the hydraulic pressure under the ice sheet is variable in both space and time.

During summer, a conduit drainage network evolves from a system of linked-cavities in response to surface meltwater input to the bed. The network grows over time from the margin inward toward the centre of the ice sheet and lowers the overall mean water pressure. However, observations and modelling suggest this network does not grow to cover more than about 20% of the ablation zone in this region (or approximately 15–20 km, under most circumstances) due to energy constraints related to channelisation of water. Both within the conduit network, and further inland where water likely flows in a highly linked-cavity network, the water pressure undergoes diurnal swings in response to the surface melt cycle. The magnitude of these swings is much larger in the fast-draining conduit system.

Some of the highest pressures observed occur during brief periods of the late afternoon in summer. Other high pressure events occur at the seasonal onset of melt (the so called ‘spring event’), during lake drainage, and during rainfall events. *Supraglacial lake* (SL) drainage events also deliver large volumes of water to the ice-bed interface yielding temporary decimetre-scale uplift due to the massive input of water to the ice-bed.

Taken together, hydraulic measurements and analyses from the ice boreholes imply that ice overburden hydraulic pressure (i.e. a hydraulic head corresponding to 92% of ice thickness) provides an appropriate and realistic description of the basal hydraulic pressure as an average value for the entire ice sheet over the year. The pressure could potentially reach 110% of overburden pressure locally where a direct connection temporarily exists between the bed and water pooled at the surface. Pressure has been shown to drop to as low as 30% of overburden, but only within a few km of the margin of the ice sheet, and only during a portion of summer days. At all sites, the basal water system is near overburden pressure during the majority of the year.

This revised conceptual understanding of the basal drainage system developed through the GAP implies that much of the bed inward of the margin is covered by water, rather than mostly drained by discrete conduits with little water in between. Further, the basal drainage system would not be expected to undergo large pressure drops in response to water input forcing, as hypothesised for a conduit dominated system that rapidly drains high volumes of water from the bed. Rather, a relatively high pressure (approximately 90% of the ice thickness) can be maintained at all times despite variable water input.

### ***Role of permafrost and taliks***

The GAP study area is located in a region with deep continuous permafrost. Close to the ice sheet margin, the permafrost thickness reaches 350–400 m, as measured in the DH-GAP03 and DH-GAP04 boreholes. The main part of the base of the ice sheet in the study area, including the marginal areas, has been shown to have basal melting conditions, with the exception of the central parts of the ice sheet. This, together with the glacial history of the region, suggests that permafrost does not exist under the major part of the large warm-based areas of the ice (see Section 5.2), with the possible exception of the ice margin, where a wedge of permafrost most likely extends underneath the ice for some distance.

The existence of unfrozen areas through the entire permafrost thickness, so-called through taliks, in close proximity to a continental-scale ice sheet has been confirmed by scientific investigations conducted on the Talik lake and in borehole DH-GAP01. Several lakes in the investigation area are larger and deeper than the investigated lake, indicating that through taliks are common features in the hydrological system in the study area. It is estimated that approximately 6% of the land surface in the periglacial part of the study area is covered by lakes that are underlain by through taliks. Through taliks are interpreted to be important features in the hydrological system, providing a potential pathway for exchange of deep groundwater and surface water. Sampling of DH-GAP01 has provided the first

information on groundwaters from within a talik located in close proximity to the ice sheet margin. Although it had been hypothesised that the Talik lake would act entirely as a discharge feature, evidence from hydraulic head measurements and the stable water isotopic composition of the sampled groundwaters are consistent with recharging conditions at this location.

### ***Meltwater end-member water compositions***

The characteristics of a meltwater end-member are needed when evaluating water compositions in glaciated areas, as well as in any numerical modelling of groundwater flow and reactive solute transport. Based on analysis of meltwater compositions conducted as part of the GAP and reported in the scientific literature, a glacial meltwater end-member has depleted  $\delta^{18}\text{O}$  (–30 to –25 per mil) and  $\delta^2\text{H}$  (–235 to –200 per mil) signatures consistent with cold climate conditions and a very low total dissolved solids content, with solute concentrations ranging from practically zero to approximately 1 mM for the main solutes, such as  $\text{Ca}^{2+}$ .

### ***Depth of glacial recharge***

The stable water isotopic signatures ( $\delta^2\text{H}$  and  $\delta^{18}\text{O}$ ) indicate that the groundwaters sampled in borehole DH-GAP04 are of glacial meltwater origin. The millions of years of predominantly glacial conditions in this region, the local structural geology and fracture distribution, the presence of high hydraulic gradients and the presence of relatively low salinity fluids at depth in the rock mass have likely facilitated the penetration of glacial meltwaters at this site to depths of at least 500 m, which is the approximate depth of the packed-off section in DH-GAP04 relative to the ice margin elevation.

The relatively low concentrations of Na and Cl in the groundwaters likely originate from within the rock matrix through water-rock interactions and diffusion, whereas Ca and  $\text{SO}_4$  in these waters originate from dissolution of gypsum, which occurs as a fracture infill mineral at depths below approximately 300 m.

A preliminary interpretation of dissolved He concentrations from the upper section of DH-GAP04 suggests that the deep groundwaters may have residence times exceeding hundreds of thousands of years. Taken together with the extensive persistence of gypsum (hydrothermal origin) below 300 m, which is a highly soluble mineral, there is strong evidence of stable conditions with limited groundwater flow at depths below 300 m. This interpretation is further supported by the absence of any chemical, isotopic or physico-chemical (EC or T) indications of changed flow conditions at depth, and by the slow decline in concentration of drilling fluid. The fast hydraulic head responses observed in borehole DH-GAP04 do not contradict these conclusions, but rather indicate a groundwater system with low storage. Additional work involving continued monitoring, isotopic and chemical analyses together with groundwater flow modelling will increase the understanding of the system.

The information gathered at DH-GAP04 is unique in the context of field investigations in glaciated terrain. The geologic, physical and chemical-hydrogeologic evidence obtained reveals a degree of complexity and non-uniqueness in the interpretation of the deep seated groundwater domain and its' evolution. This is particularly the case with respect to the timing of groundwater recharge and residence times. Further interpretation is ongoing to assess whether this timing can be better constrained.

### ***Redox stability of the groundwater system***

Below the permafrost (and/or at depths greater than about 350 m), reducing conditions are interpreted to prevail in the study area. Past penetration into the bedrock of dissolved oxygen in meltwaters has been limited in depth, as indicated by the presence of iron oxyhydroxides in fractures only in the upper parts of the rock (down to 60 m) with only two isolated occurrences of goethite down to 260 m depth. Although pyrite is observed in fractures below 300 m, iron hydroxide minerals were not observed.

## 6.2 The GAP: Applicability to safety assessments for nuclear waste repositories

The findings summarised above illustrate that the research undertaken as part of the GAP has advanced scientific understanding of hydrological processes associated with a retreating GrIS, including the temporal and spatial nature of processes occurring on the ice sheet surface, conditions at the ice sheet bed (thermal and meltwater generation) and also interactions between glacial meltwater and the underlying groundwater systems.

In assessments of the potential risk to humans and the environment from DGRs for spent nuclear fuel, uncertainties related to process understanding are typically handled using pessimistic assumptions which over- rather than underestimate the potential radiological consequences. By applying the results from the GAP in future safety assessments, it will be possible to demonstrate a significantly increased process understanding within the fields studied. Such demonstrations of process understanding are a cornerstone in safety assessment analyses. In addition, the increased understanding and associated reduction of uncertainties will reduce the need for pessimistic assumptions in certain areas, and may also allow a re-evaluation of the degree of pessimism in some of the assumptions made in previous safety assessments and modelling work.

In this context, some main points of interest are:

- advance in the scientific understanding of the interactions between the hydrology of a retreating ice sheet (GrIS) and the hydrogeology of the bedrock beneath the ice sheet. This provides important information on how the boundary conditions for groundwater flow modelling during glacial cycles should be defined, also in the case of the existence of deep permafrost at the ice sheet margin;
- the evidence of anoxic groundwaters deep in the bedrock under a warm-based ice sheet, conditions which in principle could allow the intrusion of oxygenated water. This provides confidence in the quantification of geochemical parameters at depth, especially on the solubility of solids containing redox-sensitive radionuclides;
- the evidence of the buffering capacity of the bedrock, not only for oxygen, but also pH, to maintain favourable chemical conditions at a repository at depth.

The extent to which the results of GAP can be applied to safety assessments will depend on the selected repository site(s), the chosen repository concept (e.g. repository depth, type of barriers), the selected safety assessment methodology, and the view of the implementer and regulator with respect to the use of analogue sites.

## Acknowledgements

We would like to thank Dr. Shawn Marshall (University of Calgary, Canada), Dr. F. Joe Pearson (Ground-Water Geochemistry, U.S.A.), and Dr. Mike Thorne (Mike Thorne and Associates Limited, U.K.) for conducting scientific peer reviews of this report and providing constructive comments. We would also like to thank Dr. Richard Peltier (University of Toronto, Canada) and Rick Beauheim (Consulting Hydrogeologist, U.S.A.) for their valuable comments on an earlier version of the report.

We would also like to acknowledge the guidance provided throughout the project by the GAP Technical Steering Committee: Mahrez Ben Belfadhel (NWMO, 2009-2010), Mark Jensen (NWMO, 2011-2014), Juhani Vira (Posiva) and Peter Wikberg (SKB).

Per Mikkelsen (JMM Gruppen), Basse Vaengtoft (Kangerlussuaq International Science Support) and Helena Järvinen (SKB) offered valuable support for the study.



## References

SKB's (Svensk Kärnbränslehantering AB) publications can be found at [www.skb.se/publications](http://www.skb.se/publications) and NWMO's publications can be found at [www.nwmo.ca](http://www.nwmo.ca).

- Aaltonen I, Douglas B, Claesson Liljendahl L, Frape S, Henkemans E, Hobbs M, Klint K E, Lehtinen A, Lintinen P, Ruskeeniemi T, 2010.** The Greenland Analogue Project, Sub-Project C, 2008, Field and data report. Posiva Working Report 2010-62, Posiva Oy, Finland.
- Abdalati W, Steffen K, 2001.** Greenland ice sheet melt extent: 1979–1999. *Journal of Geophysical Research: Atmospheres* 106, 33983–33988.
- Aebly F A, Fritz, S C, 2009.** Palaeohydrology of Kangerlussuaq (Søndre Strømfjord), West Greenland during the last ~8000 years. *Holocene* 19, 91–104.
- Alley R B, Dupont T K, Parizek B R, Anandakrishnan S, 2005.** Access of surface meltwater to beds of sub-freezing glaciers: preliminary insights. *Annals of Glaciology* 40, 8–14.
- Andersen B G, Mangerud J, 1989.** The last interglacial–glacial cycle in Fennoscandia. *Quaternary International* 1, 21–29.
- Andersson J-E, Nordqvist R, Nyberg G, Smellie J, Tirén S, 1991.** Hydrogeological conditions in the Finnsjön area. Compilation of data and conceptual model. SKB TR 91-24, Svensk Kärnbränslehantering AB.
- Anderson N J, Leng M L, 2004.** Increased aridity during the early Holocene in West Greenland inferred from stable isotopes in laminated-lake sediments. *Quaternary Science Reviews* 23, 841–849.
- Bamber J L, Layberry R L, Gogineni S P, 2001.** A new ice thickness and bed data set for the Greenland ice sheet: 1. Measurement, data reduction, and errors. *Journal of Geophysical Research: Atmospheres* 106, 33773–33780.
- Bamber J L, Griggs J A, Hurkmans R T W L, Dowdeswell J A, Gogineni S P, Howat I, Mouginot J, Paden J, Palmer S, Rignot E, Steinhage D, 2013.** A new bed elevation dataset for Greenland. *The Cryosphere* 7, 499–510.
- Bartholomew I, Nienow P, Sole A, Mair D, Cowton T, King M, Palmer S, 2011.** Seasonal variations in Greenland Ice Sheet motion: inland extent and behaviour at higher elevations. *Earth and Planetary Science Letters* 307, 271–278.
- Bartoli G, Sarnthein M, Weinelt M, Erlenkeuser H, Garbe-Schönberg D, Lea D W, 2005.** Final closure of Panama and the onset of northern hemisphere glaciation. *Earth and Planetary Science Letters* 237, 33–44.
- Bennike O, Björck S, 2002.** Chronology of the last recession of the Greenland Ice Sheet. *Journal of Quaternary Science* 17, 211–219.
- Booth A D, Clark R A, Kulesa B, Murray T, Carter J, Doyle S, Hubbard A, 2012.** Thin-layer effects in glaciological seismic amplitude-versus-angle (AVA) analysis: implications for characterising a subglacial till unit, Russell Glacier, West Greenland. *Cryosphere* 6, 909–922.
- Bosson E, Sabel U, Gustafsson L-G, Sassner M, Destouni G, 2012.** Influences of shifts in climate, landscape, and permafrost on terrestrial hydrology. *Journal of Geophysical Research* 117, D05120. doi:10.1029/2011JD016429
- Bosson E, Selroos J-O, Stigsson M, Gustafsson L-G, Destouni G, 2013.** Exchange and pathways of deep and shallow groundwater in different climate and permafrost conditions using the Forsmark site, Sweden, as an example catchment. *Hydrogeology Journal* 21, 225–237.
- Bottrell S H, Tranter M, 2002.** Sulphide oxidation under partially anoxic conditions at the bed of the Haut Glacier d’Arolla, Switzerland. *Hydrological Processes* 16, 2363–2368.
- Brinkerhoff D, Meierbachtol T, Johnson J, Harper J, 2010.** Sensitivity of the frozen-melted basal boundary to perturbations of basal traction: Isunnguata Sermia, western Greenland. In *International*

Symposium on Earth's Disappearing Ice, Columbus, Ohio, 15–20 August, 2010. International Glaciological Society, Abstract 59A065.

**Brinkerhoff D J, Meierbachtol T W, Johnson J V, Harper J T, 2011.** Sensitivity of the frozen/melted basal boundary to perturbations of basal traction and geothermal heat flux: Isunnguata Sermia, western Greenland. *Annals of Glaciology* 52, 43–50.

**Brown G H, 2002.** Glacier meltwater hydrochemistry. *Applied Geochemistry* 17, 855–883.

**Brown G H, Tranter M, Sharp M J, Davies T D, Tsiouris S, 1994.** Dissolved oxygen variations in alpine glacial meltwaters. *Earth Surface Processes and Landforms* 19, 247–253.

**Brown J, Ferrians O J, Heginbottom J A, Melnikov E S (eds), 1997.** Circum-Arctic map of permafrost and ground-ice conditions. Washington, DC: U.S. Geological Survey in Cooperation with the Circum-Pacific Council for Energy and Mineral Resources. Circum-Pacific Map Series CP-45, scale 1:10,000,000, 1 sheet.

**Cappelen J (ed), 2012.** Weather and climate data from Greenland 1958–2011 – Observation data with description. Technical Report 12-15, Danish Meteorological Institute.

**Cappelen J, Vraae Jørgensen B, Vaarby Laursen E, Slighting Stannius L, Sjølin Thomsen R, 2001.** The observed climate of Greenland, 1958–99 – with climaticological standard normals, 1961–90. Technical Report 00-18, Danish Meteorological Institute.

**Card K D, 1990.** A review of the Superior Province of the Canadian Shield, a product of Archean accretion. *Precambrian Research* 48, 99–156.

**Clark P U, Alley R B, Pollard D, 1999.** Northern hemisphere ice sheet influences on global climate change. *Science* 286, 1104–1111.

**Cooper R J, Wadham J L, Tranter M, Hodgkins R, Peters N E, 2002.** Groundwater hydrochemistry in the active layer of the proglacial zone, Finsterwalderbreen, Svalbard. *Journal of Hydrology* 269, 208–223.

**Csatho B, van der Veen C J, Tremper C, 2005.** Trimline mapping from multispectral Landsat ETM+ imagery. *Géographie Physique et Quaternaire* 59, 49–62.

**Cuffey K M, Paterson W S B, 2010.** The physics of glaciers. 4th rev. ed. Amsterdam: Butterworth-Heinemann.

**Das S B, Joughin I, Behn M D, Howat I M, King M A, Lizarralde D, Bhatia M P, 2008.** Fracture propagation to the base of the Greenland Ice Sheet during supraglacial lake drainage. *Science* 320, 778–781.

**Data Report, 2016.** See Harper et al. 2016a.

**Dietrich R, Rülke A, Scheinert M, 2005.** Present-day vertical crustal deformations in West Greenland from repeated GPS observations. *Geophysical Journal International* 163, 865–874.

**Dow C F, Hubbard A, Booth A D, Doyle S H, Gusmeroli A, Kulesa Y B, 2013.** Seismic evidence of mechanically weak sediments underlying Russell Glacier, West Greenland. *Annals of Glaciology* 54, 135–141.

**Doyle S H, Hubbard A L, Dow C F, Jones G A, Fitzpatrick A, Gusmeroli A, Kulesa B, Lindback K, Pettersson R, Box J E, 2013.** Ice tectonic deformation during the rapid in situ drainage of a supraglacial lake on the Greenland Ice Sheet. *The Cryosphere* 7, 129–140.

**Doyle S H, Hubbard A, Fitzpatrick A A W, van As D, Mikkelsen A B, Pettersson R, Hubbard B, 2014.** Persistent flow acceleration within the interior of the Greenland ice sheet. *Geophysical Research Letters* 41, 899–905.

**Eichinger F, Waber H N, 2013.** Matrix porewater in crystalline rocks: extraction and analysis. NWMO TR-2013-23, Nuclear Waste Management Organization, Canada.

**Engelhardt H, Humphrey N, Kamb B, Fahnestock M, 1990.** Physical conditions at the base of a fast moving Antarctic ice stream. *Science* 248, 57–59.

**Engels S, Helmens K, 2010.** Holocene environmental changes and climate development in Greenland. SKB R-10-65, Svensk Kärnbränslehantering AB.

- Engström J, Klint K E S, 2014.** Continental collision structures and post-orogenic geological history of the Kangerlussuaq area in the southern part of the Nagsugtoqidian orogen, Central West Greenland. *Geosciences* 4, 316–334.
- Engström J, Paananen M, Klint K E, 2012.** The Greenland Analogue Project. Geomodel version 1 of the Kangerlussuaq area on Western Greenland. Posiva Working Report 2012-10, Posiva Oy, Finland.
- Eronen M, Glückert G, van de Plassche O, van de Plicht J, Rantala P, 1995.** Land uplift in the Olkiluoto-Pyhäjärvi area, Southwestern Finland, during last 8000 years. YJT-95-17, Nuclear Waste Commission of Finnish Power Companies.
- Ettema J, van den Broeke M R, van Meijgaard E, van de Berg W J, Bamber J L, Box J E, Bales R C, 2009.** Higher surface mass balance of the Greenland ice sheet revealed by high-resolution climate modelling. *Geophysical Research Letters* 36. doi:10.1029/2009GL038110
- Fettweis X, Tedesco M, van den Broeke M, Ettema, J, 2011.** Melting trends over the Greenland ice sheet (1958–2009) from spaceborne microwave data and regional climate models. *The Cryosphere* 5, 359–375.
- Fitzpatrick A A W, Hubbard A, Joughin I, Quincey D J, van As D, Mikkelsen A P B, Doyle S H, Hasholt B, Jones G A, 2013.** Ice flow dynamics and surface meltwater flux at a land-terminating sector of the Greenland Ice Sheet. *Journal of Glaciology* 59, 687–696.
- Fitzpatrick A A W, Hubbard A L, Box J E, Quincey D J, van As D, Mikkelsen A P B, Doyle S H, Dow C F, Hasholt B, Jones G A, 2014.** A decade (2002–2012) of supraglacial lake volume estimates across Russell Glacier, West Greenland. *The Cryosphere* 8, 107–121.
- Flesche Kleiven H, Jansen E, Fronval T, Smith T M, 2002.** Intensification of Northern Hemisphere glaciations in the circum Atlantic region (3.5–2.4 Ma) – ice-rafted detritus evidence. *Palaeogeography, Palaeoclimatology, Palaeoecology* 184, 213–223.
- Follin S, Johansson P-O, Hartley L, Jackson P, Roberts D, Marsic N, 2007.** Hydrogeological conceptual model development and numerical modelling using CONNECTFLOW, Forsmark modelling stage 2.2. SKB R-07-49, Svensk Kärnbränslehantering AB.
- Follin S, Stigsson M, Rhén I, Engström J, Klint K E, 2011.** Greenland Analogue Project – Hydraulic properties of deformation zones and fracture domains at Forsmark, Laxemar and Olkiluoto for usage together with Geomodel version 1. SKB P-11-26, Svensk Kärnbränslehantering AB.
- Forman S L, Van Der Veen C, Tremper C, Csatho B, 2007.** Little Ice Age and neoglacial landforms at the inland ice margin, Isunguata Sermia, Kangerlussuaq, west Greenland. *Boreas* 36, 341–351.
- Fountain A G, Walder J S, 1998.** Water flow through temperate glaciers. *Reviews of Geophysics* 36, 299–328.
- Fox Maule C, Purucker M E, Olsen N, 2009.** Inferring magnetic crustal thickness and geothermal heat flux from crustal magnetic field models. Danish Climate Centre Report 09-09, Danish Meteorological Institute.
- Frape S K, Fritz P, 1987.** Geochemical trends for groundwater from the Canadian Shield. In Fritz P, Frape S K (eds). *Saline water and gases in crystalline rocks*. St. John's, Canada: Geological Association of Canada, 19–38.
- Freifeld B M, Trautz R C, Kharaka Y K, Phelps T J, Myer L R, Hovorka S D, Collins D J, 2005.** The U-tube: a novel system for acquiring borehole fluid samples from a deep geologic CO<sub>2</sub> sequestration experiment. *Journal of Geophysical Research* 110, B10203. doi:10.1029/2005JB003735
- Funder S V, 1989.** Quaternary geology of the ice-free areas and adjacent shelves of Greenland. *Quaternary geology of Canada and Greenland*. In Fulton R J (ed). *Quaternary geology of Canada and Greenland*. Boulder, CO: Geological Society of America, 743–792.
- Funder S, Hansen L, 1996.** The Greenland Ice Sheet – a model for its culmination and decay during and after the last glacial maximum. *Bulletin of the Geological Society of Denmark* 42, 137–152.

- Garde A A, Hollis J A, 2010.** A buried Paleoproterozoic spreading ridge in the northern Nagssugtoqidian orogen, West Greenland. In Kusky T M, Zhai M-G, Xiao W (eds). *The evolving continents : understanding processes of continental growth*. London: Geological Society. (Special publications 338), 213–234.
- Garde A A, Marker M, 2010.** Geological map of Greenland, 1:500 000, Kangerlussuaq/Søndre Strømfjord – Nuussuaq, Sheet 3. 2nd ed. Copenhagen: Geological Survey of Denmark and Greenland.
- Gascoyne M, 2000.** Hydrogeochemistry of the Whiteshell Research Area. Report 06819-REP-01200-10033-R00, Ontario Power Generation, Nuclear Waste Management Division, Canada.
- Gascoyne M, 2001.** <sup>36</sup>Cl in Olkiluoto groundwaters: evidence for intrusion of Litorina seawater. Posiva Working Report 2001-20, Posiva Oy, Finland.
- Gascoyne M, 2004.** Hydrogeochemistry, groundwater ages and sources of salts in a granitic batholith on the Canadian Shield, southeastern Manitoba. *Applied Geochemistry* 19, 519–560.
- Gascoyne M, Kamineni D C, 1994.** The hydrogeochemistry of fractured plutonic rocks in the Canadian Shield. *Applied Hydrogeology* 2, 43–49.
- Gascoyne M, Shewchuk M, 1998.** Results of U-series age determinations on fracture calcites in the Whiteshell Research Area. Report 06819-REP-01200-0024-R00, Ontario Power Generation, Nuclear Waste Management Division, Canada.
- Gómez J B, Laaksoharju M, Skårman E, Gurban I, 2006.** M3 version 3.0: Concepts, methods, and mathematical formulation. SKB TR-06-27, Svensk Kärnbränslehantering AB.
- Gómez J B, Auqué L F, Gimeno M J, 2008.** Sensitivity and uncertainty analysis of mixing and mass balance calculations with standard and PCA-based geochemical codes. *Applied Geochemistry* 23, 1941–1956.
- Gómez J B, Laaksoharju M, Skårman E, Gurban I, 2009.** M3 version 3.0: Verification and validation. SKB TR-09-05, Svensk Kärnbränslehantering AB.
- Graly J A, Humphrey N F, Landowski C M, Harper J T, 2014.** Chemical weathering under the Greenland Ice Sheet. *Geology* 42, 551–554.
- Grasby S E, Allen C C, Longazo T G, Lisle J T, Griffin D W, Beauchamp B, 2003.** Supraglacial sulfur springs and associated biological activity in the Canadian high Arctic – signs of life beneath the ice. *Astrobiology* 3, 583–596.
- Hanna E, Huybrechts P, Steffen K, Cappelen J, Huff R, Shuman C, Irvine-Fynn I, Wise S, Griffiths M, 2008.** Increased runoff from melt from the Greenland Ice Sheet: a response to global warming. *Journal of Climate* 21, 331–341.
- Harper J, Hubbard A, Ruskeeniemi T, Claesson Liljedahl L, Lehtinen A, Booth A, Brinkerhoff D, Drake H, Dow C, Doyle S, Engström J, Fitzpatrick A, Frape S, Henkemans E, Humphrey N, Johnson J, Jones G, Joughin I, Klint K E, Kukkonen I, Kullessa B, Landowski C, Lindbäck K, Makahnouk M, Meierbachtol T, Pere T, Pedersen K, Pettersson R, Pimentel S, Quincey D, Tullborg E-L, van As D, 2011.** The Greenland Analogue Project. Yearly report 2010. SKB R-11-23, Svensk Kärnbränslehantering AB.
- Harper J, Hubbard A, Ruskeeniemi T, Claesson Liljedahl L, Kontula A, Brown J, Dirkson A, Dow C, Doyle S, Drake H, Engström J, Fitzpatrick A, Follin S, Frape S, Graly J, Hansson K, Harrington J, Henkemans E, Hirschorn S, Hobbs M, Humphrey N, Jansson P, Johnson J, Jones G, Kinnbom P, Kennell L, Klint K E S, Liimatainen J, Lindbäck K, Meierbachtol T, Pere T, Pettersson R, Tullborg E-L, van As D, 2016a.** The Greenland Analogue Project: Data and Processes, NWMO-TR-2016-13, Nuclear Waste Management Organization, Canada.
- Harper J, Hubbard A, Ruskeeniemi T, Claesson Liljedahl L, Kontula A, Booth A, Brinkerhoff D, Chandler D, Drake H, Dow C, Doyle S, Engström J, Fitzpatrick A, Frape S, Helanow C, Henkemans E, Humphrey N, Johnson E, Johnson J, Jones G, Klint K E, Kullessa B, Landowski C, Lindbäck K, Luckman A, Maddoc L, Makahnouk M, Meierbachtol T, Pere T, Pettersson R, Pimentel S, Quincey D, Tullborg E-L, van As D, 2016b.** The Greenland Analogue Project. Yearly report 2011. Posiva Working Report 2012-79, Posiva Oy, Finland.

- Helm V, Humbert A, Miller H, 2014.** Elevation and elevation change of Greenland and Antarctica derived from CryoSat-2. *The Cryosphere* 8, 1539–1559.
- Helmens K F, 2013.** The Last Interglacial-Glacial cycle (MIS 5–2) re-examined based on long proxy records from central and northern Europe. SKB TR-13-02, Svensk Kärnbränslehantering AB.
- Henriksen N, Higgins A K, Kalsbeek F, Pulvertaft T C R, 2000.** Greenland from Archean to Quaternary: Descriptive text to the geological map of Greenland, 1:2 500 000: Geology of Greenland Survey Bulletin 185.
- Herut B, Starinsky A, Katz A, Bein A, 1990.** The role of seawater freezing in the formation of subsurface brines. *Geochimica et Cosmochimica Acta* 54, 13–21.
- Howat I M, de la Peña S, van Angelen J H, Lenaerts J T M, van den Broeke M R, 2013.** Brief communication “Expansion of meltwater lakes on the Greenland ice sheet”. *Cryosphere* 7, 201–204.
- Humphrey N, Echelmeyer K, 1990.** Hot-water drilling and bore-hole closure in cold ice. *Journal of Glaciology* 36, 287–298.
- Hökmark H, Lönnqvist M, Fälth B, 2010.** THM-issues in repository rock. Thermal, mechanical, thermo-mechanical and hydro-mechanical evolution of the rock at the Forsmark and Laxemar sites. SKB TR-10-23, Svensk Kärnbränslehantering AB.
- IAEA, 2012.** The safety case and safety assessment for the disposal of radioactive waste. Vienna: International Atomic Energy Agency. (Safety Standards Series SSG-23)
- IAEA, 2013.** Isotope methods for dating old groundwater. Vienna: International Atomic Energy Agency.
- Irvine-Fynn T D L, Hodson A J, 2010.** Biogeochemistry and dissolved oxygen dynamics at a subglacial upwelling, Midtre Lovénbreen, Svalbard. *Annals of Glaciology* 51, 41–46.
- Jansson P, 2010.** Ice sheet hydrology from observations. SKB TR-10-68, Svensk Kärnbränslehantering AB.
- Jansson P, Näslund J-O, 2009.** Spatial and temporal variations in glacier hydrology on Storglaciären, Sweden. SKB TR-09-13, Svensk Kärnbränslehantering AB.
- Jansson P, Näslund J-O, Rodhe L T, 2007.** Ice sheet hydrology – a review. SKB TR-06-34, Svensk Kärnbränslehantering AB.
- Jaquet O, Namah R, Jansson P, 2010.** Groundwater flow modelling under ice sheet conditions. Scoping calculations. SKB R-10-46, Svensk Kärnbränslehantering AB.
- Jaquet O, Namah R, Siegel P, Jansson P, 2012.** Groundwater flow modelling under ice sheet condition in Greenland (phase II). SKB R-12-14, Svensk Kärnbränslehantering AB.
- Jaquet O, Namar R, Jansson P, Siegel P, 2015.** Groundwater flow modelling under ice sheet conditions in Greenland (phase III). SKB R-15-12, Svensk Kärnbränslehantering AB.
- Johannessen O M, Khvorostovsky K, Miles M W, Bobylev L P, 2005.** Recent ice sheet growth in the interior of Greenland. *Science* 310, 1013–1016.
- Johansson P, Lunkka J P, Sarala P, 2011.** The glaciation of Finland. *Developments in Quaternary Science* 15, 105–116.
- Johansson E, Berglund S, Lindborg T, Petrone J, van As D, Gustafsson L-G, Näslund J-O, Laudon H, 2015a.** Hydrological and meteorological investigations in a periglacial lake catchment near Kangerlussuaq, west Greenland – presentation of a new multi-parameter dataset. *Earth System Science Data* 7, 713–756.
- Johansson E, Gustafsson L-G, Berglund S, Lindborg T, Selroos J-O, Claesson Liljedahl L, Destouni G, 2015b.** Data evaluation and numerical modeling of hydrological interactions between active layer, lake and talik in a permafrost catchment, Western Greenland. *Journal of Hydrology* 527, 688–703.
- Joughin I, Smith B E, Howat I M, Scambos T, Moon T, 2010.** Greenland flow variability from ice sheet-wide velocity mapping. *Journal of Glaciology* 56, 415–430.

- Jørgensen A S, Andreassen F, 2007.** Mapping of permafrost surface using ground-penetrating radar at Kangerlussuaq Airport, western Greenland. *Cold Regions Science and Technology* 48, 64–72.
- Kane D L, Yoshikawa K, McNamara J P, 2013.** Regional groundwater flow in an area mapped as continuous permafrost, NE Alaska (USA). *Hydrogeology Journal* 21, 41–52.
- Kleman J, Stroeven A P, Lundqvist J, 2008.** Patterns of Quaternary ice sheet erosion and deposition in Fennoscandia and a theoretical framework for explanation. *Geomorphology* 97, 73–90.
- Krabill W, Abdalati W, Frederick E, Manizade S, Martin C, Sonntag J, Swift R, Thomas R, Wright W, Yungel J, 2000.** Greenland ice sheet: high-elevation balance and peripheral thinning. *Science* 289, 428–430.
- Laaksoharju M, Tullborg E-L, Wikberg P, Wallin B, Smellie J, 1999a.** Hydrogeochemical conditions and evolution at the Äspö HRL, Sweden. *Applied Geochemistry* 14, 835–859.
- Laaksoharju M, Skårman C, Skårman E, 1999b.** Multivariate mixing and mass balance (M3) calculations, a new tool for decoding hydrogeochemical information. *Applied Geochemistry* 14, 861–871.
- Laaksoharju M, Gascoyne M, Gurban I, 2008a.** Understanding groundwater chemistry using mixing models. *Applied Geochemistry* 23, 1921–1940.
- Laaksoharju M, Smellie J, Tullborg E-L, Gimeno M, Hallbeck L, Molinero J, Waber N, 2008b.** Bedrock hydrogeochemistry Forsmark. Site descriptive modelling, SDM-Site Forsmark. SKB R-08-47, Svensk Kärnbränslehantering AB.
- Laaksoharju M, Skårman E, Gómez J, Gurban I, 2009a.** M3 user's manual. Version 3.0. SKB TR-09-09, Svensk Kärnbränslehantering AB.
- Laaksoharju M, Smellie J, Tullborg E-L, Wallin B, Drake H, Gascoyne M, Gimeno M, Gurban I, Hallbeck L, Molinero J, Nilsson A-C, Waber N, 2009b.** Bedrock hydrogeochemistry Laxemar. Site descriptive modelling, SDM-Site Laxemar. SKB R-08-93, Svensk Kärnbränslehantering AB.
- Lemieux J-M, Sudicky E A, Peltier W R, Tarasov L, 2008.** Simulating the impact of glaciations on continental groundwater flow systems: 2. Model application to the Wisconsinian glaciation over the Canadian landscape. *Journal of Geophysical Research* 113, F03018. doi:10.1029/2007JF000929
- Levy L B, Kelly M A, Howley J A, Virginia R A, 2012.** Age of the Ørkendalen moraines, Kangerlussuaq, Greenland: constraints of the extent of the southwestern margin of the Greenland Ice Sheet during the Holocene. *Quaternary Science Reviews* 52, 1–5.
- Lindbäck K, Pettersson R, Doyle S H, Helanow C, Jansson P, Savstrup Kristensen S, Hubbard A L, 2014.** High-resolution ice thickness and bed topography of a land-terminating section of the Greenland Ice Sheet. *Earth System Science Data Discussions* 7, 129–148.
- Lindbäck K, Pettersson R, 2015.** Spectral roughness and glacial erosion of a land-terminating section of the Greenland Ice Sheet. *Geomorphology* 238, 149–159.
- Lisiecki L E, Raymo M E, 2005.** A Pliocene-Pleistocene stack of 57 globally distributed benthic  $\delta^{18}\text{O}$  records. *Paleoceanography* 20, PA1003. doi:10.1029/2004PA001071
- Lund B, Schmidt P, Hieronymus C, 2009.** Stress evolution and fault stability during the Weichselian glacial cycle. SKB TR-09-15, Svensk Kärnbränslehantering AB.
- Lönnqvist M, Hökmark H, 2010.** Assessment of potential for glacially induced hydraulic jacking at different depths. SKB R-09-35, Svensk Kärnbränslehantering AB.
- Maslin M A, Li X-S, Loutre M-F, Berger A, 1998.** The contribution of orbital forcing to the progressive intensification of Northern Hemisphere glaciation. *Quaternary Science Reviews* 17, 411–426.
- Mathurin F A, Åström M E, Laaksoharju M, Kalinowski B E, Tullborg E-L, 2012.** Effect of tunnel excavation on source and mixing of groundwater in a coastal granitoidic fracture network. *Environmental Science & Technology* 46, 12779–12786.
- Mayborn K R, Leshner C E, 2006.** Origin and evolution of the Kangâmiut mafic dyke swarm, West Greenland. *Geological Survey of Denmark and Greenland Bulletin* 11, 61–86.

- McIntosh J C, Schlegel M E, Person M, 2012.** Glacial impacts on hydrologic processes in sedimentary basins: evidence from natural tracer studies. *Geofluids* 12, 7–21.
- McMurry J, 2004.** Reference water compositions for a deep geologic repository in the Canadian shield. Report 06819-REP-01200-10135-R01, Ontario Power Generation, Canada.
- Meese D A, Gow A J, Alley R B, Zielinski G A, Grootes P M, Ram M, Taylor K C, Mayewski P A, Bolzan J F, 1997.** The Greenland Ice Sheet Project 2 depth-age scale: methods and results. *Journal of Geophysical Research* 102, 26411–26423.
- Meierbachtol T, Harper J, Humphrey N, 2013.** Basal drainage system response to increasing surface melt on the Greenland ice sheet. *Science* 341, 777–779.
- Meierbachtol T W, Harper J T, Johnson J V, Humphrey N F, Brinkerhoff D J, 2015.** Thermal boundary conditions on Western Greenland: observational constraints and impacts on the modeled thermo-mechanical state. *Journal of Geophysical Research*. doi:10.1002/2014JF003375
- Mikkelsen A B, Hasholt B, Knudsen N T, Nielsen M H, 2013.** Jökulhlaups and sediment transport in Watson River, Kangerlussuaq, West Greenland. *Hydrology Research* 44, 58–67.
- Nielsen A B, 2010.** Present conditions in Greenland and the Kangerlussuaq area. Posiva Working Report 2010-07, Posiva Oy, Finland.
- Nilsson A-C, Tullborg E-L, Smellie J, Gimeno M J, Gómez J B, Auqué L F, Sandström B, Pedersen K, 2011.** SFR site investigation. Bedrock hydrogeochemistry. SKB R-11-06, Svensk Kärnbränslehantering AB.
- Normani S D, Sykes J F, 2012.** Paleohydrogeologic simulations of Laurentide ice sheet history on groundwater at the eastern flank of the Michigan Basin. *Geofluids* 12, 97–122.
- NWMO, 2012.** Adaptive Phased Management. Used fuel repository conceptual design and post-closure safety assessment in crystalline rock. Pre-project report NWMO TR-2012-16, Nuclear Waste Management Organization, Canada.
- Näslund J-O, Jansson P, Fastook J L, Johnson J, Andersson L, 2005.** Detailed spatially distributed geothermal heat-flow data for modeling of basal temperatures and meltwater production beneath the Fennoscandian ice sheet. *Annals of Glaciology* 40, 95–101.
- Palmer S, Shepherd A, Nienow P, Joughin I, 2011.** Seasonal speedup of the Greenland Ice Sheet linked to routing of surface water. *Earth and Planetary Science Letters* 302, 423–428.
- Peltier W R, 2003.** Long term Climate Change: Glaciation. Report 06819-REP-01200-10113-R00, Ontario Power Generation, Nuclear Waste Management Division, Canada.
- Pere T, 2014.** Geological logging of the Greenland Analogue Project drill cores DH-GAP01, 03 and 04. Posiva Working Report 2013-59, Posiva Oy, Finland.
- Petrone J, Sohlenius G, Johansson E, Lindborg T, Näslund J O, Strömberg M, 2016.** Using ground-penetrating radar, topography and classification of vegetation to model the sediment and active layer thickness in a periglacial lake catchment, western Greenland. *Earth System Science Data*, in review.
- Pitkänen P, Luukkonen A, Ruotsalainen P, Leino-Forsman H, Vuorinen U, 1998.** Geochemical modelling of groundwater evolution and residence time at the Kivetty site. Posiva 98-07, Posiva Oy, Finland.
- Pitkänen P, Luukkonen A, Ruotsalainen P, Leino-Forsman H, Vuorinen U, 2001.** Geochemical modelling of groundwater evolution and residence time at the Hästholmen site. Posiva 2001-01, Posiva Oy, Finland.
- Pitkänen P, Kaija J, Blomqvist R, Smellie J A T, Frape S K, Laaksoharju M, Negrel P, Casanova J, Karhu J, 2002.** Hydrogeochemical interpretation of groundwater at Palmottu. In Eighth EC Natural Analogue Working Group Meeting. Proceedings of an international workshop held in Strasbourg, France, 23–25 March 1999. EUR 19118, European Commission, 155–167.
- Pitkänen P, Partamies S, Luukkonen A, 2004.** Hydrogeochemical interpretations of baseline groundwater conditions at the Olkiluoto site. Posiva 2003-07, Posiva Oy, Finland.

- Pitkäranta R, 2009.** Pre-late Weichselian podzol soil, permafrost features and lithostratigraphy at Penttilänkangas, western Finland. *Bulletin of the Geological Society of Finland* 81, 53–74.
- Pollard W H, 2005.** Icing processes associated with high Arctic perennial springs, Axel Heiberg Island, Nunavut, Canada. *Permafrost and Periglacial Processes* 16, 51–68.
- Porter S C, 1989.** Some geological implications of average Quaternary glacial conditions. *Quaternary Research* 32, 245–261.
- Posiva, 2012.** Safety case for the disposal of spent nuclear fuel at Olkiluoto. Formulation of radionuclide release scenarios 2012. Posiva 2012-08, Posiva Oy, Finland.
- Posiva, 2013.** Olkiluoto site description 2011. Posiva 2011-02, Posiva Oy, Finland.
- Pöllänen J, Heikkinen P, Lehtinen A, 2012.** Difference flow measurements in Greenland, drillhole DH-GAP04 in July 2011. Posiva Working Report 2012-13, Posiva Oy, Finland.
- Raiswell R, 1984.** Chemical models of solute acquisition in glacial melt waters. *Journal of Glaciology* 30, 49–57.
- Russell A J, 2009.** Jökulhlaup (ice dammed lake outburst flood) impact within a valley-confined sandur subject to backwater conditions, Kangerlussuaq, West Greenland. *Sedimentary Geology* 215, 33–49.
- Russell A J, Aitken J F, De Jong C, 1990.** Observations on the drainage of an ice dammed lake in West Greenland. *Journal of Glaciology* 36, 72–74.
- Russell A, Carrivick L, Ingeman-Nielsen T, Yde J, Williams M, 2011.** A new cycle of jökulhlaups at Russel Glacier, Kangerlussuaq, West Greenland. *Journal of Glaciology* 57, 238–246.
- Sahlstedt E, Karhu J, Rinne K, 2009.** Paleohydrogeological implications from fracture calcites and sulfides in a major hydrogeological zone HZ19 at Olkiluoto. Posiva Working Report 2009-54, Posiva Oy, Finland.
- Sahlstedt E, Karhu J, Rinne K, 2014a.** Fracture mineral study of the hydraulic feature HZ20 and implications to paleohydrogeology: a report of investigations in 2009. Posiva Working Report 2012-93, Posiva Oy, Finland.
- Sahlstedt E, Karhu J, Rinne K, 2014b.** Fracture mineral investigations at Olkiluoto in 2010: Implications to paleohydrogeology. Posiva Working Report 2012-94, Posiva Oy, Finland.
- Scholz H, Baumann M, 1997.** An “open system pingo” near Kangerlussuaq (Søndre Strømfjord), West Greenland. *Geology of Greenland Survey Bulletin* 176, 104–108.
- Selker J S, Thévenaz L, Huwald H, Mallet A, Luxemburg W, van de Giesen N, Stejskal M, Zeman J, Westhoff M, Parlange M B, 2006.** Distributed fiber-optic temperature sensing for hydrologic systems. *Water Resources Research* 42, W12202. doi:10.1029/2006WR005326
- Shapiro N M, Ritzwoller M H, 2004.** Inferring surface heat flux distributions guided by a global seismic model: particular application to Antarctica. *Earth and Planetary Science Letters* 223, 213–224.
- Shreve R L, 1972.** Movement of water in glaciers. *Journal of Glaciology* 11, 205–214.
- Sidborn M, Neretnieks I, 2008.** Long term oxygen depletion from infiltrating groundwaters: model development and application to intra-glaciation and glaciation conditions. *Journal of Contaminant Hydrology* 100, 72–89.
- Sidborn M, Sandström B, Tullborg E-L, Delos A, Molinero J, Hallbeck L, Pedersen K, 2010.** SR-Site: Oxygen ingress in the rock at Forsmark during a glacial cycle. SKB TR-10-57, Svensk Kärnbränslehantering AB.
- Singer S N, Cheng C K, 2002.** An assessment of the groundwater resources of Northern Ontario. *Hydrogeology of Ontario Series (Report 2)*. Environmental Monitoring and Reporting Branch, Ministry of the Environment, Canada.
- Singhal B B S, Gupta R P, 2010.** Hydrogeology of crystalline rocks. In Singhal B B S, Gupta R P (eds). *Applied hydrogeology of fractured rocks*. Dordrecht: Kluwer Academic Publishers, 237–255.

- SKB, 2010a.** Climate and climate-related issues for the safety assessment SR-Site. SKB TR-10-49, Svensk Kärnbränslehantering AB.
- SKB, 2010b.** The Greenland analogue project. Yearly report 2009. SKB R-10-59, Svensk Kärnbränslehantering AB.
- SKB, 2011.** Long term safety for the final repository for spent nuclear fuel at Forsmark. Main report of the SR-Site project. SKB TR-11-01, Svensk Kärnbränslehantering AB.
- Skidmore M, Tranter M, Tulaczyk S, Lanoil B, 2010.** Hydrochemistry of ice stream beds – Evaporitic or microbial effects? *Hydrological Processes* 24, 517–523.
- Smellie J A T, Blomqvist R, Frape S K, Pitkänen P, Ruskeeniemi T, Casanova J, Gimeno M J, Kaija J, 2002.** Palaeohydrogeological implications for long term hydrochemical stability at Palmottu. In Maravic H von, Alexander W R (eds). Eighth EC Natural Analogue Working Group Meeting: Proceedings of an international workshop held in Strasbourg, France, 23–25 March, 1999. EUR 19118 EN, European Commission, 201–207.
- Smellie J, Tullborg E-L, Nilsson A-C, Sandström B, Waber N, Gimeno M, Gascoyne M, 2008.** Explorative analysis of major components and isotopes. SDM-Site Forsmark. SKB R-08-84, Svensk Kärnbränslehantering AB.
- Sole A, Nienow P, Bartholomew I, Mair D, Cowton T, Tedstone A, King M A, 2013.** Winter motion mediates dynamic response of the Greenland Ice Sheet to warmer summers. *Geophysical Research Letters* 40, 3940–3944.
- Spiessl S M, MacQuarrie K T B, Mayer K U, 2008.** Identification of key parameters controlling dissolved oxygen migration and attenuation in fractured crystalline rocks. *Journal of Contaminant Hydrology* 95, 141–153.
- Starinsky A, Katz A, 2003.** The formation of natural cryogenic brines. *Geochimica et Cosmochimica Acta* 67, 1475–1484.
- Statistics Greenland, 2008.** Greenland in figures 2008. 5th ed. Nuuk: Statistics Greenland, Greenland Home Rule Government.
- Storms J E A, de Winter I L, Overeem I, Drijkoningen G G, Lykke-Andersen H, 2012.** The Holocene sedimentary history of the Kangerlussuaq Fjord-valley fill, West Greenland. *Quaternary Science Reviews* 35, 29–50.
- Stotler R L, Frape S K, Ruskeeniemi T, Ahonen L, Onstott T C, Hobbs M Y, 2009.** Hydro-geochemistry of groundwaters in and below the base of thick permafrost at Lupin, Nunavut, Canada. *Journal of Hydrology* 373, 80–95.
- Stotler R L, Frape S K, Ahonen L, Clark I, Greene S, Hobbs M, Johnson E, Lemieux J-M, Peltier R, Pratt L, Ruskeeniemi T, Sudicky E, Tarasov L, 2010.** Origin and stability of a permafrost methane hydrate occurrence in the Canadian Shield. *Earth and Planetary Science Letters* 296, 384–394.
- Stotler R L, Frape S K, Ruskeeniemi T, Pitkänen P, Blowes D W, 2012.** The interglacial–glacial cycle and geochemical evolution of Canadian and Fennoscandian Shield groundwaters. *Geochimica et Cosmochimica Acta* 76, 45–67.
- Stumpf A R, Elwood Madden M E, Soreghan G S, Hall B L, Keiser L J, Marra K R, 2012.** Glacier meltwater stream chemistry in Wright and Taylor Valleys, Antarctica: Significant roles of drift, dust and biological processes in chemical weathering in a polar climate. *Chemical Geology* 322–323, 79–90.
- Sveinbjörnsdóttir Á E, Arnórsson S, Heinemeier J, 2001.** Isotopic and chemical characteristics of old “ice age” groundwater, North Iceland. In Cidu R (ed). *Water-Rock Interaction 2001*. Lisse: Swets & Zeitlinger, 205–208.
- Tarasov L, Peltier R W, 2002.** Greenland glacial history and local geodynamic consequences. *Geophysical Journal International* 150, 198–229.

- Taylor P L, 1984.** A hot water drill for temperate Ice. In Holdsworth G, Kulvinen K C, Rand J H (eds). Ice drilling technology. Cold regions research and engineering laboratory. Special Report 84-34, 105-117.
- Tedesco M, Fettweis X, Alexander P, Green G, Datta T, 2013.** MAR Greenland Outputs 1958-2013 ver. 3.2, CCNY Digital Archive. [https://www.aoncadis.org/dataset/CPL\\_MAR.html](https://www.aoncadis.org/dataset/CPL_MAR.html).
- Ten Brink N W, 1974.** Glacio-isostasy: new data from west Greenland and geophysical implications. Geological Society of America Bulletin 85, 219-228.
- Ten Brink N W, 1975.** Holocene history of the Greenland ice sheet based on radiocarbon-dated moraines in West Greenland. Kobenhavn: Kommissionen for Videnskabelige Undersogelse. (Meddelelser om Grønland 201, 4).
- Ten Brink N W, Weidick A, 1974.** Greenland ice sheet history since the last glaciation. Quaternary Research 4, 429-440.
- Thomas R, Csatho B, Davis C, Kim C, Krabill W, Manizade, McConnell S J, Sonntag J, 2001.** Mass balance of higher-elevation parts of the Greenland ice sheet. Journal of Geophysical Research 106, 33707-33716.
- Thomsen H H, Thorning L, Olesen O B, 1989.** Applied glacier research for planning hydro-electric power, Ilulissat/Jakobshavn. West Greenland. Annals of Glaciology 13, 257-261.
- Trincherro P, Delos A, Molinero J, Dentz M, Pitkänen P, 2014.** Understanding and modelling dissolved gas transport in the bedrock of three Fennoscandian sites. Journal of Hydrology 512, 506-517.
- Tyler S W, Selker J S, Hausner M B, Hatch C E, Torgersen T, Thodal C E, Schladow S G, 2009.** Environmental temperature sensing using Raman spectra DTS fiber-optic methods. Water Resources Research 45. doi:10.1029/2008WR007052
- van Angelen J H, Lenaerts J T M, Lhermitte S L, Fettweis X, Kuipers Munneke P, van den Broeke M R, van Meijgaard E, Smeets C J P P, 2012.** Sensitivity of Greenland Ice Sheet surface mass balance to surfacealbedo parameterization: a study with a regional climate model. The Cryosphere 6, 1175-1186.
- van Angelen J H, van den Broeke M R, Wouters B, Lenaerts J T M, 2014.** Contemporary (1960-2012) evolution of the climate and surface mass balance of the Greenland Ice Sheet. Surveys in Geophysics 35, 1155-1174.
- van As D, Hubbard A L, Hasholt B, Mikkelsen A B, van den Broeke M R, Fausto R S, 2012.** Large surface meltwater discharge from the Kangerlussuaq sector of the Greenland ice sheet during the record-warm year 2010 explained by detailed energy balance observations. The Cryosphere 6, 199-209.
- van den Broeke M R, Gallée H, 1996.** Observation and simulation of barrier winds at the western margin of the Greenland ice sheet. Quarterly Journal of the Royal Meteorological Society 122, 1365-1383.
- van der Veen C J, 2007.** Fracture propagation as means of rapidly transferring surface meltwater to the base of glaciers. Geophysical Research Letters 34, L01501. doi:10.1029/2006GL028385
- van de Wal R S W, Gruell, W, Van den Broeke M R, Reijmer C H, Oerlemans J, 2005.** Surface mass balance observations and automatic weather station data along a transect near Kangerlussuaq, West Greenland. Annals of Glaciology 42, 311-316.
- van de Wal R S W, Boot W, van den Broeke M R, Smeets C J P P, Reijmer C H, Donker J J A, Oerlemans J, 2008.** Large and rapid melt-induced velocity changes in the ablation zone of the Greenland Ice Sheet. Science 321, 111-113.
- van de Wal R S W, Boot W, Smeets C J P P, Snellen H, van den Broeke M R, Oerlemans J, 2012.** Twenty-one years of mass balance observations along the K-transect, West Greenland. Earth System Science Data 4, 31-35.

- van Gool J A M, Connelly L N, Marker M, Mengel F C, 2002.** The Nagssugtoqidian orogen of West Greenland: tectonic evolution and regional correlation from a West Greenland perspective. *Canadian Journal of Earth Sciences* 39, 665–686.
- van Tatenhove F G M, Olesen O B, 1994.** Ground temperature and related permafrost characteristics in West Greenland. *Permafrost and Periglacial Processes* 5, 199–215.
- van Tatenhove F G M, van der Meer J J M, Koster E A, 1996.** Implications for deglaciation chronology from new AMS age determinations in central west Greenland. *Quaternary Research* 45, 245–253.
- Vaughan D G, Comiso J C, Allison I, Carrasco J, Kaser G, Kwok R, Mote P, Murray T, Paul F, Ren J, Rignot E, Solomina O, Steffen K, Zhang T, 2013.** Observations: cryosphere. In Stocker T F, Qin D, Plattner G-K, Tignor M, Allen S K, Boschung J, Nauels A, Xia Y, Bex V, Midgley P M (eds). *Climate change 2013: the physical science basis. Contribution of Working Group I to the Fifth Assessment Report of the Intergovernmental Panel on Climate Change.* Cambridge: Cambridge University Press, 317–382.
- Vidstrand P, Follin S, Zugec N, 2010.** Groundwater flow modelling of periods with periglacial and glacial climate conditions – Forsmark. SKB R-09-21, Svensk Kärnbränslehantering AB.
- Vidstrand P, Follin S, Selroos J-O, Näslund J-O, Rhén I, 2013.** Modeling of groundwater flow at depth in crystalline rock beneath a moving ice sheet margin, exemplified by the Fennoscandian Shield, Sweden. *Hydrogeology Journal* 21, 239–255.
- Vidstrand P, Follin S, Selroos J-O, Näslund J-O, 2014.** Groundwater flow modeling of periods with periglacial and glacial climate conditions for the safety assessment of the proposed high-level nuclear waste repository site at Forsmark, Sweden. *Hydrogeology Journal* 22, 1251–1267.
- Vizcaíno M, Mikolajewicz U, Jungclaus J, Schurgers G, 2010.** Climate modification by future ice sheet changes and consequences for ice sheet mass balance. *Climate Dynamics* 34, 301–324.
- Wadham J L, Cooper R J, Tranter M, Bottrell S, 2007.** Evidence for widespread anoxia in the proglacial zone of an Arctic glacier. *Chemical Geology* 243, 1–15.
- Wadham J L, Tranter M, Hodson A J, Hodgkins R, Bottrell S, Cooper R, Raiswell R, 2010a.** Hydro-biogeochemical coupling beneath a large polythermal Arctic glacier: implications for sub ice sheet biogeochemistry. *Journal of Geophysical Research* 115, F04017. doi:10.1029/2009JF001602
- Wadham J L, Tranter M, Skidmore M, Hodson A J, Prisco J, Lyons W B, Sharp M, Wynn P, Jackson M, 2010b.** Biogeochemical weathering under ice: size matters. *Global Biogeochemical Cycles* 24, GB3025. doi:10.1029/2009GB003688
- Wahr J, van Dam T, Larson K, Francis O, 2001.** Geodetic measurements in Greenland and their implications. *Journal of Geophysical Research: Atmospheres* 106, 16567–16581.
- Wallroth T, Lokrantz H, Rimsa A, 2010.** The Greenland Analogue Project (GAP). Literature review of hydrogeology/hydrogeochemistry. SKB R-10-34, Svensk Kärnbränslehantering AB.
- Weidick A, 1993.** Neoglacial change of ice cover and the related response of the Earth's crust in west Greenland. *Rapport Grønlands Geologiske Undersøgelse* 159, 121–126.
- Weidick A, 1996.** Late Holocene and historical changes of glacier cover and related relative sea level in Greenland. *Zeitschrift für Gletscherkunde und Glazialgeologie* 32, 217–224.
- White D, Hinzman L, Alessa L, Cassano J, Chambers M, Falkner K, Francis J, Gutowski W J, Holland M, Holmes R M, Huntington H, Kane K, Kliskey A, Lee C, McClelland J, Peterson B, Rupp T S, Straneo F, Steele M, Woodgate R, Yang D, Yoshikawa K, Zhang T, 2007.** The arctic freshwater system: changes and impacts. *Journal of Geophysical Research* 112, G04S54. doi:10.1029/2006JG000353
- Willemse N W, Koster E A, Hoogakker B, van Tatenhove F G M, 2003.** A continuous record of Holocene Aeolian activity in West Greenland. *Quaternary Research* 59, 322–334.
- Wilson R W, Klint K E S, van Gool J A M, McCaffrey K J W, Holdsworth R E, Chalmers J A, 2006.** Faults and fractures in central West Greenland: onshore expression of continental break-up and

sea-floor spreading in the Labrador – Baffin Bay Sea. Geological Survey of Denmark and Greenland Bulletin 11, 185–204.

**Wohlfarth B, 2009.** Ice-free conditions in Fennoscandia during Marine Oxygen Isotope Stage 3? SKB TR-09-12, Svensk Kärnbränslehantering AB.

**Wohlfarth B, 2013.** A review of Early Weichselian climate (MIS 5d–a) in Europe. SKB TR-13-03, Svensk Kärnbränslehantering AB.

**Yde J C, Knudsen N T, 2004.** The importance of oxygen isotope provenance in relation to solute content of bulk meltwaters at Imersuaq Glacier, West Greenland. Hydrological Processes 18, 125–139.

**Yin Y, Normani S, Sykes J, Barnard M, 2013.** Preliminary hydrogeologic modelling of a crystalline rock setting in Western Greenland. NWMO TR-2013-20, Nuclear Waste Management Organization, Canada.

**Zwally H J, Abdalati W, Herring T, Larson K, Saba J, Steffen K, 2002.** Surface melt-induced acceleration of Greenland ice sheet flow. Science 297, 218–222.

## GAP bibliography – list of journal publications

The following list comprises *peer-reviewed* journal papers and PhD theses that have emanated from the GAP. It does not contain the reports published in the SKB, Posiva and NWMO report series, nor symposia abstracts.

### Published papers

**Ahlstrøm A P, Andersen S B, Andersen M L, Machguth H, Nick F M, Joughin I, Reijmer C H, van de Wal R S W, Merryman Boncori J P, Box J E, Citterio M, van As D, Fausto R S, Hubbard A, 2013.** Seasonal velocities of eight major marine-terminating outlet glaciers of the Greenland ice sheet from continuous in situ GPS instruments. *Earth System Science Data* 5, 277–287.

**Booth A D, Clark R A, Kulesa B, Murray T, Carter J, Doyle S, Hubbard A, 2012.** Thin-layer effects in glaciological seismic amplitude-versus-angle (AVA) analysis: implications for characterising a subglacial till unit, Russell Glacier, West Greenland. *The Cryosphere* 6, 909–922.

**Bougamont M, Christoffersen P, Hubbard A L, Fitzpatrick A A, Doyle S H, Carter S P, 2014.** Sensitive response of the Greenland Ice Sheet to surface melt drainage over a soft bed. *Nature Communications* 5, 5052. doi:10.1038/ncomms6052

**Brinkerhoff D J, Meierbachtol T W, Johnson J V, Harper J T, 2011.** Sensitivity of the frozen/melted basal boundary to perturbations of basal traction and geothermal heat flux: Isunnguata Sermia, western Greenland. *Annals of Glaciology* 52, 43–50.

**Chandler D M, Wadham J L, Lis G P, Cowton T, Sole A, Bartholomew I, Telling J, Nienow P, Bagshaw E, Mair D, Vinen S, Hubbard A, 2013.** Evolution of the subglacial drainage system beneath the Greenland Ice Sheet revealed by tracers. *Nature Geoscience* 6, 195–198.

**Charalampidis C, Van As D, 2015.** Observed melt-season snowpack evolution on the Greenland ice sheet. *Geological Survey of Denmark and Greenland Bulletin* 33, 65–68.

**Charalampidis C, Van As D, Box J E, Van den Broeke M R, Colgan W T, Doyle S H, Hubbard A L, MacFerrin M, Machguth H, Smeets C J P P, 2015.** Changing surface–atmosphere energy exchange and refreezing capacity of the lower accumulation area, West Greenland. *The Cryosphere* 9, 2163–2181. doi:10.5194/tc-9-2163-2015

**Dow C F, Hubbard A, Booth A D, Doyle S H, Gusmeroli A, Kulesa B, 2013.** Seismic evidence of mechanically weak sediments underlying Russell Glacier, West Greenland. *Annals of Glaciology* 54, 135–141. doi: 10.3189/2013AoG64A032

**Dow C F, Kulesa B, Rutt I C, Doyle S H, Hubbard A, 2014.** Upper bounds on subglacial channel development for interior regions of the Greenland ice sheet. *Journal of Glaciology* 60, 1044–1052.

**Dow C F, Kulesa B, Rutt I C, Tsai V C, Pimentel S, Doyle S H, Van As D, Lindbäck K, Pettersson R, Jones G A, Hubbard A, 2015.** Modeling of subglacial hydrological development following rapid supraglacial lake drainage. *Journal of Geophysical Research: Earth Surface* 120, 1127–1147.

**Doyle S H, Hubbard A L, Dow C F, Jones G A, Fitzpatrick A, Gusmeroli A, Kulesa B, Lindbäck K, Pettersson R, Box J E, 2013.** Ice tectonic deformation during the rapid in situ drainage of a supraglacial lake on the Greenland Ice Sheet. *The Cryosphere* 7, 129–140.

**Doyle S H, Hubbard A, Fitzpatrick A A W, van As D, Mikkelsen A B, Pettersson R, Hubbard B, 2014.** Persistent flow acceleration within the interior of the Greenland ice sheet. *Geophysical Research Letters* 41, 899–905.

**Doyle S H, Hubbard A, Fitzpatrick A A W, Van As D, Mikkelsen A B, Pettersson R, Hubbard B, 2014.** Persistent flow acceleration within the interior of the Greenland Ice Sheet. *Geophysical Research Letters* 41, 899–905.

**Doyle S H, Hubbard A, Van de Wal R S W, Box J E, Van As D, Scharrer K, Meierbachtol T W, Smeets P C J P, Harper J T, Johansson E, Mottram R H, Mikkelsen A B, Wilhelms F, Patton H, Christoffersen P, Hubbard B, 2015.** Amplified melt and flow of the Greenland ice sheet driven by late-summer cyclonic rainfall. *Nature Geoscience* 8, 647–653.

- Engström J, Klint K E, 2014.** Continental Collision Structures and Post-Orogenic Geological History of the Kangerlussuaq Area in the Southern Part of the Nagssugtoqidian Orogen, Central West Greenland. *Geosciences* 4, 316–334.
- Fausto R S, Van As D, PROMICE Project Team, 2012.** Ablation observations for 2008–2011 from the Programme for Monitoring of the Greenland Ice Sheet (PROMICE). *Geological Survey of Denmark and Greenland Bulletin* 26, 73–76.
- Fausto R S, Van As D, Box J E, Colgan W, Langen P L, Mottram R H, 2016.** The implications of non-radiative energy fluxes dominating Greenland exceptional surface melt in 2012. *Geophysical Research Letters*, 43, 2649-2658, doi: 10.1002/2016GL067720
- Fitzpatrick A A W, Hubbard A, Joughin I, Quincey D J, van As D, Mikkelsen A P B, Doyle S H, Hasholt B, Jones G A, 2013.** Ice flow dynamics and surface meltwater flux at a land-terminating sector of the Greenland ice sheet. *Journal of Glaciology* 59, 687–696.
- Fitzpatrick A A W, Hubbard A L, Box J E, Quincey D J, van As D, Mikkelsen A P B, Doyle S H, Dow C F, Hasholt B, Jones G A, 2014.** A decade (2002–2012) of supraglacial lake volume estimates across Russell Glacier, West Greenland. *The Cryosphere* 8, 107–121.
- Graly J A, Humphrey N F, Landowski C M, Harper J T, 2014.** Chemical weathering under the Greenland Ice Sheet. *Geology* 42, 551–554.
- Greenwood S L, Clason C C, Helanow C, Margold M, 2016.** Theoretical, contemporary observational and palaeo-perspectives on ice sheet hydrology: Processes and products. *Earth-Science Reviews* 155, 1–27. doi:10.1016/j.earscirev.2016.01.010
- Harrington J, Humphrey N F, Harper J T, 2015.** Temperature distribution and thermal anomalies along a flowline of the Greenland Ice Sheet. *Annals of Glaciology* 56. doi:10.3189/2015AoG70A945
- Helanow C, Meierbachtol T, 2015.** Steady-state water pressures in subglacial conduits: corrections to a model and recommendations for its use. *Journal of Glaciology* 61. doi:10.3189/2015JoG14J197202-204
- Jones G A, Kulesa B, Doyle S H, Dow C F, Hubbard A, 2013.** An automated approach to the location of icequakes using seismic waveform amplitudes. *Annals of Glaciology* 54. doi:10.3189/2013AoG64A07410.3189/2013AoG64A074
- Klint K E S, Engström J, Parmenter A, Ruskinemi T, Claesson Liljedahl L, Lehtinen A, 2013.** Lineament mapping and geological history of the Kangerlussuaq region, southern West Greenland. *Geological Survey of Denmark and Greenland Bulletin* 28, 57–60.
- Lindbäck K, Pettersson R, Doyle S H, Helanow C, Jansson P, Savstrup Kristensen S, Hubbard A L, 2014.** High-resolution ice thickness and bed topography of a land-terminating section of the Greenland Ice Sheet. *Earth System Science Data Discussions* 7, 129–148.
- Lindbäck K, Pettersson R, 2015.** Spectral roughness and glacial erosion of a land-terminating section of the Greenland Ice Sheet. *Geomorphology* 238, 149–159.
- Lindbäck K, Pettersson R, Hubbard A L, Doyle S H, Van As D, Mikkelsen A B, Fitzpatrick A A, 2015.** Subglacial water drainage, storage, and piracy beneath the Greenland Ice Sheet. *Geophysical Research Letters* 42. doi:10.1002/2015GL065393
- Machguth H, MacFerrin M, Van As D, Box J E, Charalampidis C, Colgan W, Fausto R S, Meijer H A J, Mosley-Thompson E, Van de Wal R S W, 2016.** Greenland meltwater storage in firn limited by near-surface ice formation. *Nature Climate Change*. doi:10.1038/nclimate2899
- Meierbachtol T, Harper J, Humphrey N, 2013.** Basal drainage system response to increasing surface melt on the Greenland ice sheet. *Science* 341, 777–779.
- Meierbachtol T W, Harper J T, Johnson J V, Humphrey N F, Brinkerhoff D J, 2015.** Thermal boundary conditions on Western Greenland: observational constraints and impacts on the modeled thermo-mechanical state. *Journal of Geophysical Research: Earth Surface*. doi:10.1002/2014JF003375
- Mikkelsen A B, Hubbard A, MacFerrin M, Box J, Doyle S, Fitzpatrick A, Hasholt B, Bailey H, 2016.** Extraordinary runoff from the Greenland Ice Sheet in 2012 amplified by hypsometry and depleted firn retention. *The Cryosphere*, 10, 1147-1159.

- Patton H, Hubbard A, Bradwell T, Glasser N F, Hambrey M J, Clark C D, 2013.** Rapid marine deglaciation: asynchronous retreat dynamics between the Irish Sea Ice Stream and terrestrial outlet glaciers. *Earth Surface Dynamics* 1, 53–65.
- Patton H, Swift D A, Clark C D, Livingstone S J, Cook S J, Hubbard A, 2015.** Automated mapping of glacial overdeepenings beneath contemporary ice sheets: Approaches and potential applications *Geomorphology* 232, 209–223.
- Rennermalm A K, Moustafa S E, Mioduszewski J, Chu V W, Forster R R, Hagedorn B, Harper J T, Mote T L, Robinson D A, Shuman C A, Smith L C, Tedesco M, 2013.** Understanding Greenland ice sheet hydrology using an integrated multi-scale approach, *Environmental Research Letters* 8(1), 015017. doi:10.1088/1748-9326/8/1/015017
- Smeets C J P P, Boot W, Hubbard A, Pettersson R, Wilhelms F, van den Broeke M R, Van De Wal R S W, 2015.** A wireless subglacial probe for deep ice applications. *Journal of Glaciology* 58, 841–848.
- Van As D, Hubbard A L, Hasholt B, Mikkelsen A B, van den Broeke M R, Fausto R S, 2012.** Large surface meltwater discharge from the Kangerlussuaq sector of the Greenland ice sheet during the record-warm year 2010 explained by detailed energy balance observations. *The Cryosphere* 6, 199–209.
- Van As D, Fausto R S, Colgan W T, Box J E, PROMICE project team, 2013.** Darkening of the Greenland ice sheet due to the melt-albedo feedback observed at PROMICE weather stations. *Geological Survey of Denmark and Greenland Bulletin* 28, 69–72.
- Van As D, Fausto R S, Steffen K, PROMICE project team, 2014.** Katabatic winds and piteraq storms: observations from the Greenland ice sheet. *Geological Survey of Denmark and Greenland Bulletin* 31, 83–86.
- Van de Wal R S W, Smeets C, Boot W, Stoffelen M, van Kampen R, Doyle S, Wilhelms F, van den Broeke M, Reijmer C, Oerlemans J, Hubbard A, 2014.** Self-regulation of basal water pressure and flow across the ablation zone of the Greenland ice sheet. *The Cryosphere Discussions* 8, 4619–4644.
- Van de Wal R S W, Smeets C J P P, Boot W, Stoffelen M, van Kampen R, Doyle S H, Wilhelms F, van den Broeke M R, Reijmer C H, Oerlemans J, Hubbard A, 2015.** Self-regulation of ice flow varies across the ablation area in south-west Greenland. *The Cryosphere* 9, 603–611.
- Wright P, Harper J T, Humphrey N F, Meierbachtol T W, 2016.** Measured basal water pressure variability of the western Greenland Ice Sheet: implications for hydraulic potential. *Journal of Geophysical Research, Earth Surface*. doi: 10.1002/2016JF003819

### **Papers in press**

- Charalampidis C, Van As D, Colgan W T, Fausto R S, MacFerrin M and Machguth H (accepted).** Thermal tracing of retained meltwater in the lower accumulation area of the southwestern Greenland ice sheet. *Annals of Glaciology*, 57, doi:10.1017/aog.2016.2
- Charalampidis C, Van As D, Langen P L, Fausto R S, Vandecrux B, Box J E (accepted).** Regional climate model performance in Greenland firn derived from in situ temperature observations. *Geological Survey of Denmark and Greenland Bulletin*.
- Machguth H and 31 coauthors (accepted).** Greenland surface mass balance observations from the ice sheet ablation area and local glaciers. *Journal of Glaciology*.
- Van As D, Fausto R S, Cappelen J, Machguth H, Van de Wal R S W, Braithwaite R J and PROMICE project team (accepted).** Placing Greenland ice sheet ablation observations in a multi-decadal context. *Geological Survey of Denmark and Greenland Bulletin*.
- Wang W, Zender C S, Van As D, Smeets P C J P, Van den Broeke M R, 2015.** A Retrospective, Iterative, Geometry-Based (RIGB) tilt correction method for radiation observed by Automatic Weather Stations on snow-covered surfaces: application to Greenland. *The Cryosphere Discussions* 9, 6025–6060. doi:10.5194/tcd-9-6025-2015

### Papers in review

**Butler C, Wadham J, 6 others.** Subglacially stored meltwater expulsion during outburst events on the Greenland Ice Sheet. *Journal of Geophysical Research*. *In review*.

**Fitzpatrick A, et al.** Ice loss across the western margin of the Greenland Ice Sheet moderated by interior flow dynamics. *Geophysical Research Letters*. *In review*.

**Jones G, Hubbard A, Doyle S, Kulessa B, Dow C, Fitzpatrick A, Pettersson R, in review.** Seismic imaging of hydraulic fracture and its impact on the dynamics of the Greenland Ice Sheet. *PNAS*. *In review*.

**Kulessa B. et al.** Supraglacial lake drainage persistently erodes sediment beneath the Greenland Ice Sheet. *Proceedings of the National Academy of Sciences of the United States of America (PNAS)*. *In review*.

**Tedesco M, Box J E, Cappelen J, Fausto R S, Fettweis X, Hansen K, Mote T, Smeets C J P P, Van As D, Van de Wal R S W, Velicogna I, Wahr J.** Greenland. In: *State of the Climate in 2015*. *Bulletin of the American Meteorological Society*. *In review*.

### Papers in preparation

**Claesson Liljedahl L, Näslund J-O, Lehtinen A, Ruskeeniemi T, Sundberg J, Engström J, Johansson S, Nygren C.** Observation of the lowest heat flow in Greenland. *Journal no decided*. *In preparation*.

**Henkemans E, Frape S K, Ruskeeniemi T, Claesson Liljedahl L, Kontula A.** Geochemical characterization of groundwater adjacent to the Greenland Ice Sheet. To be submitted to *Applied geochemistry* or similar journal. *In preparation*.

**Henkemans E, Pettersson R, Frape S K, Ruskeeniemi T, Annable W K, Makahnouk W M.** A spring (or open-system pingo) in front of the Leverett Glacier, Greenland. To be submitted to *Nature Geoscience*. *In preparation*.

**Henkemans E, Frape S K, Anderson J, Ruskeeniemi T, Claesson Liljedahl L, Kontula A.** Geochemical characterization of surface waters in Kangerlussuaq, southwest Greenland: an isotopic approach. *Journal no decided*. *In preparation*.

**Lindback K, Pettersson R, Fitzpatrick A, Doyle S, Hubbard A.** Comparison of subglacial hydrology with supraglacial hydrology, ice flow, and structure on West Greenland. To be submitted to *The Cryosphere Discussions*. *In preparation*.

**Ruskeeniemi T, Engström J, Lehtimäki J, Vanhala H, Korhonen K, Kontula A, Claesson Liljedahl L, Näslund J O, Pettersson R.** Subglacial permafrost evidencing late-Holocene re-advance of the Greenland Ice Sheet over frozen ground at Kangerlussuaq, West Greenland. *In preparation*.

### PhD Theses

**Doyle S H, 2014.** GPS-based investigations of Greenland Ice Sheet dynamics. Aberystwyth University, Geography and Earth sciences, 267 p.

**Fitzpatrick A A W, 2014.** The dynamic response of the Greenland Ice Sheet to climatic change. Aberystwyth University, Geography and Earth sciences, 217 p.

**Henkemans E, 2016.** Geochemical characterization of groundwaters, surface waters and water-rock interaction in an area of continuous permafrost adjacent to the Greenland Ice Sheet, Kangerlussuaq, Southwest Greenland. PhD thesis, University of Waterloo, Waterloo, Ontario, Canada. 327 p.

**Lindbäck K, 2015.** Hydrology and bed topography of the Greenland Ice Sheet. Last known surroundings. *Digital Comprehensive Summaries of Uppsala Dissertations from the Faculty of Science and Technology* 1265. 59 p. Uppsala: Acta Universitatis Upsaliensis.

**Meierbachtol T W, 2014.** Ice dynamics over a land-terminating sector of Western Greenland. University of Montana, 154 p.

**Mikkelsen A B, 2014.** Freshwater discharge and sediment transport to Kangerlussuaq Fjord, West Greenland – processes, modelling and implications. Department of Geosciences and Natural Resource Management, Faculty of Science, University of Copenhagen. 253 p.

## Monthly mean air temperatures from the DMI weather station in Kangerlussuaq

Table B-1. Monthly mean air temperatures [°C] from the DMI weather station in Kangerlussuaq. Data from Cappelen et al. (2001) and Cappelen (2012). The years 2008–2013 are the GAP period. The period 1961–1990 is often used as a reference period as to when the GrIS was considered to be in mass balance. Following this 30 year period of approximate mass balance, the mass balance of the GrIS has turned negative (e.g. van Angelen et al. 2012).

Month	2008	2009	2010	2011	2012	2013	Mean 1961-1990	Mean 1974-2013	Mean 1974-2007	Mean 1974-1999	Mean GAP (2008-2013) period
Jan	-21,6	-15,7	-12,0	-14,2	-19,8	-16,8	-19,7	-18,93	-19,33	-19,78	-16,7
Feb	-23,5	-14,3	-10,0	-17,7	-18,6	-17,2	-21,0	-20,01	-20,57	-21,45	-16,9
Mar	-15,1	-20,2	-12,9	-17,8	-21,2	-9,1	-17,5	-17,10	-17,29	-18,20	-16,1
Apr	-3,3	-7,3	-2,9	-15,9	0,6	-2,3	-8,4	-7,23	-7,59	-7,95	-5,2
May	5,6	3,2	8,2	1,4	3,5	-0,1	2,3	2,88	2,75	2,46	3,6
June	11,0	9,9	11,0	10,8	11,6	10,9	8,4	9,35	9,08	8,67	10,9
July	11,8	11,3	11,6	12,5	12,7	11,2	10,7	10,96	10,80	10,77	11,9
Aug	8,0	9,3	10,7	9,4	8,9	7,8	8,5	8,54	8,45	8,27	9,0
Sep	3,1	2,2	6,0	2,5	5,0	4,0	3,1	3,40	3,33	3,08	3,8
Oct	-4,7	-6,1	-2,5	-9,1	-2,4	-4,6	-6,0	-5,16	-5,20	-5,44	-4,9
Nov	-9,6	-16,9	-4,4	-13,3	-12,6	-10,8	-12,0	-11,56	-11,61	-12,01	-11,3
Dec	-14,9	-11,9	-5,0	-15,4	-16,4	-18,4	-16,9	-15,81	-16,19	-16,44	-13,7
Yearly mean	-4,43	-4,71	-0,18	-5,57	-4,06	-3,78	-5,7	-5,06	-5,28	-5,67	-3,8
Mean summer	10,27	10,17	11,10	10,90	11,07	9,97	9,2	9,61	9,44	9,24	10,6



### List of abbreviations

2D	Two-dimensional
3D	Three-dimensional
AD	Anno Domini
AECL URL	Atomic Energy of Canada Limited Underground Research Lab
ArcGIS	Esri's geographic information system (GIS) tool for working with maps and geographic information
AVA	Amplitude versus angle
AWS	Automatic Weather Station
BHL	Borehole Length
BP	Before Present
DGR	Deep Geological Repository
DH	Drillhole
DEM	Digital Elevation Model
DMI	The Danish Meteorological Institute
DNA	Deoxyribonucleic acid
DTs	Distributed Temperature Sensing
DTU	Danish Technical University
EC	Electrical conductivity
ELA	Equilibrium Line Altitude
EOH	End Of Hole
ESRI	ArcGIS platform, software and product supplier
FGN	Felsic gneiss
FMB	Frozen/melted boundary
GAP	Greenland Analogue Project
GEUS	Geological Survey of Denmark and Greenland
GMWL	Global Meteoric Water Line
GPS	Global Positioning System
GRASP	Greenland Analogue Surface Project
GrIS	Greenland Ice Sheet
GPR	Ground-Penetrating Radar
HFD	Heat Flux Density
ICEBridge	A NASA program of airborne remote sensing measurements over the Earth's polar ice to bridge the gap in measurements between the end of the ICESat-1 mission and the launch of ICESat-2.
IDL springs	Ice dammed lake springs
IMAU	Institute for Marine and Atmospheric Research in Utrecht
ka	Thousand years
KBS-3/ KBS-3H	A multi-barrier deep geologic repository concept for disposal of high-level radioactive waste developed in Sweden by Svensk Kärnbränslehantering AB (SKB).

KISS	Kangerlussuaq International Science Support centre
L	Litre(s)
LEL	Local Evaporation Line
LGM	Last Glacial Maximum
LIA	Little Ice Age
LMWL	Local Meteoric Water Line
M3	Multivariate Mixing and Mass balance calculations
Ma	Million years
MAAT	Mean Annual Air Temperature
MAGT	Mean Annual Ground Temperature
MAR	Regional climate model
m a.g.s.	Meters above ground surface
m b.g.s.	Meters below ground surface
m a.s.l.	Meters above sea level
MODIS	The Moderate-resolution Imaging Spectroradiometer
NWMO	Nuclear Waste Management Organization
P	Pressure
PFL	Posiva Flow Log
Posiva	Posiva Oy, Finland
PHREEQC	Geochemical thermodynamic modelling code
RACMO2	Regional Atmospheric Climate Model version 2
SAMPO	Wide-band frequency-domain electromagnetic sounding system
Sect-low	Lower section of borehole DH-GAP04
Sect-mid	Mmiddle section of borehole DH-GAP04
Sect-up	Upper section of borehole DH-GAP04
SEM	Scanning Electron Microscope
SFJ	Kangerlussuaq International Airport
SFR	The low- and intermediate level radioactive waste underground repository located in the vicinity of the Forsmark nuclear power plant
SGL	Supraglacial lake(s)
SKB	Svensk Kärnbränslehantering AB, Sweden
SMB	Surface energy balance models
T	Temperature (in °C)
TDS	Total Dissolved Solids
TOC	Top Of Casing
TU	Tritium unit(s)
UTC	Coordinated Universal Time
UofT GSM	University of Toronto Glacial Systems Model
USD	Uranium Series Disequilibrium
WGS-84	World Geodetic System from 1984
WRA	Whiteshell Research Area